



UNIVERSIDAD
DE MURCIA

Escuela
de Doctorado

Esta tesis doctoral está sometida a procesos de protección o transferencia de tecnología o de conocimiento, por lo que los siguientes contenidos están inhibidos en la publicación en los repositorios institucionales.

Autorizado por la Comisión General de Doctorado de la Universidad de Murcia con fecha de 19 de febrero de 2025

TESIS DOCTORAL

Implicaciones clínicas de los perfiles de expresión génica en sangre periférica en el cáncer de próstata metastásico resistente a la castración

Clinical implications of peripheral blood genes expression profiles in castration-resistant metastatic prostate cancer

AUTOR/A

Enrique Pérez Navarro

DIRECTOR/ES

José Tomás Palma Méndez
Juan Antonio Botía Blaya
Enrique González Billalabeitia

2025



UNIVERSIDAD
DE MURCIA

Escuela
de Doctorado

Esta tesis doctoral está sometida a procesos de protección o transferencia de tecnología o de conocimiento, por lo que los siguientes contenidos están inhibidos en la publicación en los repositorios institucionales.

Autorizado por la Comisión General de Doctorado de la Universidad de Murcia con fecha de 19 de febrero de 2025

TESIS DOCTORAL

*Implicaciones clínicas de los perfiles de expresión
génica en sangre periférica en el cáncer de próstata
metastásico resistente a la castración*

*Clinical implications of
peripheral blood genes
expression profiles in
castration-resistant
metastatic prostate cancer*

AUTOR/A

Enrique Pérez Navarro

DIRECTOR/ES

José Tomás Palma Méndez

Juan Antonio Botía Blaya

Enrique González Billalabeitia

2025



DECLARACIÓN DE AUTORÍA Y ORIGINALIDAD DE LA TESIS PRESENTADA PARA OBTENER EL TÍTULO DE DOCTOR/A

Aprobado por la Comisión General de Doctorado el 19 de octubre de 2022.

Yo, D. Enrique Pérez Navarro, habiendo cursado el Programa de Doctorado Programa de Doctorado de la Escuela Internacional de Doctorado de la Universidad de Murcia (EIDUM), como autor/a de la tesis presentada para la obtención del título de Doctor/a titulada:

Implicaciones clínicas de los perfiles de expresión génica en sangre periférica en el cáncer de próstata metastásico resistente a la castración

y dirigida por:

D.: Enrique González Billalabeitia
D.: José Tomás Palma Méndez
D.: Juan Antonio Botía Blaya

DECLARO QUE:

La tesis es una obra original que no infringe los derechos de propiedad intelectual ni los derechos de propiedad industrial u otros, de acuerdo con el ordenamiento jurídico vigente, en particular, la Ley de Propiedad Intelectual (R.D. legislativo 1/1996, de 12 de abril, por el que se aprueba el texto refundido de la Ley de Propiedad Intelectual, modificado por la Ley 2/2019, de 1 de marzo, regularizando, aclarando y armonizando las disposiciones legales vigentes sobre la materia), en particular, las disposiciones referidas al derecho de cita, cuando se han utilizado sus resultados o publicaciones.

Del mismo modo, asumo ante la Universidad cualquier responsabilidad que pudiera derivarse de la autoría o falta de originalidad del contenido de la tesis presentada, en caso de plagio, de conformidad con el ordenamiento jurídico vigente.

Murcia, a 10 de febrero 2025

(firma)

Información básica sobre protección de sus datos personales aportados:	
Responsable	Universidad de Murcia. Avenida teniente Flomesta, 5. Edificio de la Convalecencia. 30003; Murcia. Delegado de Protección de Datos: dpd@um.es
Legitimación	La Universidad de Murcia se encuentra legitimada para el tratamiento de sus datos por ser necesario para el cumplimiento de una obligación legal aplicable al responsable del tratamiento. art. 6.1.c) del Reglamento General de Protección de Datos
Finalidad	Gestionar su declaración de autoría y originalidad
Destinatarios	No se prevén comunicaciones de datos
Derechos	Los interesados pueden ejercer sus derechos de acceso, rectificación, cancelación, oposición, limitación del tratamiento, olvido y portabilidad a través del procedimiento establecido a tal efecto en el Registro Electrónico o mediante la presentación de la correspondiente solicitud en las Oficinas de Asistencia en Materia de Registro de la Universidad de Murcia

Esta DECLARACIÓN DE AUTORÍA Y ORIGINALIDAD debe ser insertada en la quinta hoja, después de la portada de la tesis presentada para la obtención del título de Doctor/a.

A mis padres.

*Y a mis abuelos Paco y Tomás, y a mi tata Isabel,
quienes me cuidan y guían desde el cielo.*

*El tiempo de Dios es perfecto.
No aceleres los procesos ni tomes decisiones erróneas.
Ten paciencia que en su momento,
Dios proveerá.*

Eclesiastés 3–1

AGRADECIMENTOS

Esta tesis doctoral es el fruto de años de esfuerzo y dedicación. Se trata de un proyecto de gran complejidad que, sin el apoyo, la guía y el aliento de quienes, de una forma u otra, han dejado su huella en este camino, no habría sido posible realizar. Por ello, deseo expresar mi más sincera gratitud a quienes me han acompañado, inspirándome y haciéndome creer siempre en la belleza de la ciencia y del trabajo en equipo.

No puedo iniciar este apartado sin expresar mi más sincero agradecimiento a mis directores y tutores de tesis, el Dr. José Tomás Palma Méndez, el Dr. Juan Botía Blaya y el Dr. Enrique González Billalabeitia. Gracias por brindarme la oportunidad de embarcarme en este apasionante proyecto bajo vuestra guía y supervisión, por abrirme las puertas de vuestro grupo de investigación y, sobre todo, por introducirme al fascinante mundo de la inteligencia artificial, que ha despertado en mí una profunda admiración y curiosidad por esta disciplina y que me ha permitido crecer tanto personal como profesionalmente.

Quiero expresar mi especial agradecimiento al Dr. González Billalabeitia. Tu apoyo, tu confianza en mí y tu disposición para ayudarme en todo momento han sido fundamentales durante este proceso. Gracias por darme la oportunidad de explorar más allá de los límites de mi doctorado, por permitirme trabajar en proyectos de tu grupo de investigación y por encontrar soluciones cuando parecía que no las había. Aprecio profundamente tu capacidad para dar sentido a lo que hacemos y para mantener siempre una perspectiva positiva, incluso en los momentos más difíciles. Gracias por ser esa persona que no solo lucha por sus propias metas, sino también por el éxito de quienes lo rodean.

Quisiera expresar mi más sincero agradecimiento a la Dra. Vincenza Conteduca y al Dr. Ugo De Giorgi, cuya colaboración ha sido esencial para la obtención de las muestras de pacientes que han permitido la validación de los experimentos realizados en esta tesis. Así como a Francesca Demichellis, mi supervisora en

Computational and Integrative Biology (CIBIO), y a todos los miembros de su grupo. Gracias por vuestra ayuda y enseñanza durante mi estancia en Trento.

Agradecer también al Instituto de Investigación 12 de Octubre y al ISCIII, por proporcionarme las instalaciones y el soporte económico para poder desarrollar esta tesis. Así como a mis compañeros del hospital: Juanma, José, Celia y Miguel. Mención especial a los dos primeros: Juanma, gracias por compartir conmigo tu conocimiento y tu experiencia. José, a ti no solo te debo lo mucho que he aprendido de ciencia básica y de tablas Excel imposibles de entender, sino también cómo disfrutar Madrid y Bilbao... y cómo sobrevivir para contarlo. Gracias a ambos por hacer de este viaje algo inolvidable.

A mis antiguos compañeros de la Unidad de Proteómica de la Universidad Complutense de Madrid: Concha Gil, María Luisa, Lola, Felipe, Inés, Edu y Ebrahim. El aprendizaje, el apoyo y las experiencias compartidas fueron esenciales para afianzar mi desarrollo como investigador y, sin duda, marcaron el camino que me ha llevado hasta aquí.

A mis compañeros del ACTI: María José, Francisco, María y Roque. Gracias por vuestro apoyo y por vuestras conversaciones durante los desayunos. En especial, quiero expresar mi especial agradecimiento a María José. Parte de los resultados que aquí se presentan son fruto de tu trabajo. Gracias por estar siempre dispuesta a ayudar, por tu profesionalidad y por contribuir de manera tan significativa a este proyecto.

A mis compañeros de facultad, mis queridos Comisionistas: Fran, Juan, Alicia, Alejandro, Ade, Antonio, Juan M., Enrique M., Adri, Belén, Dani, Andrea, Joselu... Gracias por ser mucho más que compañeros de trabajo; por compartir conmigo no solo comidas, sino risas, conversaciones y momentos que nos permiten olvidarnos hasta las 14:30 de la rutina diaria.

A mi grupo de amigos, los que se convirtieron en mi familia elegida: Los Tormos, Lorena, Celia, Ítalo... Gracias por ser mi refugio durante los años de mi doctorado, por las risas interminables que aliviaron los momentos de estrés y por los recuerdos inolvidables que hemos creado juntos. Gracias por recordarme la importancia de desconectar y disfrutar, y por estar ahí siempre que se os necesita.

A mis abuelas, Mari y Conchita, a mi hermano Francisco, a mi tito José y al resto de mi familia, os agradezco profundamente vuestro apoyo constante, que ha sido una fuente de fortaleza a lo largo de este camino. Y, por supuesto, a mi familia política albojense, gracias por acogerme con tanto cariño y hacerme

sentir siempre como en casa. Cada uno de vosotros ha contribuido un poquito en la presentación de esta tesis.

También quiero dedicar una parte de estos agradecimientos a aquellos que ya no están físicamente conmigo, pero que viven en mi corazón y me han acompañado en cada paso de esta etapa: mi tata Isabel, cuyo amor, sonrisa y alegría dejaron una marca imborrable en mí, y a mis abuelos Tomás y Paco, cuyos valores y enseñanzas sigo aplicando en mi día a día. Una parte de esta tesis es vuestra y, aunque no puedan compartir este momento con vosotros, sé que desde el cielo seguís cuidándome, celebrando conmigo y animándome a continuar creciendo. Os quiero y os echo muchísimo de menos.

Y, en un lugar muy especial, gracias a las dos personas a las que les debo todo: mis padres. Papá y mamá, gracias por vuestras palabras llenas de ánimo, por vuestra constante preocupación por mi bienestar y por estar siempre a mi lado, especialmente durante los momentos más desafiantes de este proceso. Gracias por consolarme cuando las cosas no salían como esperaba, por celebrar conmigo cada pequeño avance y por recordarme siempre que era capaz de lograrlo. Teneros como padres es, sin duda, el mayor privilegio de mi vida, y esta tesis es también un reflejo de vuestro amor, dedicación y sacrificio que habéis hecho por mí.

Quiero dedicar estas últimas palabras a lo más especial de mi vida: a ti, Ainhoa, y a nuestro pequeño Marco. Ainhoa, gracias por tu amor incondicional, por tu apoyo constante y por tu infinita paciencia durante los momentos más intensos de este doctorado, en los que las horas frente al ordenador parecían interminables. Has sido mi mayor apoyo y mi mejor compañera en esta aventura, recordándome siempre lo que realmente importa cuando las dudas o el cansancio aparecían. Y Marco, estas palabras te esperan, quizá por mucho tiempo, hasta que puedas leerlas y comprenderlas. Gracias por llegar a nuestras vidas y llenarlas de un amor que no sabíamos que podía existir. Vosotros dos sois, sin duda alguna, mi mayor logro, mi mayor orgullo y la fuerza detrás de cada página de esta tesis.

Finalmente, quiero expresar mi especial agradecimiento a los pacientes y sus familiares, cuya generosa colaboración ha hecho posible la realización de esta tesis y ha contribuido significativamente al avance en la investigación del cáncer. A todos ellos, mi más sincera y profunda gratitud.

ABSTRACT

This thesis investigates the prognostic implications of immune cell dynamics and gene expression profiles on responses to anti-androgen therapy with enzalutamide among patients with metastatic castration-resistant prostate cancer (mCRPC). mCRPC remains a major clinical challenge due to its heterogeneity and the limited efficacy of treatments to date. By integrating bioinformatics analyses, clinical data from multicentre trials and laboratory experiments, the research aims to identify biomarkers that can inform prognosis, elucidate mechanisms of treatment resistance and guide personalized therapeutic strategies.

In the initial study, an analysis was conducted on 95 whole blood samples obtained from patients who had not received enzalutamide or chemotherapy, as part of a phase II PREMIERE clinical trial. Using the CIBERSORTx algorithm, the relative proportions of 22 immune cell subsets were quantified. Elevated monocyte levels were shown to be strongly associated with a worsening of overall survival (OS), while elevated CD8 + T cell levels were associated with a longer survival. These observations were independently validated in 54 patients from an Italian cohort (IRST), suggesting that peripheral immune composition provides potential predictive value. In addition, multivariate Cox regression analyses were performed to demonstrate that CD8+ T cells retained prognostic significance independent of established clinical and molecular prognostic factors and thus may strengthen the immune profile as a potential complementary tool in mCRPC risk stratification.

Based on these findings, this thesis proposes a 22-gene prognostic signature developed by analysing gene expression profiles in peripheral blood. Using advanced Machine Learning techniques, the most relevant genes were selected to form this signature. The results demonstrated a strong predictive performance for OS, superior to existing prognostic models. In addition, it was validated in an independent cohort, highlighting its potential usefulness in clinical practice for risk stratification and personalized treatment planning.

Time-dependent Receiver Operating Characteristic (ROC) curve analyses further confirmed its robustness over clinically relevant time points, outperforming existing prognostic models. This signature now offers a promising tool for personalized treatment planning, allowing clinicians to tailor their therapeutic strategies based on the individual risk profile of each patient.

A longitudinal analysis of whole blood transcriptomes was performed to understand the immunomodulatory effects of enzalutamide and its association with resistance to treatment. Gene expression was analysed from samples before treatment, after 12 weeks of treatment, and at the time of disease progression. Differential gene expression between comparisons revealed a strong suppression of immune-related pathways, in particular those related to adaptive immunity. Immune cell profile throughout treatment showed a persistent decrease in CD8⁺ T cells and an increase in monocytes both at 12 weeks and at the time of progression. These changes indicate that enzalutamide promotes an immunosuppressive environment, which may hinder anti-tumour immune responses and favour the development of therapeutic resistance.

To elucidate whether enzalutamide exerts direct effects on immune cells, *in vitro* studies were conducted with human T-cell lines (Jurkat, MOLT-4), the monocyte cell line THP-1 and the B-cell line Raji. Enzalutamide strongly suppressed T-cell viability and, to a lesser extent, B-cell and monocyte viability at clinical concentrations by an androgen receptor-independent mechanism, which resulted in induction of apoptosis. Comparisons with other antiandrogens showed that darolutamide also reduced T-cell viability, while bicalutamide, apalutamide and abiraterone acetate did not. The gene expression profiles of enzalutamide-treated T cells showed up-regulation of sterol biosynthesis pathways and down-regulation of ribosome biogenesis and mitochondrial function, suggesting that metabolic dysregulation may be due to non-specific binding of these drugs to membrane receptors involved in apoptosis.

These current results significantly underline how enzalutamide profoundly affects the immune system, thus showing another side of the hitherto unknown mechanisms of action. Among those observed, lymphocyte suppression may explain one way in which resistance arises as part of the compromise of host immunity to tumours. Clinically, the findings appear to suggest that immune cell phenotyping and gene expression may inform the prognosis of response or resistance to this treatment. The differential effects of antiandrogens on immune cells further suggest that antiandrogen selection, based on minimal immunosuppressive effects, could improve treatment outcomes.

In summary, this thesis expands knowledge on the interplay of anti-androgen therapies, immune dynamics, and gene expression in a progressive mCRPC state, highlighting potential biomarkers for prognosis and underpinning a mechanism of resistance. It contributes to the developing landscape of personalised oncology, with the primary aim of enhancing patient results.

RESUMEN

La tesis investiga la compleja interacción entre la terapia antiandrogénica con enzalutamida, la dinámica de las células inmunitarias y los perfiles de expresión génica en pacientes con cáncer de próstata metastásico resistente a la castración (mCRPC), una patología que sigue representando un desafío clínico de gran magnitud debido a su marcada heterogeneidad y a la limitada eficacia de las terapias disponibles. Esta enfermedad, que afecta a un porcentaje significativo de hombres en etapas avanzadas, presenta una supervivencia global variable, que en muchos casos no supera los 3 años, lo que subraya la urgente necesidad de nuevos enfoques pronósticos y terapéuticos. Ante la necesidad de identificar biomarcadores capaces de predecir la evolución de la enfermedad y de dilucidar los mecanismos que subyacen a la aparición de resistencia terapéutica, este trabajo integra análisis bioinformáticos, estudios clínicos en ensayos multicéntricos y experimentos de laboratorio, con el objetivo de establecer herramientas que faciliten la estratificación del riesgo y la planificación personalizada de los tratamientos.

El impacto del mCRPC en la salud pública es significativo. Estudios epidemiológicos recientes indican que, aunque la incidencia del cáncer de próstata ha disminuido en algunos países gracias a campañas de detección temprana, la tasa de mortalidad en los estadios avanzados sigue siendo elevada. La heterogeneidad biológica del mCRPC, caracterizada por diferencias en la expresión génica y en el microambiente tumoral, complica la predicción de la respuesta a los tratamientos convencionales. En este contexto, se ha vuelto imprescindible la búsqueda de biomarcadores que permitan una clasificación más precisa de los pacientes, posibilitando el desarrollo de estrategias terapéuticas adaptadas a las características individuales.

En un primer estudio, se analizó la composición inmunitaria en sangre periférica de pacientes con mCRPC, reclutados en el ensayo clínico de fase II denominado PREMIERE. En este estudio se evaluaron 95 muestras de sangre total obtenidas en pacientes que aún no habían recibido tratamiento con

enzalutamida ni quimioterapia. La cuantificación de los distintos subconjuntos de células inmunitarias se llevó a cabo mediante el algoritmo CIBERSORTx, el cual permite descomponer el perfil transcriptómico en porcentajes relativos de 22 tipos celulares inmunitarios. Se observó que los niveles elevados de monocitos se asociaban fuertemente con un empeoramiento en la supervivencia global, mientras que mayores proporciones de linfocitos T CD8+ se correlacionaban con una supervivencia prolongada. Dichas asociaciones se confirmaron posteriormente en una cohorte independiente de 54 pacientes pertenecientes al estudio IRST, lo cual sugiere que la composición inmunitaria periférica constituye un marcador predictivo de valor clínico, capaz de complementar la estratificación del riesgo basada en factores pronósticos clínicos y moleculares tradicionales.

Paralelamente, a partir de estos hallazgos se desarrolló una firma pronóstica basada en perfiles de expresión génica obtenidos de sangre periférica, con el objetivo de mejorar la predicción de la supervivencia global en pacientes con mCRPC. Para la construcción de esta firma se aplicaron técnicas de Machine Learning que permitieron seleccionar, de entre un gran número de genes diferencialmente expresados, un panel reducido y robusto de 22 genes. Este modelo predictivo demostró un rendimiento superior en términos de capacidad discriminativa frente a modelos existentes, validándose tanto en la cohorte de desarrollo (PREMIERE) como en la cohorte de validación (IRST). El análisis de las curvas ROC dependientes del tiempo confirmó la solidez del modelo a lo largo de puntos temporales clínicamente relevantes, evidenciando una mejora significativa en la capacidad para estratificar el riesgo de muerte en comparación con otras firmas genéticas previamente publicadas. La utilidad de esta firma radica en que permite calcular un puntaje de riesgo individual para cada paciente, lo cual posibilita la adaptación de las estrategias terapéuticas en función del perfil pronóstico, contribuyendo así a la oncología personalizada.

Además, la tesis profundiza en el estudio longitudinal del transcriptoma de sangre total, con el fin de comprender los efectos inmunomoduladores de la enzalutamida y su relación con la resistencia al tratamiento. Se analizaron muestras obtenidas en tres momentos clave: antes del inicio del tratamiento, a las 12 semanas de terapia y en el momento en que se evidenció la progresión de la enfermedad. La comparación entre estos momentos permitió identificar cambios sustanciales en la expresión génica, revelando una supresión notable de las vías relacionadas con la inmunidad adaptativa, especialmente aquellas implicadas en la activación y función de las células T CD8+. De igual forma, se detectó un aumento en la proporción de monocitos en las muestras obtenidas

tanto a las 12 semanas como en la progresión, lo que sugiere que el tratamiento con enzalutamida induce un entorno inmunosupresor que podría dificultar la respuesta antitumoral y favorecer la aparición de mecanismos de resistencia. La persistencia de estos cambios a lo largo del tiempo resalta la importancia de monitorizar la dinámica del microambiente inmunitario como herramienta pronóstica y como indicador de la efectividad terapéutica.

Para dilucidar si la enzalutamida ejerce efectos directos sobre las células inmunitarias, se realizaron estudios *in vitro* utilizando líneas celulares representativas del sistema inmune. En estos experimentos se evaluó la respuesta de líneas de células T (como Jurkat y MOLT-4), de monocitos (THP-1) y de células B (Raji) tras la exposición a concentraciones clínicas del fármaco. Los resultados demostraron que enzalutamida reduce de manera significativa la viabilidad de las células T, induciendo apoptosis a través de mecanismos que resultan independientes de la presencia del receptor androgénico (AR), dado que las células utilizadas carecían de expresión de dicho receptor. Este hallazgo es de particular importancia, ya que indica que la acción citotóxica del fármaco sobre el sistema inmune no depende de la vía clásica de señalización androgénica, lo que podría tener repercusiones directas en la respuesta antitumoral. De manera complementaria, se observó que, si bien las células B y los monocitos también experimentaron una reducción en su viabilidad, el efecto fue menos pronunciado en comparación con las células T. Adicionalmente, se realizó una comparación entre distintos antiandrogénicos; se encontró que, a concentraciones plasmáticas equivalentes, enzalutamida y darolutamida reducen significativamente la viabilidad de las células T, mientras que agentes como bicalutamida, apalutamida y el acetato de abiraterona muestran efectos mínimos sobre estos linfocitos. Esta diferencia en la acción de los fármacos sobre el sistema inmune podría tener implicaciones clínicas relevantes, ya que preservar la función de las células T podría traducirse en una respuesta antitumoral más robusta y en una mejor supervivencia de los pacientes.

El análisis de los perfiles de expresión génica en las células T tratadas con enzalutamida aportó información adicional sobre los mecanismos subyacentes a la inducción de apoptosis. Se observó una regulación al alza de las vías de biosíntesis de esteroides y del metabolismo del colesterol, lo que podría interpretarse como un intento de compensación celular frente al estrés inducido por el tratamiento. En paralelo, se detectó una regulación a la baja de procesos esenciales como la biogénesis de ribosomas, la función mitocondrial y el procesamiento del ARN, lo que sugiere una afectación global de la capacidad

de síntesis proteica y energética de la célula. La combinación de estos cambios metabólicos resulta en una desregulación que culmina en la activación de rutas apoptóticas, confirmando la hipótesis de que la enzalutamida induce un daño celular que trasciende la simple inhibición de la señalización androgénica.

En conjunto, estos hallazgos evidencian que la enzalutamida ejerce un doble impacto en el tratamiento del mCRPC: por un lado, actúa sobre la vía androgénica que sustenta la proliferación tumoral, y por otro, modula el sistema inmune de forma que se favorece un entorno inmunosupresor. La reducción en la proporción de células T CD8+ –responsables de la respuesta citotóxica antitumoral– y el aumento concomitante en los monocitos, que pueden promover procesos proinflamatorios y de reparación, crean un balance que podría contribuir a la evasión inmunitaria del tumor y al desarrollo de resistencia al tratamiento. De esta manera, la identificación de estos biomarcadores inmunitarios no solo tiene valor pronóstico, sino que también abre nuevas posibilidades para la intervención terapéutica, como la combinación de antiandrogénicos con estrategias de inmunoterapia que potencien la función de los linfocitos T.

El desarrollo de la firma pronóstica de 22 genes se erige como una herramienta fundamental en la personalización del tratamiento para pacientes con mCRPC. Esta firma, obtenida a partir del análisis de perfiles de expresión génica en sangre periférica, permite clasificar a los pacientes en función de su riesgo de progresión y de muerte. La validación de la firma en una cohorte independiente respalda su robustez y su aplicabilidad clínica, ya que muestra un rendimiento superior en comparación con modelos previos. La capacidad de predecir de forma precisa la supervivencia global a través de un análisis mínimamente invasivo representa un avance significativo en la oncología personalizada, pues posibilita la identificación temprana de pacientes que podrían beneficiarse de estrategias terapéuticas más agresivas o, por el contrario, de un manejo más conservador para evitar efectos adversos innecesarios.

Asimismo, la monitorización longitudinal del transcriptoma de sangre ha permitido evidenciar que la respuesta a la enzalutamida es dinámica y evoluciona a lo largo del tiempo. Los cambios en la expresión génica observados a los 12 semanas de tratamiento, que incluyen una supresión de las vías asociadas a la inmunidad adaptativa, se mantienen en gran medida en el momento de la progresión, aunque con matices que sugieren la activación de mecanismos de resistencia específicos. Esta información es de suma importancia, ya que permite inferir que, a pesar de una respuesta inicial favorable, la persistencia de un entorno inmunosupresor podría ser el factor

determinante que conduzca al fracaso terapéutico. La integración de estos datos transcriptómicos con el análisis de la composición inmunitaria ofrece una visión global de la respuesta del paciente, que podría orientar futuras estrategias de combinación terapéutica orientadas a contrarrestar la evasión inmune y mejorar la efectividad de los tratamientos antiandrogénicos.

Por otra parte, es relevante situar estos hallazgos en el contexto de los avances previos en la investigación del mCRPC. Mientras que modelos anteriores basados en firmas génicas se centraban en un número limitado de genes o en biomarcadores aislados, la aproximación multidimensional adoptada en este trabajo permite captar la complejidad del microambiente tumoral y del sistema inmune. Esta integración no solo optimiza la precisión pronóstica, sino que también brinda una base sólida para futuras investigaciones que busquen identificar nuevos blancos terapéuticos y para el diseño de ensayos clínicos que incorporen estos biomarcadores.

La relevancia clínica de estos resultados radica en la posibilidad de incorporar biomarcadores inmunitarios y transcriptómicos en la práctica clínica para identificar de forma precisa a los pacientes con alto riesgo de progresión. Esta información facilitará la toma de decisiones terapéuticas, permitiendo adaptar el tratamiento de forma oportuna y personalizada. Además, la variabilidad en la respuesta de las células inmunitarias a distintos antiandrogénicos sugiere que la selección del fármaco podría optimizarse para minimizar la inmunosupresión y potenciar la respuesta antitumoral, lo que abre la puerta a terapias combinadas con agentes inmunomoduladores.

En definitiva, el trabajo aporta evidencia sólida de que la integración de datos inmunológicos y moleculares en el manejo del mCRPC avanza hacia una oncología personalizada, fundamentada en la caracterización precisa del perfil del paciente. Este enfoque multidimensional no solo mejora la predicción de la evolución clínica y la supervivencia global, sino que también proporciona nuevas perspectivas para el diseño de ensayos y el desarrollo de tratamientos innovadores. La posibilidad de adaptar la estrategia terapéutica en función de un puntaje de riesgo individual, calculado a partir de la firma pronóstica de 22 genes y el análisis del microambiente inmunitario, representa un avance significativo para mejorar la calidad de vida y la supervivencia de los pacientes afectados.

En conclusión, la tesis no solo profundiza en la comprensión de los mecanismos que rigen la interacción entre la terapia antiandrogénica y el sistema inmune en el mCRPC, sino que también sienta las bases para futuras investigaciones y

aplicaciones clínicas. La integración del fenotipo inmunitario y los perfiles de expresión génica permite una estratificación del riesgo más precisa, lo que se traduce en una mejor personalización del tratamiento y en la posibilidad de diseñar intervenciones terapéuticas más efectivas. Estos avances representan un paso crucial hacia la oncología de precisión en el manejo de una enfermedad que sigue siendo uno de los mayores retos en la práctica oncológica actual.

CONTENTS

Contents	xxvi
List of Figures	xxxii
List of Tables	xxxviii
Abbreviations	xli
Thesis structure	xliv
1 Introduction	1
1.1 Concept of Cancer	1
1.2 Oncogenesis	1
1.3 The Prostate	5
1.3.1 Anatomy of the prostate	5
1.4 Prostate Cancer (PCa)	7
1.4.1 Epidemiology: incidence and mortality	7
1.4.2 Risk factors	9
1.4.3 Clinical features and diagnosis	12
1.4.4 Tumour classification	16
1.5 Androgen signalling and Androgen Receptor (AR) in PCa	19
1.5.1 Androgen action in prostatic development	19
1.5.2 AR structure	21
1.5.3 AR activation and mechanisms of action	22
1.5.4 Persistent AR signalling in castration-resistant PCa	24
1.6 Therapeutic approach to PCa	24
1.6.1 Treatment of localised PCa	24
1.6.2 Treatment of advanced PCa	28
1.6.3 Treatment of Castration-resistant prostate cancer	31
1.7 Immunotherapy for castration-resistant prostate cancer	33
1.7.1 Current Immunotherapy Strategies for Prostate Cancer	34

1.8	Biomarkers	39
1.8.1	Types of biomarkers	40
1.8.2	Clinicopathological biomarkers	41
1.8.3	Molecular biomarkers	42
1.9	Whole blood assay approach to circulating biomarkers discovery .	43
1.9.1	Application of whole blood RNA assays in metastatic PCa .	43
2	Hypotheses & Objectives	46
2.1	Hypotheses	46
2.2	Objectives	48
3	Material and Methods	49
3.1	Study design	49
3.2	Clinical data collection	49
3.3	Sample collection	51
3.3.1	Inclusion criteria	51
3.3.2	Sample acquisition	51
3.4	Microarray analysis	53
3.4.1	Sample collection and RNA extraction	53
3.4.2	Microarray hybridization and data acquisition	53
3.4.3	Quality control and preprocessing	54
3.4.4	Probe annotation	54
3.5	Differential gene expression analysis	54
3.6	Gene set enrichment analysis	55
3.7	Immune cell profiling using CIBERSORTx	55
3.8	<i>In vitro</i> Experiments	56
3.8.1	Cell lines and culture conditions	56
3.8.2	Cell viability assays	56
3.8.3	Apoptosis assays	56
3.8.4	Use of different antiandrogens	57
3.8.5	Gene expression profiling in cell lines	57
3.9	Statistical analysis	57
3.9.1	Survival analysis	57
3.9.2	Development and validation of prognostic models	58
3.9.3	Data visualization	59
4	Prognostic implication of blood immune cell composition in mCRPC	60
4.1	Introduction	60
4.2	Material and methods	61
4.2.1	Study design and data collection	61

4.2.2	Inference of immune cell profiling	61
4.2.3	Statistical analysis	61
4.3	Results	62
4.3.1	Study population	62
4.3.2	Immune cell composition in peripheral blood	63
4.3.3	Association of immune cell subsets with OS	64
4.3.4	Validation in an independent cohort	65
4.3.5	Multivariate analysis	68
4.4	Summary	69
5	Prognostic Gene Expression Signature in mCRPC: Development, Validation and Analysis of Disease Progression	71
5.1	Introduction	71
5.2	Material and methods	72
5.2.1	Processing of gene expression data	72
5.2.2	Univariate Cox Proportional Hazards Regression	72
5.2.3	Development and validation of prognostic gene signature	73
5.2.4	Validation of the prognostic signature	73
5.3	Results	74
5.3.1	Univariate Cox regression	74
5.3.2	Development and validation of prognostic models	74
5.3.3	Gene model (Content censored)	76
5.3.4	Time-Dependent ROC analysis and model comparison	76
5.4	Summary	78
6	Dynamics of immune cells associated with antiandrogen therapy in mCRPC	82
6.1	Introduction	82
6.2	Material and methods	83
6.2.1	Differential expression analysis and identification of DEGs	83
6.2.2	Gene set enrichment analysis	84
6.2.3	Immune cell profiling	84
6.2.4	<i>In vitro</i> studies on immune cell populations	84
6.2.5	Statistical analysis	84
6.3	Results	85
6.3.1	Enzalutamide-induced changes in whole-blood gene expression	85
6.3.2	Hierarchical clustering analysis	86
6.3.3	Differential gene expression analysis	87

6.3.4	Gene set enrichment analysis reveals dynamic pathway regulation	90
6.3.5	Effect of enzalutamide and/or tumour progression on the immune cell components in blood	92
6.3.6	<i>In vitro</i> characterization of enzalutamide's effects on immune cell populations	94
6.3.7	Enzalutamide reduces viability of T Cells independently of AR expression	94
6.3.8	Differential sensitivity of immune cell types to enzalutamide	97
6.3.9	Comparative analysis of AR inhibitors on t-cell viability . .	99
6.3.10	Gene expression profiling reveals modulation of apoptotic and immune pathways	101
6.4	Summary	102
7	Discussion	107
8	Conclusions	122
9	Conclusiones	125
10	Bibliography	128
11	Thesis contributions	150
12	Annexes	155
12.1	Annex A	156
12.2	Annex B	165
12.3	Annex C	177

LIST OF FIGURES

1.1	Hallmarks of Cancer. This image represents the capabilities of cancer cells proposed by Hanahan and Weinberg [5]	2
1.2	Two diagrams illustrating the anatomy of the prostate gland. (a) Highlights the central zone (A), anterior fibromuscular stroma (B), transitional zone (C), peripheral zone (D), and periurethral gland region (E), with their respective structural and functional roles. (b) Provides a detailed view of the ducts and acini embedded in the stromal framework, consisting of smooth muscle cells and fibroblasts, which are critical for prostate development and function. [16]	6
1.3	Global geographical incidence and mortality of PCa. (A) Global incidence of PCa in 2022. (B) Global mortality from PCa in 2022. Global cancer observatory: cancer Today; 2022. Available from: https://gco.iarc.fr/today/en/dataviz	8
1.4	Regulation and Metabolism of Testosterone. Testosterone production initiates in the hypothalamus, where GnRH (gonadotropin-releasing hormone) is released into the hypophyseal portal system. This GnRH then acts upon the anterior pituitary gland, triggering the release of two key hormones: FSH (follicle-stimulating hormone) and LH (luteinizing hormone) [78].	20
1.5	Structure of the AR. The AR gene is situated on the X chromosome (Xq11-12) and comprises eight exons. It includes exon 1, which encodes the N-terminal domain (NTD) containing the activation function AF-1. Exons 2 and 3 are responsible for the DNA-binding domain (DBD). Exon 4 encodes the hinge region, functioning as a nuclear localization signal, and along with exons 5 through 8, forms the ligand-binding domain (LBD), which contains the activation function AF-2. AF-1 houses two primary transactivation units: TAU-1 and TAU-5. [83]	22

1.6	Mechanisms of androgen action and AR signalling in prostate cells. [86]	23
3.1	Study profile. Design and workflow of the PREMIERE trial, highlighting the three predefined time points for blood sample collection: pre-treatment, after 12 weeks (12W) of enzalutamide therapy, and at disease progression. The IRST trial is presented as an independent validation cohort, ensuring the robustness of the findings.	52
4.1	Consort diagram. This study analyses pre-treatment whole blood samples from mCRPC patients prospectively treated with enzalutamide, including PREMIERE cohort comprised of 98 patients from a phase 2 biomarkers clinical trial, and an independent validation cohort (IRST) including 54 patients	62
4.2	Blood immune-cell composition. The figure shows the relative proportion of immune cell components in the blood in the PREMIERE set.	64
4.3	Kaplan–Meier survival curves for monocytes and CD8+ T cells in PREMIERE and IRST cohorts. (A) OS based on monocyte level in the PREMIRE cohort. (B) OS based on CD8 T-cell level in the PREMIRE cohort. (C) OS based on monocyte level in the IRST cohort. (D) OS based on CD8 T-cell level in the IRST cohort.	67
5.1	Curves comparing our 22-Gene signature with existing models. (A) PREMIERE cohort (B) IRST cohort	78
6.1	Principal Component Analysis (PCA) of whole-blood transcriptomes reveals distinct temporal patterns in response to enzalutamide treatment in mCRPC patients. (A) PCA plot comparing pre-treatment (green triangles) and 12-week treatment (blue triangles) samples. (B) PCA plot of pre-treatment (green triangles) versus progression (red circles) samples. (C) PCA plot comparing 12-week treatment (blue triangles) and progression (red circles) samples.	86
6.2	Unsupervised hierarchical clustering of whole-blood transcriptomes reveals distinct temporal patterns in mCRPC patients treated with enzalutamide. (A) Clustering of pre-treatment (green) versus 12-week (blue). (B) Pre-treatment (green) versus progression (red). (C) Clustering of 12-week (blue) versus progression (red).	88

6.3	Venn diagram showing the overlap of DEGs across different treatment time point comparisons in mCRPC patients treated with enzalutamide.	90
6.4	Gene Set Enrichment Analysis (GSEA) of differentially expressed genes in mCRPC patients treated with enzalutamide. (A) GSEA results comparing progression samples to pre-treatment samples. (B) GSEA results comparing 12-week treatment samples to pre-treatment samples. (C) GSEA results comparing progression samples to 12-week treatment samples. . .	93
6.5	Boxplots comparing the relative proportions of 22 immune cell subsets in peripheral blood across key treatment time points in mCRPC patients. (A) Progression vs. Pre-treatment, (B) 12-week vs. Pre-treatment, and (C) Progression vs. 12-week. Statistically significant changes are highlighted ($*p < 0.01$). Persistent reductions in CD8+ T cells and increases in monocytes were observed across comparisons.	96
6.6	Validation cohort: Boxplots comparing the proportions of CD8+ T cells and monocytes between progression and pre-treatment samples. Results confirm the significant reduction in CD8+ T cells and increase in monocytes at progression, consistent with findings from the discovery cohort ($*p < 0.01$).	97
6.7	Enzalutamide reduces cell viability in Jurkat T cells. (A) Dose-dependent reduction in viability after 72 hours. (B) Representative dose-response curve relative to untreated controls.	98
6.8	Western blot analysis of AR expression in various cell lines. Jurkat T cells do not express AR, while LNCaP and 22Rv1 prostate cancer cells are AR-positive. DU145 prostate cancer cells and Jurkat cells cultured in charcoal-stripped FBS (CS-FBS) are AR-negative controls. GAPDH is used as a loading control.	98
6.9	Enzalutamide treatment with Jurkat cells. (A) Western blot analysis showing cleavage of Caspase-3 after 24-hour treatment with enzalutamide (35.7 μ M), indicating activation of apoptosis. (B) Western blot analysis showing cleavage of PARP under the same conditions, further confirming apoptotic activity.	99

6.10	Effects of enzalutamide on viability across different immune cell lines. (A) Cell viability analysis of Jurkat (T cells), Raji (B cells), MOLT-4 (T cells), and THP-1 (monocytes) treated with 25 μ M enzalutamide for 24, 48, and 72 hours. The graph demonstrates a concentration- and time-dependent reduction in cell viability, with Jurkat cells showing the most pronounced sensitivity. (B) Western blot analysis confirming the absence of AR expression in MOLT-4, THP-1, and Raji cells, suggesting the observed cytotoxic effects are independent of AR signaling.	100
6.11	Comparison of antiandrogens on Jurkat T-cell viability. Cells were treated with clinically relevant plasma concentrations of bicalutamide (20 μ M), enzalutamide (25 μ M), darolutamide (25 μ M), apalutamide (10 μ M), and abiraterone acetate (5 μ M) for 48 hours. Cell viability was assessed by MTT assay. Data represent mean \pm SD of three independent experiments. ** p < 0.01 compared to control.	101
6.12	Enrichment and pathway analysis of gene expression changes induced by enzalutamide in Jurkat T cells. (A) GSEA enrichment plot in enzalutamide-treated Jurkat T cells. (B) KEGG pathway map in enzalutamide-treated cells.	103

LIST OF TABLES

1.1	TNM 2017 classification for PCa	17
1.2	Interpretation of Gleason Scores	17
1.3	Gleason Score and ISUP grade	18
1.4	Stages of PCa	18
1.5	D’Amico classification system for PCa risk assessment	19
1.6	Comparison of active surveillance versus watchful waiting	26
3.1	Definitions for clinical endpoints	50
4.1	Patients’ characteristics. Characteristics of patients included in the PREMIERE clinical trial	63
4.2	Univariate Cox regression analyses of immune cell subsets and OS in the PREMIERE cohort	65
4.3	Univariate Cox regression analyses of immune cell subsets and OS in the validation cohort	68
4.4	Multivariate Cox regression analysis including clinical variables	69
4.5	Multivariate Cox regression analysis including molecular variables	69
5.1	Comparison of regularized regression models	75
5.2	Lasso regression model coefficients (Gene names censored due to patenting process)	76
5.3	Time-Dependent AUC values for our 22-gene signature	77
6.1	Summary of DEGs across treatment time points	87
6.2	Summary of top enriched biological pathways identified by GSEA across comparisons	91

ABBREVIATIONS

ADT	Androgen Deprivation Therapy
ALP	Alkaline Phosphatase
ALT	Alanine Aminotransferase
AR	Androgen Receptor
AR-V7	Androgen Receptor Splice Variant 7
ARG1	Arginase 1
ARPIs	Androgen Receptor Pathway Inhibitors
ARs	Androgen Receptors
AST	Aspartate Aminotransferase
AUC	Area Under the Curve
BPI	Brief Pain Inventory
C-index	Concordance Index
CAB	Combined Androgen Blockade
CEL	Data File Format from Affymetrix GeneChip
cfDNA	Cell-Free DNA
cfRNA	Cell-Free RNA
CI	Confidence Interval
CIBERSORT	Cell-Type Identification By Estimating Relative Subsets of RNA Transcripts
COX	Cox Proportional Hazards
CRPC	Castration-Resistant Prostate Cancer
CT	Computed Tomography
CTC	Circulating Tumor Cell
CTLA-4	Cytotoxic T-Lymphocyte-Associated Antigen 4
CXCR2	C-X-C Motif Chemokine Receptor 2
DEG	Differentially Expressed Gene

DGE	Differential Gene Expression
DHT	Dihydrotestosterone
DRE	Digital Rectal Examination
EBRT	External Beam Radiation Therapy
ECOG	Eastern Cooperative Oncology Group
EM	Epithelial-Mesenchymal (transition)
FDR	False Discovery Rate
FSH	Follicle-Stimulating Hormone
GnRH	Gonadotropin-Releasing Hormone
GO	Gene Ontology
GSEA	Gene Set Enrichment Analysis
HIFU	High-Intensity Focused Ultrasound
HR	Hazard Ratio
HSP	Heat Shock Protein
HTA	Human Transcriptome Array
ICI	Immune Checkpoint Inhibitor
IGF	Insulin-Like Growth Factor
iNOS	Inducible Nitric Oxide Synthase
IRB	Independent Review Board
IRST	Istituto Scientifico Romagnolo per lo Studio e la Cura dei Tumori
ISUP	International Society of Urological Pathology
KEGG	Kyoto Encyclopedia of Genes and Genomes
LASSO	Least Absolute Shrinkage and Selection Operator
LBD	Ligand Binding Domain
LDH	Lactate Dehydrogenase
LH	Luteinizing Hormone
LM22	Leukocyte Gene Signature Matrix
Log₂FC	Logarithmic Fold Change
mCRPC	Metastatic Castration-Resistant Prostate Cancer
MDSC	Myeloid-Derived Suppressor Cell

mHSPC	Metastatic Hormone-Sensitive Prostate Cancer
MMR	Mismatch Repair
Mo-MDSC	Monocytic Myeloid-Derived Suppressor Cell
MRI	Magnetic Resonance Imaging
NK	Natural Killer
NLR	Neutrophil-to-Lymphocyte Ratio
nmCRPC	Non-Metastatic Castration-Resistant Prostate Cancer
NSAA	Non-Steroidal Anti-Androgens
NTD	N-terminal Transactivation Domain
OR	Odds Ratio
OS	Overall Survival
PARP	Poly(ADP-Ribose) Polymerase
PCA	Principal Component Analysis
PCa	Prostate Cancer
PET/CT	Positron Emission Tomography/Computed Tomography
PREMIERE	Name of a Clinical Trial (treated as acronym)
PSA	Prostate-Specific Antigen
PSA PFS	Prostate-Specific Antigen Progression-Free Survival
PSMA	Prostate-Specific Membrane Antigen
qRT-PCR	Quantitative Reverse Transcription Polymerase Chain Reaction
RARP	Robot-Assisted Radical Prostatectomy
RMA	Robust Multi-array Average
RNA	Ribonucleic Acid
ROC	Receiver Operating Characteristic
RP	Radical Prostatectomy
RSF	Random Survival Forests
s-PSA	Serum Prostate-Specific Antigen
SDS-PAGE	Sodium Dodecyl Sulfate Polyacrylamide Gel Electrophoresis
ssDNA	Single-Strand DNA
SVR	Support Vector Regression
TAA	Tumor-Associated Antigen

TAC	Transcriptome Analysis Console
TdT	Terminal Deoxynucleotidyl Transferase
TME	Tumor Microenvironment
TNM	Tumor-Node-Metastasis Classification
Treg	Regulatory T cell
TRUS	Transrectal Ultrasound
TURP	Transurethral Resection of the Prostate
UDG	Uracil-DNA Glycosylase

THESIS STRUCTURE

The whole thesis is structured as eight well-differentiated chapters:

The first chapter, Chapter 1, is the introductory chapter that motivates the need for the study. It outlined and explained some concepts that could be useful for the reader to reach an adequate understanding of all the topics covered in this research project. It established the objectives that will serve as the basis for the entire work.

Chapter 2 presents the hypotheses and objectives, which sets the basis for the experimental and analytical work developed in the following chapters.

Chapter 3 presents the material and methods used in this work and includes the design of research, data collection techniques, and experimental techniques such as microarray analyses, immune cell profiling, and in vitro assays. It also includes the statistical methods applied.

Chapter 4 initiates the results section by exploring the prognostic significance of the immune cell profile in the bloodstream of individuals with metastatic castration-resistant prostate cancer. This chapter also includes the validation of findings in independent cohorts.

Chapter 5 describes the development and provides the validation of a 22-gene prognostic signature, which has shown great potency in predicting survival among mCRPC patients, and elaborates on the mechanism behind it.

Chapter 6 presents clinical and in vitro analyses that show changes in gene expression and immune cell composition associated with enzalutamide treatment.

Chapter 7 summarizes the main research findings, their clinical relevance, the limitations, and implications of the work to suggest possible directions for future studies.

The conclusions of the thesis in English are summarized in Chapter 8. And

Chapter 9 presents the conclusions of the thesis in Spanish. These chapters have underlined the main contributions made by the research and wrapped up its relevance. It enumerates the scientific output produced and collaborative projects that have been derived from there.

The final section is dedicated to the bibliography, compiling all references cited throughout the thesis.

In Chapter 9, the primary contributions of the thesis are detailed, including the scientific articles published during the research period, the development of a patent derived from the findings of this work, and the presentations delivered at international and national congresses. The patent represents a key innovation resulting from this research, highlighting its practical applications and potential for broader impact within the field.

Chapter 10 compiles all references cited throughout the thesis, providing the theoretical and methodological foundation that supports the research.

Chapter 11 acknowledges all contributors to the research, detailing their roles, and highlighting collaborative efforts that were instrumental in achieving the research outcomes.

Finally, Chapter 12 is dedicated to annexes, which include supplementary materials.

INTRODUCTION

1.1 Concept of Cancer

The term "cancer" includes a diversity of diseases that, despite their variability in origin and manifestations, share a fundamental characteristic: the abnormal and excessive growth of neoplastic cells. These cells, with an invasive and destructive capacity, can spread from their origin to other parts of the body via the circulatory and lymphatic systems, a phenomenon known as metastasis. This process highlights the aggressive and systemic characteristics of the disease, which presents in various clinical forms and prognoses, yet is linked by its genetic basis and its capacity to avoid typical cellular regulatory mechanisms.

1.2 Oncogenesis

Cancer develops from a gradual accumulation of dynamic modifications in the genome. Neoplastic cells are able to gain distinct features from normal cells due to these modifications, which also release them from the homeostatic systems that govern regular, controlled cell multiplication [1, 2].

In 2000, Hanahan and Weinberg proposed a model based on six key characteristics of altered cell physiology that are required for tumour transformation [3]. All cell types share similar changes, each serving as a means of escape for cancer defence mechanisms. Then, in 2011, they added four more attributes to this model, emphasizing the importance of the tumour microenvironment and the complexity of tumour biology [4]. Emerging

hallmarks and facilitating characteristics have recently been introduced [5], including the activation of phenotypic plasticity, non-mutational epigenetic alterations, diverse microbiomes, and the influence of senescent cells. The fourteen fundamental characteristics have been outlined below, highlighting each critical aspect of the transition from a cell's typical physiological state to the cancerous state (Figure 1.1)

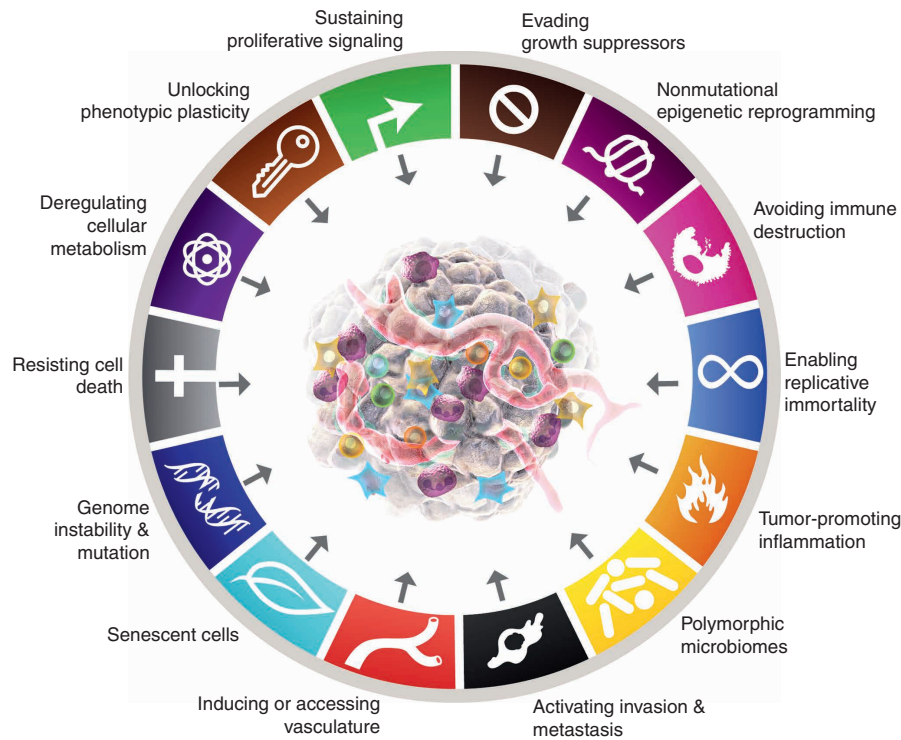


Figure 1.1: Hallmarks of Cancer. This image represents the capabilities of cancer cells proposed by Hanahan and Weinberg [5]

1. **Sustaining Proliferative Signalling:** In their normal state, cells need to wait for an external signal that will give them permission to start multiplying; one emancipation of cancer cells is from this prerequisite. The mechanism is the acquisition of a self-stimulating growth ability that could be achieved by the synthesis of the mitogenic signals themselves or interfacing with some mitogenic signalling machineries that would allow growth receptors to remain active even without the stimulatory ligands. This autonomy involves proliferative signalling that may not be dependent on any extracellular context.
2. **Evasion of Growth Suppressors:** While healthy tissues have a number of anti-proliferative signals to balance the proliferation and survival together, cancer cells would again develop a different capacity to overcome these constraints. A prominent example is the disruption of

the RB1 (retinoblastoma protein) pathway, which controls cell cycle progression. Mutations in genes such as RB1 deactivate these inhibitory pathways and promote uncontrolled proliferation.

3. **Nonmutational Epigenetic Reprogramming:** Alteration of the tumourigenic phenotype of tumour cells, which is purely epigenetically regulated and independent of genome instability and mutation, is associated with the acquisition of distinctive capabilities during both tumour development and progression.
4. **Avoiding immune destruction:** Tumour cells develop multiple strategies that enable evasion from recognition, surveillance, and destruction by the immune system. These include modulation of antigen presentation, secretion of immunosuppressive factors, and recruitment of immune regulatory cells, enabling protracted unsuspected proliferation counteracted by the immune system.
5. **Enabling Replication Capacity:** Normal cells are subject to a Hayflick division limit, at which point they undergo senescence. Activation of telomerase, or alternative telomere and chromosome end maintenance mechanisms that allow unlimited replication, allows cancer cells to bypass senescence.
6. **Induction of an Inflammatory Environment:** In tissue, tumour cells induce a general or chronic inflammatory microenvironment that, far from combating tumour growth and survival, is a substantial element in neoplastic progression. Chronic inflammation not only provides growth and survival factors, but also contributes to genomic instability and tissue remodelling.
7. **Polymorphic microbiomes:** Microbiome diversity, which encompasses microbial species and communities that may protect or promote tumour formation and cancer progression, plays an important role in tumorigenesis, the malignancy process itself and the response to treatments.
8. **Tissue Invasion and Metastasis:** Extending beyond their local growth, cancer cells turn on invasion capabilities to grow into neighbouring tissues and have the capacity to seed cancer elsewhere in the body (metastasize). This process involved restructuring of cell-cell and cell-matrix interactions, as well as activation of enzymes that degrade extracellular components that facilitate infiltration and movement of

cells.

9. **Induction of angiogenesis:** Tumour cells, in order to maintain this rapid growth, induce the formation of new blood vessels, in a process known as angiogenesis. They tip the balance in favour of intravenous irrigation of the new tissue for continuous supply of oxygen and nutrients by secreting proangiogenic factors.
10. **Senescent Cells in the Tumour Microenvironment:** Functionally, senescent cells of various origins that populate the tumour microenvironment contribute to tumorigenesis and malignant progression, through complex interaction networks which pose challenges.
11. **Mutations and genomic instability:** Tumour cells exhibit a high rate of mutations and genomic changes that provide the basis for heterogeneity and adaptability in their environment. Although this instability is decisive for the malignant properties, at the same time, it presents a picture of clear target potential in a targeted therapy scenario.
12. **Resistance to programmed cell death (apoptosis):** Apoptosis functions as a protective mechanism that eliminates damaged or unneeded cells. However, tumour cells develop ways to evade death, in particular by switching off genes involved in activating apoptosis. This blocking of the cellular 'escape pathway' allows tumour cells to accumulate and proliferate.
13. **Metabolic reprogramming:** Metabolic reprogramming induces tumour cells to afford high proliferation rates and facilitates their survival under adverse conditions. A classic example is the Warburg effect, in which cancer cells switch from a conventional respiratory mechanism, involving mitochondrial respiration, to aerobic glycolysis even in the presence of oxygen, thus optimally synthesising precursor biomolecules and ATP.
14. **Unlocking Phenotypic Plasticity:** Cancer cells evade or escape terminal differentiation, adopting phenotypic plasticity that facilitates tumour pathogenesis through dedifferentiation, blocked differentiation and transdifferentiation.

This collection of features not only emphasizes the complexity and cunning of tumour cells on their path to malignancy, but also the multiple means of

therapeutic interference that could be harnessed in each of these hedging mechanisms to achieve resolution around oncogenesis.

1.3 The Prostate

The prostate is a glandular organ with the size and shape of a walnut that is attached to the bladder and lies beneath it. The initial segment of the urethra passes through it. The terminal section of the vas deferens, or ejaculatory duct, enters the prostate from above and behind. The primary role of the prostate is to provide vital secretions to semen, which help to create ejaculates and sustain sperm viability [6].

1.3.1 Anatomy of the prostate

Structurally, the prostate is divided into mainly five different morphological zones, as can be seen in [Figure 1.2A](#). The 25% of the glandular tissue is concentrated in a central zone (A) at the base of the prostate. This zone is formed by the periurethral submucosal glands. It is the most resistant to carcinoma and inflammation. There is the anterior fibromuscular tissue (B), which is largely devoid of glands and is located in front of the urethra. A transitional region (C) that houses 5% of glandular tissue. This zone is formed by the periurethral mucous glands. Benign prostatic hyperplasia develops in this zone. A peripheral zone (D) that constitutes the posterior, lateral, and apical portions of the glandular tissue and represents 70% of the glandular tissue. Nearly 80% of prostate tumours in older men develop in this region, making it the most frequent location of origin for neoplasms [7–9], as well as being the area examined during the digital rectal examination (DRE). The region of the periurethral gland (E) is a narrow area with short ducts adjacent to the prostatic urethra, which surrounds the urethra and is responsible for producing mucus-like secretions that help protect and lubricate the urethra [6, 10–12].

The normal gland is made up of ducts and acini that are embedded in a supportive tissue called stroma. These ducts and acini are lined with a single layer of simple columnar epithelium, which is surrounded by a layer of basal epithelium. The basal epithelium produces the basement membrane, an extracellular matrix anchored to stromal cells. These stromal cells are mainly

smooth muscle myocytes that help with spontaneous contractility and prevent fluid from stagnating [13] **Figure 1.2B**. Within the stroma, fibroblasts predominantly provide support to the ducts in the adult prostate. Paracrine signalling from fibroblasts is thought to play a crucial role in ductal patterning during prostate development. The stromal microenvironment is essential in both prostate development and cancer [14, 15].

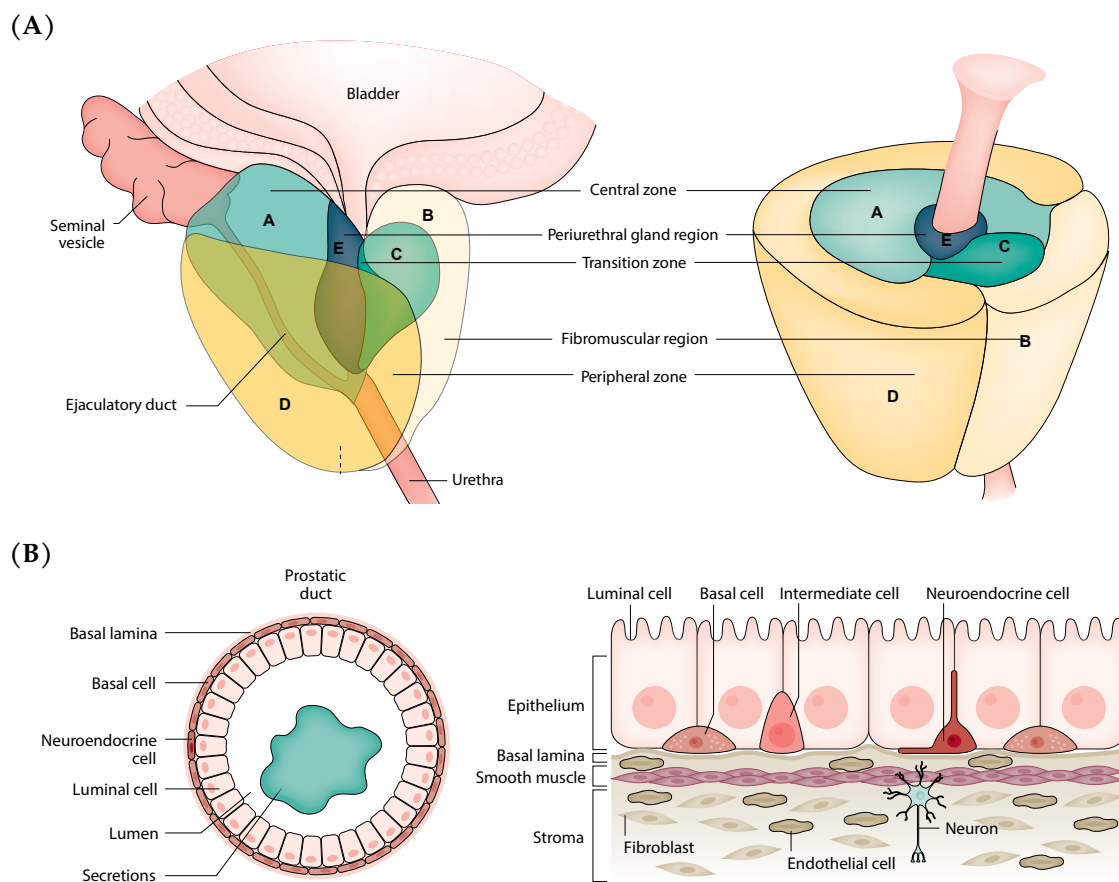


Figure 1.2: Two diagrams illustrating the anatomy of the prostate gland. (a) Highlights the central zone (A), anterior fibromuscular stroma (B), transitional zone (C), peripheral zone (D), and periurethral gland region (E), with their respective structural and functional roles. **(b)** Provides a detailed view of the ducts and acini embedded in the stromal framework, consisting of smooth muscle cells and fibroblasts, which are critical for prostate development and function. [16]

1.4 Prostate Cancer (PCa)

1.4.1 Epidemiology: incidence and mortality

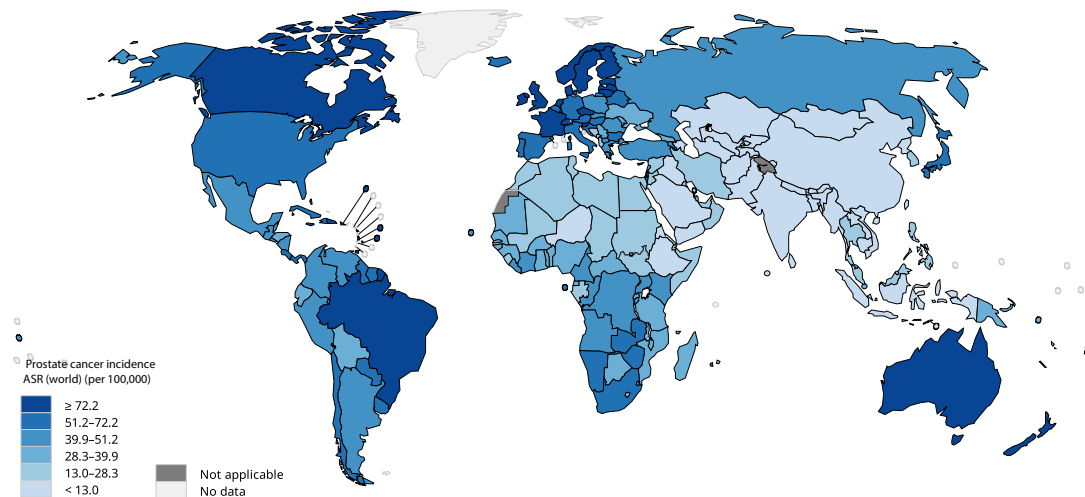
PCa is the second most frequently diagnosed cancer after lung cancer and constitutes 7% of all new cancer cases in men worldwide, this figure rising to 15% in developed areas. According to the last statistics, PCa is the most common cancer in men and the second leading cause of death in them, with an estimated 1,414,000 new cancer cases and 375,304 deaths in 2020 [17] **Figure 1.3A**. More specifically in Spain, predictions of the number of PCa cases (PCa) for 2023 reached 29.002 new cases, thus taking the first place classification as a pathology afflicting male cancer more than colorectal or lung and bladder cancer [18].

The risk of developing PCa is closely associated with age, with more than 85% of new diagnoses occurring in individuals over 60 years of age [19, 20]. As a result, regions with higher life expectancies experience a higher incidence of this disease. Globally, PCa rates are positively correlated with the Human Development Index (HDI) and the gross domestic product (GDP), which means that developed countries generally have higher incidences than developing countries [20].

The rise in PCa incidence rates may be partly attributed to increased awareness and access to diagnostic screening. More frequent screening often leads to higher incidence rates due to overdiagnosis. These regions also have the highest age-standardized rates of PCa-related deaths.

The incidence rates for prostate cancer have been particularly influenced by blood prostate-specific antigen (PSA) screening tests. The incidence often shows great variation between countries and is usually affected by the degree to which PSA screening has been implemented. Countries in the developed world, in which screening programmes and, consequently, prostatic biopsies are common, tend to report higher incidence rates for PCa. However, the usefulness of PSA screening in general population-based programmes remains a very controversial issue. While it does identify early-stage PCa, it often detects rather indolent tumours, which will not benefit from intervention, thereby exposing individuals to treatments they do not need. In addition, it is poorly specific for distinguishing those with the indolent rather than more aggressive and dangerous forms.

(A)



(B)

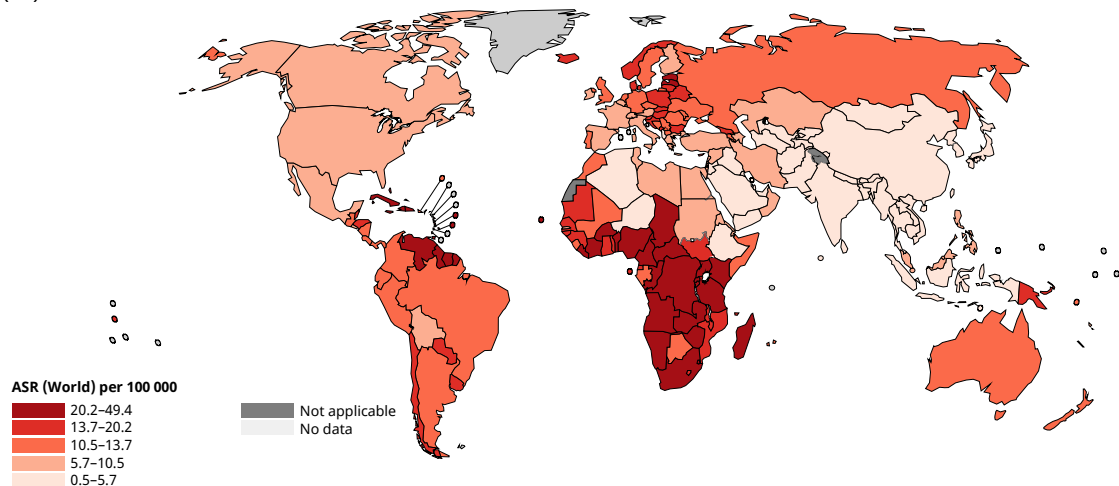


Figure 1.3: Global geographical incidence and mortality of PCa. (A) Global incidence of PCa in 2022. (B) Global mortality from PCa in 2022.

Global cancer observatory: cancer Today; 2022. Available from: <https://gco.iarc.fr/today/en/dataviz>

Despite these challenges, evidence would suggest that PSA screening conveys an absolute benefit, albeit modest, regarding reduction in PCa related mortality and the risk of metastatic disease. This benefit is likely to be enhanced by concurrent advances in treatment. Indeed, during the past decade, improvements in diagnosis and therapy have led to a decline in PCa mortality, especially in regions where early detection programmes are widely practised.

Global variations in PCa mortality rates, as shown in **Figure 1.3B**, highlight the influence of diverse factors such as genetic susceptibility, environmental exposures, dietary habits, healthcare access, and the quality of available

treatment.

In Spain, the incidence of prostate cancer in Spain was 30,316 new cases in 2024 [18], ranking first in terms of new cases in men, as in the rest of Europe. It was followed by lung cancer and colorectal cancer. The main reason for this significant increase in incidence, as in other developed countries, is due to the introduction and widespread use of the PSA test, which has even led to the undesirable effect of overdiagnosis [21]. The ease of PSA determination from a blood sample has contributed to the widespread use of this test in primary and specialized care consultations.

In term of mortality in Spain due to prostate cancer, in 2024 it was the leading cause of death, accounting for 26.6% of all deaths. Specifically, deaths from PCa accounted for 5.9% of all cancer deaths, making it the third leading cause of male mortality after lung and colon cancer [22].

1.4.2 Risk factors

PCa is a multifactorial disease influenced by a combination of genetic, environmental, and lifestyle-related factors. Numerous studies have identified a variety of factors that contribute to the risk of developing PCa [23].

Age

PCa predominantly affects older people, with relatively infrequent diagnoses in people younger than 50 years of age [24, 25]. Beyond this age range, the incidence of PCa increases exponentially, exceeding the growth rates of other tumour types. According to this pattern, PCa usually has a moderate growth rate and a prolonged preclinical phase. Consequently, symptoms and clinical diagnoses manifest themselves primarily in older men, if they appear at all. In many cases, men with PCa die of unrelated causes long before the disease presents noticeable symptoms or manifests itself clinically.

Ethnicity

People of African and Asian ancestry typically show less sensitivity to the disease [26]. In contrast to other racial and ethnic groups, African-American, Caribbean and black men living in Europe, for example, have the highest prevalence of PCa

and tend to develop the disease earlier in life [26, 27]. These people have genetic similarities that increase their risk of developing cancer, including certain genes (such as chromosome 8q24) that are more likely to experience mutations [26–28].

Ethnic group prevalence can be associated with the history of European colonization and the extent of genetic intermingling. According to some research [26], the genetic makeup of northern Europeans includes a heritable propensity for PCa. Two common polymorphisms on chromosome 8q24, which are transmitted by genetic mixing, are present in a subset of patients of European, European American, and African American origins [29–31].

The uncommon presence of these alleles in indigenous African populations and other ethnicities implies genetic mixing between Europeans and African-Americans as a transmission vector. Historical records indicate that European colonization, particularly by Scandinavian explorers, occurred in the Caribbean. Concurrently, the transatlantic slave trade introduced a substantial African population to the region. Consequently, the prevalence of PCa is now notably high in numerous Caribbean nations.

Family history and genetic factors

Genetic elements are a well-established risk determinant for PCa. The probability of developing PCa for an individual is known to increase when a close relative is affected by the same, the risk amplifying if the relative is diagnosed at an early age. This correlation was clearly demonstrated in a 2003 meta-analysis comprising 33 distinct studies, which concluded that the risk was particularly high when a sibling, rather than a father, was diagnosed, and increased further with multiple affected family members. Interestingly, the risk only slightly increased for second-degree relatives [32].

Remarkably, a mere 9% of PCa patients are classified as familial cases, defined as having three or more affected family members or two family members diagnosed before the age of 55 [33]. Not only has the relationship among family members been recognized, but certain genetic variations have also been identified as more common among PCa patients. An estimated 10% of PCa metastatic patients are found to possess mutations in DNA repair genes, a relationship established in a study involving 692 metastatic PCa patients without familial history. The proportion of DNA repair gene mutations was significantly lower in patients with localized PCa, comprising only 4.6% compared to more aggressive variants [34]. BRCA2, a DNA repair gene, is the

most frequently mutated in these patients. Current trials are investigating PCa screening with BRCA mutations [35]. Such trials could signal a future where early diagnosis is possible for families carrying related mutations, potentially reducing the incidence of metastatic PCa.

Obesity

Research indicates that obesity is linked to a higher likelihood of mortality and recurrence in prostate cancer (PCa) patients, as well as an unfavorable prognosis. Multiple studies have demonstrated that obesity correlates with an elevated risk of disease recurrence, exacerbation of treatment-related side effects, emergence of obesity-associated comorbid conditions, premature disease progression, development of metastatic cancer, and heightened all-cause and PCa-specific mortality rates. [36–38]. However, the physiological mechanisms associated with obesity and poor CaP outcomes remain unknown. Obesity is associated with the disruption of several hormonal pathways in the body. This alteration may lead to increased levels of insulin and insulin-like growth factor (IGF), as well as increased oxidative stress and inflammatory cytokines. Conversely, research indicates that in individuals with obesity, there is a reduction in adiponectin, testosterone, and sex hormone-binding globulin concentrations. Such variations in hormone levels and associated cellular mechanisms can exert a notable influence on general health. [39–41]

Dietary and Nutritional Factors

Dietary factors have been associated with the risk of prostate cancer (PCa). A diet rich in inflammatory components, such as processed and red meats, sweetened beverages, and trans fats, is correlated with a greater likelihood of developing PCa [42]. In turn, adherence to plant-based diets, those rich in phytoestrogens including, for example, soy, and legumes, and also the elements that constitute the Mediterranean diet appear to show a limited protective role. [43, 44].

Lifestyle factors

Physical activity has been shown to play a preventive role, while the higher the intensity or frequency, the lower the PCa-specific mortality. Sedentary or passive lifestyles, along with poor exercise, contribute to increased risk [45]. Smoking is

not directly attributed in most of the literature to the overall risk of PCa [46], but has been used in conjunction with higher subtype grades and higher mortality among smokers [47].

Environmental and occupational exposures

Occupational exposure to pesticides, petroleum products, and other industrial chemicals was associated with an increased risk of PCa in a number of occupations [48, 49].

Medical and health conditions

Chronic inflammatory diseases, such as prostatitis and autoimmune diseases such as Sjogren syndrome, may increase the risk of PCa [50]. Type 2 diabetes is associated with an increased risk of more aggressive disease types [51, 52]. Infectious agents such as human papillomavirus were associated with an increased risk of developing PCa [53].

1.4.3 Clinical features and diagnosis

Most men with early-stage PCa do not experience symptoms; however, clinical features can also be present in the early stages, though they are more common in advanced disease. In advanced stages, patients might encounter urinary issues including burning sensations or pain while urinating, trouble starting or stopping urination, and a higher frequency of urination during the night. Additionally, they may experience incontinence and reduced flow rate or velocity of the urine stream. The presence of blood in urine, known as haematuria, and in semen can also occur, often along with erectile dysfunction or painful ejaculation.

As the illness extends past the prostate, further symptoms might manifest, such as leg or pelvic area swelling, hip, leg, or foot numbness or discomfort, and bone pain. In case of recurrence of prostate cancer, haematuria or blood in the urine, difficulty urinating, lower back pain, fatigue, dyspnoea or shortness of breath and jaundice may occur; these symptoms, if present, usually require further examination.

Because early stage PCa is asymptomatic, the detection of this disease is heavily based on routine diagnostic and screening tools. The suspicion of PCa usually arises either from elevated PSA levels or abnormalities detected by Digital Rectal Examination (DRE). The absence of early symptoms underscores how diagnostic interventions are so crucial in the early identification of the disease before it progresses to a symptomatic stage.

There are several methods available to achieve this, each contributing to a comprehensive diagnostic approach.

Digital Rectal Examination

The DRE is still useful today because about 70-80% of PCas originate in the peripheral zone of the prostate. According to a recent comprehensive analysis, DRE has a sensitivity of 28.6% and a specificity of 90.7% for the detection of PC in individuals presenting symptoms [54]. These statistics suggest that many cases of PCa are not detected through DRE alone, as its low sensitivity means that it can miss a significant number of cancers, especially in asymptomatic individuals. Despite these limitations, the high specificity of DRE makes it a useful initial screening tool to identify prostate abnormalities that warrant further investigation.

Prostate-Specific Antigen (PSA)

PSA is an enzyme that originates from cells of the prostate glandular epithelium and plays a vital role in the process of dissolution of semen clots [55]. Primarily produced in prostate epithelial cells, PSA is released into the prostatic ducts, with only a negligible amount making its way into the bloodstream [56]. The penetration of PSA into the bloodstream is constrained by the histological integrity of the prostate gland, which is made up of basal cells. Certain pathological conditions such as PCa and prostatitis can cause a breach of this barrier, particularly affecting the basement membrane of epithelial cells. This disintegration can lead to an increase in the concentration of PSA in the bloodstream, a situation that is often observed in tumours. This results in elevated serum PSA levels (s-PSA) in individuals diagnosed with PCa compared to those who do not, despite the fact that cancer cells generally produce less PSA than normal epithelial cells [55, 57, 58].

The efficacy of this test in identifying PCa and tracking its progress is quite low

[59]. This is attributed to its restricted sensitivity, which stands at 20.5%, precision that ranges from 62 to 75%, and specificity between 51 and 91% [59]. Factors such as diagnostic or therapeutic interventions, intensive DRE, prostatitis, ejaculation, prostatic infarction, and benign prostatic hyperplasia can also contribute to elevated PSA levels. PSA value greater than or equal to 4.0 ng/ml is the consensus standard for further PCa evaluation. However, there is no universally accepted cutoff value, and repeated evaluation after a few weeks under standardized conditions for the individual is recommended to avoid unnecessary biopsies.

Biopsy

The most common technique for detecting PCa is a needle biopsy. Most often, a transrectal ultrasound guided biopsy is performed. The sampling locations in the peripheral gland should be bilateral from the apex to the base, as far back as practicable, and laterally. The cores should be collected from additional suspect locations. In prostates of at least 30 cm in size, at least eight biopsy samples are recommended [60], while ten to twelve samples are recommended for larger prostates [61, 62].

Generally, a prostate biopsy is performed based on clinical findings integrated with the results of diagnostic tests. One of the main indications for biopsy includes increased PSA levels. Abnormal DRE findings such as palpable nodules or asymmetry raise suspicion of PCa and can also indicate a biopsy even if PSA levels are within normal limits. Imaging techniques, especially mpMRI, also play an important role in the detection of suspicious lesions and the assistance in targeted biopsies. Other factors are considered during this decision-making process, including patient age, overall health, comorbidities, and the potential therapeutic implications of PCa diagnosis. Shared decision-making between the physician and the patient is essential, weighing the risks of biopsy, such as infection or bleeding, against the benefits of early detection and treatment.

In cases where a transrectal biopsy is contraindicated or where additional tissue sampling is needed, transurethral resection of the prostate (TURP) may be performed. This urological intervention, usually performed to relieve urinary obstruction, may provide tissue for histopathological examination and incidentally lead to the diagnosis of PCa. [63].

Magnetic Resonance Imaging (MRI)

In the process of diagnosing PCa, MRI has grown in significance [64]. Its features include tumour detection, risk classification, staging, and improved biopsy sampling under MRI guidance. In the past ten years, multiparametric MRI has become more effective in detecting clinically significant tumours [65]. A radiologist evaluates the images to report the degree of suspicion of PCa. Furthermore, employing magnetic resonance biopsies makes it easier to find and sample worrisome prostate regions.

Liquid biopsies

Liquid biopsies represent an advanced diagnostic technique that involves obtaining a blood sample and analyzing it for indicators of cancer cells, DNA, or RNA. Circulating Tumor Cells (CTCs) [66] are cancer cells that have detached from the primary tumor and entered the bloodstream. Additionally, cell-free DNA (cfDNA) and Cell-Free RNA (cfRNA) are genetic materials released by cancer cells into the circulatory system [67].

These three entities - CTCs, cfDNA, and cfRNA - offer promising avenues for diagnosing PCa. Among them, CTCs are particularly significant due to their increased sensitivity as markers for PCa. This means that a positive CTC test result can strongly suggest the presence of PCa, even when PSA levels appear normal, adding another layer of detection beyond traditional methods [68].

Although liquid biopsies represent an exciting innovation in the field of cancer diagnostics, it is important to recognise that this is a relatively new technology. As such, further research is paramount to define their optimal utility in the diagnosis, management, and potential early detection of PCa. Nevertheless, the potential of liquid biopsies as a valuable diagnostic tool is undeniable, especially in high-risk individuals, where it may revolutionize the early detection and treatment of PCa.

Positron Emission Tomography/Computed Axial Tomography (PET/CAT)

PET/CT (Positron Emission Tomography/Computed Tomography) is a powerful imaging technique that combines two methods to provide detailed images of the body's internal structures. PET uses a radioactive tracer to highlight areas of the body where cells are more active (such as cancer cells),

while CT provides detailed cross-sectional images of the body. The combination of these two methods can provide a more accurate diagnosis [69].

1.4.4 Tumour classification

Systems for determining the stage and risk of a prostate tumour vary depending on the method used, but are essential as therapy is based on the clinical stage of the tumour. A patient with PCa is usually classified according to the extent of the tumour, the clinical or pathological stage of the patient, the Gleason grade or histological grade, and the PSA level.

Tumour Node Metastasis (TNM) classification

Tumour-Node-Metastasis (TNM) classification is a universally recognized system used to stage cancer, including PCa [70]. This system is based on the evaluation of the extension of the tumour, the number of lymph nodes affected and the presence or absence of distant metastases, according to the classification of The Union for International Cancer Control (UICC) (Table 1.1).

- **Tumour (T):** The 'T' in the TNM classification refers to the size and extent of the main tumour. In the context of PCa, it specifically assesses how much of the prostate is affected by the cancer and whether it has grown to nearby tissues. The categories range from T1 (cancer is not detectable through a physical exam or imaging tests but may be found in a biopsy for other reasons), T2 (cancer is confined to the prostate without evidence of extra-glandular extension), T3 (cancer extends beyond the prostate capsule), to T4 (cancer has invaded tissues adjacent to the prostate).
- **Node (N):** 'N' represents lymph nodes, indicating the degree to which cancer has metastasized to adjacent lymph nodes. The classifications include two categories: N0, where cancer remains absent from nearby lymph nodes, and N1, where cancer has spread to one or more nearby lymph nodes.
- **Metastasis (M):** The 'M' in the TNM system signifies metastasis, which is when cancer spreads from the primary site (in this case, the prostate) to other parts of the body. The categories are M0 (no distant metastasis) and M1, which is subdivided further: M1a (cancer has spread to lymph

nodes away from the prostate), M1b (cancer has spread to bones), and M1c (cancer has spread to other organs).

Stage	Description	Stage	Description
TX	Primary tumour cannot be assessed.	T0	No evidence of primary tumour.
T1	Cancer is not detectable through a physical exam or imaging tests.	T2	Cancer is confined to the prostate.
T1a	Tumour incidental histological finding in 5% or less of tissue resected.	T2a	Tumour involves one half of one lobe or less.
T1b	Tumour incidental histological finding in more than 5% of tissue resected.	T2b	Tumour involves more than half of one lobe, but not both lobes.
T1c	Tumour identified by needle biopsy (e.g. because of elevated PSA).	T2c	Cancer involves both lobes.
T3	Cancer has spread beyond the outer layer of the prostate and may have spread to the seminal vesicles.	T3b	Tumour invades seminal vesicle(s).
T3a	Extracapsular extension (unilateral or bilateral).	T4	Tumour is fixed or invades adjacent structures.
N0	No regional lymph node metastasis.	N1	Regional lymph node metastasis.
M0	No distant spread.	M1a	Cancer has spread to lymph nodes
M1	Distant sites.	M1b	Cancer has spread to bones.
		M1c	Cancer has spread to distant organs.

Table 1.1: TNM 2017 classification for PCa

Gleason Score

The Gleason score is a system used to grade the aggressiveness of PCa. It is based on how the cancer cells look under a microscope. The Gleason score provides important information for treatment decisions and prognosis [71]. **Table 1.2** summarizes the interpretation of Gleason scores.

Gleason Score	Interpretation
6 or lower	Well-differentiated (low-grade) cancer
7	Moderately differentiated (intermediate-grade) cancer
8-10	Poorly differentiated (high-grade) cancer

Table 1.2: Interpretation of Gleason Scores

The score ranges from 2 to 10, with 2 being the least aggressive and 10 being the most aggressive. A Gleason score of 6 or less is considered a low-grade cancer. These cancers are slow-growing and less likely to spread. A Gleason score of 7 is considered an intermediate-grade cancer. These cancers are more likely to grow and spread than low-grade cancers, but are not as aggressive as high-grade

cancers. A Gleason score of 8, 9 or 10 is considered a high-grade cancer. These cancers are the most aggressive and the most likely to grow and spread.

The International Society of Urological Pathology (ISUP) and World Health Organization (WHO) have adopted a new grading system for PCa, known as the ISUP/WHO grade groups [72, 73]. This system aims to help patients better understand the behavior of their diagnosed prostate carcinoma. Notably, it separates Gleason Score (GS) 7 adenocarcinoma into two prognostically distinct categories: grade group 2 for GS 7(3+4) and grade group 3 for GS 7(4+3). This distinction provides more precise prognostic information for patients and clinicians. See Table 1.3 for the Gleason and ISUP grades organisation.

Gleason Score	ISUP Grade
2-6	1
7(3+4)	2
7(4+3)	3
8(4+4 or 3+5 or 5+3)	4
9-10	5

Table 1.3: Gleason Score and ISUP grade

Stage

The combination of the T, N and M values allows the oncological stage of each patient to be determined. The Union for International Cancer Control (UICC) in the 8th edition of the TNM Classification of Malignant Tumours [70] defined the stages of PCa described in Table 1.4.

The stage of cancer is a crucial factor in determining the prognosis and guiding treatment decisions. [74]. Patients with early stage PCa (stages I and II) may be candidates for active surveillance, radical prostatectomy, or radiation therapy [75]. In contrast, those with more advanced disease (stages III and IV) often require multimodal approaches, potentially including hormone therapy, chemotherapy, or novel targeted therapies [75].

Stage	T	N	M	G
Stage I	T1, T2a	N0	M0	G1
Stage II	T2b, T2c	N0	M0	G2-4, Any G
Stage III	T3, T4	N0	M0	Any G
Stage IV	Any T	N1	M0	Any G
	Any T	Any N	M1	Any G

Table 1.4: Stages of PCa

Risk groups

The management of patients diagnosed with PCa varies according to their risk of progression. The use of cancer prognostic risk groups plays an important role in therapeutic treatment decision-making, clinical trial design and outcome reporting. While several approaches exist, the D'Amico classification remains one of the most widely adopted [76]. This system uses PSA level (blood test), Gleason grade (microscopic appearance of the cancer cells), and T stage (size of the tumour on rectal exam and/or ultrasound) to group men as low, intermediate, or high-risk (Table 1.5)

Risk Group	PSA Level	Gleason Score	Clinical Stage
Low-Risk	10	6	T1-T2a
Intermediate-Risk	10 - 20	7	T2b
High-Risk	>20	8	T2c-T3a

Table 1.5: D'Amico classification system for PCa risk assessment

1.5 Androgen signalling and Androgen Receptor (AR) in PCa

1.5.1 Androgen action in prostatic development

Steroid hormones known as androgens play a crucial role in the human body. Although commonly associated with male development, these hormones are important for both sexes. Their primary function involves the growth and maintenance of male sexual traits, both primary and secondary.

Androgen synthesis is probably one of the most important parts of male reproductive physiology and occurs mainly in the testes under the regulation of the hypothalamic-pituitary-gonadal axis. Figure 1.4. This axis orchestrates more than 95% of total circulating testosterone, the principal androgen of the body. The balance of the remaining circulating androgens is contributed by the adrenal glands, but in lesser amounts. These testicular androgens are the most important for the development and maintenance of the prostate gland, which is an important organ of the male reproductive system [77].

Stimulated by an increase in serum testosterone levels during puberty, the size of a normal prostate increases to 20 grams. This period of rapid growth is

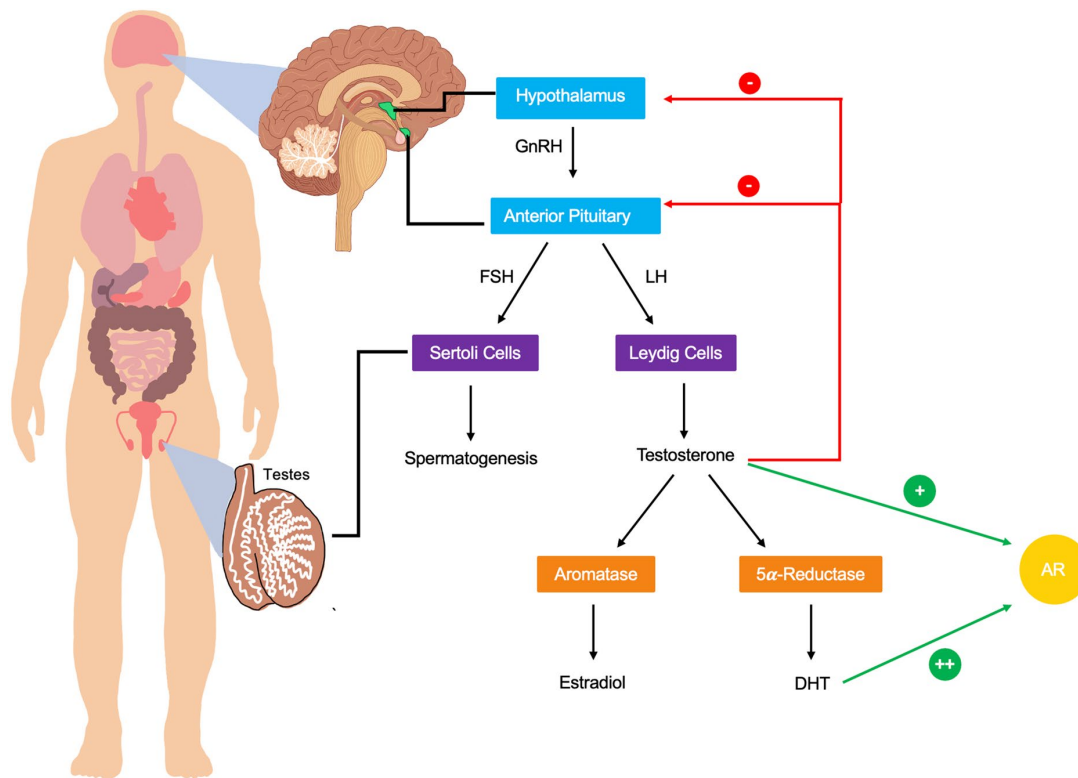


Figure 1.4: Regulation and Metabolism of Testosterone. Testosterone production initiates in the hypothalamus, where GnRH (gonadotropin-releasing hormone) is released into the hypophyseal portal system. This GnRH then acts upon the anterior pituitary gland, triggering the release of two key hormones: FSH (follicle-stimulating hormone) and LH (luteinizing hormone) [78].

followed by a period of stabilization, in which the continued presence of androgens does not cause growth [77]. The transition from growth to steady state is tightly regulated with a fine balance between cell proliferation and apoptosis, so that the structural and functional integrity of the prostate is maintained.

Androgens also appear to play a role in the formation of reproductive organs of the male embryo. Their secretion is under the regulation of negative feedback that involves not only the hypothalamic LHRH but also the LH. The hypothalamus has the responsibility of releasing LHRH, which will act on the pituitary gland to release LH. LH will also act on the Leydig cells, which will respond by synthesizing most of the body testosterone, while the remaining is secreted by the adrenal gland and its androgens. Once synthesized, androgens circulate in the bloodstream and are absorbed by body tissues, including the prostate, causing growth and maintenance of the organ.

1.5.2 AR structure

The AR is encoded by a solitary copy of the AR gene located at chromosome position Xq11-12. The gene has also been referred to as NR3C4 gene and forms an essential member of the nuclear receptors (NRs) that play a critical role as a transcription factor. The receptors exert their action through binding to specific regulatory sequences found in the promoter regions of DNA upon binding with hydrophobic ligands and hence play a central role in gene expression. As reported in different studies [79–81], the importance of this mechanism in gene regulation has been highlighted, underlining a fundamental role in cellular and molecular biology.

AR gene belongs to the class I group of nuclear receptors that also include of the androgen (AR), progesterone (PR), estrogen (ER α and ER β), mineralocorticoid (MR) and glucocorticoid (GR) receptors all of which mediate the cellular responses to the steroid hormones. The AR gene is located on the long arm of the X chromosome (band q11-12). This gene consists of 8 exons and, with a length of 2,757 nucleotides, encodes the synthesis of a large protein of about 110 kDa and 919 amino acid residues. Notably, AR gene expression is mainly observed in reproductive tissues such as the prostate, ovaries and endometrium [82].

Functionally, it is the AR gene that serves as the main mediator of androgen action, which influences the course of male sexual differentiation and even further contributes to the development and maintenance of male reproductive tissues [82]. This versatile role points out the central place of AR in human biological processes. The broad tissue activity it induces underlines its importance beyond mere reproduction, as well as allowing hypothesising possible implications for metabolic, neurological and other physiological systems in humans.

The AR consists of functional domains that allow receptor dimerization, DNA binding and complexing via cofactors with the basal transcription machinery. It consists of four functional domains (Figure 1.5):

- **N-terminal transactivation domain (NTD):** Encodes the transcriptional activation function 1 (AF1) and is responsible for the formation of the cellular transcription complex. Within AF1, two transactivation units (TAU-1 and TAU-5) shape the activity of the receptor. TAU-5 specifically confers strong constitutive transcriptional determinant activity and has been shown to be involved in aberrant AR

activation in some disease states.

- **DNA-binding domain (DBD):** Encoded by exons 2 and 3, which contain two zinc finger motifs, it is involved in the specific sequences in the DNA and the homodimerization of this receptor.
- **Ligand binding domain (LBD):** It is translated from exons 5-8. This domain contains AF-2 and binds ligands of androgens, thus constituting the predominant mode of regulation of the androgen signalling pathway.
- **Hinge region:** The nuclear translocation signal found in the hinge region, which divides the DBD from the LBD, is crucial for mediating the translocation of the active AR into the nucleus.

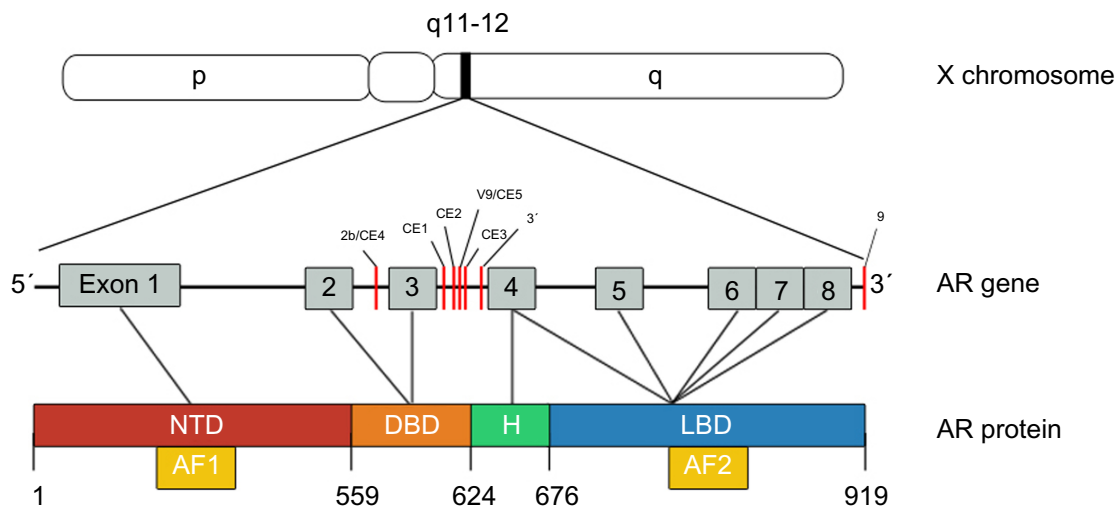


Figure 1.5: Structure of the AR. The AR gene is situated on the X chromosome (Xq11-12) and comprises eight exons. It includes exon 1, which encodes the N-terminal domain (NTD) containing the activation function AF-1. Exons 2 and 3 are responsible for the DNA-binding domain (DBD). Exon 4 encodes the hinge region, functioning as a nuclear localization signal, and along with exons 5 through 8, forms the ligand-binding domain (LBD), which contains the activation function AF-2. AF-1 houses two primary transactivation units: TAU-1 and TAU-5. [83]

1.5.3 AR activation and mechanisms of action

In the absence of its ligand, AR is found in the cytoplasm, where it forms complexes with chaperone proteins, such as heat shock proteins (HSP) 70 and HSP40, to form a mature aporeceptor complex. This form is associated with additional microtubules and HSPs that ensure the proper conformation of the receptor to bind ligand. Binding of testosterone or DHT induces a

conformational change of the LBD, leading to HSP dissociation, phosphorylation, and dimerization of the AR. This indicates that it has dimerisation motifs and possesses nuclear localization signals that allow the AR to translocate to the nucleus **Figure 1.6** [82, 84].

In the nucleus, AR binds to AREs resulting in the transcription of specific genes and interacts with other transcription factors, such as nuclear factor IB (NFIB), with a far-reaching effect on regulation of genes within PCa cells. Some of the best known target genes are PSA, transmembrane serine protease type 2 (TMPRSS2), kallikrein 2 (KLK2) and hexokinase 2 (HK2). Significantly, receptor binding to AREs leads to the recruitment of a set of enzymatic and regulatory proteins, including histone acetyltransferases, demethylases, as well as kinases and other co-regulators. Disruption of ligand binding prompts the re-exposure of nuclear export sites, with the receptor recycled back to the cytoplasm. There, it associates with the cytoskeleton and primes itself for interactions with new ligands. The AR has significant genomic action, primarily regulated through a spectrum of coregulators interaction with it. These interactions may occur via the N-terminal domain (NTD) and/or the ligand binding domain (LBD), with the specificity of the cofactor recruitment determined by the state of the receptor conformation and post-translational modifications of the receptor domains [85].

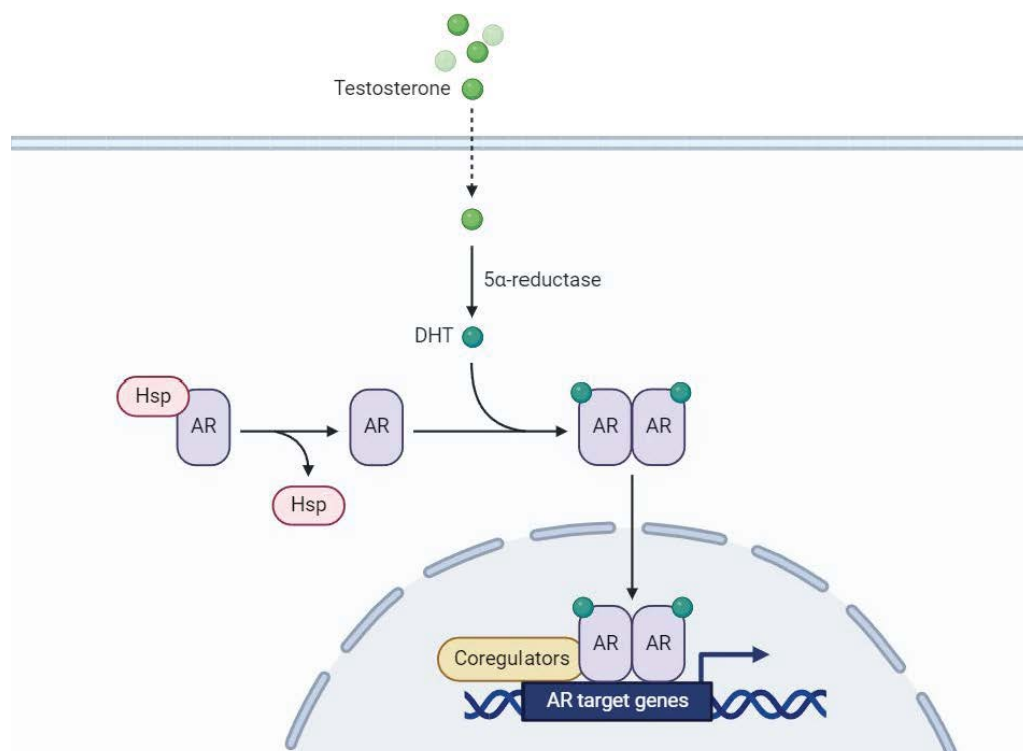


Figure 1.6: Mechanisms of androgen action and AR signalling in prostate cells. [86]

In addition, there are different AR variants (ARvs) arising from alternative splicing of mRNA that give rise to variants lacking or containing variable portions of LBD. In some ARvs, dimerization can be promoted in the absence of ligand to AR target genes either through homodimerization or by heterodimerization with full-length ARs.

1.5.4 Persistent AR signalling in castration-resistant PCa

The paradigm of castration-resistant PCa (CRPC) has undergone significant evolution in recent years. Initially, the scientific community posited that CRPC progression was completely independent of androgen signaling, rendering further hormonal interventions futile [87]. However, contemporary research has elucidated a more nuanced understanding of CRPC biology. Current evidence suggests that while subpopulations of truly androgen-independent neoplastic cells may exist, sustained AR signaling remains a critical driver in CRPC progression [88, 89]. This persistent AR activity is facilitated through multiple molecular mechanisms, including AR gene amplification or overexpression, mutations in the AR gene sequence, intratumoral de novo androgen synthesis, dysregulation of kinase signaling cascades, alterations in AR coregulator dynamics, expression of constitutively active AR splice variants etc.

The recognition of AR reactivation as a central component in CRPC pathogenesis has catalyzed extensive research efforts aimed at developing novel therapeutic agents targeting the AR signaling axis [90]. These pharmacological agents have demonstrated significant clinical efficacy and have been integrated into the standard treatment protocols for patients with metastatic CRPC. A detailed discussion of their mechanisms of action will be presented in the Treatment of advanced PCa section of this thesis.

1.6 Therapeutic approach to PCa

1.6.1 Treatment of localised PCa

In local PCa, Treatment decisions depend on an accurate assessment of the stage and risk of the disease. In this phase of the disease, low-risk patients typically do not require extensive staging, as the likelihood of metastasis is low.

However, for higher-risk categories, thorough imaging is crucial to detect potential metastases, which plays a pivotal role in guiding treatment choices. In the treatment of localized PCa, several options are available, each tailored to the specific stage and aggressiveness of the disease, as well as the patient's general health and treatment preferences.

Active surveillance/ watchful waiting

Active surveillance and watchful waiting are conservative management strategies for PCa that aim to avoid or delay the potential side effects of definitive treatments while maintaining oncological safety (Table 1.6). These approaches are particularly relevant for men with low-risk PCa or those with limited life expectancy due to age or comorbidities [91].

In active surveillance, low-risk patients with PCa are regularly followed up for PSA tests, DRE, and periodic prostate biopsies to monitor the patient's condition. It has the objective of early detection of possible disease progression and offers an opportunity for curative treatment in such cases. Recent research indicates that active surveillance is a safe approach for carefully selected patients, with a risk of cancer-related death or metastasis less than 1% over extended follow-up periods [92]. However, approximately 25% of patients under active surveillance will require definitive treatment within 5 years due to disease reclassification or progression [93].

In watchful waiting, PCa patients who are considered unsuitable for curative treatment, either due to limited life expectancy or the presence of significant comorbidities, are managed conservatively. Here, the approach will shift from trying to cure the disease to monitoring the patient for the appearance of signs and symptoms caused by progression. In case such symptomatology develops, palliative treatment is performed to preserve the patient's quality of life. [94, 95].

Radical prostatectomy

Radical prostatectomy (RP) is a surgical intervention designed to excise the prostate gland while preserving pelvic organ function. The procedure involves complete removal of the prostate gland, including the entire capsule and seminal vesicles, followed by vesicourethral anastomosis [96–98]. Since its initial description in 1904, the approach has undergone significant evolution,

	Active Surveillance	Watchful Waiting
Treatment intent	Curative	Palliative
Follow-up	Predefined schedule	Patient-specific
Assessment/markers used	DRE, PSA, rebiopsy, optional MRI	Not predefined
Life expectancy	>10 years	<10 years
Aim	Minimize treatment-related toxicity without compromising survival	Minimize treatment-related toxicity
Comments	Only for low-risk patients	Can apply to patients at all stages

Table 1.6: Comparison of active surveillance versus watchful waiting

particularly in recent years with the advent of advanced technologies [99]. Traditional open retropubic and perineal approaches have largely been replaced by minimally invasive techniques, namely laparoscopic and robot-assisted radical prostatectomy (RARP) [100–102]. RARP, in particular, has gained prominence due to its potential benefits in terms of surgical precision, reduced blood loss, and faster postoperative recovery [103–105]. Although surgical techniques have improved, radical prostatectomy (RP) is still linked with frequent postoperative issues, including erectile dysfunction, dry ejaculation due to seminal vesicle resection, altered orgasm quality, orgasm-related pain, and penile shortening. Additionally, long-term urinary incontinence is noted as the second most prevalent complication. [106–109].

Radiotherapy

Radiotherapy is a crucial component in the management of PCa, with the primary aim of eradicating the tumour through precisely targeted therapeutic radiation while minimizing exposure to adjacent healthy tissues. This approach is pivotal not only for the effective elimination of cancerous cells but also for mitigating potential side effects. Currently, there are different modalities of radiotherapy administration:

The aim of this treatment, like that of surgery, is to eradicate the tumour by means of a precisely targeted dose of therapeutic radiation, while concurrently ensuring minimal exposure to adjacent tissues. This approach is pivotal not only for the effective elimination of cancerous cells, but also for mitigating potential side effects. There are currently different modalities of radiotherapy

administration:

1. **External Beam Radiation Therapy (EBRT):** Using sophisticated machinery, highly focused radiation beams are precisely targeted at the tumour and delivered to the prostate gland. This accuracy reduces exposure to and potential harm to nearby tissues, especially important organs like the bladder and rectum which are located close to the prostate. There are several advanced EBRT techniques available, each with its own distinct strategy and advantages. The choice of EBRT technique is tailored to the individual patient's disease characteristics, overall health status, and treatment preferences
2. **Brachytherapy:** Brachytherapy places radioactive seeds or pellets right inside the prostate gland [110, 111]. Depending on the isotope being utilized, the duration of the radiation delivered by these seeds to the tumour over a predetermined period can range from days to many months. Direct implantation ensures that the malignant cells receive an intense radiation dose while significantly lowering radiation exposure to the surrounding environment.

Nevertheless, the effectiveness of radiation therapy is intricately linked to multiple patient-specific elements. These include the cancer's stage and grade, the patient's overall health condition, and personal treatment preferences. It is crucial for patients to participate in detailed discussions with their oncologist to establish a personalized treatment plan, considering both the advantages and possible adverse effects.

Other available Treatments

Apart from these two main modalities, surgery and radiotherapy, there are new and emerging options for PCa patients. These involve cryotherapy and high-intensity focused ultrasound. Cryotherapy utilizes freezing techniques in the destruction of cells that cause PCa. Dehydrating the cells leads to protein denaturation, direct disruption of cell membranes by ice crystals, vascular stasis, and microthrombi, which then work in a cascading effect to finally cause stagnation of the microcirculation, consequently resulting in ischemic apoptosis. Under transrectal ultrasound guidance, two freeze-thaw cycles are performed to achieve the desired temperature of -40°C in the medial gland and the neurovascular bundle [112–114].

High-intensity ultrasound therapy (HIFU) uses specialized transducers to emit

focused ultrasonic waves, which induce tissue damage through a combination of mechanical and thermal effects, alongside cavitation processes [115]. The primary goal of HIFU is to elevate the temperature of the malignant tissues beyond 65°C, thereby inducing their eradication through coagulative necrosis). This non-invasive technique has shown promise as a treatment option for PCa [116].

1.6.2 Treatment of advanced PCa

Despite treatment with surgery or radiotherapy, relapses occur in approximately 30% of men treated for localized PCa and advanced disease is associated with poor outcomes. In these patients, treatments are mainly focused on increasing longevity, slowing disease progression and improving general well-being, without aiming for the total eradication of the disease. The cases of advanced PCa can then be divided into three broad categories based on the absence or presence of metastases and serum testosterone concentrations:

- **Metastatic Hormone-Sensitive PCa (mHSPC):** represents a disease entity that includes patients with clinician-assessed, radiologically documented metastatic disease and normal testosterone grades (>50 ng/dL). A clear distinction should be drawn between those patients with a 'de novo' (synchronous) metastatic disease and those with metachronous recurrent metastatic disease, since these subgroups are reported to have different baseline prognostic outcomes.
- **Non-metastatic castration-resistant PCa (nmCRPC):** is a category of patients with maintained castration levels of testosterone (<50 ng/dL) without distant metastases on conventional images. These patients show biochemical progression with increasing PSA during androgen deprivation therapy (ADT) alone.
- **Metastatic castration-resistant PCa (mCRPC):** This is the very last and most lethal stage of the disease, where patients have a castration level of testosterone along with documented metastatic disease on imaging studies.

Surgical castration: Orchiectomy

Orchiectomy is a surgical procedure in which both testicles are removed. This produces a dramatic and fast decrease in testosterone serum levels to values below 15 ng/dl, usually within the first 12 hours after surgery. Although this decrease is permanent, no differences have been found regarding survival or progression of the disease compared to LHRH analogues [117]. It is indicated when patients have not followed treatment adequately or in urgent reduction in serum testosterone levels.

Androgen Deprivation Therapy

Huggins and Hodges in 1941 highlighted the dependence of PCa on androgens for its growth and spread [118]. This milestone won them the Nobel Prize in Physiology and marked the beginning of ADT as a mainstay in the treatment of advanced PCa. Androgens, particularly testosterone, play a critical role in the development and function of the male reproductive system, including the prostate gland. In PCa, these hormones bind to Androgen Receptors located on PCa cells, triggering a cascade of signaling events that lead to cell growth, division, and survival. ADT aims to disrupt this androgen-driven signaling pathway by suppressing androgen production or blocking AR activity. This deprivation of androgens effectively starves PCa cells, causing them to shrink, slow down their growth, and eventually die.

ADT induces a decrease in prostate size and disease regression by reducing or inhibiting androgen production. This is achieved by suppressing up to 90-95% of testosterone production. These therapies fall into several main categories:

- **Estrogens:**

Estrogens were among the first agents used to inhibit testosterone production by suppressing the hypothalamic-pituitary-gonadal axis [118]. Estrogens reduce testosterone levels by providing negative feedback to the hypothalamus, thus decreasing the secretion of luteinizing hormone (LH) and follicle-stimulating hormone (FSH), which are necessary for testosterone production. However, due to significant cardiovascular side effects, such as thromboembolic events, their use in clinical practice has largely been replaced by other ADT strategies [119].

- **GnRH Analogues:**

A class of medications known as gonadotropin-releasing hormone (GnRH) agonists is commonly used to treat PCa. GnRH downregulate the pituitary gland, reducing LH and FSH production. This results in a significant decrease in testosterone levels, which can help slow or stop the growth of PCa cells. However, GnRH agonists initially cause a surge in LH and FSH levels, temporarily increasing testosterone production (the "flare" effect), leading to increased symptoms of PCa, especially in people with advanced disease. Leuprolide, goserelin, and triptorelin are commonly prescribed GnRH agonists.

- **GnRH antagonists:**

GnRH antagonists offer a distinct mechanism of action. Unlike GnRH agonists, which initially stimulate hormone production before suppressing it, antagonists bind directly to GnRH receptors, preventing them from activating the pituitary gland. The competitive blocking of the GnRH receptor results in a rapid, but reversible, decrease in LH, FSH and testosterone without any flare. This can be particularly beneficial for patients with advanced PCa, as it helps to prevent or minimize the temporary worsening of symptoms that can occur with a sudden increase in testosterone [120].

GnRH antagonists are generally well-tolerated, with fewer side effects compared to earlier generations of these drugs. While some patients may experience histamine-mediated side effects, newer versions have been developed to minimize these issues [121].

- **Androgen biosynthesis inhibitors:**

Androgen biosynthesis inhibitors, such as abiraterone acetate, selectively inhibit the enzyme CYP17A1, which is crucial in the production of androgens. This enzyme is involved in two steps of androgen synthesis: converting pregnenolone and progesterone into their 17 α -hydroxylated derivatives, and then converting these into dehydroepiandrosterone (DHEA) and androstenedione, precursors of testosterone. By blocking this pathway, abiraterone acetate effectively reduces the production of testosterone and other androgens not just in the testes, but also in the adrenal glands and within prostate tumors themselves [122, 123].

Abiraterone is usually given alongside prednisone, a corticosteroid, to mitigate side effects associated with its mechanism of action.

Specifically, by inhibiting CYP17A1, abiraterone also inadvertently increases levels of mineralocorticoids (e.g., aldosterone), leading to side effects like fluid retention, hypertension, and hypokalemia. Prednisone helps to counteract these effects by reducing the production of adrenocorticotrophic hormone (ACTH) from the pituitary gland, which in turn reduces the production of adrenal steroids, including those that can cause these side effects [123, 124].

1.6.3 Treatment of Castration-resistant prostate cancer

CRPC is identified by a biochemical recurrence indicated by rising PSA levels in the blood and/or metastatic spread demonstrated through imaging studies, despite maintaining castrate-level testosterone (below 50 ng/dL). Patients with CRPC frequently experience pain, discomfort, and weakness due to metastatic tumours present in bone, lymph nodes, and soft tissues. During the metastatic stage, CRPC is associated with a median survival of 2 to 4 years, and there are presently no treatments capable of curing the disease. Available therapeutic strategies focus on extending survival and providing symptomatic relief. Among the most commonly employed options are the use of second generation anti-androgens, chemotherapy and more recently the use of radiopharmaceuticals, immunotherapy and the use of PARP inhibitors. Each of these options addresses different aspects of CRPC progression, offering a range of mechanisms to manage the disease.

Anti-androgens

Unlike androgen biosynthesis inhibitors, which decrease the levels of androgens, anti-androgens compete with natural androgens for binding to the AR, inhibit these hormones from activating the receptor, and hence stimulate the growth of PCa cells. There are two major divisions of antiandrogens: steroidal and nonsteroidal.

Steroidal anti-androgens e.g. cyproterone acetate, aside from blocking the AR, also have directly acting progestogenic activity that further suppresses LH, hence testosterone production. However, these are not as commonly used because of associated side effects and elicit androgenic effects at high concentrations due to partial agonist activity

[125, 126].

Non-Steroidal Anti-Androgens (NSAA), such as flutamide, enzalutamide and bicalutamide, are more used in the treatment of PCa. These compounds exhibit significant affinity for the AR, thereby hindering its translocation from the cytoplasm to the nucleus. In the nuclear environment, antiandrogens obstruct AR binding to deoxyribonucleic acid (DNA), decreasing the transcription of genes responsive to AR. Consequently, this halts the proliferation of androgen-dependent prostate cancer (PCa) cells.

Non-steroidal anti-androgens are commonly used for advanced PCa, usually in combination with ADT, which decreases androgen production by the testes. The combination is called Combined Androgen Blockade (CAB) has been reported to have greater efficacy than monotherapy in some cases. Enzalutamide, a new generation NSAA, showed activity both in castration-resistant and hormone-sensitive PCa with significantly prolonged survival in clinical trials [127, 128]. However, long-term administration of anti-androgens, particularly NSAA, has attendant side effects like gynaecomastia, hot flashes, and gastrointestinal disturbances. Because they inhibit androgen action, it is expected to decrease libido and lead to erectile dysfunction. In most cases, the management involves dose adjustments and some supportive therapies that help maintain good quality of life for patients during their treatment.

Chemotherapy

Before 2004, there was no standard of care for first-line and second-line chemotherapy in PCa treatment. Chemotherapy at that time had the principal palliative effects; this simply means symptom alleviation without any survival advantage to patients.

The most commonly used chemotherapeutic agents in PCa are docetaxel and cabazitaxel. Both drugs bind to tubulin, a protein essential for cell division, and stabilize microtubules. This stabilization prevents microtubules from disassembling, which inhibits mitosis and leads to apoptosis. [129, 130].

Radioactive therapies

Radiopharmaceuticals represent a significant advance in the therapeutic strategy for metastatic PCa. Targeted radiation involves new treatment approaches that take advantage of the unique nature of radioactive isotopes to specifically target and deliver lethal doses to stateruled malignant cells, thus sparing the healthy tissues surrounding each tumour [131]. Nowadays, the most commonly used radiopharmaceutical treatments are lutetium and radium

The combination of Lutetium-177 with the ligand PSMA-617 (177Lu-PSMA-617) is gaining recognition as a highly promising treatment approach for advanced metastatic prostate cancer. The expression of prostate-specific membrane antigen, a type II membrane glycoprotein, is significantly elevated in prostate cancer (PCa) cells. PSMA is an excellent target for both molecular imaging and therapeutics with high specificity. Lu-PSMA-617 exhibited substantial effectiveness in the management of mCRPC. In its latest phase III study, called VISION, 177Lu-PSMA-617 standard care, compared to standard care, has been shown to offer significant OS and radiographic progression-free survival benefits in patients with PSMA-positive mCRPC [132]. Numerous additional trials are currently underway to investigate in more depth its treatment outcomes, as well as its potential use at earlier stages of the disease [133].

Radium-223, is an alpha-emitter that entraps itself much like calcium at sites of increased bone turnover. Bone metastases are a common site of PCa spread. Following uptake by bone, Radium-223 emits high-energy alpha particles that, in turn, break double strands of DNA in the cancer cells surrounding it, destroying them [134]. Radium-223 is significantly effective in increasing OS and delaying time to first symptomatic skeletal event in patients with mCRPC and bone metastases [135].

1.7 Immunotherapy for castration-resistant prostate cancer

Immunotherapy has emerged as a transformati ve approach in cancer treatment, utilizing the immune system of the body to identify and eliminate malignant cells. Unlike traditional therapies such as surgery, radiation, and chemotherapy, immunotherapy targets the immune system's ability to

recognize cancer-specific antigens, offering the potential for durable responses and improved survival outcomes. The success of immunotherapy in malignant neoplasms such as melanoma, lung cancer, and renal cell carcinoma highlights its potential to redefine the therapeutic landscape in various cancers.

However, prostate cancer presents a unique set of challenges for immunotherapy. Unlike immunologically "hot" tumours, which are characterized by a high mutational burden and abundant tumour-infiltrating lymphocytes, prostate cancer is considered an "immune cold" tumour. This designation reflects a relatively low neoantigen burden, a paucity of cytotoxic T-cell infiltration, and the presence of immunosuppressive elements within the tumour microenvironment, such as myeloid-derived suppressor cells and regulatory T cells.

According to recent studies, AR is a key factor in reducing CD8 + T cell activity, which is a crucial reason for resistance to immunotherapy in CRPC. By downregulating vital genes including TNF, granzyme B, and IFN γ in CD8+ T cells, Guan et al. showed that AR adversely affects the anticancer immune response [136]. Adding a new dimension of complexity, sex-based differences further complicate immunotherapy outcomes. Epidemiological data indicate that men have higher incidence and mortality rates for many malignancies of non-reproductive organs compared with women [137]. This male bias could be due to unique molecular and cellular mechanisms of antitumor immunity that are regulated by genes, hormones, and lifestyle factors [138]. For example, the X chromosome contains numerous immune-related genes whose inactivation in females is incomplete, and earlier studies have mentioned that this can result in increased immune surveillance [139]. However, external factors such as smoking and obesity reshape the tumour microenvironment in favour of chronic inflammation or immunosuppression, conditions more common in men [137].

1.7.1 Current Immunotherapy Strategies for Prostate Cancer

Dendritic cell (DC) based immunotherapy

Sipuleucel-T was the first therapeutic vaccine approved for cancer treatment. Treatment consists of autologous treatment with peripheral blood mononuclear cells obtained by leukoapheresis and pulsed ex-vivo with a fusion protein named PA2024 (Granulocyte-macrophage colony stimulating factor -GM-CSF-

and prostatic acid phosphatase -PAP-). This treatment fosters dendritic cells maturation and antigen presentation to the T-cells increasing both humoral and cellular responses. Sipuleucel-T (Provenge) is currently the only FDA-approved immunotherapy for prostate cancer. A phase 3 clinical trial demonstrated its significant contribution to prolonging OS in men with mCRPC, with a 22% reduction in risk of death and a median survival improvement of 4.1 months. Despite its benefits in prolonging survival, it does not affect disease progression, and its high costs and logistic challenges remain barriers to widespread use [140].

Immune checkpoint inhibitors (ICIs)

Malignant tumour cells have thus far succeeded in elaborating very efficient mechanisms for evading immune surveillance, among which activation of immune checkpoints that dampen T lymphocyte cytotoxic functions stands out. By this way, tumours successfully avoid T cell responses and thereby prevent immune destruction of tumour cells. Immune checkpoint inhibitors represent a class of monoclonal antibodies designed to neutralize this process by blocking particular checkpoint proteins in T cells or tumour cells. While doing this, they remove the inhibitory signals and restore the immune system's ability to eliminate cancer cells. Immune checkpoint inhibitors (ICIs), such as those targeting programmed death-1 (PD-1), its ligand (PD-L1) or cytotoxic T lymphocyte-associated antigen-4 (CTLA-4) pathways, have shown limited efficacy as monotherapies for prostate cancer. The immunologically "cold" nature of prostate tumours, characterized by low mutation burdens and limited T-cell infiltration, hampers the response to ICI.

Several studies have addressed the efficacy of PD-1/PD-L1 blockade in castration-resistant prostate cancer, obtaining variable results: Treatment with pembrolizumab, an anti-PD1 monoclonal antibody, was studied in KEYNOTE-028, a phase 1b clinical trial that included 23 mCRPC patients. The overall response rate was 17% (4/23) with a median duration of response of 13.5 months [141]. A phase 2 study including pembrolizumab, KEYNOTE-199, that included 258 patients observed a 5% response rate (including 2 complete responses) with a median duration of response of 16.8 months [142]. Atezolizumab, a PD-L1 inhibitor, obtained a response rate of 8.6% in a phase 2 study [143].

CTLA-4 can induce immune regulation by binding to CD80 and CD86 and sending a negative signal to the T cell. Ipilimumab is a monoclonal antibody

directed towards CTLA4 and blocks its function inducing increased T-Cell activation. Despite preliminary studies suggesting increased and prolonged PSA responses in mCRPC, two large randomized phase 3 trials in post-docetaxel CA184-043 [144, 145] and pre-chemotherapy [146] have failed to improve OS, although there are preliminary signs of a subgroup of patients with prolonged treatment responses.

The combination of CTLA4 inhibition and PD1/PD-L1 has increase response rate and toxicity. The combination of Ipilimumab (3 mg/kg) and nivolumab (1 mg/kg) resulted in a 25% response rate pre-chemotherapy and 10% in the post-chemotherapy scenario although with 50% of patients with grade 3 or higher toxicities, including 4/90 treatment-related deaths [147].

The combination of pembrolizumab with enzalutamide obtained a 18% of PSA decline equal or greater than 50% in a randomised phase 2 trial. However, two large randomized phase 3 trials in mCRPC (KEYNOTE-641) [148] and metastatic castration-sensitive prostate cancer (KEYNOTE-991) [149] were closed early for futility.

Despite these disappointing results in unselected patients, the presence of signs of activity highlighted the importance of identifying the patients that benefit the most. Molecular subtypes with greater benefit with immunotherapy include: patients with mismatch repair deficiency (MMRd) [150], CDK12 biallelic mutations [151] and high-tumour mutational burden [152].

PARP inhibitors

One of the most promising therapeutic strategies to address defective DNA repair genes is to take advantage of synthetic lethality resulting from the combination of PARP inhibition with dysfunction of the homologous recombination pathway. Several PARP inhibitors (iPARP) that differ in their ability to bind to the enzyme are in various stages of clinical development.

The first strong indications of the efficacy of iPARPs in mCRPC emerged with the TOPARP-A study (Phase 2) [153], in which olaparib was administered to patients with genetic alterations in DNA repair and showed a notable clinical benefit, with long-lasting responses over time. Based on these results, TOPARP-B [154], also in Phase 2, confirmed olaparib activity at different doses, demonstrating a particularly marked efficacy profile in carriers of BRCA1/2 mutations. Although some toxicity was observed that required dose adjustment

in some cases, the study supported the use of this drug in advanced prostate cancer.

The clinical relevance of iPARPs increased with the PROfound trial (Phase 3) [155], in which olaparib was compared with an alternative inhibitor of androgen receptor signaling (ARSi). Two cohorts were established according to the alterations in the genes involved in repair, distinguishing mutations in BRCA1, BRCA2, and ATM in one cohort, and other alterations in the second. This study demonstrated a clear benefit in radiological progression-free survival, as well as OS, especially in people with BRCA2 mutations. In addition, a more discrete effect was observed in mutations such as ATM, raising doubts about the efficacy of iPARPs in these specific cases. After positive results were published in the main cohort, the European Medicines Agency (EMA) approved olaparib for the treatment of mCRPC with BRCA1/2 mutations, provided there was progression after iPARP.

In parallel, other iPARPs such as rucaparib were investigated in the TRITON2 study (Phase 2) [156], which included a wide range of genetic alterations in the DNA repair pathway. The results highlighted significant responses in carriers of the BRCA1 / 2 mutation, evidenced by radiological evaluation and the decline in PSA. The next step was the TRITON3 trial (phase 3) [157], where rucaparib was compared directly against docetaxel or a second ARSi. With this more demanding comparison, a clear benefit of rucaparib was found in radiological progression-free survival for BRCA1 / 2 mutations, but the same advantage was not found in the ATM subgroup. This finding reaffirmed the hypothesis that iPARP activity is particularly strong in BRCA2 alterations, remaining more undefined in other genomic defects.

Another iPARP, niraparib, was analyzed in the GALAHAD study (Phase 2) [158], which focused on patients with biallelic defects in several genes related to DNA repair. In particular, remarkable responses were described in BRCA1/2 mutations, although it could not be fully clarified whether biallelic alterations conferred an additional advantage over monoallelic ones reported in other trials. A subsequent publication confirmed that tumours with BRCA2 mutations, regardless of whether they were somatic or germline, or whether they were monoallelic or biallelic, are often highly sensitive to iPARP.

In light of these results, it is clear that iPARPs today represent an essential therapeutic option for mCRPC with alterations in BRCA2 and, to a lesser extent, BRCA1. However, there is controversy regarding the efficacy in ATM and other less frequent genes, so new avenues are being explored, such as ATR, ATM, or

Chk inhibitors, in order to effectively treat these subgroups. However, patients with mutations in genes such as CDK12 and in genes of the MMR (mismatch repair) system could respond to immunotherapy, according to the first available data. This genomic diversity calls for a precision medicine strategy to target specific therapies to defined mutations, often combining iPARP with other agents to enhance response and delay resistance.

Combinations of PARP inhibitors and inhibitors of AR signaling.

Preclinical data indicate a synergy between AR inhibition and PARP inhibition, since AR blockade decreases the expression of homologous recombination-related genes while PARP1 participates in AR-regulated transcription. Based on this, three Phase 3 trials (PROpel, MAGNITUDE and TALAPRO-2) [159–161] have investigated the combination of different iPARPs and ARSi in first-line mCRPC. MAGNITUDE included a previous molecular screening that allowed to separate patients according to the presence of alterations in homologous recombination genes; benefit of the combination (Niraparib + abiraterone) was only observed in cases with BRCA1/2 mutations, proving futile for the others. In contrast, PROpel (Olaparib + abiraterone) [159] and TALAPRO-2 (Talazoparib + enzalutamide) [161] adopted an all-comer approach and also demonstrated an overall benefit in radiological progression-free survival, with a particularly marked impact on those with BRCA2 alterations. However, it must be considered that in clinical practice, most of the patients in mCRPC have already received ARSi at an earlier stage, and this subgroup was under-represented in these studies. Future trials in earlier stages, such as metastatic hormone-sensitive prostate cancer, are expected to help better define the place of these combinations in the therapeutic strategy.

In August 2023, the FDA approved a combination of niraparib and abiraterone acetate for treating BRCA-mutated mCRPC [162]. Similarly, in June 2023, the FDA approved talazoparib in combination with enzalutamide for HRR gene-mutated mCRPC [161].

Antigen Receptor T-cell (CAR-T) therapy

Chimeric Antigen Receptor T-cell (CAR-T) therapy represents another promising avenue for prostate cancer treatment. A phase 1 clinical trial evaluating PSCA-directed CAR-T cell therapy in mCRPC highlighted notable

responses, including PSA declines and radiographic improvements in some patients [163]. However, challenges such as toxicity, cytokine release syndrome, and limited CAR-T cell persistence beyond 28 days remain significant hurdles. These findings suggest potential for CAR-T therapy in prostate cancer but underscore the need for further research to optimize dosing and combination strategies for enhanced efficacy.

1.8 Biomarkers

Biomarkers, also known as biological markers, are measurable indicators that offer significant insights into normal biological activities, disease-related processes, or pharmacological responses to treatments. These attributes, which can be molecular, histological, radiographic, or physiological, provide quantitative assessments of health and disease conditions, serving as essential tools for diagnosis, prognosis, and therapeutic monitoring in clinical practice. The National Institutes of Health Biomarkers Definitions Working Group has established a comprehensive definition: "A biomarker is a feature that is objectively quantified and assessed to serve as an indicator of normal biological processes, disease-related processes, or pharmacologic responses resulting from a therapeutic intervention." [164]. This definition underscores the versatility and significance of biomarkers across various biological contexts.

During the last ten years, the treatment of metastatic PCa has undergone a sea change and rewrote our way of management of mCRPC. These advances have resulted in a more marked survival rate among men suffering from metastatic PCa, thus instilling new optimism in both the affected men and the clinicians as well. However, the following section will outline that, even with these recent advances, there remain several key issues in this arena which require and need further consideration and a response.

Although current treatments have already demonstrated their clinical utility in large cohorts of patients, this overall effect varies significantly between individuals. There is a significant percentage of patients who show little or no response to treatment [165]. This phenomenon is known as primary resistance. Another type of resistance is called acquired resistance, in which disease progression occurs in response to treatment over time after an initial positive response.

The variability in treatment responses can be largely attributed to the

traditional approach that applies the same treatment to all patients, underscoring the need for personalized therapeutic strategies. With the continued rapid incorporation of multiple active therapies into daily clinical practice, the therapeutic challenges have only become more pronounced, with complex clinical decision-making. Identifying the best sequence and combination remains a major challenge.

These challenges underscore the critical need to find robust predictive and prognostic biomarkers that allow for appropriate individualization of therapeutic decisions. Overcoming this challenge requires a better understanding of the tumour biology underlying primary and acquired resistance to current therapies. This information is essential to design strategies to overcome these resistances and thus improve patient outcomes. Biomarkers that are valid and reliable to predict response and prognosis to treatment are an important need for personalization of treatments, which can lead to better quality of life outcomes for patients [166].

Well-designed clinical trials comparing various treatment sequences and combinations are essential to provide evidence-based guidance for clinicians through this complex landscape. The search for novel treatment modalities, including immunotherapies, targeted agents, and combination approaches, deserves further research to further improve outcomes in patients with metastatic PCa. The application of advanced technologies in the future, including artificial intelligence and machine learning combined with clinical and molecular data, could revolutionize treatment decisions for metastatic PCa.

1.8.1 Types of biomarkers

The BEST (Biomarkers, EndpointS, and other Tools) Resource, a collaborative effort between the FDA and NIH, has further refined the classification of biomarkers into seven distinct categories according to their intended use and biological significance [167].

- **Diagnostic Biomarkers:** These are the molecular markers that help in diagnosing cancer or finding out a subtype of cancer. Theoretically, an ideal diagnostic biomarker should have absolute sensitivity and absolute specificity, 100% each, rightly identifying every subject with disease and excluding all others who are healthy. Examples include PSA in PCa diagnosis, though there are many limitations related to its use. This has been explained in detail in the section 1.4.3

- **Monitoring Biomarkers:** Biomarkers are usually measured serially in order to follow disease activity, response to therapy, or the effects of medication or environmental exposures. In the case of PCa, one of the most common biomarkers used is PSA, which is serially measured after treatment-most commonly radical prostatectomy or radiation therapy-to estimate disease control and recurrence.
- **Predictive Biomarkers:** Such biomarkers help stratify patient populations according to the likelihood of benefit from a certain therapeutic intervention or be at risk for an adverse outcome based on exposure to medical products or environmental agents. For example, the presence or absence of Androgen Receptor Splice Variant 7 (AR-v7) in PCa patients would show differential responses to either taxane-based chemotherapy or AR-targeted therapies.
- **Prognostic Biomarkers:** These biomarkers reflect the likely course of the disease in terms of progression, recurrence, or other clinical outcomes independent of treatment. In PCa, both PSA dynamics and Gleason scores have been used as prognostic biomarkers for estimating the risk of recurrence and guiding treatment intensity. Biomarkers of Susceptibility/Risk: This is because these biomarkers provide details about the risk that an individual carries of developing a particular type of cancer in the case where apparent diseases are absent. Among the genetic markers also come the BRCA2 mutations, which might pre-dispose one to an enhanced tendency of developing highly dangerous forms of PCa besides their already well-known connection with breast as well as ovarian cancers.

1.8.2 Clinicopathological biomarkers

Clinicopathological biomarkers are measurable parameters derived from clinical data, laboratory tests, and pathological assessments that provide information on the biological behaviour of tumours and their response to treatment. These biomarkers are imperative for understanding disease progression, guiding treatment decisions and predicting patient outcomes, especially in mCRPC.

Early efforts to develop prognostic models for mCRPC focused on easily detectable clinical and laboratory parameters. The prognostic factors that were determined include lactate dehydrogenase (LDH), PSA, Alkaline Phosphatase

(ALP), Albumin, Gleason Score, Eastern Cooperative Oncology Group (ECOG) performance status. These factors were integrated into nomograms to predict OS in patients with mCRPC. More recent research has expanded the repertoire of clinicopathological biomarkers, such as neutrophil-to-lymphocyte ratio (NLR), hemoglobin, and the number of bone metastases.

The integration of these diverse biomarkers into clinical practice has significantly improved our ability to stratify patients, predict treatment responses, and estimate survival outcomes. This wealth of information allows for more personalized treatment approaches, potentially improving patient outcomes and quality of life. Moreover, the ongoing identification and validation of new biomarkers continue to refine our prognostic models, paving the way for increasingly precise and effective management strategies in mCRPC. As research in this field progresses, there is growing interest in combining clinicopathological biomarkers with molecular and genetic markers. This integrative approach promises to provide an even more comprehensive understanding of individual tumour characteristics and patient-specific factors, further advancing the field of personalized medicine in PCa management.

1.8.3 Molecular biomarkers

Considerable progress has been made in prostate cancer (PCa) research, particularly in the search for dependable molecular biomarkers. Metastatic PCa exhibits a distinctive pattern of recurrent mutations, alterations in copy number, and structural rearrangements in crucial genes and pathways. These include AR, DNA repair mechanisms, the PI3K-AKT pathway, ERG, regulators of the cell cycle, the WNT signaling pathway, tumor suppressors such as TP53, RB1, PTEN, and chromatin modifiers, among others. [168–170]

Several studies have focused on analyzing different molecular biomarkers, such as AR-V7 [171]. AR-V7 has shown promise in predicting resistance to AR-targeted therapies in castration-resistant PCa patients [172]. Additionally, investigations into the inactivation of tumour suppressor genes like PTEN or the amplification of oncogenes such as c-MYC have provided valuable insights into PCa progression [173].

An important finding is the TMPRSS2-ERG gene fusion, occurring in roughly 50% of prostate cancer (PCa) cases [174]. The transmembrane protease serine 2 (TMPRSS2), which is a prostate-specific gene influenced by androgens, is located near the ERG gene on the same chromosome. Research has shown that

overproduction of ERG in significant PCa cases is driven by its fusion with TMPRSS2 [175]. Recent investigations reveal that the TMPRSS2-ERG gene fusion is the predominant variant found in approximately 40% to 70% of PCa cases [176]. This recurrent genomic rearrangement, which results in the overexpression of the ERG transcription factor, has shown promise as both a diagnostic biomarker and a therapeutic target [177, 178].

Despite these promising findings, to date, regulatory bodies have not approved any of these biomarkers alone as prognostic markers. This process underlines the complexity of PCa biology, as well as the challenge of translating molecular discovery into clinically useful tools. Such heterogeneity of PCa really demands a multiple-face approach-perhaps a combination of many biomarkers-reaching the sensitivity and specificity required for clinical application.

1.9 Whole blood assay approach to circulating biomarkers discovery

The clinical utility of circulating biomarkers in revolutionizing PCa management has become increasingly apparent, driven by rapid technological advancements and a deeper understanding of tumour biology. CTCs and circulating cell-free nucleic acids (cfNAs) have emerged as promising tools, with the ability to analyse tumour-derived macromolecules at an unprecedented level of detail [179]. The scope of their application continues to expand, yet the integration of these discoveries into routine clinical practice remains challenging. The implementation of such advanced techniques is constrained by the complexity of the methodologies and the specialized infrastructure required, which are largely confined to academic and research institutions [180]. Consequently, there has been a growing emphasis on using biomarker identification techniques that prioritize automation or simplicity of preanalytical factors. Examining the gene expression of peripheral whole blood has become a practical and promising strategy for treating metastatic PCa, as explained in the sections that follow.

1.9.1 Application of whole blood RNA assays in metastatic PCa

Gene expression profiling in whole blood has become an indispensable tool for the study of molecular mechanisms in solid tumours. This technique allows for

the analysis of RNA in blood samples, hence providing information on tumour biology and potential biomarkers. However, by nature, RNA is unstable and easily degraded by RNases, which are enzymes that cleave RNA. If not processed appropriately, this may lead to inaccurate results.

Collection systems, such as the PAXgene™ Blood RNA System of Qiagen and Tempus™ Blood RNA Tubes of Applied Biosystems, have been developed in this regard. These blood collection systems specially stabilize RNA right after blood has been drawn. Rapid preservation of RNA and its protection against degradation mean that these systems ensure that gene expression data will accurately reflect the biological state of the sample at the time of collection without introducing artificial changes caused by RNA instability or enzymatic activity. [181].

In mCRPC, whole blood RNA assays have historically served as a crucial tool for investigating molecular biomarkers associated with prognosis. These assays have primarily focused on identifying and validating multigene signatures that provide insight into disease progression and therapeutic response. Early studies in this area leveraged the capabilities of multiplexed quantitative reverse transcription polymerase chain reaction (qRT-PCR) and microarray platforms to measure the expression of numerous gene transcripts that were overexpressed in advanced PCa. Some previous studies conducted by Ross et al. [182], Olmos et al. [183] and Wang et al. [184] investigated several gene signatures in the context of treatment response and patient outcomes, demonstrating the potential of whole blood RNA profiling to stratify patients according to their risk of disease progression and survival.

Ross et al. developed a six-gene model focusing on inflammation, immune response, and tumour progression. This model stratified patients into low-risk and high-risk groups, with the high-risk cohort experiencing median survival rates as low as 7.8 months. Notably, the study highlighted systemic immune dysregulation, emphasizing the roles of genes such as SEMA4D and ITGAL in immune evasion, a hallmark of advanced disease [182].

Olmos et al. employed whole blood gene expression profiling to develop a nine-gene prognostic signature that identified a subgroup of mCRPC patients with significantly poorer survival outcomes. Using Bayesian latent process decomposition (LPD), they stratified patients into subgroups, with the LPD1 cohort exhibiting elevated PSA levels, higher lactate dehydrogenase, and adverse survival metrics. This nine-gene signature, validated through qRT-PCR, also implicated erythroid progenitor cells (characterized by CD71

expression) as contributors to poor outcomes, potentially through immunosuppressive effects [183].

Wang et al. constructed a four-gene model derived from stable co-expression modules identified through integrative genomic analysis. This model, which outperformed prior signatures in prognostic accuracy, revealed significant immune dysregulation. Upregulated genes were associated with myeloid lineage cells, while downregulated genes were enriched in lymphocytic pathways, suggesting immune cell-specific shifts that influence patient survival [184].

Together, these studies underscore the utility of whole blood RNA profiling in capturing systemic molecular alterations and reflecting the molecular heterogeneity of mCRPC. By measuring genes involved in AR signalling, immune response, and cell proliferation, these assays offer valuable insights into therapeutic vulnerabilities and patient stratification. However, despite their contributions, several limitations of these foundational studies highlight the need for further research in the modern therapeutic context.

However, these studies were limited in several important respects. All predated the widespread use of Androgen Receptor Pathway Inhibitors (ARPIs) such as abiraterone, enzalutamide, and apalutamide, leaving a gap in understanding how these biomarkers evolve in response to these modern therapies or contribute to resistance mechanisms. Moreover, the variability among patient cohorts, considering disease burden, previous therapies, and clinical features, obstructed the interpretation of the findings. Furthermore, the absence of comprehensive immunological profiles in these studies restricted the investigation of tumor-immune system interactions, an essential factor in the context of treatments that potentially influence systemic immunity and the tumor microenvironment.

HYPOTHESES & OBJECTIVES

2.1 Hypotheses

Prostate cancer is the most frequently diagnosed cancer among men and represents the second leading cause of cancer-related mortality in the male population. Despite the marked advancements made in early diagnosis and first-line treatments, a substantial number of patients with the disease develop mCRPC, a condition characterized by resistance to ADT, when treatment options become severely limited. Customizing cancer therapies relies on a more profound insight into the tumor's biology and the intricate interactions between the tumor and its surrounding environment. Advanced PCa has been shown to induce changes in the tumour microenvironment and in the broader environment, such as the blood. These changes have been shown to have prognostic value, including in blood tests (e.g. neutrophil to lymphocyte ratio) or at the gene expression level. Alterations in peripheral blood immune cell composition and gene expression profiles may reflect tumour-induced immunomodulation and could serve as valuable prognostic biomarkers and therapeutic targets.

We hypothesize that:

- (a) The composition of peripheral blood immune cells may be related to clinical outcomes in patients with mCRPC. Specific patterns in immune cell proportions may correlate with prognosis, providing independent prognostic information beyond established clinical factors.
- (b) Gene expression profiles of peripheral blood can serve as robust prognostic biomarkers in mCRPC, reflecting tumour-induced

alterations in the immune system and hematopoietic environment.

- (c) Enzalutamide treatment induces significant immunomodulatory effects on peripheral blood immune cells, leading to changes in immune cell composition and gene expression profiles associated with therapeutic resistance and disease progression.
- (d) Dynamic assessment of peripheral blood gene expression and immune profiling during enzalutamide therapy can identify early biomarkers of resistance and unveil potential therapeutic vulnerabilities within the tumour microenvironment.

The goal of evaluating these hypotheses is to enhance our comprehension of the interplay between the tumour and the immune system in mCRPC, as well as to identify new prognostic indicators and therapeutic targets that could potentially improve patient outcomes.

2.2 Objectives

- **Objective 1: Comprehensive assessment of immune cell blood composition in patients with mCRPC.**

In this objective, we assess the feasibility of using CIBERSORT, a machine learning algorithm previously validated in cancers other than PCa, for immune cell deconvolution in peripheral blood samples from patients with mCRPC. We will evaluate associations between detailed profiling of the subsets of immune cells with key clinical outcomes, including OS and PFS in pre-treatment patients with mCRPC.

- **Objective 2: To develop and validate a whole blood gene expression signature in mCRPC patients.**

To address the prognostic value of genes expressed in pre-treatment samples, we will analyse the dynamics of gene expression during disease progression and perform univariate and penalized multivariable analyses to obtain a parsimonious prognostic model that can be validated in an external series.

- **Objective 3. Dynamic assessment of enzalutamide-induced changes in the blood immune cells of mCRPC patients.**

In contrast to other common cancers, immunotherapy with immune checkpoint inhibitors has not shown relevant efficacy in PCa. It is often combined with new anti-androgen therapies, the most common of which is enzalutamide. The effect of antiandrogen therapies on immune cells in the microenvironment and in the blood brings conflicting results. In this study, we will evaluate the effect of new anti-androgen therapies on blood immune cells from patients diagnosed with mCRPC.

Each of these targets is designed to address different aspects of the complex molecular and cellular environment associated with mCRPC, providing a deeper understanding of the interplay between therapy, tumour biology, and host response.

MATERIAL AND METHODS

3.1 Study design

The PREMIERE trial (NCT02288936) was a phase 2 translational, multicenter, single-arm, open-label clinical study designed to evaluate the efficacy and safety of enzalutamide as a first-line treatment in chemotherapy-naïve patients with mCRPC. Conducted across 17 hospitals in Spain, the study aimed to explore the potential of enzalutamide in delaying disease progression and improving survival outcomes in this patient population. Ethical approval was obtained from the Germans Trias i Pujol Independent Review Board (IRB) in Spain (approval number: AC-14-112-R), ensuring adherence to international ethical standards and protection of participant rights.

To further validate the findings in treatment outcomes, a distinct validation cohort was formed at the Istituto Scientifico Romagnolo per lo Studio e la Cura dei Tumori (IRST) located in Meldola, Italy. This cohort was approved by the IRST Institutional Review Board with approval number REC 2192/2013, adhering to the same stringent ethical guidelines as the main study.

3.2 Clinical data collection

Prior to treatment initiation, comprehensive baseline demographic and clinicopathological data were collected. Data collection was standardized across participating institutions through the provision of a data collection manual, and a designated data collector at each site ensured adherence to the defined protocols. Patient data were recorded and managed using a Microsoft

Excel spreadsheet, with unique identification numbers assigned to maintain patient anonymity.

The data collection involved a comprehensive set of clinical and biochemical parameters. Clinical parameters included age, race, Gleason score, PSA levels at diagnosis, disease stage, ECOG performance status, and sites of metastatic disease, specifically in bones, liver, lungs, and lymph nodes. Laboratory tests focused on hematologic parameters like hemoglobin, absolute neutrophil and lymphocyte counts, the neutrophil-to-lymphocyte ratio, and biochemical markers such as albumin, lactate dehydrogenase (LDH), and alkaline phosphatase (ALP).

The study evaluated a variety of clinical endpoints to determine the efficacy of treatment: PSA response rates, PSA progression-free survival (PSA PFS), clinical progression-free survival and radiographic progression-free survival, and the OS as defined in [Table 3.1](#). More information was also obtained concerning pain as presented, previous treatments-surgery, radiotherapy, corticosteroids, antiandrogen therapy, GnRH therapy-sequential determinations of PSA, and important dates such as diagnosis, treatment start, and progression events. Patients were followed until death or loss to follow-up, allowing for the calculation of various time-to-event measures, including time from diagnosis to metastasis and overall follow-up duration.

Clinical Endpoint	Definition
PSA response	PSA decline of 50% or greater from baseline (PSAresponse50) or 90% or greater from baseline (PSAresponse90)
PSA progression-free survival	Time from treatment initiation until date of PSA progression
Clinical progression-free survival	Time from treatment initiation until date of clinical progression
Radiographic progression-free survival	Time from treatment initiation until date of radiographic progression
OS	Time from treatment initiation until death from any cause (death)

Table 3.1: Definitions for clinical endpoints

3.3 Sample collection

3.3.1 Inclusion criteria

Patients were included in the study based on the following criteria: male patients aged 18 years or older with histologically confirmed prostate adenocarcinoma lacking neuroendocrine differentiation or small cell characteristics; documented metastatic disease with evidence of progression despite androgen-deprivation therapy (serum testosterone ≤ 50 ng/dL); ECOG performance status of 0 or 1; asymptomatic or mildly symptomatic disease (Brief Pain Inventory Short Form question 3 score < 4); and adequate organ function as evidenced by specific laboratory thresholds (e.g., absolute neutrophil count $\geq 1500/\mu\text{L}$, platelet count $\geq 100,000/\mu\text{L}$, hemoglobin ≥ 9 g/dL, bilirubin, Aspartate Aminotransferase (AST), and Alanine Aminotransferase (ALT) $\leq 2.5\times$ the upper limit of normal, creatinine ≤ 2 mg/dL, albumin ≥ 3.0 g/dL).

The exclusion criteria included any active infections or serious underlying medical conditions that may impair the effectiveness of the study; any known brain metastases or leptomeningeal involvement; any history of other malignancies, except for those patients who had been treated successfully, without evidence of recurrence, for non-melanoma skin cancer; significant haematologic, hepatic, or renal dysfunction; history of seizures or conditions that promote seizures; significant cardiovascular disease; and previous therapy that might interfere with assay results, including prior cytotoxic chemotherapy, and abiraterone acetate for PCa.

Every enrolled patient received enzalutamide at the standard oral dosage of 160 mg daily, continuing until either disease progression occurred or they experienced severe toxicity.

3.3.2 Sample acquisition

The PREMIERE study recruited 98 patients who had not previously undergone chemotherapy and were diagnosed with mCRPC. This multi-center approach ensured a diverse patient population, enhancing the generalizability of the study results. All patients received enzalutamide as a first-line treatment at a standard dose of 160 mg daily.

Figure 3.1 outlines the pre-defined time-points. Peripheral blood samples were collected from patients at three key time points:

- Pre-treatment: Prior to initiation of enzalutamide therapy.
- 12 Weeks of Treatment: After 12 weeks of continuous enzalutamide therapy.
- At Disease Progression: Upon clinical or radiographic evidence of disease progression.

A total of 238 whole-blood samples were prospectively collected from PREMIERE cohort. After quality controls, 3 blood samples were excluded due to poor RNA integrity.

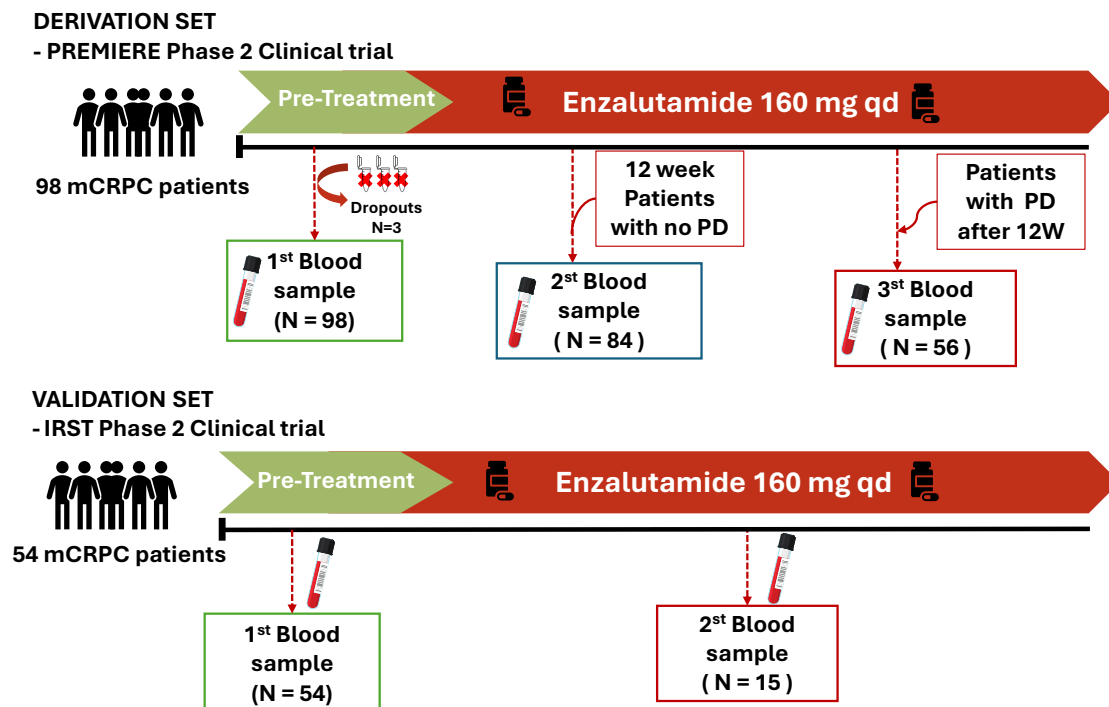


Figure 3.1: Study profile. Design and workflow of the PREMIERE trial, highlighting the three predefined time points for blood sample collection: pre-treatment, after 12 weeks (12W) of enzalutamide therapy, and at disease progression. The IRST trial is presented as an independent validation cohort, ensuring the robustness of the findings.

The IRST trial served as an independent validation set to validate the findings from the PREMIERE study, ensuring the robustness and generalizability of the results. Whole blood samples were obtained that met the same inclusion and exclusion criteria as those of the PREMIERE cohort, with the distinction that these patients had previously been treated with abiraterone acetate at 1 g daily in combination with prednisone 6 mg twice daily, before receiving enzalutamide as a second-line treatment. Samples were collected both before

treatment and during tumour progression. In total, 69 whole blood samples were acquired.

3.4 Microarray analysis

3.4.1 Sample collection and RNA extraction

Blood samples were serially collected from each participant in the study using PAXgene RNA tubes (PreAnalytiX GmbH, Hombrechtikon, Switzerland) to maintain RNA integrity. RNA isolation and purification were performed using the PAXgene Blood RNA Kit (Qiagen, Hilden, Germany) according to the manufacturer's protocol, with optimizations for maximum yield and purity. RNA quantity and quality were assessed using two complementary methods. Spectrophotometry with a NanoDrop 2000 (Thermo Scientific, Newark, DE, USA) was used to measure RNA concentration and purity ratios (A260/A280 and A260/A230). Microfluidic electrophoresis using an Agilent 2100 Bioanalyzer (Agilent Technologies, Palo Alto, CA, USA) with the RNA 6000 Nano Kit was employed to determine the RNA Integrity Number (RIN). For subsequent analyses, only RNA samples with a RIN of at least seven were chosen, thereby guaranteeing high-quality input for further applications.

3.4.2 Microarray hybridization and data acquisition

The GeneChip™ Human Transcriptome Array HTA 2.0 (902162, Affymetrix, ThermoFisher, Newark, DE, USA) was utilized for microarray analysis in order to examine comprehensive gene expression profiles. This high-density array provides comprehensive coverage of all known coding transcripts in the human genome, as well as various non-coding RNAs.

The hybridization process involved incubating 5.2 µg of biotin-labeled single-strand DNA (ssDNA) with the GeneChip™ Human Transcriptome Array HTA 2.0 for 16 hours at 45°C in a GeneChip™ Hybridization Oven 645. Following hybridization, the arrays underwent washing and staining using the GeneChip™ Fluidics Station 450 to remove non-specifically bound probes and amplify the signal. The hybridized and stained arrays were then scanned using the GeneChip Scanner 3000 7G (Affymetrix, Thermo Scientific, Newark, DE, USA) at a resolution of 0.7 µm.

3.4.3 Quality control and preprocessing

Raw microarray data were processed using the Transcriptome Analysis Console (TAC) Software (version 4.0.1, Thermo Fisher Scientific). Quality control metrics included examination of background intensity, scaling factors, and hybridization controls. Arrays failing quality control were excluded from further analysis.

Data preprocessing involved background correction, normalization, and summarization using the Robust Multi-array Average (RMA) method implemented in the "affy" package [185]. Batch effects were identified and corrected using the ComBat algorithm from the "sva" package [186]. Logarithmic transformation was applied to stabilize variance across expression levels.

3.4.4 Probe annotation

Probe set annotation was performed using the "pd.hta.2.0" package [187], ensuring accurate mapping to gene symbols and transcript IDs. Non-informative and control probe sets were filtered out prior to downstream analysis.

3.5 Differential gene expression analysis

Differentially expressed genes (DEGs) were identified using the limma package [188]. We performed individual paired-wise comparisons of whole-blood gene expression (GE) in mCRPC patients treated with enzalutamide. To ensure more accurate results, the sample numbers were reduced by applying strict filtering criteria. In the 12-week patient group, we excluded patients with a progression-free survival (PFS) of less than 3 months and those without a 50% reduction in PSA levels (PSAresponse50).

Pairwise comparisons were performed between pre-treatment and 12 weeks of treatment, pre-treatment and disease progression, and 12 weeks of treatment and disease progression.

Statistical significance was determined using paired t-tests, with p-values adjusted for multiple comparisons using the Benjamini-Hochberg false

discovery rate (FDR). Significant DEGs were identified using thresholds of adjusted p-value (FDR) < 0.05 and absolute \log_2 fold change ($|\log_2FC| > 1$).

3.6 Gene set enrichment analysis

Gene set enrichment analysis was performed using the clusterProfiler [189] package in the R environment for statistical analysis. Within the R environment, the normalized enrichment score (NES), p-value, and false discovery rate (FDR) for all variables and signatures were calculated. The analysis utilized the Gene Ontology (GO) biological processes/pathways database [190] along with the Kyoto Encyclopedia of Genes and Genomes (KEGG) pathways [191]. GSEA was performed using a pre-sorted gene list based on \log_2FC values. Pathways with FDR-adjusted p-values < 0.05 were considered significantly enriched.

3.7 Immune cell profiling using CIBERSORTx

For the immune cell profiling in our study, we used CIBERSORT [192, 193], a machine learning algorithm that quantifies 22 different immune cell subtypes. The platform employs a specific leukocyte gene signature matrix, known as LM22, which consists of 547 genes that are able to distinguish these immune cell subtypes.

Normalized gene expression data were uploaded to the CIBERSORTx platform¹, selecting the LM22 database, disabling normalization by quartiles, and setting the allowances to 1000 to improve the accuracy and reliability of the deconvolution results. Relative mode was selected to estimate the proportion of each immune cell type within the sample.

Only samples with a CIBERSORTx deconvolution p-value < 0.05 were considered for further analysis, ensuring high confidence in the estimated immune cell fractions.

¹ <https://cibersortx.stanford.edu>

3.8 *In vitro* Experiments

3.8.1 Cell lines and culture conditions

The cells used in this study were obtained from a private collection at Hospital 12 de Octubre, as well as from the American Type Culture Collection (ATCC). The following human cell lines were used: Jurkat and MOLT-4 T-cell lines, the THP-1 monocyte line, the Raji B-cell line, and prostate cancer cell lines LNCaP, 22Rv1, and DU145. All cell lines were cultured in RPMI-1640 medium supplemented with 10% fetal bovine serum (FBS), 100 U/mL penicillin, and 100 µg/mL streptomycin, and maintained at 37°C.

3.8.2 Cell viability assays

Cell viability was measured using the CellTiter-Glo Luminescent Cell Viability Assay (Promega). Cells were plated in white 96-well plates at a density of 1×10^5 cells/well, treated with the respective drugs, and processed according to the manufacturer's protocol. Luminescence was recorded using a BioTek Synergy HT microplate reader, and viability was calculated relative to untreated controls.

3.8.3 Apoptosis assays

Apoptosis was assessed by Western blot analysis to detect the cleavage of caspase-3 and poly (ADP-ribose) polymerase (PARP). Protein lysates were prepared using RIPA buffer containing protease and phosphatase inhibitors, and protein concentrations were determined using the Bicinchoninic Acid (BCA) Protein Assay Kit (Thermo Fisher Scientific). Proteins (30 µg per sample) were separated by SDS-PAGE, transferred to PVDF membranes, and probed with primary antibodies, including cleaved caspase-3 (Cell Signaling Technology, 1:1,000), cleaved PARP (Cell Signaling Technology, 1:1,000), AR (Santa Cruz Biotechnology, 1:500), and GAPDH (Cell Signaling Technology, 1:5,000) as a loading control. Membranes were incubated with HRP-conjugated secondary antibodies (1:5,000) and visualized using the SuperSignal West Femto Maximum Sensitivity Substrate (Thermo Fisher Scientific). Images were captured using a ChemiDoc MP Imaging System (Bio-Rad).

3.8.4 Use of different antiandrogens

Cells were treated with enzalutamide and other AR inhibitors, including abiraterone acetate, bicalutamide, apalutamide, and darolutamide, at physiologically relevant concentrations for 72 hours. Apoptosis was evaluated by measuring the expression of cleaved PARP and cleaved Caspase 3 using Western blot analysis. Cells were treated with enzalutamide for 48 hours before protein extraction and analysis. For gene expression profiling, RNA was extracted from treated and untreated cells using the RNeasy Mini Kit (Qiagen) following the manufacturer's instructions.

3.8.5 Gene expression profiling in cell lines

Total RNA was extracted from treated and control cells using the RNeasy Mini Kit (Qiagen). RNA quality was assessed using an Agilent 2100 Bioanalyzer. Gene expression profiling was performed using the Affymetrix Human Transcriptome Array 2.0. Data preprocessing, normalization, and analysis were conducted as described in the [Section 3.4](#).

3.9 Statistical analysis

A comprehensive statistical analysis was conducted to determine the association of gene expression profiles and immune cell compositions with clinical outcomes in mCRPC patients treated with enzalutamide. All statistical analyses were performed using R statistical software (version 4.4.1) [194] and Rstudio [195]. To ensure transparency and reproducibility, all scripts used for data processing, statistical modelling, and visualization are publicly available at GitHub repository (<https://github.com/enriiquee/thesis-script>).

3.9.1 Survival analysis

The main endpoint of the study was OS, defined as the time from the start of enzalutamide therapy to death due to any cause. Patients alive at last follow-up were censored at that date. Survival analyses were performed by using the Kaplan-Meier method and Cox proportional hazards regression models implemented in "survival" [196] and "survminer" [197] packages.

Univariate analysis

The univariate Cox proportional hazards regression model was used to identify the relationship between OS and individual variables, including immune cell proportions estimated from gene expression data and the expression levels of specific genes. Variables with a p-value less than 0.05 were considered statistically significant and included in further analyses. The Kaplan-Meier survival plot was used to compare OS between subgroups of patients. Based on median values of immune cell proportions or risk scores from prognostic models, patients were divided into "high" and "low" groups. The log-rank test, a non-parametric method, was used for testing the difference in survival distribution between the two groups.

Multivariable analysis

Multivariable Cox proportional hazards regression models were constructed for the various potential confounders. Clinical factors included ECOG performance status, pattern of metastatic spread, PSA levels, ALP, lactate dehydrogenase (LDH), pain score assessed by the Brief Pain Inventory, neutrophil-lymphocyte ratio (NLR), and corticosteroid use. Molecular variables studied included the presence of CTC and AR gene amplification detected in circulating tumor DNA.

In the multivariable model, backward stepwise selection was used to identify significant predictors. The model iteratively dropped variables according to the Akaike Information Criterion, AIC, toward the most parsimonious model that best fit the data. This approach balances model complexity with explanatory power, reducing the risk of overfitting.

3.9.2 Development and validation of prognostic models

The candidate genes were identified using univariable Cox regression analyses on DEGs, taking into consideration genes with a p-value less than 0.05. These candidate genes were further used with machine learning techniques to develop predictive models for risk stratification of the patients concerning adverse outcome.

First, the lasso regression was a type of regularized Cox regression applied for variable selection and shrinkage. It conducts feature selection by shrinking the coefficients of less important variables to zero using the L1 penalty controlled

by the parameter λ . For Lasso, the penalty parameter λ was optimized separately with 10-fold cross-validation in order to minimize partial likelihood deviance for enhanced model generalizability. This is particularly useful in high-dimensional data analyses, as it handles multicollinearity and selects the most relevant features for the predictive model.

Complementary to the Lasso regression, Elastic Net regression was also performed, which contains features of both L1 and L2 penalties. Just like Lasso, the best value for the parameter λ in Elastic Net is also chosen by performing a grid search through possible values to strike an optimal balance among feature selection, coefficient shrinkage, and overall model performance.

To evaluate the performance of the model, several statistical parameters were taken into account. First, the C-index was calculated as a measure of the model's discrimination ability. An integrated Brier score was calculated to measure the overall accuracy of survival predictions over time. In addition, time-dependent receiver operating characteristic analyses were performed with the "timeROC" package [198], calculating AUCs at several time points, for instance, at 12, 24, and 36 months, to assess the performance of the models across different timeframes.

The final prognostic model was verified by the independent IRST cohort. Risk scores for each patient were calculated in accordance with the expression level of genes in the signature and coefficients derived from Lasso regression. Patients were divided into two groups: the high-risk group and the low-risk group, based on the median cutoff value of the risk score. Survival curves were drawn in accordance with the Kaplan-Meier method for the validation cohort, and differences in survival among the different risk groups were compared by the log-rank test.

3.9.3 Data visualization

Principal component analysis (PCA) was performed using the "prcomp" function in R to reduce the dimensionality of the gene expression data to visualize sample clustering based on treatment time points, including pre-treatment, 12 weeks, and progression. "hclust" function was performed for hierarchical clustering analysis with Euclidean distance and complete linkage to group the samples of similar expression profiles and make it easier to identify patterns linked to treatment response and disease course. Boxplots were generated using the "ggplot2" package [199] for the visualization of the distribution of immune cell proportions and gene expression levels.

PROGNOSTIC IMPLICATION OF BLOOD IMMUNE CELL COMPOSITION IN mCRPC

4.1 Introduction

The prognosis for metastatic prostate cancer (PCa) shows considerable variability, with survival times ranging from a few months to several years [200]. Numerous prognostic factors and variant prognostic models have been developed based on specific clinical contexts and treatment regimens.

The peripheral blood of patients with mCRPC offers prognostic insights beyond merely identifying tumour constituents. This arises from a complex interaction among the tumour, bone marrow, and host immune system. Prior studies have demonstrated the prognostic significance of whole-blood RNA signatures [182, 183], notably in genes related to hematopoiesis and immune function. Additionally, blood composition assessed through specific cellular elements in the complete blood count, such as an elevated neutrophil-to-lymphocyte ratio (NLR), can also serve as a prognostic indicator [201–207]. An enhanced understanding of the dynamic interactions between cancer and immune cells could yield vital prognostic information regarding mCRPC.

The composition of immune cells in the blood comprises over 22 unique cell types that can be identified either by flow cytometry or recently by blood cell deconvolution using gene expression arrays. CIBERSORT-X is a machine learning deconvolution algorithm validated for blood immune cell analyses [192, 193]. This approach provides technical benefits for the analysis of samples

in central reference laboratories and offers a methodology suitable for implementation in multicenter clinical trials.

This chapter focuses on elucidating how various immune cell populations influence the prognosis of patients with mCRPC. We conducted analyses on pre-treatment blood samples that were prospectively collected from participants in a phase 2 multicenter biomarker study, which evaluated the deployment of enzalutamide as an initial treatment for mCRPC. The findings were subsequently confirmed in a separate cohort of mCRPC patients.

4.2 Material and methods

4.2.1 Study design and data collection

In this chapter, only the pretreatment patients described in [Section 3.3](#) are used. The RNA-seq expression data were analysed following the protocols described in [Section 3.4](#) of the [Microarray analysis](#) chapter.

4.2.2 Inference of immune cell profiling

For the immune cell profiling in our study, we used CIBERSORT. This tool has been explained in detail in [Section Immune cell profiling using CIBERSORTx](#)

4.2.3 Statistical analysis

All statistical analyses were performed using R software (version 4.4.1) [[194](#)]. The survival analyses utilized the Cox proportional hazards regression model [[208](#)], the log-rank test [[209](#)], and the Kaplan–Meier approach [[210](#)]. Hazard ratios (HRs) were presented as relative risks with their associated 95% confidence intervals (CIs). A two-tailed $p < 0.05$ was regarded as statistically significant. Survival curves were developed to illustrate the effects of different immune cell populations on patient outcomes. Patients were classified into ‘high’ and ‘low’ groups, defined by whether their immune cell counts were above or below the median values, respectively. This stratification method facilitates an unbiased comparison of survival outcomes across the groups. The relationship between immune cell proportions and patient survival was

analyzed using multivariate Cox proportional hazards models. This analysis adjusted for confounding factors such as ECOG performance status, disease dissemination pattern, PSA levels, ALP, LDH, Brief Pain Inventory pain scores, NLR, and corticosteroid usage. These adjustments enabled a thorough assessment of each variable’s independent impact on survival outcomes.

4.3 Results

4.3.1 Study population

The study included 152 chemotherapy-naïve individuals diagnosed with mCRPC, from whom blood samples were collected prior to commencing enzalutamide treatment. The PREMIERE cohort consisted of 98 patients who were part of a phase 2 clinical trial focused on biomarkers. All participants had whole-blood samples accessible for pre-treatment analysis. Gene expression data arrays were obtained for 95 participants, while three were excluded due to technical issues stemming from low-quality RNA (Figure 4.1).

The characteristics of the patients for the PREMIERE cohort are described in Table 4.1.

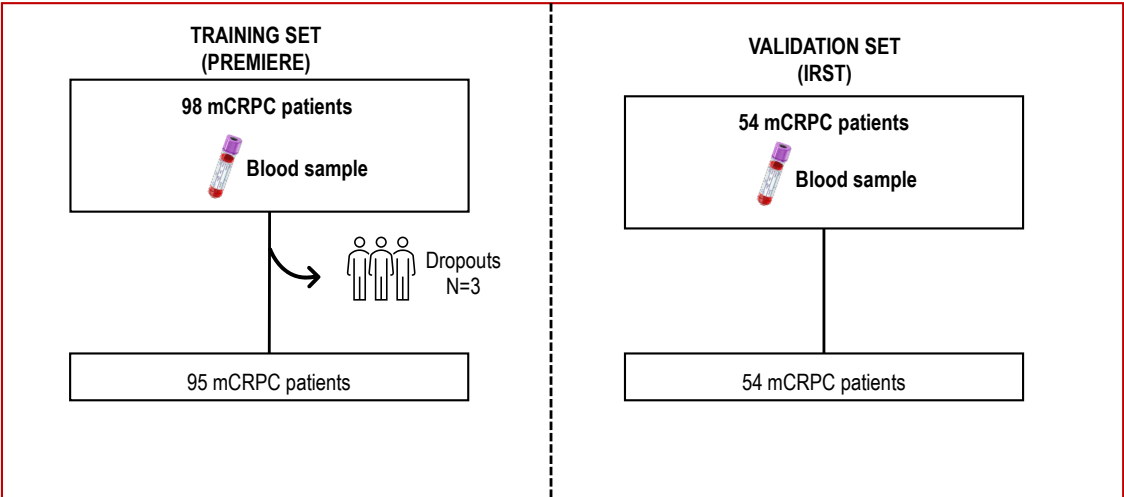


Figure 4.1: Consort diagram. This study analyses pre-treatment whole blood samples from mCRPC patients prospectively treated with enzalutamide, including PREMIERE cohort comprised of 98 patients from a phase 2 biomarkers clinical trial, and an independent validation cohort (IRST) including 54 patients

Patient characteristics	Values	Patient characteristics	Values
Age median (range)	77 (57-95)	Metastases N (%)	
OS [months]	34.35 (2.3-44.69)	Bone metastasis (BM)	80 (81.63 %)
PFS [months]		Visceral metastasis (VM)	17 (17.35 %)
PSA	10.86 (0.92-44.68)	Lung	16 (16.33 %)
Rad.	16.57 (0.89-44.68)	Liver	4 (4.08 %)
Death		Lymph nodes metastasis	47 (47.96 %)
Yes	50 (51.02 %)	Metastases N (range)	2 (0-10)
No	48 (48.98 %)	PSA basal [ng/mL]	24.95 (0.59-4318.78)
Gleason score		PSA kinetics	
<= 7	53 (54.08 %)	PSA50%	
>7	43 (43.88 %)	Yes	81 (82.65 %)
ECOG score		No	17 (17.35 %)
0	53 (54.08 %)	PSA90%	
1	45 (45.92 %)	Yes	52 (53.06 %)
Primary treatment		No	46 (46.94 %)
Yes	45 (45.92 %)	Sero albumin [g/L]	4.16 (3.29-5)
No	53 (54.08 %)	Haemoglobin [g/L]	13.2 (7.5-17.3)
Surgery		ALP	
Yes	22 (22.45 %)	High	28 (28.57 %)
No	76 (77.55 %)	Low	70 (71.43 %)
Radiotherapy		LDH	
Yes	25 (25.51 %)	High	31 (31.63 %)
No	73 (74.49 %)	Low	66 (67.35 %)
Pain		NLR	
Mild (≤ 3 BPI score)	52 (53.06 %)	≤ 5	90 (91.84 %)
No pain	45 (45.92 %)	>5	8 (8.16 %)
Bicalutamide		CTCs	
Yes	85 (86.73 %)	Yes	35 (35.71 %)
No	13 (13.27 %)	No	63 (64.29 %)

Table 4.1: Patients' characteristics. Characteristics of patients included in the PREMIERE clinical trial

4.3.2 Immune cell composition in peripheral blood

The relative proportions of 22 immune cell types in peripheral blood of the PREMIERE cohort were quantified using the CIBERSORT algorithm. The distribution of immune cell subsets is illustrated in [Figure 4.2](#). Neutrophils constituted the predominant immune cell population, with a median proportion of 62.5% (interquartile range [IQR]: 55.0%–69.8%). Resting natural killer (NK) cells were the second most abundant cell type (median: 8.3%, IQR: 5.6%–11.2%), followed by resting memory CD4+ T cells (median: 7.4%, IQR: 5.4%–10.0%), monocytes (median: 6.5%, IQR: 4.7%–9.1%), and CD8+ T cells (median: 5.2%, IQR: 3.4%–7.8%). Memory B cells and resting mast cells were present in lower proportions.

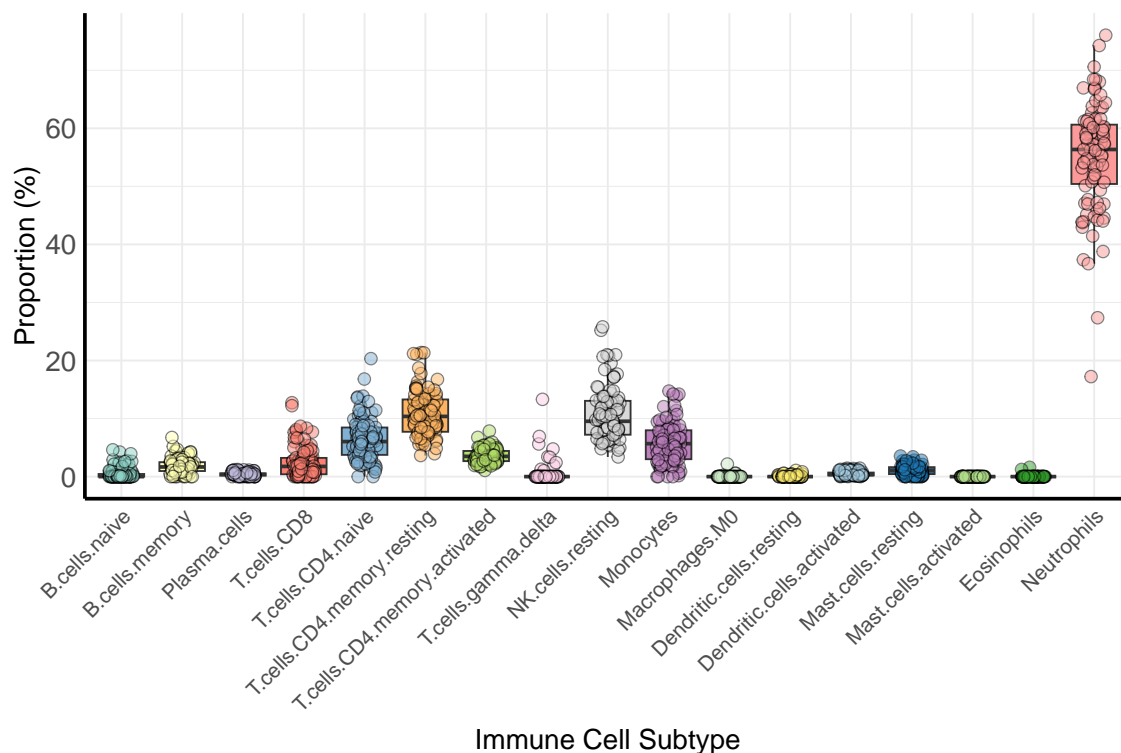


Figure 4.2: Blood immune-cell composition. The figure shows the relative proportion of immune cell components in the blood in the PREMIERE set.

4.3.3 Association of immune cell subsets with OS

To assess the prognostic value of distinct immune cell subsets, Cox regression analyses were conducted to determine the impact of specific immune cell types on overall survival (OS) within the PREMIERE cohort. The findings are detailed in [Table 4.2](#).

Elevated monocyte levels were significantly associated with shorter OS (hazard ratio [HR] 1.96, 95% confidence interval [CI] 1.11–3.45; $p < 0.019$). Specifically, an increase of one unit in the proportion of monocytes doubles the risk of death. In contrast, higher levels of CD8+ T cell infiltrates were associated with improved OS, with an HR of 0.51, 95% CI 0.29–0.90; $p < 0.018$, indicating that patients with higher levels of these cells had approximately half the risk of death compared to those with lower levels. Although activated dendritic cells showed a trend toward significance, this did not reach the statistical threshold (HR 1.65, 95% CI 0.94–2.89; $p = 0.081$).

For visualizations, the median proportions of infiltrated monocytes and CD8+ T cells in samples stratified patients into the “high” and “low” groups. Kaplan-Meier survival analyses showed that those with high levels of

Blood Immune Cell Type	HR (95% CI)	p Value
B cells Memory	1.21 (0.69–2.12)	0.506
T cells CD4 memory, resting	0.72 (0.41–1.26)	0.252
Plasma cells	1.32 (0.76–2.31)	0.323
T cells CD8	0.51 (0.29–0.9)	0.018
T cells CD4-naive	1.11 (0.64–1.94)	0.71
T cells CD4 memory, activated	0.87 (0.50–1.51)	0.617
NK cells, resting	0.92 (0.53–1.61)	0.78
Monocytes	1.96 (1.11–3.45)	0.019
Neutrophils	0.98 (0.56–1.71)	0.935
Dendritic cells, activated	1.65 (0.94–2.89)	0.081
Mast cells, resting	0.92 (0.53–1.61)	0.775

Table 4.2: Univariate Cox regression analyses of immune cell subsets and OS in the PREMIERE cohort

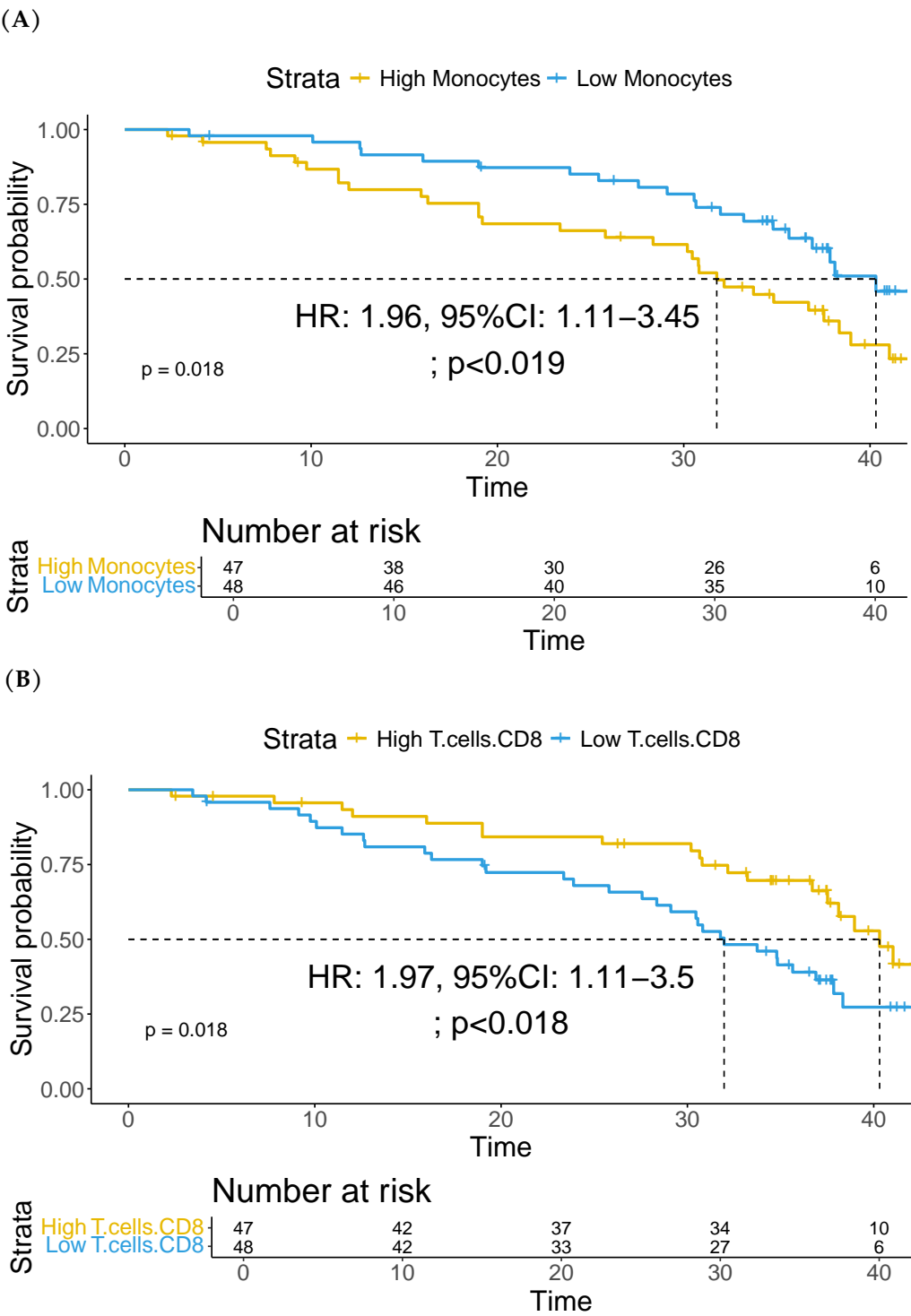
monocytes demonstrated considerably worse median OS when compared with the low-infiltration group (32.2 months vs 40.3 months; log-rank $p = 0.018$; [Figure 4.3A](#). Similarly, patients with low levels of CD8+ T cells had a lower median OS than patients with high levels of CD8+ T cells: 31.8 months versus 40.3 months, log-rank $p = 0.009$; [Figure 4.3B](#).

4.3.4 Validation in an independent cohort

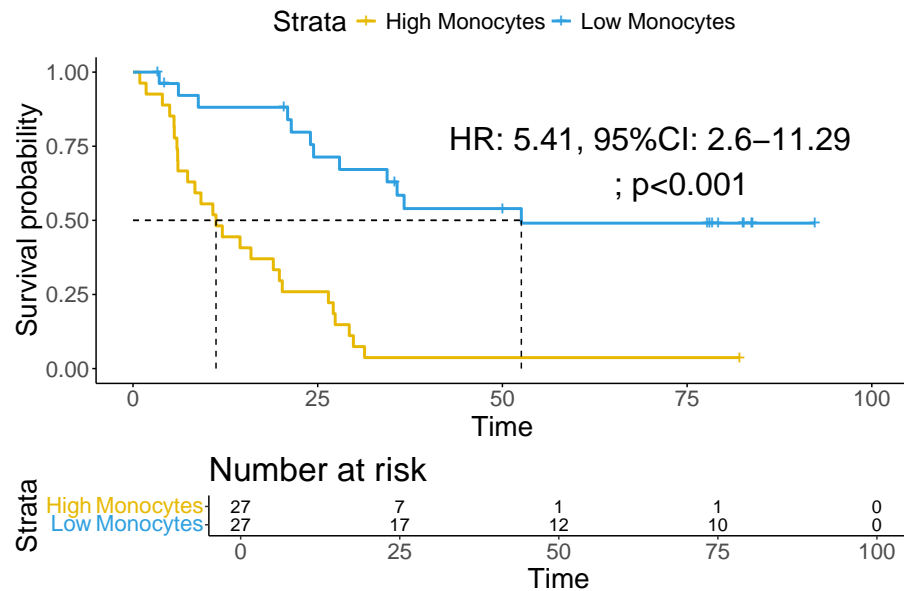
These findings were validated in a separate validation cohort (IRST) of 54 mCRPC patients treated with enzalutamide.

The adverse prognostic impact of elevated monocyte levels was replicated in the IRST cohort (HR 5.41, 95% CI 2.60–11.29; $p < 0.001$). Interestingly, the effect size of the hazard ratio in the IRST cohort was greater, which reinforces that a higher number of monocytes has a constant and positive impact on survival status. Again, the interaction that improved OS based on an increasing proportion of CD8+ T cells was reaffirmed within this model [HR 0.48, 95% CI 0.25–0.92; $p = 0.027$]. A summary of these findings is provided in [Table 4.3](#), and the associated Kaplan–Meier plots for OS in this cohort are shown in [Figure 4.3C](#) and [Figure 4.3D](#).

A summary of these findings is provided in [Table 4.3](#), and the associated Kaplan–Meier plots for OS in this cohort are shown in [Figure 4.3C](#) and [Figure 4.3D](#).



(C)



(D)

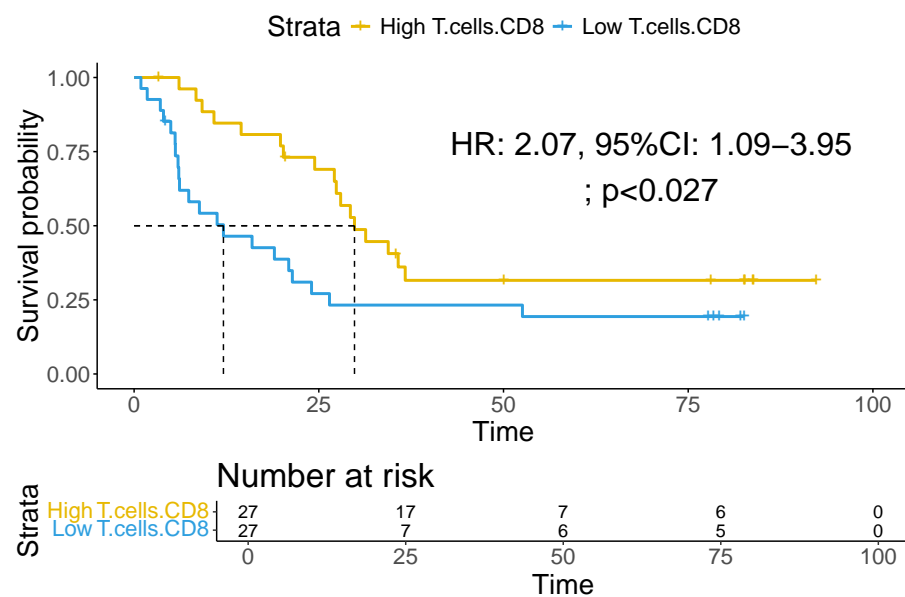


Figure 4.3: Kaplan–Meier survival curves for monocytes and CD8+ T cells in PREMIERE and IRST cohorts. (A) OS based on monocyte level in the PREMIERE cohort. (B) OS based on CD8 T-cell level in the PREMIERE cohort. (C) OS based on monocyte level in the IRST cohort. (D) OS based on CD8 T-cell level in the IRST cohort.

Blood Immune Cell Type	HR (95% CI)	Pa
B cells memory	0.88 (0.46-1.67)	0.695
Plasma cells	1.66 (0.87 -3.14)	0.123
T cells CD8	0.48 (0.25 -0.92)	0.027
T cells CD4 naive	0.47 (0.25 -0.91)	0.023
T cells CD4 memory resting	0.65 (0.34 -1.24)	0.194
T cells CD4 memory activated	0.68 (0.36 -1.29)	0.235
NK cells resting	0.98 (0.52 -1.85)	0.943
Monocytes	5.41 (2.60 -11.29)	0.001
Dendritic cells activated	2.49 (1.28 -4.81)	0.006
Mast cells resting	0.83 (0.44 -1.56)	0.557
Neutrophils	1.08 (0.57 -2.05)	0.811

Table 4.3: Univariate Cox regression analyses of immune cell subsets and OS in the validation cohort

4.3.5 Multivariate analysis

Multivariate Cox regression analyses adjusting for established clinical prognostic factors were performed to assess the independence of the prognostic significance of monocyte and CD8+ T cells. ECOG performance status, metastatic spread pattern (bone-only vs. visceral involvement), log-transformed PSA levels, ALP, LDH, pain score (BPI), neutrophil to lymphocyte ratio (NLR) and corticosteroid use were included in the multivariate model. The results are shown in [Table 4.4](#).

In this adjusted model, the levels of CD8+ T cells were still significantly associated with OS: HR 0.63, 95% CI 0.41-0.98; $p = 0.040$, while this means that their prognostic value is independent of other clinical factors. Likewise, in the multivariate analysis, the statistical significance was not held by the levels of monocytes: HR 1.05, 95% CI 0.74-1.49; $p = 0.770$, suggesting their prognostic impact might be mediated by other clinical variables. In particular, higher LDH levels (HR 1.91, 95% CI 1.02–3.60; $p = 0.045$) and higher log-transformed PSA levels (HR 1.44, 95% CI 1.18–1.76; $p = 0.001$) were independently associated with worse OS.

In addition, we performed a multivariate analysis including molecular prognostic markers such as AR gene amplification (AR gain) and the presence of circulating tumour cells (CTCs). In this model ([Table 4.5](#)), CD8+ T cell levels continued to show independent prognostic value (HR 0.54, 95% CI 0.35–0.83; $p = 0.006$). AR gain (HR 6.17, 95% CI 2.83–13.46; $p < 0.001$) and the presence of CTCs (HR 4.63, 95% CI 2.58–8.31; $p < 0.001$) were both strongly associated with poorer OS.

Prognostic	HR (95% CI)	p Value
LDH_Mod	1.91 (1.02–3.60)	0.045
ALP_Mod	1.84 (0.99–3.342)	0.055
Pattern Of Spread	1.08 (0.24–4.82)	0.922
BPI	0.59 (0.30–1.14)	0.117
LogPSA	1.44 (1.18–1.76)	0.001
NLR	0.70 (0.36–1.34)	0.279
Monocytes	1.05 (0.74–1.49)	0.770
CD8 T cells	0.63 (0.41–0.98)	0.04
ECOG	1.33 (0.71–2.50)	0.371

Table 4.4: Multivariate Cox regression analysis including clinical variables

	HR (95% CI)	p Value
ARgain	6.17 (2.83–13.46)	<0.001
T cells CD8	0.54 (0.35–0.83)	0.006
CTCs	4.63 (2.58–8.31)	<0.001

Table 4.5: Multivariate Cox regression analysis including molecular variables

4.4 Summary

In this chapter, we have demonstrated that the composition of peripheral blood immune cells, in particular the proportions of monocytes and CD8+ T cells, holds a significant prognostic value in mCRPC patients. Applying the CIBERSORT algorithm to pre-treatment blood gene expression of patients, we determined that high monocytes exhibit a negative effect on OS, while their survival improves with higher proportional abundances of CD8+T cells. These findings have been subjected to internal validation in a second set apart from our series, increasing external validity and clinical utility in perspective.

Notably, the prognostic value of CD8+ T cells remained after adjustment for established clinical and molecular prognostic variables, including ECOG performance status, levels of PSA, ALP, lactate dehydrogenase, NLR, AR gene amplification, and the presence of CTCs. This underlines the potential value of CD8+ T cell levels as a possible independent biomarker for the risk stratification of patients with mCRPC.

Our study demonstrates the feasibility and utility of gene expression-based immune cell profiling using CIBERSORT in a multicenter clinical trial setting. This approach offers a practical and scalable method for assessing immune cell populations without the need for complex flow cytometry techniques and is thus suitable for large-scale clinical applications.

Thus, the identification of monocyte and CD8+ T-cell biomarkers has enormous implications in terms of prognosis and treatment of mCRPC. This should not only improve the immune profile in clinical management, aiding in better stratification of patients, but should also aid in therapeutic choice to include those who are likely to benefit from the use of immunotherapeutic interventions alone or in combinations of immune-modulating therapies. In addition, variations in immune cellular composition measured over time may indicate plausible response to treatment and disease development.

In summary, our findings point to circulating monocytes and CD8+ T cells as significant predictors of clinical outcomes in patients with mCRPC. Immune cell profiles may add significant value to clinical protocols regarding risk stratification and treatment personalization with a view to improving outcomes in advanced prostate cancer. These findings warrant further investigation of immunological biomarkers and therapeutic strategies in mCRPC.

PROGNOSTIC GENE EXPRESSION SIGNATURE IN mCRPC: DEVELOPMENT, VALIDATION AND ANALYSIS OF DISEASE PROGRESSION

5.1 Introduction

The management of mCRPC remains a significant challenge in oncology, and patients exhibit various responses to available treatments. In recent years, the emergence of high-throughput genomic technologies has facilitated the development of more individualized strategies for predicting cancer outcomes and tailoring treatment plans. Gene expression signatures, in particular, have emerged as powerful tools for stratifying patients and predicting disease outcomes.

In this chapter, we used an integrated machine learning approach to develop a novel gene expression-based signature that predicts the prognosis in mCRPC. Our approach combined the power of multiple machine learning algorithms like LASSO, Ridge regression, Elastic Net regression, and RSF to identify a robust set of genes associated with OS. This integrative approach allowed us to leverage the strengths of each technique while ensuring model generalizability and reproducibility.

The study utilized gene expression data from the PREMIERE trial, a multicenter phase II clinical trial of enzalutamide in mCRPC, and validated the findings in an independent cohort from the IRST study. Peripheral blood samples were

analyzed to capture the systemic molecular landscape of mCRPC, reflecting both the tumour microenvironment and the host's response to therapy. We found a 22-gene prognostic signature that demonstrated strong predictive performance across both cohorts by integrating state-of-the-art computational tools with rigorous statistical evaluation.

The prognostic signature developed in this chapter has the potential to significantly impact clinical practice. It could enable more accurate risk stratification of patients, inform treatment selection, and ultimately improve patient outcomes and quality of life. Furthermore, elucidating the biological pathways represented by signature genes may provide novel insights into the mechanisms of disease progression and therapeutic resistance in mCRPC, potentially revealing new therapeutic targets.

5.2 Material and methods

All patients included in this analysis were selected from the PREMIERE and IRST studies. Genomic data were previously processed and explained in the **Material and Methods** section of this thesis. Here, we detail the specific selection and analysis methods applied to the pre-treatment patients to derive the prognostic gene signature.

5.2.1 Processing of gene expression data

As explained in the **Material and Methods** section of this PhD thesis, this and the following chapters will use samples from PREMIERE and IRST studies, as well as genomic results obtained from microarray analysis conducted following the protocols outlined in **Section 3.4** of the **Microarray analysis** chapter and **Differential gene expression analysis** chapter.

5.2.2 Univariate Cox Proportional Hazards Regression

Univariate Cox proportional hazards regression was explored to find out the relationship between OS and DEG expression levels. Each gene was separately analysed for its possible prognostic value. This was done using the survival package in R, where for each gene, a calculation of HRs and p-values was

performed. Those genes whose $p < 0.05$ were considered significant for survival and were therefore selected as further candidate predictors for modelling.

5.2.3 Development and validation of prognostic gene signature

We explored both linear and nonlinear modelling strategies to derive a robust prognostic gene signature from candidate predictors. Linear methods included L1-regularized (LASSO), L2-regularized (Ridge), and their combination through the Elastic Net algorithm, while Random Forests provided a non-linear alternative. These penalized Cox models, Lasso and Ridge and Elastic Net, were performed using the "glmnet" package [211], while RSF was fit by using the "randomForestSRC" package [212]. Model training and hyperparameter tuning have been executed in a 10-fold cross-validation manner with the aim of robustness in performance and avoidance of overfitting.

In penalized Cox models, hyperparameter tuning was performed by minimizing the partial likelihood deviance over a range of penalty strengths. For Elastic Net, an additional hyperparameter, alpha, was optimized to balance L1 and L2 regularization. Optimal hyperparameters were identified by selecting the parameter combination that produced the lowest partial likelihood deviation across all cross-validation folds. For RSF, two primary hyperparameters, ntree and nodesize, were systematically varied via grid search, and each configuration was evaluated by measuring concordance indices to determine the combination displaying consistent predictive performance.

From these compared models, the final prognostic signature was chosen to balance performance considering the C-index, which quantifies the ability of each algorithm to distinguish between the high- and low-risk patient groups. Following cross-validation, the final models were retrained on the entire dataset, and the C-index was recalculated to confirm their predictive performance.

5.2.4 Validation of the prognostic signature

The independent IRST cohort was utilized to validate the prognostic signature. Risk scores for patients were obtained by calculating gene expression levels against the coefficients of the final model. Based on the median risk score, patients were categorized into high-risk and low-risk groups. Kaplan-Meier

survival analyses were conducted, and the divergence between the risk groups was evaluated using the log-rank test.

Time-dependent ROC analyses were performed at clinically relevant time points (12, 18, 24, 30, 33, and 36 months). The predictive performance of our signature was compared with established prognostic models from Olmos et al. (15-gene signature) [183], Ross et al. (6-gene signature) [182], and Wang et al. (4-gene signature) [184].

5.3 Results

Our study aimed to develop and validate a robust gene expression signature to predict OS in patients with mCRPC. Our analysis of gene expression profiles revealed 1,920 DEGs between progression and pre-treatment samples. This robust set of DEGs formed the foundation for our subsequent analyses aimed at developing a prognostic gene signature for mCRPC.

5.3.1 Univariate Cox regression

To refine our list of candidate genes, we performed univariate Cox proportional hazards regression on each of the 1,920 DEGs. This rigorous statistical approach identified 74 genes significantly associated with OS (Log-rank $P < 0.05$). These genes represent potential prognostic markers and offer insights into the molecular mechanisms underlying mCRPC progression.

5.3.2 Development and validation of prognostic models

We employed four advanced machine learning techniques to develop prognostic models: Ridge regression, Lasso regression and Elastic Net regression. Model performance was evaluated using 10-fold cross-validation, with the concordance index (c-index) serving as our primary metric of discriminative ability. All validations were carried out using an independent dataset, IRST, to ensure robust assessment of model generalizability.

Table 5.1 summarizes the performance of these models, including the number of genes retained, training c-index, and validation c-index on the IRST dataset.

Model	Number of Genes	Training C-index	Validation C-index
Ridge	74	0.826	0.737
Lasso	22	0.868	0.774
Elastic Net	23	0.873	0.772

Table 5.1: Comparison of regularized regression models

Ridge regression

Ridge regression, which applies L2 regularization to all features, was the first model trained on the candidate genes identified through univariate analysis. The model aims to retain all genes while shrinking their coefficients toward zero, reducing the risk of overfitting when many genes are weakly correlated with the outcome. Ridge regression performed well, achieving a train c-index of 0.826. The test c-index of Ridge regression on an independent dataset set was 0.737, indicating good generalization ability. Ridge regression is particularly suitable for high-dimensional data where many features contribute marginally to the outcome.

Lasso regression

Lasso regression was applied to further reduce the dimensionality of the data by penalizing the absolute value of the coefficients (L1 regularization), driving some coefficients to zero and thus performing variable selection. This approach identified a subset of the most relevant genes while discarding less informative features.

Lasso regression, employing L1 regularization, emerged as our top-performing model. It achieved a training c-index of 0.868 and a test c-index of 0.774 on the IRST validation set, demonstrating superior generalization capability. Crucially, Lasso regression distilled our initial gene set to a focused 22-gene signature, capturing the most informative prognostic markers for mCRPC.

Elastic Net regression

Elastic Net regression combines both L1 and L2 penalties, offering a balance between Ridge and Lasso regression. This method is especially useful when multiple features are correlated, as it retains the advantages of both regularization techniques. Elastic Net showed comparable performance to Lasso, with a training c-index of 0.873 and a test c-index of 0.772 on the IRST

dataset. This method identified a 23-gene signature, providing a balance between model parsimony and comprehensive gene representation.

5.3.3 Gene model (Content censored)

Given its optimal performance in terms of both parsimony and predictive power, we selected the Lasso regression model for our final 22-gene prognostic signature. The coefficients of this model, which represent the contribution of each gene to the overall prognostic score, are presented in Table 5.2. These coefficients can be used to calculate a risk score for individual patients, with higher positive coefficients indicating genes associated with a poorer prognosis and negative coefficients indicating genes associated with a better prognosis.

Note

This section has been removed in this version because it is subject to technology protection and/or knowledge transfer processes. The original content is only available in the unabridged version of the thesis, temporarily restricted by the General Doctoral Commission of the University of Murcia.

Gene	Coefficient	Gene	Coefficient
G***1	0.517364	G***12	0.119308
G***2	0.469121	G***13	0.100680
G***3	0.290974	G***14	0.058931
G***4	0.290191	G***15	0.021022
G***5	0.287535	G***16	0.011279
G***6	0.235089	G***17	0.007688
G***7	0.231427	G***18	-0.039713
G***8	0.178509	G***19	-0.120376
G***9	0.131916	G***20	-0.168221
G***10	0.129305	G***21	-0.224362
G***11	0.128270	G***22	-0.310436

Table 5.2: Lasso regression model coefficients (Gene names censored due to patenting process)

5.3.4 Time-Dependent ROC analysis and model comparison

To evaluate the dynamic predictive accuracy of our 22-gene signature and compare it with existing models, we performed a time-dependent Receiver

Time (months)	PREMIERE Cohort			IRST Cohort		
	AUC	95% CI Lower	95% CI Upper	AUC	95% CI Lower	95% CI Upper
12	0.972	0.944	1.000	0.813	0.638	0.933
18	0.898	0.796	0.981	0.834	0.690	0.950
24	0.936	0.878	0.981	0.826	0.711	0.928
30	0.905	0.821	0.975	0.842	0.726	0.943
33	0.897	0.796	0.966	0.830	0.714	0.945
36	0.898	0.805	0.966	0.829	0.697	0.944

Table 5.3: Time-Dependent AUC values for our 22-gene signature

Operating Characteristic (ROC) analysis using the riskRegression R package [213]. We assessed the models at clinically relevant time points (12, 18, 24, 30, 33, and 36 months) in both the PREMIERE development cohort and the IRST validation cohort. Table 5.3 presents the Area Under the Curve (AUC) values at these time points for our model in both cohorts:

Our 22-gene signature demonstrated excellent predictive accuracy across all time points in both cohorts. In the PREMIERE cohort, the AUC values ranged from 0.897 to 0.972, indicating a consistently high level of discrimination. The model's performance in the IRST validation cohort was also robust, with AUC values ranging from 0.813 to 0.842, confirming the signature's generalizability to an independent dataset. To contextualize the performance of our signature, we compared it with three established prognostic models: Olmos et al. (15-gene), Ross et al. (6-gene), and Wang et al. (4-gene). Figure 5.1 illustrates the ROC curves for all models in both the PREMIERE and IRST cohorts.

In the PREMIERE cohort, our 22-gene signature achieved an AUC of 0.891 (95% CI: 0.807-0.974), significantly outperforming the Olmos et al. model (AUC = 0.757, 95% CI: 0.646-0.867), the Ross et al. model (AUC = 0.611, 95% CI: 0.489-0.734), and the Wang et al. model (AUC = 0.633, 95% CI: 0.509-0.757). The superior performance of our signature was further validated in the IRST cohort, where it achieved an AUC of 0.958 (95% CI: 0.911-1.000), again surpassing the Olmos et al. model (AUC = 0.893, 95% CI: 0.801-0.985), the Ross et al. model (AUC = 0.744, 95% CI: 0.599-0.888), and the Wang et al. model (AUC = 0.830, 95% CI: 0.716-0.944). These results demonstrate the robust and consistent prognostic power of our 22-gene signature across different patient populations and over extended follow-up periods. The significant improvement in predictive accuracy over existing models underscores the potential clinical utility of our signature in guiding treatment decisions and risk stratification for patients with mCRPC.

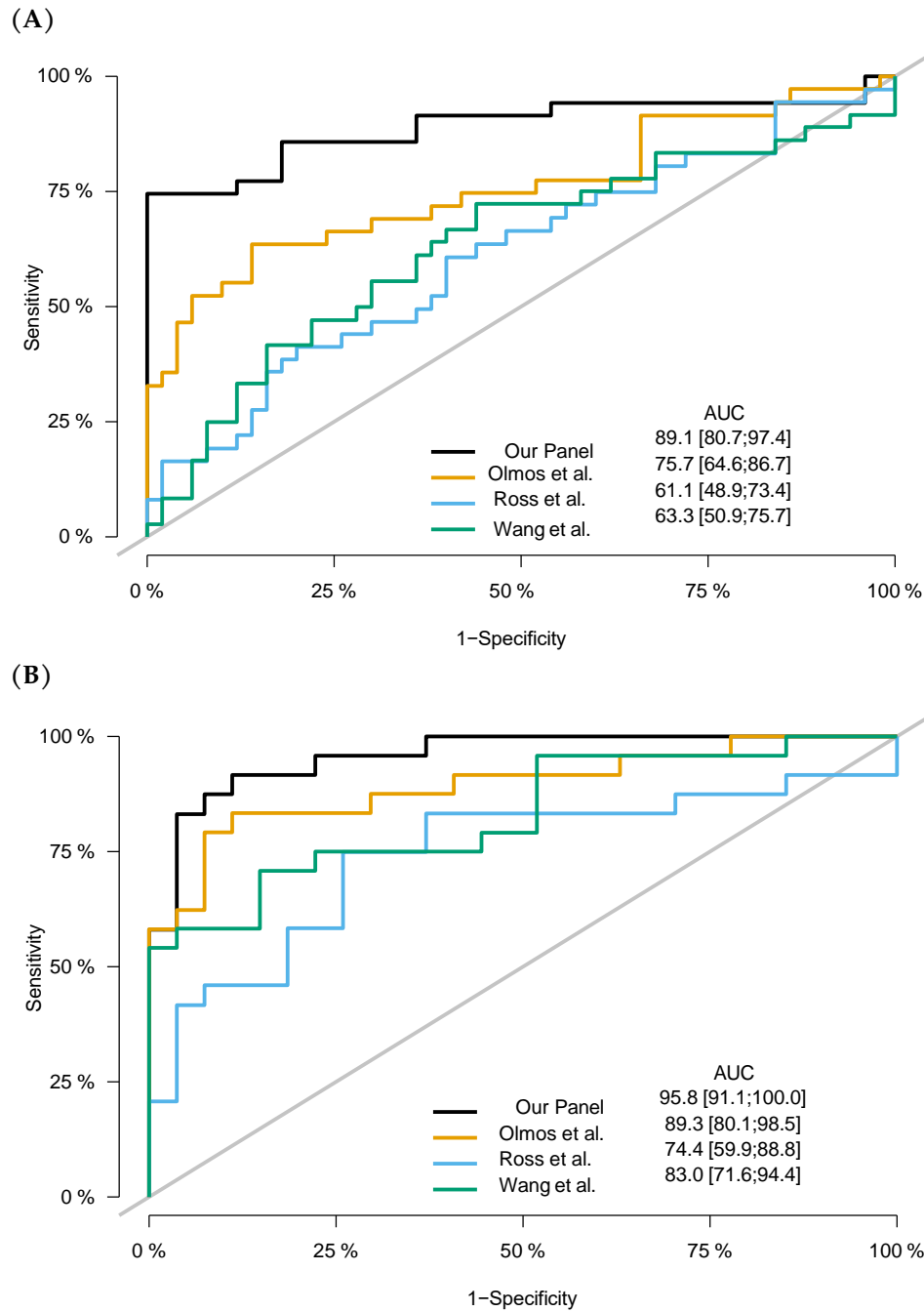


Figure 5.1: Curves comparing our 22-Gene signature with existing models. (A) PREMIERE cohort (B) IRST cohort

5.4 Summary

In this chapter, we have developed and validated a novel 22-gene expression signature derived from peripheral blood samples that robustly predicts OS in patients with mCRPC. Using advanced machine learning techniques, especially Lasso regression, we distilled a large set of differentially expressed genes into a

focused panel that demonstrates superior prognostic performance compared to existing models. It has been rigorously validated within an independent cohort, identifying the generalizability and clinical relevance of the signature. Previous efforts, such as the six-gene model by Ross et al., the nine-gene model by Olmos et al., and the four-gene model by Wang et al., laid the groundwork for blood-based prognostic signatures in mCRPC.

Our 22-gene signature holds great promise for impacting clinical practice in that it will enable much more precise risk stratification of patients with mCRPC. Clinicians will be better positioned to tailor treatment strategies, possibly opting for more aggressive or alternative therapies for high-risk patients while avoiding unnecessary side effects for low-risk patients.

Furthermore, since the signature is from peripheral blood, it represents a minimally invasive biomarker that can be easily integrated into clinical workflows. The superior predictive accuracy of our model, compared to existing gene signatures, underscores the importance of leveraging high-throughput genomic data and advanced analytics methods in the quest for personalized cancer care. Future studies should be conducted to validate the signature in larger studies and diverse patient populations, and to explore the biological functions of identified genes to uncover novel targets. In summary, we identified a 22-gene prognostic signature that represents, to date, a very significant step forward in personalised mCRPC treatment, which could improve patient outcomes by timely administration of more appropriate effective therapies.

DYNAMICS OF IMMUNE CELLS ASSOCIATED WITH ANTIANDROGEN THERAPY IN mCRPC

6.1 Introduction

Castration-resistant prostate cancer (CRPC) continues to pose a considerable clinical challenge, even with the progress made in recent therapeutic developments. Approximately 20-30% of patients develop resistance to treatment, with metastatic progression resulting in a survival rate of only 15-36 months [214]. The heterogeneous nature of PCa, characterized by diverse molecular signatures and varying sensitivities to treatment, is a primary contributor to this resistance. As the disease progresses, it becomes increasingly heterogeneous, leading to a diverse collection of cells with distinct molecular signatures and differential levels of sensitivity to treatment. This heterogeneity is the main source of resistance, making its correct assessment essential for proper prognosis and the development of effective therapies.

Blood-based approaches offer a minimally invasive method to stratify patients based on tumour biology, which is particularly relevant for mCRPC patients where biological heterogeneity and stratification approaches are limited. The interaction between mCRPC and the hematopoietic and immune systems leads to changes detectable in peripheral blood, potentially yielding valuable prognostic information. Previous studies have hypothesized that the interaction between immune cell components and cancer tissue leads to changes in general expression levels in blood, which could provide prognostic information about

mCRPC.

In this chapter, we investigate the dynamics of immune cells and gene expression patterns associated with antiandrogen therapy in mCRPC. Emerging evidence suggests that enzalutamide, while primarily targeting AR signaling, may also have significant effects on the immune system [215]. Understanding these immunomodulatory effects is crucial, as they may contribute to both the therapeutic efficacy and the development of resistance to enzalutamide.

Our objective in this study is to uncover novel biomarkers and therapeutic targets for enzalutamide-resistant mCRPC, with a particular focus on the immune-related changes induced by the treatment. By analyzing blood samples taken prior to treatment, at the 12-week point of enzalutamide treatment, and after progression, we aim to ascertain the overexpressed genes in each condition, identify putative pathways implicated in the development of enzalutamide resistance, and characterize the immunomodulatory effects of enzalutamide. This research seeks to provide insights into the complex interplay between antiandrogen therapy and the immune system in mCRPC.

6.2 Material and methods

All the methodologies applied in this work have been carried out following the protocols described in the sections **Material and Methods** chapter and related sections.

6.2.1 Differential expression analysis and identification of DEGs

The identification of differentially expressed genes (DEGs) followed the detailed preprocessing and analysis process in **Differential gene expression analysis** section. This included rigorous quality control, normalization, and statistical analysis using "limma" package. Thresholds for the selection of DEGs (P -value < 0.05 , Q -value < 0.01 and $|\log_2FC| > 0.3$) were set as in the previous description.

6.2.2 Gene set enrichment analysis

GSEA was performed using the approach described in [Gene set enrichment analysis](#) section using the clusterProfiler package and curated gene sets from GO and KEGG databases. It allowed the identification of biological processes and pathways associated with the DEGs identified in this study, using the same statistical thresholds ($FDR < 0.05$) and methodological parameters.

6.2.3 Immune cell profiling

Immune cell profiling by CIBERSORTx was performed as described in [Immune cell profiling using CIBERSORTx](#) section, focusing on deconvolution of immune subtypes from transcriptomic data. To further investigate functional impacts, in vitro experiments targeted immune populations including T cells, monocytes, and B cells, using methodologies consistent with those outlined in.

6.2.4 *In vitro* studies on immune cell populations

The *In vitro* experiments employed immune cell lines (Jurkat, MOLT-4, THP-1, and Raji) and prostate cancer cell lines (LNCaP, 22Rv1, and DU145), maintained under the conditions described in [In vitro Experiments](#) section. Cell viability was measured using the CellTiter-Glo assay, and apoptosis was assessed via Western blot to detect cleaved caspase-3 and PARP, following the protocols previously outlined. Drug treatments included enzalutamide and other AR inhibitors (abiraterone acetate, bicalutamide, apalutamide, and darolutamide), administered at concentrations specified earlier.

Gene expression profiling was conducted using the Affymetrix Human Transcriptome Array 2.0, with RNA extraction, quality control, and data analysis performed as described in [Microarray analysis](#) section.

6.2.5 Statistical analysis

All statistical analyses were performed using R (version 4.4.0) and figures described in [Statistical analysis](#) section

6.3 Results

To elucidate the molecular mechanisms underlying the response to enzalutamide in mCRPC patients, we performed a comprehensive longitudinal analysis of whole-blood transcriptomes. Our time-course study design allowed us to capture the dynamic changes in gene expression profiles at key clinical milestones: pre-treatment, early response (12 weeks), and disease progression.

6.3.1 Enzalutamide-induced changes in whole-blood gene expression

Initial exploratory data analysis using principal component analysis (PCA) revealed distinct temporal clustering of samples. In [Figure 6.1A](#) compares pre-treatment samples with those collected after 12 weeks of enzalutamide therapy. The clear separation between these two groups along the first principal component axis demonstrates a pronounced shift in gene expression profiles following treatment initiation. This distinct clustering indicates that enzalutamide induces a rapid and consistent transcriptomic response within the first 12 weeks of treatment. In [Figure 6.1B](#), pre-treatment samples are shown with those obtained at the time of disease progression. The persistent separation between these groups suggests that the transcriptomic alterations induced by enzalutamide are largely maintained even as the disease progresses. This observation implies that while the treatment continues to exert a strong influence on gene expression, the development of resistance may involve more subtle changes or alterations in specific pathway activities rather than a wholesale reversion to the pre-treatment state. [Figure 6.1C](#) presents a comparison between 12 weeks samples and those collected at progression. Interestingly, these two groups show a greater degree of overlap in the PCA plot, indicating a more nuanced transition in gene expression patterns as patients move from initial response to treatment resistance. This partial overlap suggests that the development of resistance is a gradual process, potentially characterized by patient-specific alterations in gene expression superimposed on the broader enzalutamide-induced transcriptomic landscape.

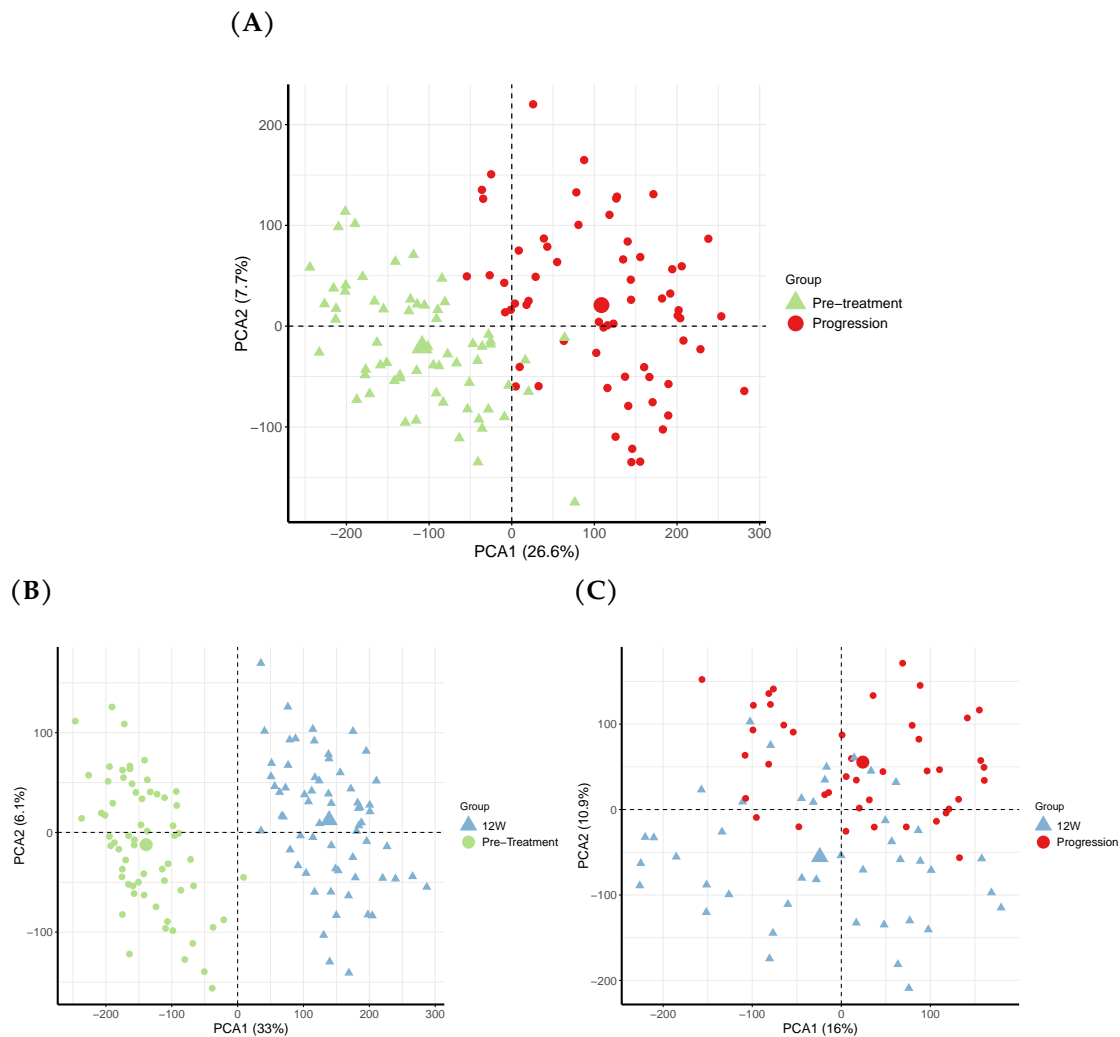


Figure 6.1: Principal Component Analysis (PCA) of whole-blood transcriptomes reveals distinct temporal patterns in response to enzalutamide treatment in mCRPC patients. (A) PCA plot comparing pre-treatment (green triangles) and 12-week treatment (blue triangles) samples. (B) PCA plot of pre-treatment (green triangles) versus progression (red circles) samples. (C) PCA plot comparing 12-week treatment (blue triangles) and progression (red circles) samples.

6.3.2 Hierarchical clustering analysis

Our PCA results were further corroborated and extended by unsupervised hierarchical clustering analysis to provide additional detail about the temporal dynamics of gene expression patterns after enzalutamide treatment (Figure 6.2). In Figure 6.2A, the dendrogram indicates a perfect separation between pretreatment and 12-week samples. These results stress the rapidity and coherence of the transcriptomic remodeling induced by enzalutamide. This clear delineation supports the notion of a robust early response signature across

patients. Similarly, **Figure 6.2B** shows a perfect separation between pre-treatment and progression samples, indicating that while resistance has taken hold, the global transcriptome remains significantly different from the treatment-naïve state. This durability in difference would imply that resistance mechanisms themselves may involve pathway-specific rather than global reverting expression modifications. Intriguingly, the clustering of 12-week and progression samples (**Figure 6.2C**) reveals a more complex pattern: although there is a certain degree of separation, there is also considerable intermingling of samples from these two time points. This would suggest a more nuanced-and perhaps patient-specific-evolution of gene expression as resistance develops. This less pronounced separation between these later time points indicates that subtle transcriptomic changes superimposed on the overall enzalutamide-induced expression landscape underlie the transition to a resistant state.

6.3.3 Differential gene expression analysis

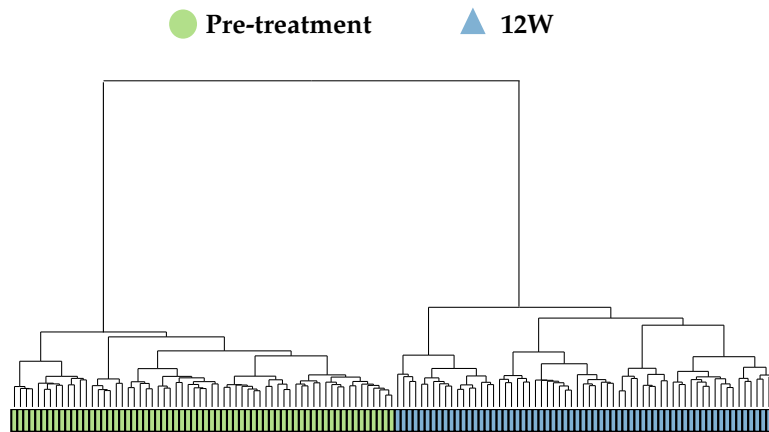
We therefore performed pairwise DGE analyses comparing key time points in order to quantify the extent of transcriptional reprogramming induced by enzalutamide treatment. To ensure more accurate results, the sample numbers were reduced by applying strict filtering criteria. In the 12-week patient group, we excluded patients with a progression-free survival (PFS) of less than 3 months and those without a 50% reduction in PSA levels (PSAresponse50). This approach revealed substantial and dynamic changes in gene expression profiles throughout the course of treatment **6.1**.

Comparison	Number of DEGs	Upregulated	Downregulated
12 weeks vs. Pre-treatment	4,162	1,832	2330
Progression vs. Pre-treatment	1,774	716	1058
Progression vs. 12 weeks	517	347	170

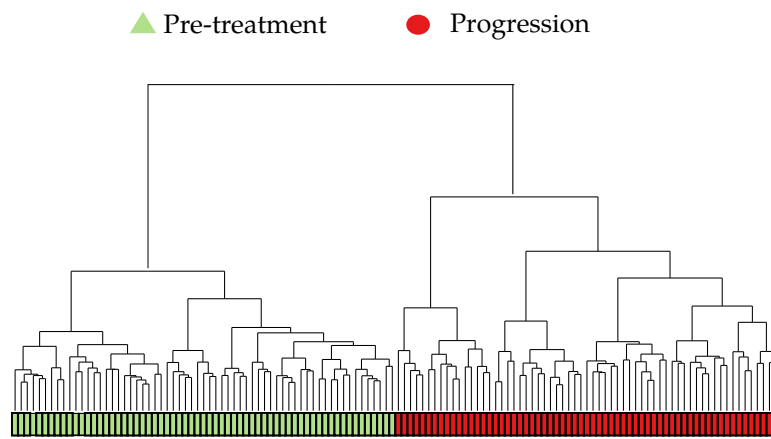
Table 6.1: Summary of DEGs across treatment time points

The most pronounced changes were observed when comparing the 12-week time point to pre-treatment, with 4,162 genes showing significant differential expression. This finding underlines rapid and extensive transcriptomic remodeling upon enzalutamide treatment. Noticeably, there was a slight bias toward downregulation, with 2,330 genes downregulated compared to 1,832 upregulated. This may reflect the suppressive action of enzalutamide on specific cellular processes. A comparison of the progression samples to

(A)



(B)



(C)

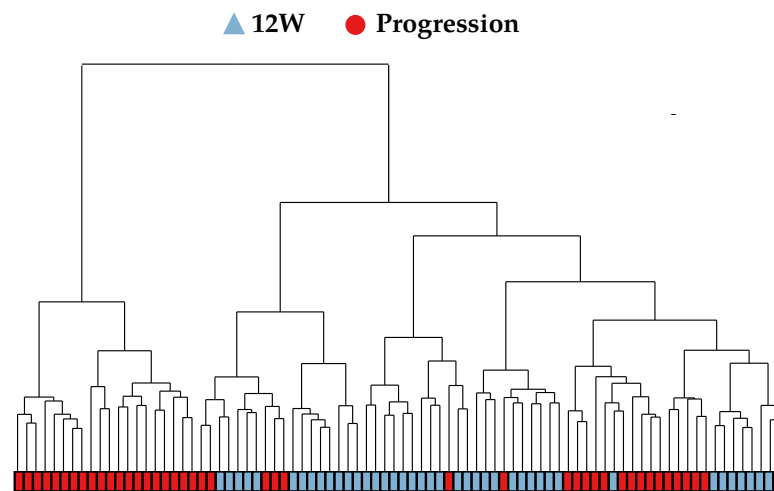


Figure 6.2: Unsupervised hierarchical clustering of whole-blood transcriptomes reveals distinct temporal patterns in mCRPC patients treated with enzalutamide. (A) Clustering of pre-treatment (green) versus 12-week (blue). **(B)** Pre-treatment (green) versus progression (red). **(C)** Clustering of 12-week (blue) versus progression (red).

pre-treatment revealed 1,774 differentially expressed genes, suggesting that although some of the early treatment-induced changes persist, there is a significant shift in the transcriptome as resistance develops. Interestingly, this comparison exhibited a greater bias toward downregulation, with 1,058 genes downregulated versus 716 upregulated. Such a trend might indicate that one component of the development of resistance includes the active suppression of some enzalutamide-induced changes. Therefore, the transition from week 12 to progression was characterized by subtle changes, represented by 517 differentially expressed genes. On the contrary, compared with other comparisons, this transition was mainly characterized by an upregulated gene prevalence over the downregulated one: 347 versus 170, respectively. This upregulation might reflect the turning on of specific resistance mechanisms during disease progression. These dynamic changes in gene expression patterns provide important insight into the molecular mechanisms that underlie the response to enzalutamide and the emergence of treatment resistance in mCRPC patients. Identification of time point-specific and consistently altered gene sets is a rich resource for further functional studies and potential biomarker development.

To further elucidate the relationships between differentially expressed genes across different time points, we generated a Venn diagram to visualize the overlap of DEGs between comparisons ([Figure 6.3](#)). This analysis provides insights into the persistence and evolution of gene expression changes throughout the course of treatment. Notably, the most profound impact on gene regulation occurs at the initiation of treatment, as evidenced by the substantial number of differentially expressed genes (2,832) when comparing the 12-week time point to pre-treatment samples. This observation underscores the rapid and extensive transcriptomic remodeling induced by enzalutamide.

The analysis also highlights the dynamic nature of gene expression changes over time. While many genes show persistent differential expression, there are also unique sets of genes associated with specific stages of treatment. For instance, 267 genes are uniquely differentially expressed when comparing progression to pre-treatment samples, but not at the 12-week time point. These genes may be indicative of specific resistance mechanisms that emerge over time or adaptive responses that only become apparent with prolonged treatment.

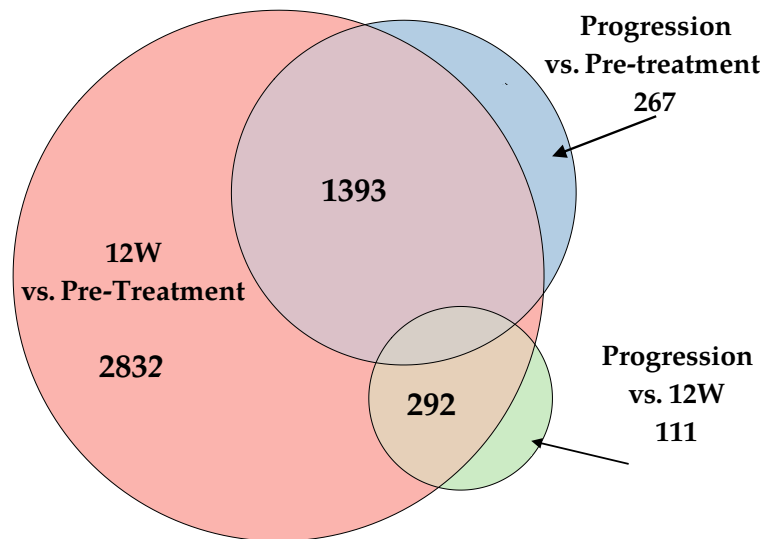


Figure 6.3: Venn diagram showing the overlap of DEGs across different treatment time point comparisons in mCRPC patients treated with enzalutamide.

6.3.4 Gene set enrichment analysis reveals dynamic pathway regulation

To interpret the functional implications of the DEGs, we performed GSEA using GO Biological Processes. The top enriched pathways for each comparison are summarized in [Table 6.2](#).

Enrichment plots illustrating the significance and directionality of these pathways are presented in [Figure 6.4](#) revealing significant alterations in several biological pathways throughout the course of enzalutamide treatment. At 12 weeks of treatment ([Figure 6.4A](#)), we observed a marked downregulation of immune-related pathways, particularly those associated with B-cell activation and signaling, as well as antigen processing and presentation ($\text{FDR} < 0.05$). Conversely, pathways involved in chemical stimulus detection and response were significantly upregulated ($\text{FDR} < 0.05$), suggesting a novel effect of enzalutamide on sensory perception processes.

The interesting observation was that the progression samples shared a similar pathway modulation compared to the samples at 12 weeks, where immune-related pathways were persistently downregulated and processes related to chemical stimulus remained upregulated. This consistency supports the idea that such changes are integral to the mechanism either of action of the drug or to the adaptive response of the tumour. The distinctive features of the progression samples are then also reported. Curiously, there is a significantly

Progression vs. Pre-treatment	
GO Term	Description
GO:0050911	Detection of chemical stimulus involved
GO:0007608	Sensory perception of smell
GO:0050907	Detection of chemical stimulus involved in sensory perception
GO:0007606	Sensory perception of chemical stimulus
GO:0009593	Detection of chemical stimulus
GO:0050906	Detection of stimulus involved in sensory perception
GO:0061515	Myeloid cell development
GO:0016064	Immunoglobulin mediated immune response
GO:0019724	B cell mediated immunity
GO:0030099	Myeloid cell differentiation
12 weeks vs. Pre-treatment	
GO Term	Description
GO:0030099	Myeloid cell differentiation
GO:0050911	Detection of chemical stimulus involved in sensory perception of smell
GO:0050907	Detection of chemical stimulus involved in sensory perception
GO:0007608	Sensory perception of smell
GO:0016064	Immunoglobulin mediated immune response
GO:0019724	B cell mediated immunity
GO:0030218	Erythrocyte differentiation
GO:0050853	B cell receptor signaling pathway
GO:0007606	Sensory perception of chemical stimulus
GO:0030217	T cell differentiation
12 weeks vs. Progression	
GO Term	Description
GO:0006457	Protein folding
GO:0002831	Regulation of response to biotic stimulus
GO:0008380	RNA splicing
GO:0006397	mRNA processing
GO:0000377	RNA splicing, via transesterification
GO:0000398	mRNA splicing, via spliceosome
GO:0050684	Regulation of mRNA processing
GO:0000375	RNA splicing, via transesterification reactions
GO:1903311	Regulation of mRNA metabolic process
GO:0033044	Regulation of chromosome organization

Table 6.2: Summary of top enriched biological pathways identified by GSEA across comparisons

upregulated keratinization pathway-FDR <0.05- **Figure 6.4B** possibly implying epithelial-mesenchymal transition or other adaptation mechanisms evolutionarily linked to disease progression.

Comparing these samples to the progression and 12-week samples **Figure 6.4C**, we observed a concomitant upregulation of pathways relating to mRNA splicing and DNA detoxification and downregulation of pathways relating to DNA and protein conformation and mRNA metabolic processing. These models emphasize the dynamic nature of transcriptomic remodelling in this disease accustomed to developing treatment resistance.

6.3.5 Effect of enzalutamide and/or tumour progression on the immune cell components in blood

To evaluate the immune landscape dynamics during enzalutamide treatment and tumour progression, we analyzed immune cell proportions at three key time points: pre-treatment (baseline), 12-week treatment, and progression. Immune subsets were estimated using CIBERSORTx, which deconvolutes transcriptomic data into proportions of 22 immune cell types. Comparisons were performed for (A) progression vs. pre-treatment, (B) 12 weeks vs. pre-treatment, and (C) progression vs. 12 weeks. A validation cohort was also analyzed for progression vs. pre-treatment to confirm the reproducibility of findings.

In the progression vs. pre-treatment comparison (**Figure 6.5A**), significant changes were observed in several immune cell subsets. CD8+ T cells exhibited a marked reduction at progression ($p < 0.001$), while monocytes and resting mast cells were significantly increased ($p < 0.001$). These results suggest that tumour progression is associated with a suppression of cytotoxic immune responses and a shift toward a myeloid-dominated immune profile, potentially promoting an immunosuppressive tumour microenvironment.

The 12 weeks vs. pre-treatment comparison (**Figure 6.5B**) revealed similar patterns of immune remodeling. Monocytes, resting NK cells, and resting mast cells were significantly increased ($p < 0.001$), while memory B cells and CD8+ T cells were significantly reduced ($p < 0.001$). These findings indicate that enzalutamide treatment induces rapid and significant changes in the immune landscape, characterized by the suppression of adaptive immune subsets such as CD8+ T cells and memory B cells, along with an increase in innate immune cells like NK cells and monocytes.

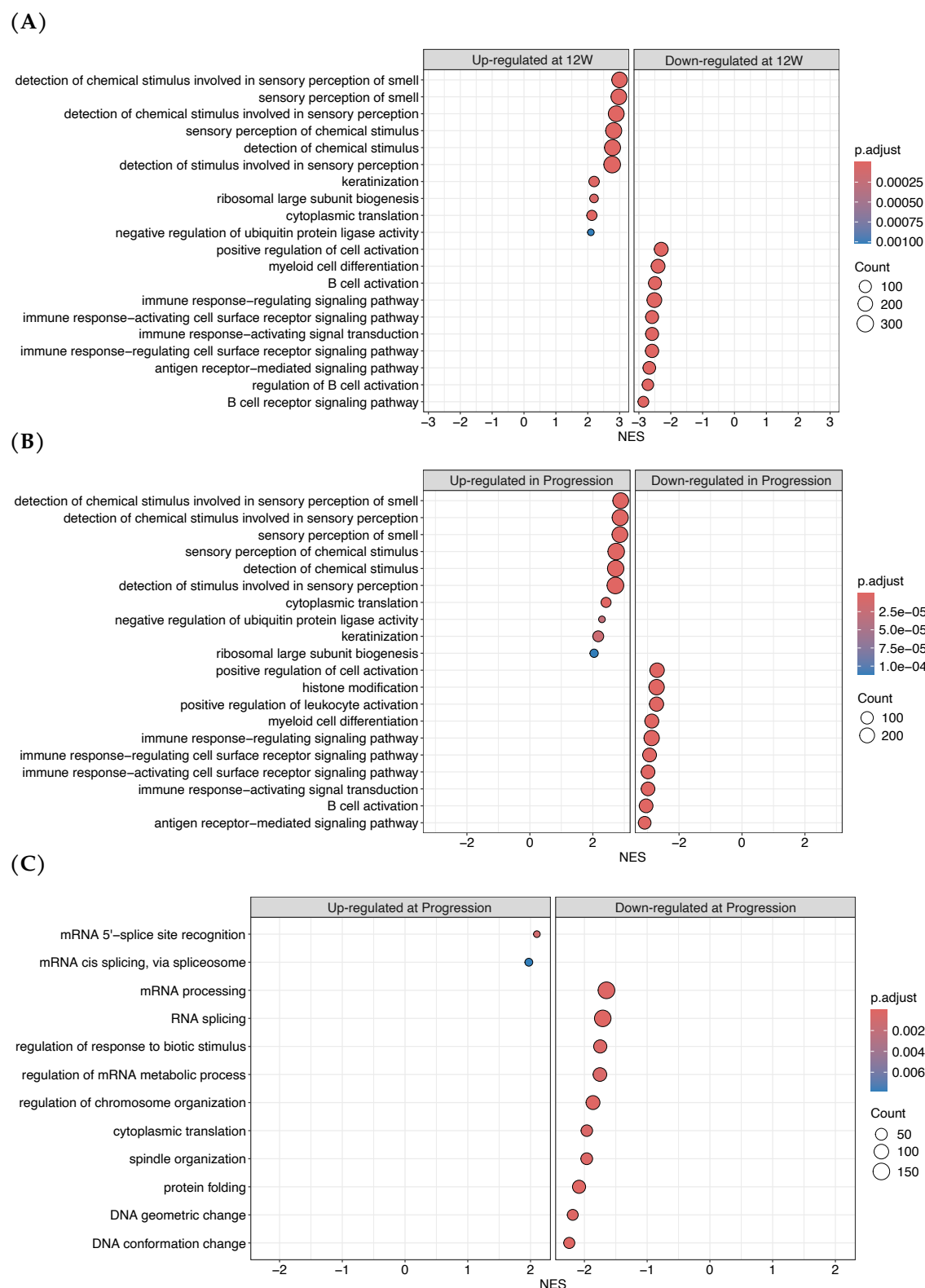


Figure 6.4: Gene Set Enrichment Analysis (GSEA) of differentially expressed genes in mCRPC patients treated with enzalutamide. (A) GSEA results comparing progression samples to pre-treatment samples. (B) GSEA results comparing 12-week treatment samples to pre-treatment samples. (C) GSEA results comparing progression samples to 12-week treatment samples.

In the progression vs. 12 weeks comparison (**Figure 6.5C**), memory B cells and monocytes were significantly increased ($p < 0.001$), while resting NK cells were significantly reduced ($p < 0.001$). These findings suggest that as resistance to enzalutamide develops, adaptive immune components such as memory B cells increase, possibly reflecting tumour-driven recruitment or immune compensation. Meanwhile, the continued rise in monocytes reinforces their potential role in maintaining a pro-tumourigenic or immunosuppressive environment. The reduction in resting NK cells may indicate a weakening of innate immune surveillance as the tumour progresses.

To validate these findings, we analyzed a second independent cohort comparing progression vs. pre-treatment samples. Consistent with the discovery cohort, this analysis confirmed the significant reduction in CD8+ T cells ($p < 0.01$) and the significant increase in monocytes ($p < 0.01$) at progression (**Figure 6.6**). This reproducibility across cohorts highlights the robustness of the observed immune shifts and their potential relevance in understanding treatment resistance in mCRPC.

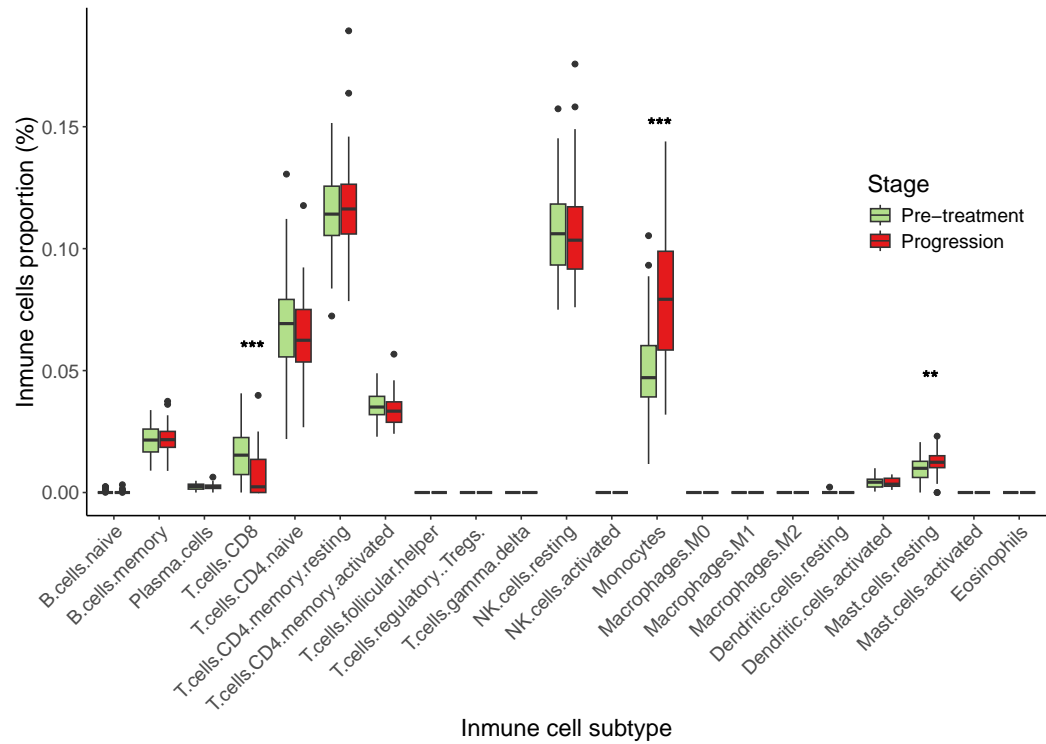
6.3.6 *In vitro* characterization of enzalutamide's effects on immune cell populations

Given the immunosuppressive effects observed of enzalutamide in mCRPC patients, we conducted *In vitro* experiments to investigate the direct impact of enzalutamide on key immune cell populations. We focused on T cells, monocytes, and B cells, utilizing established human cell lines: Jurkat and MOLT-4 for T cells, THP-1 for monocytic cells, and Raji for B cells. Our studies included viability assays, apoptosis assays, and gene expression profiling to elucidate the mechanisms underlying enzalutamide's effects on these immune cells.

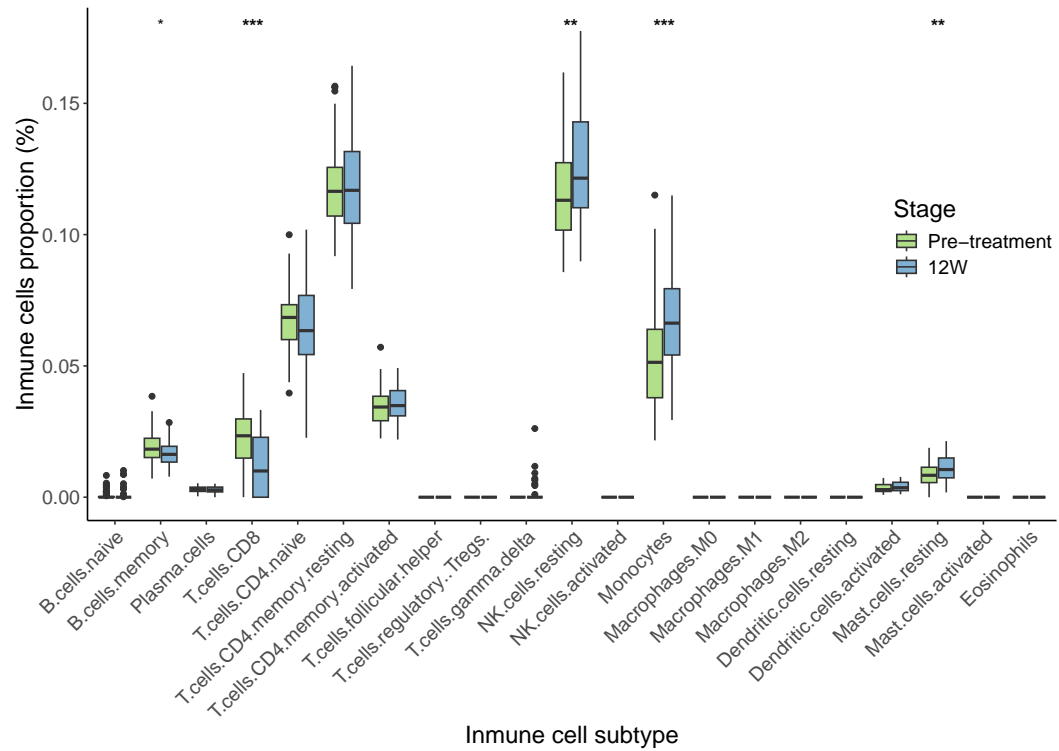
6.3.7 Enzalutamide reduces viability of T Cells independently of AR expression

We first assessed the effect of enzalutamide on T-cell viability using the Jurkat cell line. Cells were treated with increasing concentrations of enzalutamide (1–100 μ M) for 48 hours, and cell viability was measured using the CellTiter-Glo. Enzalutamide significantly reduced the viability of Jurkat cells in

(A)



(B)



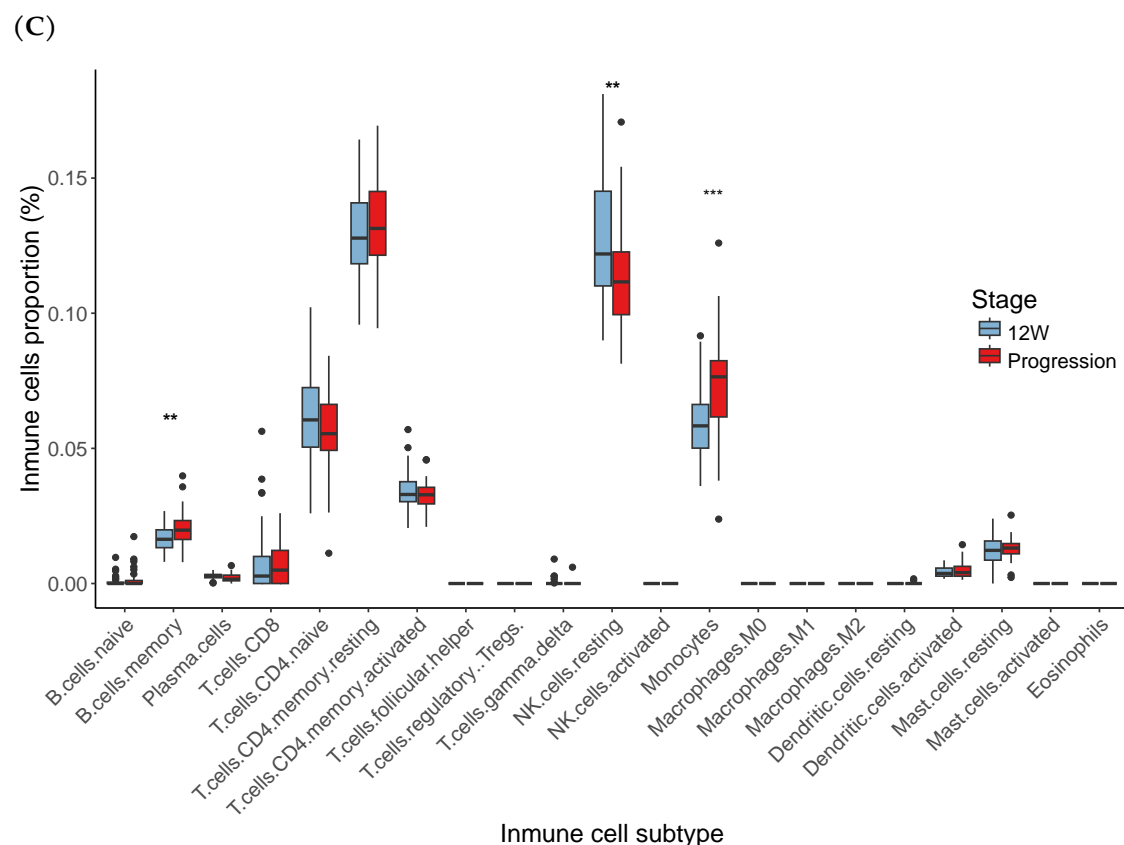


Figure 6.5: Boxplots comparing the relative proportions of 22 immune cell subsets in peripheral blood across key treatment time points in mCRPC patients. (A) Progression vs. Pre-treatment, (B) 12-week vs. Pre-treatment, and (C) Progression vs. 12-week. Statistically significant changes are highlighted ($*p < 0.01$). Persistent reductions in CD8+ T cells and increases in monocytes were observed across comparisons.

a dose-dependent manner [Figure 6.7A](#), with an IC_{50} of approximately $18.71 \mu M$ ([Figure 6.7B](#)).

To determine whether this cytotoxic effect was mediated through AR signaling, we examined AR expression in Jurkat cells compared to prostate cancer cell lines known to express AR (LNCaP and 22Rv1) and an AR-negative prostate cancer cell line (DU145). Western blot analysis confirmed that Jurkat cells do not express AR, while LNCaP and 22Rv1 cells showed strong AR expression ([Figure 6.8](#)). DU145 and Jurkat cells served as AR-negative controls. These results indicate that enzalutamide's effect on T-cell viability is independent of AR signaling.

To determine whether loss of viability was due to apoptosis, we measured the activation of apoptotic markers in Jurkat cells exposed to clinically relevant plasma concentrations of enzalutamide ($35.7 \mu M$). Cells were treated for 24

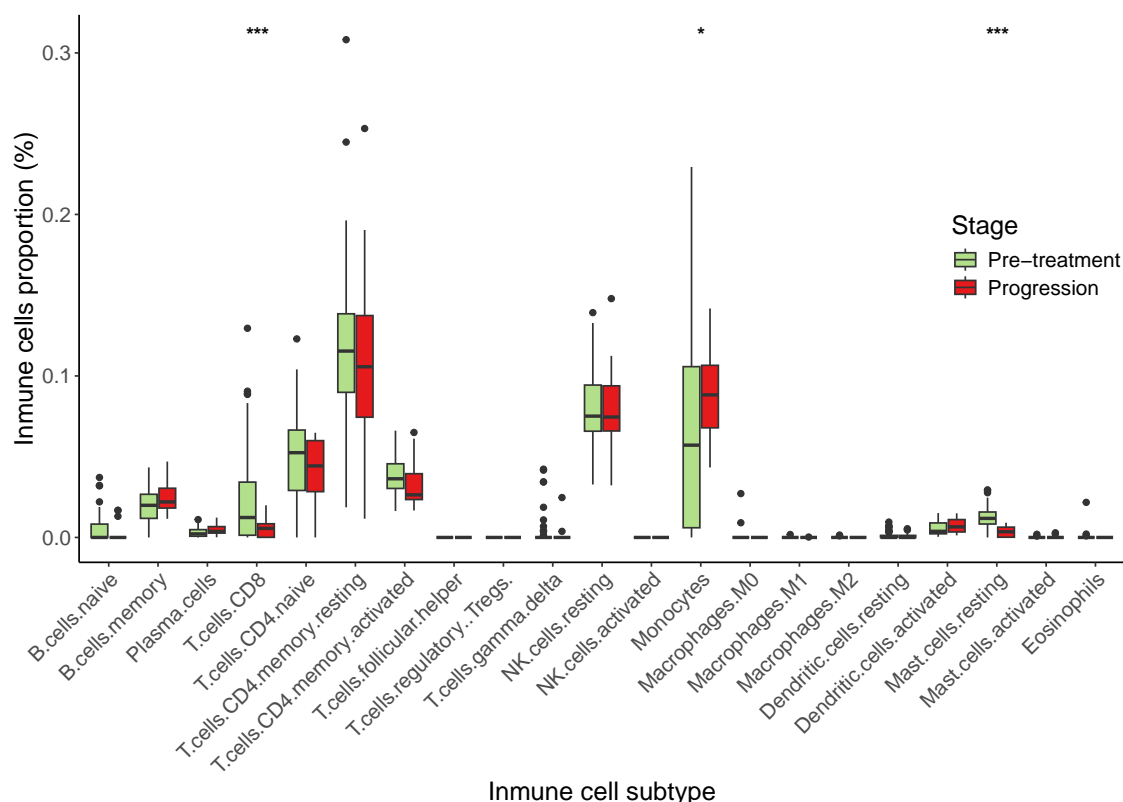


Figure 6.6: Validation cohort: Boxplots comparing the proportions of CD8+ T cells and monocytes between progression and pre-treatment samples. Results confirm the significant reduction in CD8+ T cells and increase in monocytes at progression, consistent with findings from the discovery cohort ($*p < 0.01$).

hours with enzalutamide and cleavage of Caspase-3 and PARP were determined by Western blot. Enzalutamide promoted marked cleavage of Caspase-3 (Figure 6.9A) and PARP (Figure 6.9B) compared to untreated controls, indicating induction of apoptosis. These observations suggest that the pro-apoptotic effects of enzalutamide on T cells are mediated through an AR-independent mechanism.

6.3.8 Differential sensitivity of immune cell types to enzalutamide

We extended our investigation to other immune cell lines to assess the broader impact of enzalutamide. Thus, we treated the following lymphocytic cell lines: Jurkat, MOLT-4 (T cells), THP-1 (monocytes) and Raji (B cells) with enzalutamide at 25 μ M concentrations for 24, 48, and 72 hours. Treatment of the cell line resulted in the loss of its viability at all tested concentrations and time intervals in a concentration and time-dependent manner, despite

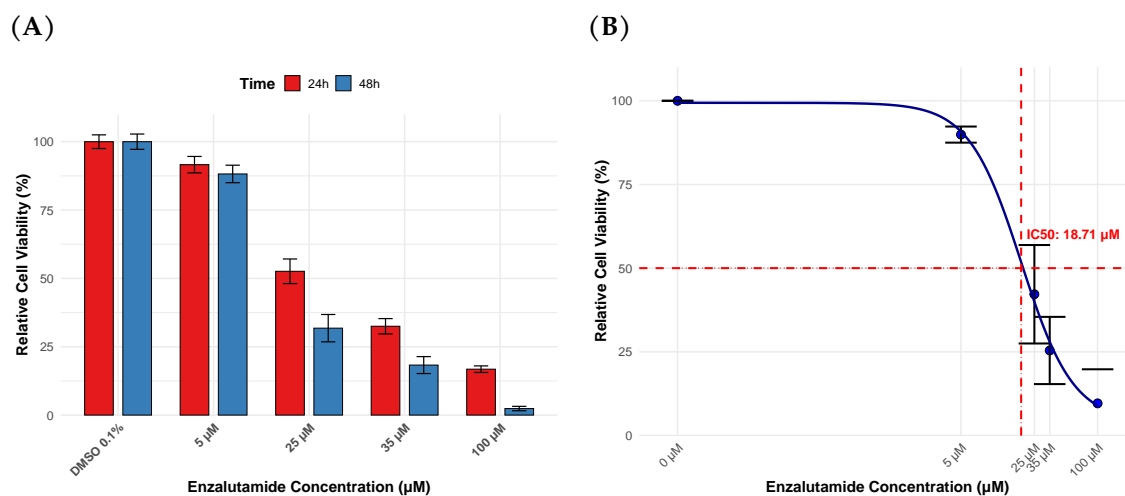


Figure 6.7: Enzalutamide reduces cell viability in Jurkat T cells. (A) Dose-dependent reduction in viability after 72 hours. (B) Representative dose-response curve relative to untreated controls.

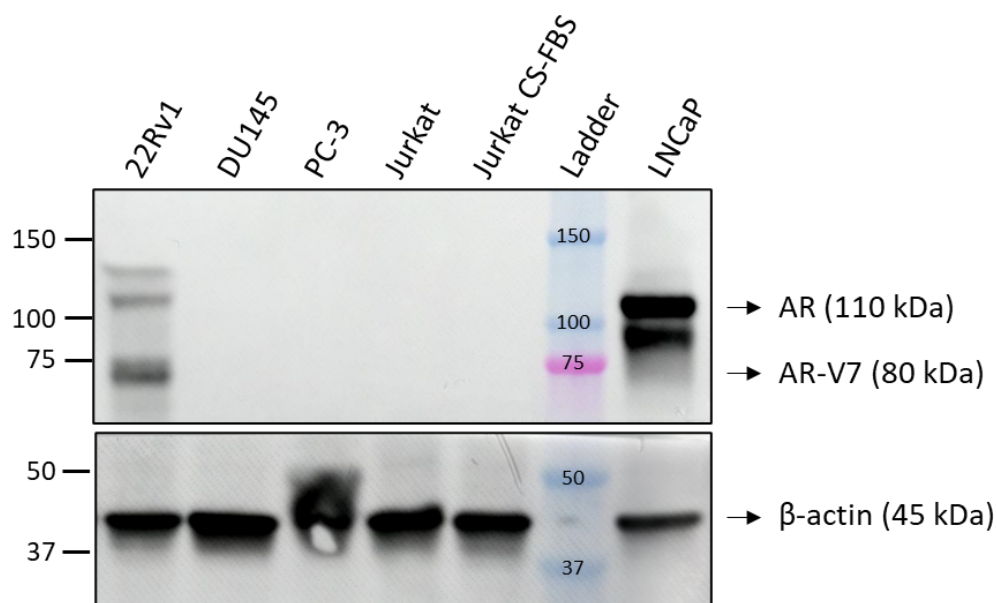


Figure 6.8: Western blot analysis of AR expression in various cell lines. Jurkat T cells do not express AR, while LNCaP and 22Rv1 prostate cancer cells are AR-positive. DU145 prostate cancer cells and Jurkat cells cultured in charcoal-stripped FBS (CS-FBS) are AR-negative controls. GAPDH is used as a loading control.

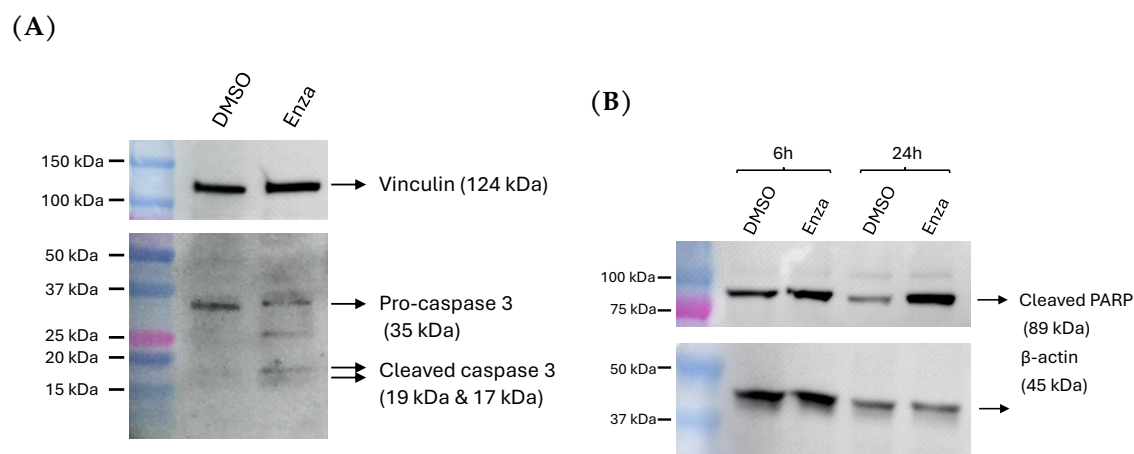


Figure 6.9: Enzalutamide treatment with Jurkat cells. (A) Western blot analysis showing cleavage of Caspase-3 after 24-hour treatment with enzalutamide (35.7 μ M), indicating activation of apoptosis. (B) Western blot analysis showing cleavage of PARP under the same conditions, further confirming apoptotic activity.

inter-individual variations (Figure 6.10A). At 24 hours, Jurkat cells exhibited a significant reduction in viability to less than 55% compared to untreated controls. Raji B cells also showed a substantial decrease in viability to approximately 60%. MOLT-4 T cells and THP-1 monocytes were less affected at this early time point, with viability remaining around 80%. Over extended treatment durations (48 and 72 hours), all cell lines exhibited further reductions in viability, indicating that prolonged exposure enhances the cytotoxic effects of enzalutamide. Notably, Jurkat cells continued to show the most significant decrease in viability, reinforcing their heightened sensitivity.

We also confirmed that MOLT-4, THP-1, and Raji cells do not express AR by Western blot analysis (Figure 6.10B), reinforcing that the observed effects are independent of AR signaling.

6.3.9 Comparative analysis of AR inhibitors on t-cell viability

To determine whether the cytotoxic effects observed with enzalutamide are unique to this compound or shared among other antiandrogens, we evaluated the impact of several clinically relevant antiandrogens on the viability of Jurkat T cells. Cells were treated for 48 hours with plasma equivalent concentrations of bicalutamide (20 μ M), enzalutamide (25 μ M), darolutamide (25 μ M), apalutamide (10 μ M), and abiraterone acetate (5 μ M).

Our results demonstrated that enzalutamide and darolutamide significantly reduced Jurkat cell viability, with viability decreasing to less than 50%

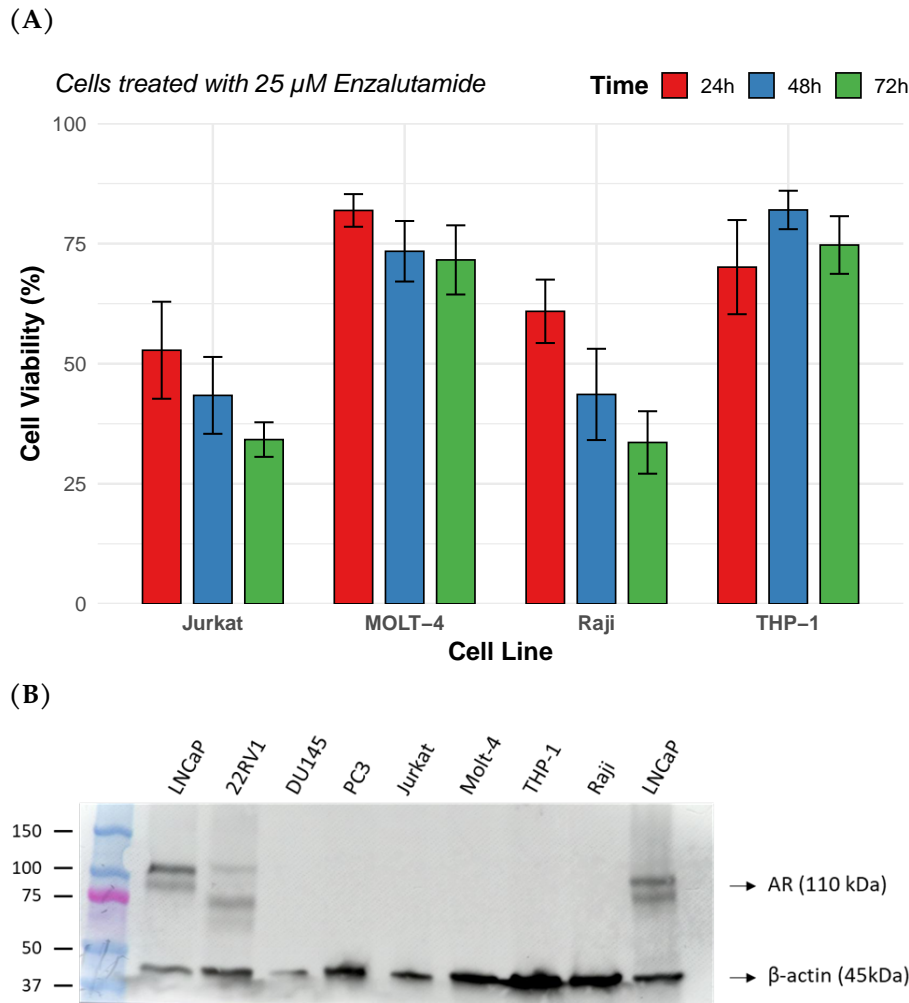


Figure 6.10: Effects of enzalutamide on viability across different immune cell lines. (A) Cell viability analysis of Jurkat (T cells), Raji (B cells), MOLT-4 (T cells), and THP-1 (monocytes) treated with 25 μ M enzalutamide for 24, 48, and 72 hours. The graph demonstrates a concentration- and time-dependent reduction in cell viability, with Jurkat cells showing the most pronounced sensitivity. (B) Western blot analysis confirming the absence of AR expression in MOLT-4, THP-1, and Raji cells, suggesting the observed cytotoxic effects are independent of AR signaling.

compared to untreated controls (Figure 6.11). In contrast, bicalutamide, apalutamide, and abiraterone acetate had minimal effects on cell viability, with viability remaining above 80%. These findings indicate that enzalutamide and darolutamide exert more pronounced cytotoxic effects on T cells compared to other antiandrogens.

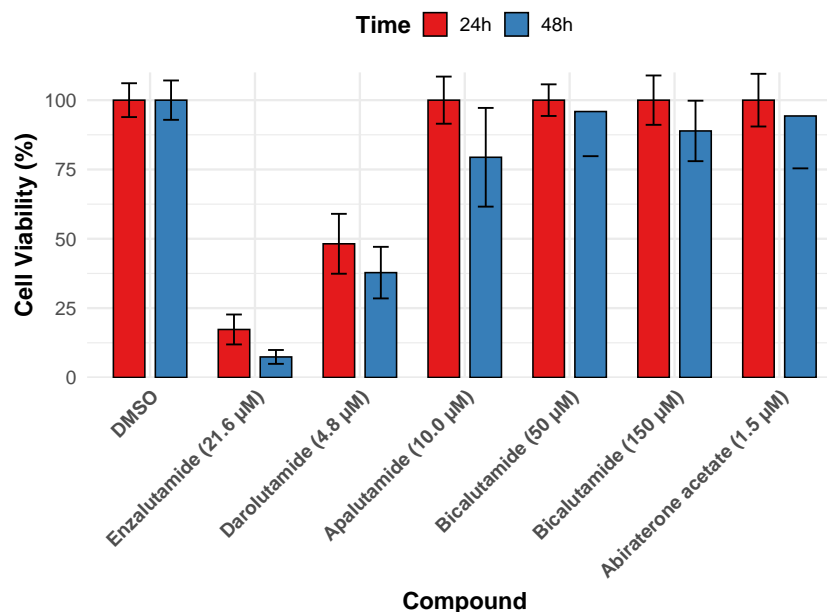


Figure 6.11: Comparison of antiandrogens on Jurkat T-cell viability. Cells were treated with clinically relevant plasma concentrations of bicalutamide (20 μ M), enzalutamide (25 μ M), darolutamide (25 μ M), apalutamide (10 μ M), and abiraterone acetate (5 μ M) for 48 hours. Cell viability was assessed by MTT assay. Data represent mean \pm SD of three independent experiments. $**p < 0.01$ compared to control.

6.3.10 Gene expression profiling reveals modulation of apoptotic and immune pathways

To investigate the molecular changes induced by enzalutamide in T cells, we performed gene expression profiling using microarrays. We treated Jurkat T cells with 35 μ M for 24 hours in three biological replicates for both enzalutamide-treated cells and DMSO-treated controls. RNA was extracted and analyzed using Affymetrix Human Transcriptome Array 2.0 microarrays.

DEGs detected were 1,077, while logFC was ≥ 1 with p value < 0.05 . We use GSEA and KEGG pathway analysis as ways of exploring the change in gene expression in systems biology and biological pathways targeted by enzalutamide treatment. We conducted a GSEA and KEGG pathway analysis. GSEA revealed a significant enrichment of genes involved in sterol biosynthesis and cholesterol metabolism pathways [Figure 6.12A](#). Conversely, GSEA also identified significant downregulation of pathways related to ribosome biogenesis, mitochondrial translation, and RNA processing.

The analysis of the KEGG pathway corroborated these findings [Figure 6.12B](#). The Steroid Biosynthesis Pathway was significantly up-regulated, aligning with the

GSEA results. Additionally, KEGG analysis highlighted the downregulation of pathways such as Ribosome and Oxidative Phosphorylation, further supporting the impact of enzalutamide on protein synthesis machinery and mitochondrial function.

These results suggest that enzalutamide causes prominent changes in metabolic pathways in T cells by upregulating sterol and cholesterol biosynthesis while downregulating protein synthesis and mitochondrial functions. Such an up-regulation of the metabolic pathways in lipid biosynthesis could point to a compensatory process or stress for the preservation of cellular membrane integrity. However, down-regulation of pathways related to ribosome biogenesis and mitochondrial translation may indicate compromise in protein synthesis and energy production capability, which will ultimately culminate in disrupted cell functionality and viability.

6.4 Summary

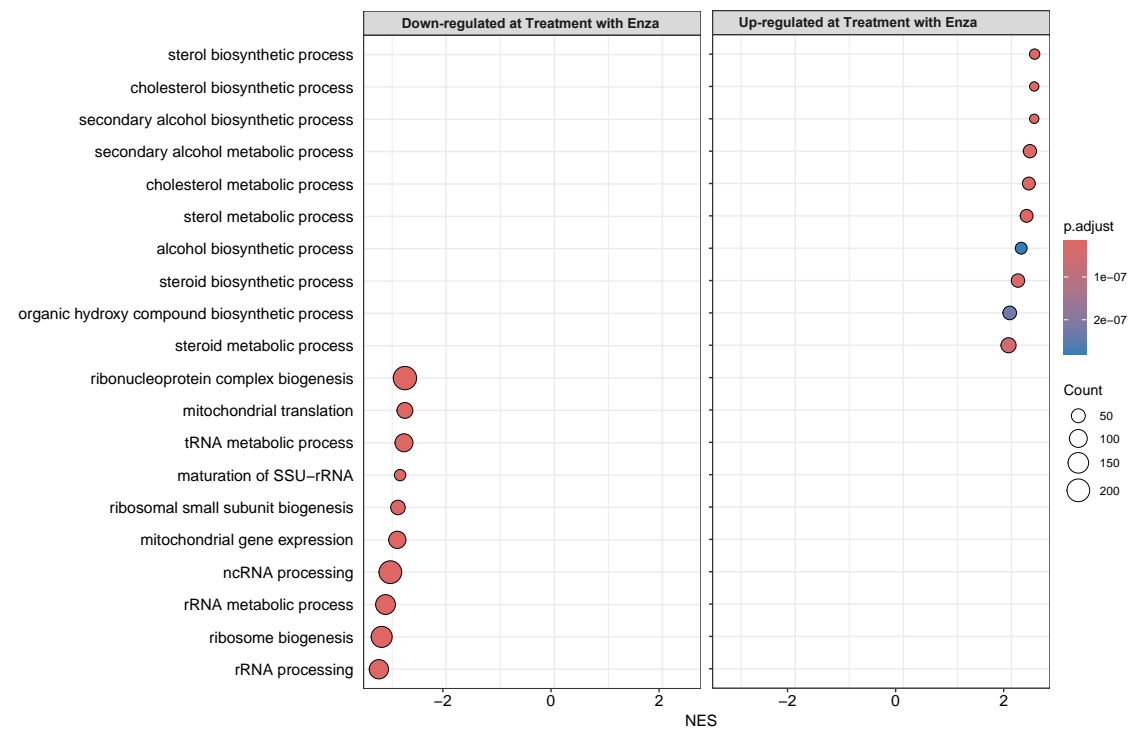
Our integrated longitudinal analysis of mCRPC patients treated with enzalutamide has revealed key aspects of the dynamic interplay between antiandrogen treatment, immune modulation, and disease progression. We demonstrated that enzalutamide treatment causes rapid and profound transcriptomic changes in peripheral blood, particularly with regard to immune-related pathways.

In particular, suppression of adaptive immune responses was characterized by a marked reduction in CD8+ T cells and memory B cells, with an increase in monocytes and innate immune cells, which was evident from 12 weeks of treatment and persisted throughout disease progression.

These data suggest that enzalutamide exerts an immunosuppressive effect impairing antitumour immunity, thus contributing to the development of therapeutic resistance. These were further corroborated by our *In vitro* studies showing that enzalutamide induces AR-independent apoptosis of T cells, an off-target effect of this drug that was previously unknown.

These differential sensitivities of the various antiandrogen therapies to immune cells suggest a role for immunomodulatory properties in the choice of treatment strategies in patients with mCRPC. In particular, although enzalutamide and darolutamide display potent cytotoxic effects against T cells, other AR

(A)



(B)

Up-regulated

Enrichment FDR	nGenes	Pathway Genes	Fold Enrichment	Pathways (click for details)
7.1E-07	10	20	10.1	Steroid biosynthesis
1.3E-04	8	38	8.1	Allograft rejection
1.2E-04	9	23	7.3	Terpenoid backbone biosynthesis
3.9E-02	5	42	5.8	Graft-versus-host disease
6.6E-04	10	53	5.2	Autoimmune thyroid disease
3.3E-02	6	43	5.1	Type I diabetes mellitus
2.6E-02	9	60	3.7	Viral myocarditis
3.9E-02	12	74	2.8	Biosynthesis of amino acids
1.7E-09	59	433	2.6	Olfactory transduction

Down-regulated

Enrichment FDR	nGenes	Pathway Genes	Fold Enrichment	Pathways (click for details)
1.2E-03	13	36	3.8	DNA replication
8.7E-05	22	77	3.3	Ribosome biogenesis in eukaryotes
3.1E-02	12	46	3	Nucleotide excision repair
1.1E-03	29	126	2.4	Cell cycle
3.9E-02	24	128	2	Purine metabolism

Figure 6.12: Enrichment and pathway analysis of gene expression changes induced by enzalutamide in Jurkat T cells. (A) GSEA enrichment plot in enzalutamide-treated Jurkat T cells. (B) KEGG pathway map in enzalutamide-treated cells.

inhibitors demonstrated minimal effects, suggesting alternative therapies with better preservation of immune function.

Clinically, our findings emphasize the integration of immunological assessments in the management of mCRPC. Monitoring immune cell populations and gene expression may provide biomarker information on treatment decisions and identify patients prone to immunosuppression and resistance. Furthermore, the potential immunosuppressive effects of enzalutamide should be carefully considered in the design of combination treatments, especially with immunotherapeutic agents. Together, the study in this article highlights how our investigation of enzalutamide's influence on the immune system reveals complexity and significant effects in patients with mCRPC. An explanation of these immunomodulatory actions is needed to maximize therapy and ultimately benefit patients in advanced prostate cancer.

DISCUSSION

mCRPC is one of the leading causes of cancer death in men and constitutes one of the biggest challenges for cancer immunotherapy. Despite recent developments in treatment, mCRPC remains currently incurable, with variable survival rates and outcomes ranging from a few months to several years.

In this thesis, we have conducted a comprehensive investigation of the prognostic significance of blood gene expression signatures and immune cell dynamics in patients with mCRPC who undergo enzalutamide treatment, integrating bioinformatics analysis, clinical data, and laboratory experiments to address the main gaps in mCRPC research. Our multifaceted approach encompassed the evaluation of the composition of blood immune cells and their prognostic implications (Chapter 4), the development and validation of a novel 22-gene prognostic signature (Chapter 5), and the exploration of the immunomodulatory effects of enzalutamide and other antiandrogens on immune cells both *in vivo* and *In vitro* (Chapter 6). The integration of bioinformatics and clinical oncology provided profound insight into the molecular underpinnings of mCRPC progression and resistance to treatment.

Peripheral blood analysis in patients with mCRPC provides not only the possibility of identifying tumour components, but also prognostic information. This prognostic data results from the intricate interactions among the tumor, bone marrow, and the host's immune system. Blood samples from individuals with mCRPC have previously been shown to provide prognostic information for the disease beyond the simple identification of tumour components. This is supported by studies involving analysis of gene expression [182, 183, 216] and evaluating relative cell proportions in blood counts, specifically focussing on the neutrophil to lymphocyte ratio (NLR) [201–206]. Analyses of gene expression in whole blood have been shown to be significant prognostic

indicators in advanced prostate cancer. Specifically, Olmos et al. [183] discovered a nine-gene signature linked to the T cell immune response, whereas Ross et al. [182] formulated a six-gene signature associated with the regulation of cellular immunity and monocyte differentiation. Notably, this research is pioneering in assessing the roles of 22 distinct immune cell components in blood, which are generally not reported in clinical trial blood tests.

Assessing the composition of immune cells within the blood is crucial for comprehending the dynamic interplay between cancer and the immune system, offering significant prognostic information for diseases like mCRPC. Technological advances now facilitate detailed analyses of these elements. CIBERSORT is an advanced deconvolution technique that deciphers cell composition using gene expression data [192, 193]. It applies linear support vector regression (SVR) for precise deconvolution of gene expression mixtures from these tissues. The method has shown a high correlation with the conventional flow cytometric technique and, therefore, is considered quite accurate and reliable by many studies [217–219].

In this chapter, our objective was to improve our understanding of the prognostic environment in mCRPC by examining the involvement of various types of immune cells. To achieve this, we rigorously evaluated pre-treatment blood samples from patients participating in an innovative phase 2 multicenter study. The study specifically aimed to assess the therapeutic effectiveness of enzalutamide as an initial treatment for mCRPC. Recognising the paramount importance of repeatability and applicability in biomarker studies, we included an independent validation group of patients with mCRPC. This group was vital in confirming the reliability and potential clinical value of our initial results, providing a robust basis for potentially personalized treatment approaches.

This study represents an initial effort in assessing the practicality of blood immune profiling in patients enrolled in a multicenter clinical trial. It explores the prognostic impact of blood CD8 T cells in individuals with mCRPC. We analyzed twenty-two types of blood immune cells in pre-treatment samples from mCRPC patients taking part in a multicenter phase 2 biomarker clinical trial using enzalutamide. Our findings indicated that elevated monocyte levels and reduced CD8 T-cell counts were linked to poorer survival outcomes. These findings were corroborated in a separate cohort of mCRPC patients. Low CD8 T-cell levels remained an independent prognostic factor when incorporated into a validated clinical prognostic model. This study validates the feasibility of analyzing immune cell components at a centralized laboratory using samples obtained from patients in a multicenter clinical trial. The results hold potential

for patient stratification in future studies, especially in clinical trials concerning agents that stimulate immune cells.

To analyze the composition of immune cells in blood, we employed CIBERSORT, a machine learning method designed to determine the cellular makeup of complex tissues from gene expression data. CIBERSORT has been shown to precisely quantify the immune-cell components of blood samples [192, 193, 220], correlating well with flow cytometry methods for detailing the phenotypic range of the twenty-two immune-cell subsets evaluated in this study [220]. This methodological approach not only improves reproducibility among different studies but also offers a scalable solution for regular clinical evaluation.

Currently, several prognostic models for mCRPC are available, depending on the clinical context and the treatments chosen. A specific model for chemotherapy-naïve mCRPC patients treated with enzalutamide was constructed using clinical data from both the PREVAIL phase 3 trial and our own study scenario and treatments. Recently, we improved this model by incorporating molecular factors such as circulating tumour cells (CTCs) and amplification of the AR in plasma DNA [221]. Through multivariate analysis, we examined the independent prognostic importance of these cellular components compared to validated clinical models, finding that the proportion of CD8 T-Cell lymphocytes retained independent prognostic value. Interestingly, in our cohort, NLR was not prognostic, likely due to the prevalence of low NLR in patients primarily with low tumour burden.

Various elements, such as steroid therapies, may impact the composition of immune cells in the blood and act as confounding factors in prognostic assessments. Steroid use is associated with elevated neutrophil levels and reduced lymphocyte numbers [222]. We observed that a minor segment of our patient cohort was initially on low-dose steroids, specifically 6 patients taking low-dose prednisone (≤ 10 mg). To account for potential confounding effects of steroids on the prognostic relevance of immune-cell components, we incorporated steroid usage into a comprehensive multivariate analysis that included recognized clinical and laboratory factors alongside the prognostic immune cell components. Steroid usage did not alter prognostic significance for CD8 T-Cells or monocytes, and was not prognostically significant. Consequently, we conclude that the small group of patients on low-dose steroids did not influence the previously reported prognostic significance of these immune cell components, thus bolstering the reliability and applicability of our findings.

While our study offers innovative contributions, we acknowledge certain limitations. The evaluation of immune-cell composition using CIBERSORT, like all methods based on gene expression, can be restricted by the accuracy of the reference profiles, which may vary under specific conditions. Additionally, certain cell types might be consistently overestimated or underestimated, though inter-group relative comparisons can mitigate this effect. Despite these challenges, it continues to be a validated method for evaluating and monitoring immune cell populations within complex tissues, including blood. A further constraint concerns the inclusion of patients with asymptomatic or minimally symptomatic chemotherapy-naïve mCRPC. Although this scenario is the most prevalent in the clinical, it would be insightful examining the immune elements in the blood of patients with other clinical characteristics, such as those experiencing pain or exhibiting aggressive or neuroendocrine disease features, and those undergoing alternative treatments like other AR pathway inhibitors (ARPIs), docetaxel, ¹⁷⁷Lu-PSMA or Radium-223.

Ultimately, our results suggest the need to reconsider the integration of immune profiles into clinical studies. They pave the way for further exploration into the prognostic and/or predictive importance of immune cell components in clinical trials. This approach may be particularly beneficial for immunotherapy trials. These findings were recently published by Perez-Navarro E, et al. [223]

Currently, our therapeutic decisions are based on the clinical features and safety profile of the treatments. To individualize treatment, it is essential to dissect tumour heterogeneity at both the clinical and biological levels. To address clinical heterogeneity, we have nomograms that include the most significant clinical prognostic factors [224] and to address biological heterogeneity, we need to integrate qualified biomarkers. An ideal biomarker in mCRPC must be reliable, reproducible, easy to obtain, preferably by a minimally invasive method, able to capture tumour heterogeneity and dynamism, and repeatable in the different clinical scenarios in which it is used.

Peripheral blood studies are an ideal source of biomarkers. The so-called liquid biopsy aims to capture tumour-related information from blood samples. Studies included in this heading include the study of circulating tumour cells (CTCs) [225], nucleic acids (plasma DNA)[226], circulating RNA and microvesicle studies [227].

In previous work, we presented findings from a phase 2 multicenter clinical study that focused on biomarkers in chemo-naïve mCRPC patients treated with enzalutamide as a first-line therapy. The study's main goal was to explore the

link between TMPRSS2-ERG and the drug's effectiveness, yet no significant correlation was found. Nonetheless, our analysis revealed that circulating tumor cells (CTCs) measured by AdnaTest® and AR gain were significant, independent prognostic factors. Furthermore, we performed external validation of a clinical prognostic model from the PREVAIL trial, noting that both CTCs and AR gain enhanced the model's prognostic accuracy. Consequently, we formulated a streamlined model comprising clinical variables and AR gain, validated using an independent cohort of mCRPC patients undergoing enzalutamide treatment in a comparable clinical context.

Prior investigations into the predictive significance of TMPRSS2-ERG concerning novel antiandrogens have yielded inconsistent outcomes with abiraterone. An early phase I/II trial involving abiraterone observed heightened PSA responses in tumors displaying TMPRSS2-ERG fusion [89, 228]. Our findings involving patients administered enzalutamide, in conjunction with earlier research with abiraterone, suggest that the TMPRSS2-ERG fusion gene is of limited utility as a predictive biomarker in mCRPC subjected to anti-androgen treatments.

Additionally, we assessed plasma AR-gain alongside other prospective biomarkers such as CTCs identified via AdnaTest® and AR-V7 expression within CTCs. Our prior publication documented the correlation between plasma AR-gain and negative outcomes to enzalutamide treatment after a median follow-up period of 11 months. These results were updated with a median follow-up of 37 months that confirms its strong independent prognostic value in first line mCRPC. AR-gain prognostic value was independent of other clinical and molecular prognostic variables. We observed a numerical increase in AR gain in AR-V7 positive patients compared with AR-V7 negative and CTC negative (40% vs 17% vs 8%). This result, although limited by the low numbers, agreed with previous publications in prostate cancer metastatic tissue, that observe an association between AR gain and AR-V7 expression in prostate cancer metastases [229].

Our study demonstrated that AdnaTest® enables the detection of CTCs in approximately one-third (35%) of patients with low to intermediate risk mCRPC. Furthermore, CTCs serve as a robust and independent prognostic biomarker. Additionally, landmark survival analysis revealed that the conversion of CTC status at 12 weeks of therapy is correlated with treatment outcomes, indicating a positive prognosis when CTCs become negative and a negative prognosis when they become positive. However, prospective randomized clinical trials are needed in order to fulfil the Prentice criteria [230] and fully qualify as a meaningful biomarker for regulatory matters. AR-V7 in

CTCs has previously demonstrated clinical value in mCRPC patients treated with a new anti-androgen therapy [171, 231]. In this first-line study, we observed a low detection rate for AR-V7 (5% of all patients; N= 5/98) and low PSA50 response rate (40% vs 82%). These results are consistent with a recently published phase 3 trial [232] in this same scenario, with a detection rate of 7-10% (N=38/953) and a response rate of 42% in 19 patients treated with enzalutamide. These results have been recently published by Fernandez-Perez MP et al. [221] (Annex 12.1), Perez-Navarro E et al. [223] (Annex 12.2).

The investigators of the pivotal trial of enzalutamide in first-line mCRPC published a clinical prognostic model able to stratify patients based on pre-treatment clinical variables. The initial model suffered from constraints due to the absence of external validation and lack of molecular variables. By validating this clinical prognostic model, we achieved a C-index of 0.70 and found that both circulating tumor cells (CTCs) and AR gain were independent variables enhancing the model's prognostic capability. Subsequently, we developed a streamlined clinical-molecular model incorporating three variables: AR gain, ALP, and PSA, which underwent independent validation. Lactate dehydrogenase (LDH) has been a frequent choice in various prognostic models for mCRPC, including those incorporating CTCs [225, 233]. Interestingly, LDH did not prove significant in our penalized regression model. This could be due to LDH's association with high-risk factors not captured by our model, potentially explaining the absence of statistical significance. In this phase 2 biomarker trial, we presented further evidence with extensive follow-up concerning the prognostic influence of AR gain alongside other biomarkers, including CTCs and AR-V7 in chemo-naïve mCRPC patients. We demonstrate the enhancement of clinical prognostic models through AR gain and propose a novel parsimonious model with plasma AR gain. Further investigations featuring extensive biomarker panels and detailed clinical datasets are necessary to reformulate prognostic models in prostate cancer.

Clinical prognostic models for mCRPC, such as the model for patients receiving first-line enzalutamide [234], aim to address the condition's heterogeneity. This particular model requires external validation and may benefit from enhancements that incorporate molecular data.

Blood cells interact with tumour cells in tissue, especially in the bone marrow. This interaction generates changes in expression, chromosomal alterations, and epigenetic changes in stromal cells associated with tumour aggressiveness.

Peripheral blood (PB) expression profiling has been shown to have diagnostic

and prognostic capabilities in multiple malignancies [235–238]. Peripheral blood expression profiles with prognostic ability have also been described in mCRPC. The first study published by Olmos D. et al. [183], conducted at the Royal Marsden/Institute of Cancer Research-UK, identifies a signature in the peripheral blood of mCRPC. Cancer Research-UK, identifies a signature composed of 9 genes with the capacity to identify a subgroup of patients with very aggressive tumours with prognostic patients with highly aggressive tumours with a decreased median survival of (10.7 vs. 25.6 months). This signature was associated with other poor prognostic factors such as elevated PSA or presence of CTCs. This signature, which was obtained from the selection of genes studied by gene expression arrays that were validated by RT-PCR, is composed of the following genes: HMBS, TMCC2, SNCA, SLC4A1, STOM, GABRRAPL2, TERF2IP, RIOK3, and TFDP1. These genes are predominantly expressed by immature erythroid cells CD71+ (transferrin receptor), possibly related to the movement of haematopoietic cells from the bone marrow and, to a lesser extent, genes involved in a decrease in the immune response. Independently, researchers at Dana Farber Cancer [182] identify a signature composed of 6 genes capable of identifying a group with a very adverse prognosis (7.8 vs 34.9 months) and independent of known clinical prognostic factors. This gene signature, which was obtained by studying by RT-PCR a pre-selected subgroup of genes involved in inflammatory processes, includes the following genes: C1QA, TIMP1, and CDKN1A which are related to an enrichment in macrophages; ITGAL which is expressed in natural killer (NK) cells; and ABL2 and SEMA4D which are enriched and involved in motility, immune surveillance function and T cell activity. A third study, carried out jointly by researchers from the above groups, identifies a prognostic signature composed of 4 genes and a prognostic signature composed of four genes that is more prognostic than the previous ones [184]. To this end, it again analyses the expression data published by Dr. Olmos using computational techniques including the elastic-net technique and is validated in 2 independent cohorts. Although these signatures include different genes, together they identify a subgroup of patients with very poor prognosis associated with bone marrow infiltration and immune system dysfunction. These studies suggest that tumour progression is associated with a decrease in the expression of genes related to lymphocyte activation and cytotoxic function and an increase in genes related to type 2 macrophages, associated with tumour progression. These results are consistent with findings observed in serial samples of tumour tissue treated with anti-CTLA4, demonstrating low pre-treatment lymphocyte infiltration in relation to other tumours and post-treatment associated immuno-regulatory

mechanisms lymphocyte mechanisms together with M2-type macrophage activation [239], which may explain the limited efficacy of these treatments.

In this thesis, we develop a 22-gene prognostic signature derived from peripheral blood gene expression profiles. We applied high-throughput microarray data from the PREMIERE trial and, after stringent preprocessing and quality control procedures, focused our analysis on well-characterized transcripts with consistent expression patterns. First, DEG associated with OS were identified by univariate Cox regression. This gave us a large pool of candidate biomarkers. These candidates were further polished and confirmed through a variety of supervised learning approaches, including linear and non-linear methods. For linear models, these included L1-regularized regression, L2-regularized regression, and their combination in the Elastic Net model that balances L1 and L2 penalties. In addition to these, Random Survival Forests were considered to possibly uncover complex nonlinear relationships among gene predictors. Every model was subjected to systematic hyperparameter tuning within a 7.3. Dynamics of immune cells in response to antiandrogen therapy 10-fold cross-validation framework to optimize the C-index. From these models, LASSO and Elastic Net emerged as the leading contenders, predominantly due to their strong predictive capacity. The signature demonstrated excellent predictive performance, with high concordance indices (C-indices) in both the training cohorts (0.868) and the validation cohorts (0.774), and maintained its prognostic value across multiple clinically relevant time points, as evidenced by time-dependent ROC analyses.

The signature outperformed existing models, such as those by Olmos et al. [183], Ross et al. [182] and Wang et al. [216], in both the PREMIERE training cohort and the MELDOLA validation cohort. The strength of our model lies in its rigorous statistical foundation and validation. Using Lasso regression, we effectively reduced dimensionality and selected the most relevant genes from a large pool of candidates identified through univariate Cox regression analysis. Time-dependent ROC analyses further confirmed the robustness of our signature across clinically relevant time points, indicating its potential utility in guiding treatment decisions and risk stratification.

The identification of this 22-gene signature has significant clinical implications. It provides a robust tool for risk stratification, enabling clinicians to tailor treatment strategies based on individual patient risk profiles. High-risk patients, as identified by our signature, may benefit from more aggressive or alternative therapeutic interventions, including enrolment in clinical trials investigating novel agents. Conversely, low-risk patients might avoid

unnecessary side effects associated with intensive treatments.

We have applied for an invention related to methods for predicting the progression of prostate cancer, specifically mCRPC, in an individual. The invention employs gene expression profiling combined with predictive modeling to assess the likelihood of OS and biochemical recurrence following treatment. Details of the application of the invention are available in the annexes. (HE-Ref. 909 356; Annex 12.3).

Immunotherapy has been revolutionary over the past several years, particularly immunocheckpoint inhibitors (ICI) that are already available in clinical settings. However, ICIs in PCa have shown disappointing results compared to other malignancies [142, 144, 145]. The PCa immune microenvironment may be inhospitable to immune cells and soon develop immune-tolerance strategies that can promote tumour growth, dissemination, and immune evasion.

Several efforts have been made to improve immunotherapy development in prostate cancer. Zhao et al. [218] interrogated the immune landscape using gene expression data from 9393 primary prostate tissue obtained from prostatectomy. Deconvolution using CIBERSORT revealed that tumour infiltration by macrophages and T lymphocytes conferred a worse prognosis, while mast cells, natural killers (NK) and dendritic cells (DC) were associated with an improved prognosis. Despite the huge number of samples included in the analyses, this study is limited by the study of only localized disease and the estimation of cell populations. However, the authors identify PD-L2 as a relevant biomarker for immune tolerance in PCa. Consistent with previous results, Jairath et al. [217] recently analysed TCGA RNA-Seq data and identified that localised prostate cancer subtypes enriched with macrophages and plasma cells depleted localized prostate cancer subtypes were associated with a worse prognosis.

Since immunotherapy is currently aimed at treating distant and lethal diseases, there is a pressing need to address the different stages of prostate cancer, including metastatic tissue in an androgen-deprived environment. In particular, ADT is associated with a short-term increase in the number of naïve T cells and Th-1 cells and a decrease in the number of T-regs, supporting the antitumor immune response to ADT [240]. However, emerging evidence suggests that anti-androgens, including enzalutamide, may have immunosuppressive effects on T cell priming [241]. These results suggest that the correct timing of ADT when treating PCa in combination with other immunotherapies is crucial to avoid unintended immunosuppressive effects. In

fact, sequencing of a therapeutic vaccine (Prostvac) and nilutamide demonstrated that using Prostvac first, followed by nilutamide, prolonged survival compared to reverse sequence [242].

The tumour microenvironment represents a complex medium in which innate immunity enhances tumour progression, metastases, and resistance to treatment, including resistance to castration [243] and to immunotherapy. However, the precise determinants that trigger a specific immunological landscape are not fully understood. Different genetic backgrounds have been shown to profoundly influence the composition of the tumour microenvironment, inducing diverse immune-cell components with different natures and roles. Bezzi et al. [244] demonstrated that gene-specific intrinsic pathways are at the core of various pro-tumour immune cell recruitment and infiltration. The loss of PTEN has been shown to be associated with an increased number of mononuclear myeloid derived suppressor cells (Mo-MDSCs; Gr-1+CD11b+ cells). These cells support prostate tumour growth and metastases by opposing the senescence response essential for immunosuppression by expressing Arginase 1 (Arg1) and inducible nitric oxide (iNOS) [245]. TP53 directly regulates the expression of CXCL17 at the promoter, and loss of TP53 is associated with up-regulation of CXCL17 expression. This cytokine acts as a cell attractant for Mo-MDSCs. Genetically modified prostate cancer models have increased intratumoural Gr-1+CD11b+ cells that exhibit a tumour-promoting phenotype associated with T-reg-mediated antitumour immunosuppression. Mo-MDSCs observed at an earlier stage are subsequently derived from PMN cells and macrophages. *In silico* analysis of the TCGA data supports these findings in humans. This interaction between PTEN and P53 defective tumours and MoMDSCs can be druggable. Vidotto et al. [246] observed using *in silico* analysis that gene expression in a human data set increased Treg infiltration (FOXP3) in PTEN-deficient prostate cancers. CXCR2 has been shown to increase the immunosuppressive tumour microenvironment and drives tumour progression through the attraction of Gr-1 + CD11b + cells. Inhibition of CXCR2, using SB225002, inhibits the attraction of Gr-1 + CD11b + cells, which subsequently inhibits tumour growth. Navarixin (MK-7123) is a CXCR2 inhibitor currently in clinical trials in prostate cancer in combination with pembrolizumab or enzalutamide. Further understanding of the complex interaction between the genetic background and its targeted agents, and the immune components of the TME is key to drive tailored immunotherapy. In addition, we need to unravel complex interactions between both components and its variation in diverse scenarios

Despite these promising insights, immune-checkpoint inhibitors including anti-CTLA4 and anti-PD1/PD-L1 therapies—have so far failed in advanced prostate cancer [138, 142, 144, 147, 247, 248]. Two large randomized trials in metastatic castration-resistant disease, combining enzalutamide with anti-PD-L1 (atezolizumab; IMbassador 250 [249]) or with anti-PD1 (pembrolizumab; KEYNOTE-641 [250]), did not improve survival; similarly, the phase 3 KEYNOTE-991 trial of ADT plus enzalutamide and pembrolizumab in metastatic castration-sensitive disease ended for futility [149].

Host-immune interactions with sex hormones could explain this lack of success, as well as gender differences in incidence and mortality across many cancers [137, 138, 251]. Prostate cancer intimately interacts with the immune system during initiation and progression [16, 252, 253], and androgens drive tumourigenesis while also suppressing T cells and IFN- γ production. As the standard of care in advanced disease, ADT, whether chemical (GnRH analogues or antagonists) or surgical (orchiectomy) can enhance antitumor immunity [254–256], regenerate the thymus [257], and increase intratumoural CD4+, CD8+ T cells, and macrophages in localized tumours when used preoperatively [258, 259]. ADT is also capable of inducing new antibody specificities in patients [260, 261].

Although prostate cancer is considered a “cold” tumour, compared to other cancers, immune infiltrates can be commonly observed in primary and metastatic tissue of advanced prostate cancer. Several immune populations, including CD4, CD8 lymphocytes, NK, and monocytes, are commonly observed in the tumour microenvironment of metastatic prostate cancer [136]. Furthermore, ADT increases PD-1 blockade through direct interactions of androgen receptors in T cells, boosting IFN- γ -mediated activity and creating a CD8+ T-cell signature linked to responses. Interestingly, although the combination of ADT, enzalutamide, and anti-PD1 was synergistic, enzalutamide alone did not enhance PD-1 blockade in preclinical models [136]. Parallel synergy was clinically observed in the PRIME-CUT phase 2 trial (NCT03951831), where metastatic sites such as liver, bone, lung and lymph nodes became highly infiltrated by CD8+, CD4+ T cells, and Tregs under combined ADT and anti-PD1 [262]. These findings suggest that lowering plasma testosterone may differ from directly blocking the AR with enzalutamide, which can have off-target effects. Consequently, while ADT combined with enzalutamide and anti-PD1 seems promising, enzalutamide alone may not recapitulate the same immune synergy [136]. Together, these results underscore the intricate interplay between sex hormones and immune

responses in prostate cancer and highlight the importance of aligning genomic characteristics, TME complexity, and therapeutic sequencing (particularly the timing of ADT and immunotherapies) to develop more effective individualized treatment approaches.

Integrating our results from the three chapters provides a comprehensive overview of the role of the immune system in the prognosis and treatment in mCRPC. The identification of both monocytes and CD8+ T cells as significant prognostic markers underlines the importance of immune surveillance and regulation in disease progression. We developed a 22-gene prognostic signature that could be of value in personalized medicine, allowing clinicians to predict outcomes in patients with greater certainty. Our finding on the off-target effects of enzalutamide and other antiandrogens on T-cell survival has revealed one mechanism by which resistance to this drug arises. This implies that the depletion of cytotoxic T cells and the perturbation of immune cell dynamics are indicative of a more permissive environment for enzalutamide-induced tumour growth. These findings also underscore the need for evaluation of treatment in mCRPC, not only targeting direct antitumor effects but also considering impacts on the immune system.

Inclusion of immune profiling in clinical trials will allow the selection of therapies with the least effect on immunosuppression that could result in improvement of combination treatments involving immunotherapies.

Although our studies contribute significantly to the knowledge about mCRPC, several limitations should be underlined: Despite rigorous selection and validation, patient cohorts were relatively small and findings may need validation in larger and more diverse populations. Immune cell profiling relies on computational deconvolution algorithms, which, for all their power, cannot compete with direct measurements such as flow cytometry in capturing the full details of the immune landscape. The extension of patient cohorts to include all ethnicities and stages of disease in future studies would provide a better generalization of the findings. Further immune cell types, including regulatory T cells and myeloid-derived suppressor cells, could be studied to provide a deeper understanding of the immune dynamics in mCRPC. Longitudinal studies of immune changes through different treatment modalities would also be informative in identifying optimal therapeutic windows and strategies.

In addition, a deeper investigation of the molecular processes that determine the AR-independent action of antiandrogens on immune cells might show new targets for reducing immunosuppression. Future research into combination

regimens with other such immune-activating agents will hopefully unlock synergies to breakthrough resistance in a clinical attempt to improve patient outcomes.

CONCLUSIONS

The following are the final conclusions that can be drawn from the results obtained in this thesis:

- **Conclusion 1.-** A comprehensive evaluation of the composition of immune cells in mCRPC patients has shown that high levels of monocytes prior to treatment and reduced proportions of CD8+ T cells in peripheral blood are independently associated with poorer OS in patients with mCRPC. These findings highlight the critical role of host immune responses and how immune profiling could add value to risk stratification.
- **Conclusion 2.-** We have identified a new peripheral blood 22-gene expression signature that is a strong predictor of patient outcome in mCRPC. This signature has been validated in an independent data set and outperforms existing blood-based prognostic models. A patent has been sought and is currently being evaluated.
- **Conclusion 3.-** Treatment with enzalutamide is associated with changes in immune cell composition in the blood of patients with mCRPC, including a decrease in CD8-T cells. In vitro experiments demonstrate decreased survival induced by enzalutamide in an AR independent manner. This off-target effect might be variable between different AR targeting agents.

CONCLUSIONES

A continuación se exponen las conclusiones finales que se pueden extraer de los resultados obtenidos en esta tesis:

- **Conclusión 1.-** Una evaluación exhaustiva de la composición sanguínea de las células inmunes en pacientes con CPRCm ha demostrado que los niveles elevados de monocitos antes del tratamiento y las proporciones reducidas de células T CD8+ en sangre periférica se asocian de forma independiente con una peor supervivencia global en pacientes con cáncer de próstata metastásico resistente a la castración. Estos hallazgos ponen de relieve el papel fundamental de las respuestas inmunitarias del huésped y cómo los perfiles inmunológicos podrían añadir valor a la estratificación del riesgo.
- **Conclusión 2.-** Hemos identificado una nueva firma de expresión de 22 genes en sangre periférica que es un fuerte predictor del resultado de los pacientes con cáncer de próstata metastásico resistente a la castración. Esta firma ha sido validada en un conjunto de datos independiente y supera a los modelos de pronóstico basados en sangre existentes. Se ha solicitado una patente, que se está evaluando actualmente.
- **Conclusión 3.-** El tratamiento con enzalutamida se asocia con cambios en la composición inmune de la sangre de pacientes con CPRCm, incluyendo descenso en linfocitos T CD8. Experimentos in vitro demuestran una menor supervivencia inducida por la enzalutamida de forma independiente del receptor de andrógenos. Este efecto, independiente de la diana, puede ser variable entre los distintos agentes dirigidos frente al receptor androgénico.

BIBLIOGRAPHY

BIBLIOGRAPHY

- [1] William C. Hahn et al. "Creation of human tumour cells with defined genetic elements". In: *Nature* 400.6743 (July 1999), pp. 464–468. ISSN: 00280836. DOI: 10.1038/22780.
- [2] William C. Hahn et al. "Rules for Making Human Tumor Cells". In: *The New England journal of medicine* 347.20 (Nov. 2002), pp. 1593–603. ISSN: 1533-4406. DOI: 10.1056/NEJMra021902.
- [3] Douglas Hanahan et al. "The Hallmarks of Cancer". In: *Cell* 100.1 (Jan. 2000), pp. 57–70. ISSN: 00928674. DOI: 10.1016/S0092-8674(00)81683-9.
- [4] Douglas Hanahan et al. "Hallmarks of Cancer: The Next Generation". In: *Cell* 144.5 (Mar. 2011), pp. 646–674. ISSN: 00928674. DOI: 10.1016/j.cell.2011.02.013.
- [5] Douglas Hanahan. "Hallmarks of Cancer: New Dimensions". In: *Cancer Discovery* 12.1 (Jan. 2022), pp. 31–46. ISSN: 2159-8274. DOI: 10.1158/2159-8290.CD-21-1059.
- [6] F J Wilson et al. *Histology Image Review*. Lange educational library. McGraw-Hill Professional Publishing, 1999. ISBN: 9780838537480.
- [7] John E. McNeal. "The zonal anatomy of the prostate". In: *The Prostate* 2.1 (1981), pp. 35–49. ISSN: 02704137. DOI: 10.1002/pros.2990020105.
- [8] Alexandre R. Zlotta et al. "Prevalence of Prostate Cancer on Autopsy: Cross-Sectional Study on Unscreened Caucasian and Asian Men". In: *JNCI: Journal of the National Cancer Institute* 105.14 (July 2013), pp. 1050–1058. ISSN: 1460-2105. DOI: 10.1093/jnci/djt151.
- [9] Barry G. Timms. "Prostate development: a historical perspective". In: *Differentiation* 76.6 (July 2008), pp. 565–577. ISSN: 0301-4681. DOI: 10.1111/J.1432-0436.2008.00278.X.
- [10] H. Rui et al. "Accessory Sex Gland Function in Normal Young (20-25 Years) and Middle-aged (50-55 Years) Men". In: *Journal of Andrology* 7.2 (1986), pp. 93–99. ISSN: 19394640. DOI: 10.1002/j.1939-4640.1986.tb00887.x.
- [11] Lalani el-N et al. "Molecular and cellular biology of prostate cancer." In: *Cancer metastasis reviews* 16.1-2 (June 1997), pp. 29–66. ISSN: 0167-7659. DOI: 10.1023/a:1005792206377.

- [12] A. Fritjofsson et al. "Anatomy of the prostate. Aspects of the secretory function in relation to lobar structure." In: *Scandinavian journal of urology and nephrology. Supplementum* 107 (Jan. 1988), pp. 5–13. ISSN: 03008886.
- [13] Cory Abate-Shen et al. "Molecular genetics of prostate cancer". In: *Genes & Development* 14.19 (Oct. 2000), pp. 2410–2434. ISSN: 0890-9369. DOI: 10.1101/gad.819500.
- [14] B. Orr et al. "Identification of stromally expressed molecules in the prostate by tag-profiling of cancer-associated fibroblasts, normal fibroblasts and fetal prostate". In: *Oncogene* 31.9 (Mar. 2012), pp. 1130–1142. ISSN: 1476-5594. DOI: 10.1038/ONC.2011.312.
- [15] Noemi Eiro et al. "Stromal factors involved in human prostate cancer development, progression and castration resistance". In: *Journal of cancer research and clinical oncology* 143.2 (Feb. 2017), pp. 351–359. ISSN: 1432-1335. DOI: 10.1007/S00432-016-2284-3.
- [16] Angelo M. De Marzo et al. *Inflammation in prostate carcinogenesis*. Apr. 2007. DOI: 10.1038/nrc2090.
- [17] Rebecca L Siegel et al. "Cancer statistics, 2024." In: *CA: a cancer journal for clinicians* 74.1 (Jan. 2024), pp. 12–49. ISSN: 0007-9235. DOI: 10.3322/caac.21820.
- [18] <https://redecana.org/storage/documents/02d62122-9adb-4d35-b6d0-551435dbe4ae.pdf>. REDECAN. Red Española de Registros de Cáncer. [Internet]. Available from: 2024.
- [19] Rebecca L Siegel et al. "Cancer statistics, 2023". In: *CA: A Cancer Journal for Clinicians* 73.1 (Jan. 2023), pp. 17–48. ISSN: 0007-9235. DOI: 10.3322/caac.21763.
- [20] Hyuna Sung et al. "Global Cancer Statistics 2020: GLOBOCAN Estimates of Incidence and Mortality Worldwide for 36 Cancers in 185 Countries". In: *CA: A Cancer Journal for Clinicians* 71.3 (May 2021), pp. 209–249. ISSN: 1542-4863. DOI: 10.3322/CAAC.21660.
- [21] N. Larrañaga et al. "Prostate cancer incidence trends in Spain before and during the prostate-specific antigen era: Impact on mortality". In: *Annals of Oncology* 21.SUPPL.3 (2010). ISSN: 15698041. DOI: 10.1093/annonc/mdq087.
- [22] SEOM; *Las cifras del cáncer en España*. 2024. URL: https://www.seom.org/images/LAS_CIFRAS_2024.pdf.
- [23] Amit R. Patel et al. *Risk factors for prostate cancer*. 2009. DOI: 10.1038/ncpuro1290.
- [24] G. S.M. Harrison. "The Prognosis of Prostatic Cancer in the Younger Man". In: *British Journal of Urology* 55.3 (1983), pp. 315–320. ISSN: 1464410X. DOI: 10.1111/j.1464-410X.1983.tb03307.x.
- [25] Douglas E. Johnson et al. "Prostatic adenocarcinoma occurring in men under 50 years of age". In: *Journal of Surgical Oncology* 4.3 (1972), pp. 207–216. ISSN: 10969098. DOI: 10.1002/jso.2930040305.
- [26] Kristin Gunderson et al. "Global prostate cancer incidence and the migration, settlement, and admixture history of the Northern Europeans". In: *Cancer*

- Epidemiology* 35.4 (Aug. 2011), pp. 320–327. ISSN: 18777821. DOI: 10.1016/j.canep.2010.11.007.
- [27] Timothy R. Rebbeck. “Prostate cancer disparities by race and ethnicity: From nucleotide to neighborhood”. In: *Cold Spring Harbor Perspectives in Medicine* 8.9 (Sept. 2018). ISSN: 21571422. DOI: 10.1101/cshperspect.a030387.
- [28] Lorelei A. Mucci et al. “Epidemiology of prostate cancer”. In: *Pathology and Epidemiology of Cancer*. Vol. 10. 2016, pp. 107–125. ISBN: 9783319351537. DOI: 10.1007/978-3-319-35153-7_{_}9.
- [29] Miia Suuriniemi et al. “Confirmation of a positive association between prostate cancer risk and a locus at chromosome 8q24”. In: *Cancer Epidemiology Biomarkers and Prevention* 16.4 (Apr. 2007), pp. 809–814. ISSN: 10559965. DOI: 10.1158/1055-9965.EPI-06-1049.
- [30] Michael N. Okobia et al. “Chromosome 8q24 variants are associated with prostate cancer risk in a high risk population of African ancestry”. In: *Prostate* 71.10 (July 2011), pp. 1054–1063. ISSN: 02704137. DOI: 10.1002/pros.21320.
- [31] Matthew L. Freedman et al. “Admixture mapping identifies 8q24 as a prostate cancer risk locus in African-American men”. In: *Proceedings of the National Academy of Sciences of the United States of America* 103.38 (Sept. 2006), pp. 14068–14073. ISSN: 00278424. DOI: 10.1073/pnas.0605832103.
- [32] K. J. Pienta et al. *Risk factors for prostate cancer*. 1993. DOI: 10.7326/0003-4819-118-10-199305150-00007.
- [33] Brittany Szymaniak et al. *Genetics in prostate cancer: implications for clinical practice*. Dec. 2021. DOI: 10.1097/SPC.0000000000000575.
- [34] David V. Conti et al. “Trans-ancestry genome-wide association meta-analysis of prostate cancer identifies new susceptibility loci and informs genetic risk prediction”. In: *Nature Genetics* 53.1 (Jan. 2021), pp. 65–75. ISSN: 15461718. DOI: 10.1038/s41588-020-00748-0.
- [35] Veda N. Giri et al. “Role of genetic testing for inherited prostate cancer risk: Philadelphia prostate cancer consensus conference 2017”. In: *Journal of Clinical Oncology* 36.4 (Feb. 2018), pp. 414–424. ISSN: 15277755. DOI: 10.1200/JCO.2017.74.1173.
- [36] Eugenia E. Calle et al. “Overweight, Obesity, and Mortality from Cancer in a Prospectively Studied Cohort of U.S. Adults”. In: *New England Journal of Medicine* 348.17 (Apr. 2003), pp. 1625–1638. ISSN: 0028-4793. DOI: 10.1056/nejmoa021423.
- [37] Christopher J. Keto et al. “Obesity is associated with castration-resistant disease and metastasis in men treated with androgen deprivation therapy after radical prostatectomy: Results from the SEARCH database”. In: *BJU International* 110.4 (Aug. 2012), pp. 492–498. ISSN: 14644096. DOI: 10.1111/j.1464-410X.2011.10754.x.
- [38] Rebekah L. Wilson et al. *Obesity and prostate cancer: A narrative review*. Jan. 2022. DOI: 10.1016/j.critrevonc.2021.103543.

- [39] Adriana C. Vidal et al. *Obesity and Prostate Cancer: A Focused Update on Active Surveillance, Race, and Molecular Subtyping*. July 2017. doi: 10.1016/j.eururo.2016.10.011.
- [40] Bamidele A. Adesunloye. *Mechanistic insights into the link between obesity and prostate cancer*. Apr. 2021. doi: 10.3390/ijms22083935.
- [41] Kazutoshi Fujita et al. *Obesity, inflammation, and prostate cancer*. Feb. 2019. doi: 10.3390/jcm8020201.
- [42] Saeedeh Nouri-Majd et al. *Association Between Red and Processed Meat Consumption and Risk of Prostate Cancer: A Systematic Review and Meta-Analysis*. Feb. 2022. doi: 10.3389/fnut.2022.801722.
- [43] Lukas Schwingshackl et al. *Adherence to mediterranean diet and risk of cancer: An updated systematic review and meta-analysis*. Sept. 2017. doi: 10.3390/nu9101063.
- [44] Sheng Cheng et al. *Mediterranean dietary pattern and the risk of prostate cancer a meta-analysis*. 2019. doi: 10.1097/MD.00000000000016341.
- [45] Felix F. Berger et al. *Sedentary behavior and prostate cancer: A systematic review and meta-analysis of prospective cohort studies*. 2019. doi: 10.1158/1940-6207.CAPR-19-0271.
- [46] Sarah Al-Fayez et al. "Cigarette smoking and prostate cancer: A systematic review and meta-analysis of prospective cohort studies". In: *Tobacco Induced Diseases* 21 (Feb. 2023). ISSN: 16179625. doi: 10.18332/tid/157231.
- [47] Farhad Islami et al. *A systematic review and meta-analysis of tobacco use and prostate cancer mortality and incidence in prospective cohort studies*. Dec. 2014. doi: 10.1016/j.eururo.2014.08.059.
- [48] Felix M. Onyije et al. *Cancer incidence and mortality among petroleum industry workers and residents living in oil producing communities: A systematic review and meta-analysis*. Apr. 2021. doi: 10.3390/ijerph18084343.
- [49] Kayo Togawa et al. "Cancer incidence in agricultural workers: Findings from an international consortium of agricultural cohort studies (AGRICOH)". In: *Environment International* 157 (Dec. 2021). ISSN: 18736750. doi: 10.1016/j.envint.2021.106825.
- [50] Hui Zhong et al. *Primary Sjögren's syndrome is associated with increased risk of malignancies besides lymphoma: A systematic review and meta-analysis*. May 2022. doi: 10.1016/j.autrev.2022.103084.
- [51] Huayang Ding et al. "Does prostatitis increase the risk of prostate cancer? A meta-analysis". In: *International Journal of Clinical and Experimental Medicine* 10.3 (2017), pp. 4798–4808. ISSN: 19405901.
- [52] Haiying Cui et al. *Antidiabetic medications and the risk of prostate cancer in patients with diabetes mellitus: A systematic review and meta-analysis*. Mar. 2022. doi: 10.1016/j.phrs.2022.106094.
- [53] Giorgio I. Russo et al. *Human papillomavirus and risk of prostate cancer: a systematic review and meta-analysis*. Apr. 2020. doi: 10.1080/13685538.2018.1455178.

- [54] Daniel Jones et al. *The diagnostic test accuracy of rectal examination for prostate cancer diagnosis in symptomatic patients: A systematic review*. June 2018. DOI: 10.1186/s12875-018-0765-y.
- [55] Thomas A. Stamey et al. "Prostate-Specific Antigen as a Serum Marker for Adenocarcinoma of the Prostate". In: *New England Journal of Medicine* 317.15 (Oct. 1987), pp. 909–916. ISSN: 0028-4793. DOI: 10.1056/nejm198710083171501.
- [56] H. Lilja. "A kallikrein-like serine protease in prostatic fluid cleaves the predominant seminal vesicle protein". In: *Journal of Clinical Investigation* 76.5 (1985), pp. 1899–1903. ISSN: 00219738. DOI: 10.1172/JCI112185.
- [57] T. Y. Wang et al. "Preliminary evaluation of measurement of serum prostate-specific antigen level in detection of prostate cancer". In: *Annals of Clinical and Laboratory Science* 16.6 (1986), pp. 461–466. ISSN: 00917370.
- [58] William J. Catalona et al. "Measurement of Prostate-Specific Antigen in Serum as a Screening Test for Prostate Cancer". In: *New England Journal of Medicine* 324.17 (Apr. 1991), pp. 1156–1161. ISSN: 0028-4793. DOI: 10.1056/nejm199104253241702.
- [59] Ana Rita Lima et al. *Advances and perspectives in prostate cancer biomarker discovery in the last 5 years through tissue and urine metabolomics*. Mar. 2021. DOI: 10.3390/metabo11030181.
- [60] Jenny Donovan et al. *Prostate testing for cancer and treatment (ProtecT) feasibility study*. 2003. DOI: 10.3310/hta7140.
- [61] Klaus Eichler et al. *Diagnostic Value of Systematic Biopsy Methods in the Investigation of Prostate Cancer: A Systematic Review*. May 2006. DOI: 10.1016/S0022-5347(05)00957-2.
- [62] Mengxin Lu et al. "Transrectal versus transperineal prostate biopsy in detection of prostate cancer: a retrospective study based on 452 patients". In: *BMC Urology* 23.1 (Dec. 2023), pp. 1–7. ISSN: 14712490. DOI: 10.1186/s12894-023-01176-y.
- [63] Richard Zigeuner et al. "Detection of prostate cancer by TURP or open surgery in patients with previously negative transrectal prostate biopsies". In: *Urology* 62.5 (2003), pp. 883–887. ISSN: 00904295. DOI: 10.1016/S0090-4295(03)00663-0.
- [64] Louise Dickinson et al. "Magnetic resonance imaging for the detection, localisation, and characterisation of prostate cancer: Recommendations from a European consensus meeting". In: *European Urology* 59.4 (Apr. 2011), pp. 477–494. ISSN: 03022838. DOI: 10.1016/j.eururo.2010.12.009.
- [65] John V. Hegde et al. *Multiparametric MRI of prostate cancer: An update on state-of-the-art techniques and their performance in detecting and localizing prostate cancer*. May 2013. DOI: 10.1002/jmri.23860.
- [66] Giuseppe Galletti et al. *Circulating tumor cells in prostate cancer diagnosis and monitoring: An appraisal of clinical potential*. 2014. DOI: 10.1007/s40291-014-0101-8.
- [67] Dmitry Enikeev et al. *A Systematic Review of Circulating Tumor Cells Clinical Application in Prostate Cancer Diagnosis*. Aug. 2022. DOI: 10.3390/cancers14153802.

- [68] Yaqiong Wang et al. *Liquid biopsy in prostate cancer: current status and future challenges of clinical application*. 2021. doi: 10.1080/13685538.2021.1944085.
- [69] Frédéric E. Lecouvet et al. *Use of modern imaging methods to facilitate trials of metastasis-directed therapy for oligometastatic disease in prostate cancer: a consensus recommendation from the EORTC Imaging Group*. Oct. 2018. doi: 10.1016/S1470-2045(18)30571-0.
- [70] Brierley J.D. et al. *TNM Classification of Malignant Tumours, 8th edition due December 2016*. Wiley-Blackwell, 2017, pp. 1–272. ISBN: 978-1-119-26357-9.
- [71] D. F. Gleason et al. “Prediction of prognosis for prostatic adenocarcinoma by combined histological grading and clinical staging”. In: *Journal of Urology* 111.1 (1974), pp. 58–64. ISSN: 00225347. doi: 10.1016/S0022-5347(17)59889-4.
- [72] Jonathan I. Epstein et al. “The 2014 international society of urological pathology (ISUP) consensus conference on gleason grading of prostatic carcinoma definition of grading patterns and proposal for a new grading system”. In: *American Journal of Surgical Pathology* 40.2 (2016), pp. 244–252. ISSN: 15320979. doi: 10.1097/PAS.0000000000000530.
- [73] International Agency for Research on Cancer. *Urinary and Male Genital Tumours*. Ed. by H. Moch. Vol. 8. International Agency for Research on Cancer, 2022, p. 576. ISBN: 978-92-832-4512-4.
- [74] Philip Cornford et al. *EAU-EANM-ESTRO-ESUR-ISUP-SIOG Guidelines on Prostate Cancer—2024 Update. Part I: Screening, Diagnosis, and Local Treatment with Curative Intent*. Aug. 2024. doi: 10.1016/j.eururo.2024.03.027.
- [75] Edward M. Schaeffer et al. “Prostate Cancer, Version 4.2023”. In: *JNCCN Journal of the National Comprehensive Cancer Network* 21.10 (Oct. 2023), pp. 1067–1096. ISSN: 15401413. doi: 10.6004/jnccn.2023.0050.
- [76] Anthony V. D’Amico et al. “Biochemical outcome after radical prostatectomy, external beam radiation therapy, or interstitial radiation therapy for clinically localized prostate cancer”. In: *Journal of the American Medical Association* 280.11 (Sept. 1998), pp. 969–974. ISSN: 00987484. doi: 10.1001/jama.280.11.969.
- [77] Stephen J. Berry et al. “The development of human benign prostatic hyperplasia with age”. In: *Journal of Urology* 132.3 (Sept. 1984), pp. 474–479. ISSN: 00225347. doi: 10.1016/S0022-5347(17)49698-4.
- [78] Justin M. Ketchem et al. *Male sex hormones, aging, and inflammation*. Feb. 2023. doi: 10.1007/s10522-022-10002-1.
- [79] Ana Aranda et al. “Nuclear Hormone Receptors and Gene Expression”. In: *Physiological Reviews* 81.3 (July 2001), pp. 1269–1304. ISSN: 0031-9333. doi: 10.1152/physrev.2001.81.3.1269.
- [80] V Laudet. “Evolution of the nuclear receptor superfamily: early diversification from an ancestral orphan receptor”. In: *Journal of Molecular Endocrinology* 19.3 (Dec. 1997), pp. 207–226. ISSN: 0952-5041. doi: 10.1677/jme.0.0190207.

- [81] Pierre Chambon. "The Nuclear Receptor Superfamily: A Personal Retrospect on the First Two Decades". In: *Molecular Endocrinology* 19.6 (June 2005), pp. 1418–1428. ISSN: 0888-8809. DOI: 10.1210/me.2005-0125.
- [82] Rachel A Davey et al. "Androgen Receptor Structure, Function and Biology: From Bench to Bedside." In: *Clinical biochemist reviews* 37.1 (Feb. 2016), pp. 3–15. ISSN: 0159-8090.
- [83] Rosa Greasley et al. *A profile of enzalutamide for the treatment of advanced castration resistant prostate cancer*. June 2015. DOI: 10.2147/CMAR.S50585. URL: <https://pmc.ncbi.nlm.nih.gov/articles/PMC4472073/>.
- [84] MH Eileen Tan et al. "Androgen receptor: structure, role in prostate cancer and drug discovery". In: *Acta Pharmacologica Sinica* 36.1 (Jan. 2015), pp. 3–23. ISSN: 1671-4083. DOI: 10.1038/aps.2014.18.
- [85] Wenqing Gao et al. "Chemistry and structural biology of androgen receptor". In: *Chemical Reviews* 105.9 (Sept. 2005), pp. 3352–3370. ISSN: 00092665. DOI: 10.1021/CR020456U/ASSET/CR020456U.FP.PNG{_}V03.
- [86] Bisheng Cheng et al. "Expanding horizons in overcoming therapeutic resistance in castration-resistant prostate cancer: targeting the androgen receptor-regulated tumor immune microenvironment". In: *Cancer Biology and Medicine* 20.8 (Aug. 2023), pp. 568–574. ISSN: 20953941. DOI: 10.20892/j.issn.2095-3941.2023.0256.
- [87] John T. Isaacs et al. "Adaptation Versus Selection as the Mechanism Responsible for the Relapse of Prostatic Cancer to Androgen Ablation Therapy as Studied in the Dunning R-3327-H Adenocarcinoma". In: *Cancer Research* 41 (1981), pp. 5070–5074. ISSN: 15387445.
- [88] Howard I. Scher et al. *Targeting the androgen receptor: Improving outcomes for castration-resistant prostate cancer*. Sept. 2004. DOI: 10.1677/erc.1.00525.
- [89] Gerhardt Attard et al. "Characterization of ERG, AR and PTEN gene status in circulating tumor cells from patients with castration-resistant prostate cancer". In: *Cancer research* 69.7 (Apr. 2009), pp. 2912–2918. ISSN: 1538-7445. DOI: 10.1158/0008-5472.CAN-08-3667.
- [90] Yien Ning Sophia Wong et al. *Evolution of androgen receptor targeted therapy for advanced prostate cancer*. 2014. DOI: 10.1038/nrclinonc.2014.72.
- [91] Laurence Klotz. *Active surveillance for low-risk prostate cancer*. May 2017. DOI: 10.1097/MOU.0000000000000393.
- [92] Jeffrey J. Tosoian et al. "Active Surveillance of Grade Group 1 Prostate Cancer: Long-term Outcomes from a Large Prospective Cohort". In: *European Urology* 77.6 (June 2020), pp. 675–682. ISSN: 18737560. DOI: 10.1016/j.eururo.2019.12.017.
- [93] Freddie C. Hamdy et al. "10-Year Outcomes after Monitoring, Surgery, or Radiotherapy for Localized Prostate Cancer". In: *New England Journal of Medicine* 375.15 (Oct. 2016), pp. 1415–1424. ISSN: 0028-4793. DOI: 10.1056/nejmoa1606220.

- [94] John Kirkpatrick. *Radical prostatectomy versus watchful waiting in early prostate cancer*. May 2002. doi: 10.1097/s0022-5347(01)68600-2.
- [95] Peter C. Albertsen. *Re: Radical prostatectomy or watchful waiting in early prostate cancer*. Mar. 2014. doi: 10.1016/j.eururo.2014.08.043.
- [96] Hugh H. Young. "The early diagnosis and radical cure of carcinoma of the prostate: A study of fifty cases and presentation of a radical operation". In: *Journal of the American Medical Association* XLVI.10 (1906), pp. 699–704. ISSN: 23768118. doi: 10.1001/jama.1906.62510370005001b.
- [97] J. H. Carver. "Retropubic urinary surgery". In: *International Journal of Clinical Practice* 1.12 (Dec. 1947), pp. 41–42. ISSN: 1368-5031. doi: 10.1111/j.1742-1241.1947.tb02012.x.
- [98] W. G. Reiner et al. "An anatomical approach to the surgical management of the dorsal vein and Santorini's plexus during radical retropubic surgery". In: *Journal of Urology* 121.2 (1979), pp. 198–200. ISSN: 00225347. doi: 10.1016/S0022-5347(17)56718-X.
- [99] Herbert Lepor. "A review of surgical techniques for radical prostatectomy." In: *Reviews in urology* 7 Suppl 2.Suppl 2 (2005), pp. 11–7. ISSN: 1523-6161.
- [100] Reza Ghavamian et al. "Comparison of operative and functional outcomes of laparoscopic radical prostatectomy and radical retropubic prostatectomy: Single surgeon experience". In: *Urology* 67.6 (June 2006), pp. 1241–1246. ISSN: 00904295. doi: 10.1016/j.urology.2005.12.017.
- [101] Giorgio Guazzoni et al. "Intra- and Peri-Operative Outcomes Comparing Radical Retropubic and Laparoscopic Radical Prostatectomy: Results from a Prospective, Randomised, Single-Surgeon Study". In: *European Urology* 50.1 (July 2006), pp. 98–104. ISSN: 03022838. doi: 10.1016/j.eururo.2006.02.051.
- [102] Vincenzo Ficarra et al. "Systematic Review and Meta-analysis of Studies Reporting Urinary Continence Recovery After Robot-assisted Radical Prostatectomy". In: *European Urology* 62.3 (Sept. 2012), pp. 405–417. ISSN: 03022838. doi: 10.1016/j.eururo.2012.05.045.
- [103] Yuefeng Du et al. "Robot-assisted radical prostatectomy is more beneficial for prostate cancer patients: A system review and meta-analysis". In: *Medical Science Monitor* 24 (Jan. 2018), pp. 272–287. ISSN: 16433750. doi: 10.12659/MSM.907092.
- [104] Anna Lantz et al. "Functional and Oncological Outcomes After Open Versus Robot-assisted Laparoscopic Radical Prostatectomy for Localised Prostate Cancer: 8-Year Follow-up". In: *European Urology* 80.5 (Nov. 2021), pp. 650–660. ISSN: 18737560. doi: 10.1016/j.eururo.2021.07.025.
- [105] Jianglei Ma et al. "Robotic-assisted versus laparoscopic radical prostatectomy for prostate cancer: the first separate systematic review and meta-analysis of randomised controlled trials and non-randomised studies". In: *International journal of surgery (London, England)* 109.5 (May 2023), pp. 1350–1359. ISSN: 17439159. doi: 10.1097/JS9.000000000000193.

- [106] James A. Eastham et al. "Risk factors for urinary incontinence after radical prostatectomy". In: *Journal of Urology* 156.5 (1996), pp. 1707–1713. ISSN: 00225347. DOI: 10.1016/S0022-5347(01)65488-0.
- [107] Emilio Sacco et al. "Urinary incontinence after radical prostatectomy: Incidence by definition, risk factors and temporal trend in a large series with a long-term follow-up". In: *BJU International* 97.6 (June 2006), pp. 1234–1241. ISSN: 14644096. DOI: 10.1111/j.1464-410X.2006.06185.x.
- [108] Ganesh Sivarajan et al. "Ten-year outcomes of sexual function after radical prostatectomy: Results of a prospective longitudinal study". In: *European Urology* 65.1 (2014), pp. 58–65. ISSN: 03022838. DOI: 10.1016/j.eururo.2013.08.019.
- [109] Yoshifumi Kadono et al. "Changes in penile length after radical prostatectomy: investigation of the underlying anatomical mechanism". In: *BJU International* 120.2 (Aug. 2017), pp. 293–299. ISSN: 1464410X. DOI: 10.1111/bju.13777.
- [110] W. F. Whitmore et al. "Retropubic implantation to iodine 125 in the treatment of prostatic cancer." In: *The Journal of urology* 108.6 (1972), pp. 918–920. ISSN: 00225347. DOI: 10.1016/S0022-5347(17)60906-6.
- [111] H. H. Holm et al. "Transperineal 125iodine seed implantation in prostatic cancer guided by transrectal ultrasonography". In: *Journal of Urology* 130.2 (1983), pp. 283–286. ISSN: 00225347. DOI: 10.1016/S0022-5347(17)51108-8.
- [112] Mike Shelley et al. *Cyrotherapy for localised prostate cancer*. 2007. DOI: 10.1002/14651858.CD005010.pub2.
- [113] Kae Jack Tay et al. "Focal cryotherapy for localized prostate cancer". In: *Archivos Espanoles de Urologia* 69.6 (2016), pp. 317–326. ISSN: 00040614.
- [114] Taimur T. Shah et al. "Early-Medium-Term Outcomes of Primary Focal Cryotherapy to Treat Nonmetastatic Clinically Significant Prostate Cancer from a Prospective Multicentre Registry". In: *European Urology* 76.1 (July 2019), pp. 98–105. ISSN: 18737560. DOI: 10.1016/j.eururo.2018.12.030.
- [115] James E. Kennedy. *High-intensity focused ultrasound in the treatment of solid tumours*. Apr. 2005. DOI: 10.1038/nrc1591.
- [116] Deepika Reddy et al. "Cancer Control Outcomes Following Focal Therapy Using High-intensity Focused Ultrasound in 1379 Men with Nonmetastatic Prostate Cancer: A Multi-institute 15-year Experience". In: *European Urology* 81.4 (Apr. 2022), pp. 407–413. ISSN: 18737560. DOI: 10.1016/j.eururo.2022.01.005.
- [117] Ankur Agarwala et al. "Bilateral Orchiectomy Revisited in Management of Metastatic Hormone-Sensitive Prostate Cancer". In: *Indian Journal of Surgical Oncology* 12.3 (Sept. 2021), pp. 565–570. ISSN: 09766952. DOI: 10.1007/s13193-021-01390-w.
- [118] Charles Huggins. "Studies on prostatic cancer". In: *Archives of Surgery* 43.2 (Aug. 1941), p. 209. ISSN: 0272-5533. DOI: 10.1001/archsurg.1941.01210140043004.

- [119] Kevin T. Nead et al. "Association of Androgen Deprivation Therapy and Thromboembolic Events: A Systematic Review and Meta-analysis". In: *Urology* 114 (2018), pp. 155–162. ISSN: 15279995. DOI: 10.1016/j.urology.2017.11.055.
- [120] Hein Van Poppel et al. *Gonadotropin-releasing hormone: An update review of the antagonists versus agonists*. July 2012. DOI: 10.1111/j.1442-2042.2012.02997.x.
- [121] N. D. Shore et al. *Re: Oral Relugolix for Androgen-Deprivation Therapy in Advanced Prostate Cancer*. Jan. 2021. DOI: 10.1056/NEJMoa2004325.
- [122] Gerhardt Attard et al. "Phase I clinical trial of a selective inhibitor of CYP17, abiraterone acetate, confirms that castration-resistant prostate cancer commonly remains hormone driven". In: *Journal of Clinical Oncology* 26.28 (Oct. 2008), pp. 4563–4571. ISSN: 0732183X. DOI: 10.1200/JCO.2007.15.9749.
- [123] Charles J. Ryan et al. "Phase I clinical trial of the CYP17 inhibitor abiraterone acetate demonstrating clinical activity in patients with castration-resistant prostate cancer who received prior ketoconazole therapy". In: *Journal of Clinical Oncology* 28.9 (Mar. 2010), pp. 1481–1488. ISSN: 0732183X. DOI: 10.1200/JCO.2009.24.1281.
- [124] Johann S. de Bono et al. "Abiraterone and Increased Survival in Metastatic Prostate Cancer". In: *New England Journal of Medicine* 364.21 (May 2011), pp. 1995–2005. ISSN: 0028-4793. DOI: 10.1056/nejmoa1014618.
- [125] S. L. Goldenberg et al. "Use of cyproterone acetate in prostate cancer". In: *Urologic Clinics of North America* 18.1 (Feb. 1991), pp. 111–122. ISSN: 00940143. DOI: 10.1016/s0094-0143(21)01398-7.
- [126] Herman J. De Voogt. "The position of cyproterone acetate (CPA), a steroidal anti-androgen, in the treatment of prostate cancer". In: *The Prostate* 21.4 S (Jan. 1992), pp. 91–95. ISSN: 10970045. DOI: 10.1002/pros.2990210514.
- [127] Howard I. Scher et al. "Increased Survival with Enzalutamide in Prostate Cancer after Chemotherapy". In: *New England Journal of Medicine* 367.13 (Sept. 2012), pp. 1187–1197. ISSN: 0028-4793. DOI: 10.1056/nejmoa1207506.
- [128] Ian D. Davis et al. "Enzalutamide with Standard First-Line Therapy in Metastatic Prostate Cancer". In: *New England Journal of Medicine* 381.2 (July 2019), pp. 121–131. ISSN: 0028-4793. DOI: 10.1056/nejmoa1903835.
- [129] Ian F. Tannock et al. "Docetaxel plus Prednisone or Mitoxantrone plus Prednisone for Advanced Prostate Cancer". In: *New England Journal of Medicine* 351.15 (Oct. 2004), pp. 1502–1512. ISSN: 0028-4793. DOI: 10.1056/nejmoa040720.
- [130] Stéphane Oudard et al. "Cabazitaxel versus docetaxel as first-line therapy for patients with metastatic castration-resistant prostate cancer: A randomized phase III trial - FIRSTANA". In: *Journal of Clinical Oncology* 35.28 (Oct. 2017), pp. 3189–3197. ISSN: 15277755. DOI: 10.1200/JCO.2016.72.1068.
- [131] Hossein Jadvar. "Targeted radionuclide therapy: An evolution toward precision cancer treatment". In: *American Journal of Roentgenology* 209.2 (Aug. 2017), pp. 277–288. ISSN: 15463141. DOI: 10.2214/AJR.17.18264.

- [132] Oliver Sartor et al. "Lutetium-177-PSMA-617 for Metastatic Castration-Resistant Prostate Cancer". In: *New England Journal of Medicine* 385.12 (Sept. 2021), pp. 1091–1103. ISSN: 0028-4793. DOI: 10.1056/nejmoa2107322.
- [133] Louise Emmett et al. "[177Lu]Lu-PSMA-617 plus enzalutamide in patients with metastatic castration-resistant prostate cancer (ENZA-p): an open-label, multicentre, randomised, phase 2 trial". In: *The Lancet Oncology* 25.5 (May 2024), pp. 563–571. ISSN: 14745488. DOI: 10.1016/S1470-2045(24)00135-9.
- [134] C. Parker et al. "Alpha Emitter Radium-223 and Survival in Metastatic Prostate Cancer". In: *New England Journal of Medicine* 369.3 (July 2013), pp. 213–223. ISSN: 0028-4793. DOI: 10.1056/nejmoa1213755.
- [135] Han Chung Yang et al. "Complete cycles of radium-223 improve overall survival in patients with metastatic castration-resistant prostate cancer: A retrospective study". In: *Anticancer Research* 43.4 (Apr. 2023), pp. 1809–1816. ISSN: 17917530. DOI: 10.21873/anticancer.16334.
- [136] Xiangnan Guan et al. "Androgen receptor activity in T cells limits checkpoint blockade efficacy". In: *Nature* 606.7915 (June 2022), pp. 791–796. ISSN: 14764687. DOI: 10.1038/s41586-022-04522-6.
- [137] Sabra L. Klein et al. *Sex differences in immune responses*. Aug. 2016. DOI: 10.1038/nri.2016.90.
- [138] Fabio Conforti et al. "Cancer immunotherapy efficacy and patients' sex: a systematic review and meta-analysis". In: *The Lancet Oncology* 19.6 (June 2018), pp. 737–746. ISSN: 14745488. DOI: 10.1016/S1470-2045(18)30261-4.
- [139] J. G. Markle et al. *SeXX matters in immunity*. Mar. 2014. DOI: 10.1016/j.it.2013.10.006.
- [140] Philip W. Kantoff et al. "Sipuleucel-T Immunotherapy for Castration-Resistant Prostate Cancer". In: *New England Journal of Medicine* 363.5 (July 2010), pp. 411–422. ISSN: 0028-4793. DOI: 10.1056/nejmoa1001294.
- [141] A. R. Hansen et al. "Pembrolizumab for advanced prostate adenocarcinoma: Findings of the KEYNOTE-028 study". In: *Annals of Oncology* 29.8 (Aug. 2018), pp. 1807–1813. ISSN: 15698041. DOI: 10.1093/annonc/mdy232.
- [142] Emmanuel S. Antonarakis et al. "Pembrolizumab for treatment-refractory metastatic castration-resistant prostate cancer: Multicohort, open-label phase II KEYNOTE-199 study". In: *Journal of Clinical Oncology*. Vol. 38. 5. American Society of Clinical Oncology, Feb. 2020, pp. 395–405. DOI: 10.1200/JCO.19.01638.
- [143] Daniel P. Petrylak et al. "Safety and clinical activity of atezolizumab in patients with metastatic castration-resistant prostate cancer: A phase i study". In: *Clinical Cancer Research* 27.12 (June 2021), pp. 3360–3369. ISSN: 15573265. DOI: 10.1158/1078-0432.CCR-20-1981.
- [144] Eugene D. Kwon et al. "Ipilimumab versus placebo after radiotherapy in patients with metastatic castration-resistant prostate cancer that had

- progressed after docetaxel chemotherapy (CA184-043): A multicentre, randomised, double-blind, phase 3 trial". In: *The Lancet Oncology* 15.7 (2014), pp. 700–712. ISSN: 14745488. DOI: 10.1016/S1470-2045(14)70189-5.
- [145] Karim Fizazi et al. "Final Analysis of the Ipilimumab Versus Placebo Following Radiotherapy Phase III Trial in Postdocetaxel Metastatic Castration-resistant Prostate Cancer Identifies an Excess of Long-term Survivors". In: *European Urology* 78.6 (Dec. 2020), pp. 822–830. ISSN: 18737560. DOI: 10.1016/j.eururo.2020.07.032.
- [146] Tomasz M. Beer et al. "Randomized, double-blind, phase III trial of ipilimumab versus placebo in asymptomatic or minimally symptomatic patients with metastatic chemotherapy-naïve castration-resistant prostate cancer". In: *Journal of Clinical Oncology* 35.1 (Jan. 2017), pp. 40–47. ISSN: 15277755. DOI: 10.1200/JCO.2016.69.1584.
- [147] Padmanee Sharma et al. "Nivolumab Plus Ipilimumab for Metastatic Castration-Resistant Prostate Cancer: Preliminary Analysis of Patients in the CheckMate 650 Trial". In: *Cancer Cell* 38.4 (Oct. 2020), pp. 489–499. ISSN: 18783686. DOI: 10.1016/j.ccell.2020.08.007.
- [148] J.N. Graff et al. "1771MO Pembrolizumab (pembro) plus enzalutamide (enza) for patients (pts) with metastatic castration-resistant prostate cancer (mCRPC): Randomized double-blind phase III KEYNOTE-641 study". In: *Annals of Oncology* 34 (Oct. 2023), S957. ISSN: 09237534. DOI: 10.1016/j.annonc.2023.09.2721.
- [149] Christian Gratzke et al. *KEYNOTE-991: pembrolizumab plus enzalutamide and androgen deprivation for metastatic hormone-sensitive prostate cancer*. Dec. 2022. DOI: 10.2217/fon-2022-0776.
- [150] Laura S. Graham et al. "Mismatch repair deficiency in metastatic prostate cancer: Response to PD-1 blockade and standard therapies". In: *PLoS ONE* 15.5 (May 2020), e0233260. ISSN: 19326203. DOI: 10.1371/journal.pone.0233260.
- [151] Emmanuel S. Antonarakis et al. "CDK12 -Altered Prostate Cancer: Clinical Features and Therapeutic Outcomes to Standard Systemic Therapies, Poly (ADP-Ribose) Polymerase Inhibitors, and PD-1 Inhibitors". In: *JCO Precision Oncology* 4.4 (Nov. 2020), pp. 370–381. ISSN: 2473-4284. DOI: 10.1200/po.19.00399.
- [152] Ryon P. Graf et al. "Comparative Effectiveness of Immune Checkpoint Inhibitors vs Chemotherapy by Tumor Mutational Burden in Metastatic Castration-Resistant Prostate Cancer". In: *JAMA Network Open* 5.3 (Mar. 2022). ISSN: 25743805. DOI: 10.1001/jamanetworkopen.2022.5394.
- [153] Joaquin Mateo et al. "DNA-Repair Defects and Olaparib in Metastatic Prostate Cancer". In: *New England Journal of Medicine* 373.18 (Oct. 2015), pp. 1697–1708. ISSN: 0028-4793. DOI: 10.1056/nejmoa1506859.
- [154] Joaquin Mateo et al. "Olaparib in patients with metastatic castration-resistant prostate cancer with DNA repair gene aberrations (TOPARP-B): a multicentre,

- open-label, randomised, phase 2 trial". In: *The Lancet Oncology* 21.1 (Jan. 2020), pp. 162–174. ISSN: 14745488. DOI: 10.1016/S1470-2045(19)30684-9.
- [155] Johann de Bono et al. "Olaparib for Metastatic Castration-Resistant Prostate Cancer". In: *New England Journal of Medicine* 382.22 (May 2020), pp. 2091–2102. ISSN: 0028-4793. DOI: 10.1056/nejmoa1911440.
- [156] Wassim Abida et al. "Rucaparib for the Treatment of Metastatic Castration-resistant Prostate Cancer Associated with a DNA Damage Repair Gene Alteration: Final Results from the Phase 2 TRITON2 Study". In: *European Urology* 84.3 (Sept. 2023), pp. 321–330. ISSN: 03022838. DOI: 10.1016/j.eururo.2023.05.021.
- [157] Karim Fizazi et al. "Rucaparib or Physician's Choice in Metastatic Prostate Cancer". In: *New England Journal of Medicine* 388.8 (Feb. 2023), pp. 719–732. ISSN: 0028-4793. DOI: 10.1056/nejmoa2214676.
- [158] Matthew R. Smith et al. "Niraparib in patients with metastatic castration-resistant prostate cancer and DNA repair gene defects (GALAHAD): a multicentre, open-label, phase 2 trial". In: *The Lancet Oncology* 23.3 (Mar. 2022), pp. 362–373. ISSN: 14745488. DOI: 10.1016/S1470-2045(21)00757-9.
- [159] Noel W. Clarke et al. "Abiraterone and Olaparib for Metastatic Castration-Resistant Prostate Cancer". In: *NEJM Evidence* 1.9 (June 2022). ISSN: 2766-5526. DOI: 10.1056/evidoa2200043.
- [160] K. N. Chi et al. "Niraparib plus abiraterone acetate with prednisone in patients with metastatic castration-resistant prostate cancer and homologous recombination repair gene alterations: second interim analysis of the randomized phase III MAGNITUDE trial". In: *Annals of Oncology* 34.9 (Sept. 2023), pp. 772–782. ISSN: 15698041. DOI: 10.1016/j.annonc.2023.06.009.
- [161] Neeraj Agarwal et al. "Talazoparib plus enzalutamide in men with first-line metastatic castration-resistant prostate cancer (TALAPRO-2): a randomised, placebo-controlled, phase 3 trial". In: *The Lancet* 402.10398 (July 2023), pp. 291–303. ISSN: 1474547X. DOI: 10.1016/S0140-6736(23)01055-3.
- [162] Kim N. Chi et al. "Niraparib and Abiraterone Acetate for Metastatic Castration-Resistant Prostate Cancer". In: *Journal of Clinical Oncology* 41.18 (June 2023), pp. 3339–3351. ISSN: 15277755. DOI: 10.1200/JCO.22.01649.
- [163] Tanya B. Dorff et al. "PSCA-CAR T cell therapy in metastatic castration-resistant prostate cancer: a phase 1 trial". In: *Nature Medicine* 30.6 (June 2024), pp. 1636–1644. ISSN: 1546170X. DOI: 10.1038/s41591-024-02979-8.
- [164] A. J. Atkinson et al. *Biomarkers and surrogate endpoints: Preferred definitions and conceptual framework*. Jan. 2001. DOI: 10.1067/mcp.2001.113989.
- [165] Himisha Beltran et al. "Emerging Molecular Biomarkers in Advanced Prostate Cancer: Translation to the Clinic". In: *American Society of Clinical Oncology Educational Book* 35.36 (May 2016), pp. 131–141. ISSN: 1548-8748. DOI: 10.1200/edbk{_}159248.

- [166] Semini Sumanasuriya et al. *Consensus Statement on Circulating Biomarkers for Advanced Prostate Cancer*. June 2018. DOI: 10.1016/j.euo.2018.02.009.
- [167] Silver Spring (MD): Food and Drug Administration (US); Bethesda (MD): National Institutes of Health (US). *FDA-NIH Biomarker Working Group. BEST (Biomarkers, EndpointS, and other Tools) Resource*. Food and Drug Administration (US), 2016.
- [168] Wassim Abida et al. "Prospective Genomic Profiling of Prostate Cancer Across Disease States Reveals Germline and Somatic Alterations That May Affect Clinical Decision Making". In: *JCO Precision Oncology* 2017.1 (Nov. 2017), pp. 1–16. ISSN: 2473-4284. DOI: 10.1200/po.17.00029.
- [169] Joshua Armenia et al. "The long tail of oncogenic drivers in prostate cancer". In: *Nature Genetics* 50.5 (Apr. 2018), pp. 645–651. ISSN: 15461718. DOI: 10.1038/s41588-018-0078-z.
- [170] Nathalia Oliveira Alqualo et al. *Molecular biomarkers in prostate cancer tumorigenesis and clinical relevance*. Feb. 2024. DOI: 10.1016/j.critrevonc.2023.104232.
- [171] Emmanuel S. Antonarakis et al. "AR-V7 and Resistance to Enzalutamide and Abiraterone in Prostate Cancer". In: *New England Journal of Medicine* 371.11 (Sept. 2014), pp. 1028–1038. ISSN: 0028-4793. DOI: 10.1056/nejmoa1315815.
- [172] Howard I. Scher et al. "Association of AR-V7 on circulating tumor cells as a treatment-specific biomarker with outcomes and survival in castration-resistant prostate cancer". In: *JAMA Oncology* 2.11 (Nov. 2016), pp. 1441–1449. ISSN: 23742445. DOI: 10.1001/jamaoncol.2016.1828.
- [173] Xintao Qiu et al. "MYC drives aggressive prostate cancer by disrupting transcriptional pause release at androgen receptor targets". In: *Nature Communications* 13.1 (May 2022), pp. 1–17. ISSN: 20411723. DOI: 10.1038/s41467-022-30257-z.
- [174] Daphne Hessels et al. "Detection of TMPRSS2-ERG fusion transcripts and prostate cancer antigen 3 in urinary sediments may improve diagnosis of prostate cancer". In: *Clinical Cancer Research* 13.17 (Sept. 2007), pp. 5103–5108. ISSN: 10780432. DOI: 10.1158/1078-0432.CCR-07-0700.
- [175] Scott A. Tomlins et al. *ETS Gene Fusions in Prostate Cancer: From Discovery to Daily Clinical Practice*. Aug. 2009. DOI: 10.1016/j.eururo.2009.04.036.
- [176] Sven Perner et al. "TMPRSS2-ERG fusion prostate cancer: An early molecular event associated with invasion". In: *American Journal of Surgical Pathology* 31.6 (June 2007), pp. 882–888. ISSN: 01475185. DOI: 10.1097/01.pas.0000213424.38503.aa.
- [177] Jan C. Brase et al. "TMPRSS2-ERG -specific transcriptional modulation is associated with prostate cancer biomarkers and TGF- β signaling". In: *BMC Cancer* 11.1 (Dec. 2011), pp. 1–8. ISSN: 14712407. DOI: 10.1186/1471-2407-11-507.

- [178] Enrique Grande et al. "A phase II multicenter biomarker trial to study the predictive value of TMPRSS2-ERG before enzalutamide treatment in chemo-naïve metastatic castration-resistant prostate cancer." In: *Journal of Clinical Oncology* 37.15_suppl (May 2019), pp. 5040–5040. ISSN: 0732-183X. DOI: 10.1200/jco.2019.37.15{_}suppl.5040.
- [179] Catherine Alix-Panabières et al. *Clinical applications of circulating tumor cells and circulating tumor DNA as liquid biopsy*. May 2016. DOI: 10.1158/2159-8290.CD-15-1483.
- [180] Marius Ilie et al. *Current challenges for detection of circulating tumor cells and cell-free circulating nucleic acids, and their characterization in non-small cell lung carcinoma patients. What is the best blood substrate for personalized medicine?* Nov. 2014. DOI: 10.3978/j.issn.2305-5839.2014.08.11.
- [181] Lynne Rainen et al. "Stabilization of mRNA expression in whole blood samples". In: *Clinical Chemistry* 48.11 (Nov. 2002), pp. 1883–1890. ISSN: 00099147. DOI: 10.1093/clinchem/48.11.1883.
- [182] Robert W. Ross et al. "A whole-blood RNA transcript-based prognostic model in men with castration-resistant prostate cancer: A prospective study". In: *The Lancet Oncology* 13.11 (Nov. 2012), pp. 1105–1113. ISSN: 14702045. DOI: 10.1016/S1470-2045(12)70263-2.
- [183] David Olmos et al. "Prognostic value of blood mRNA expression signatures in castration-resistant prostate cancer: A prospective, two-stage study". In: *The Lancet Oncology* 13.11 (Nov. 2012), pp. 1114–1124. ISSN: 14702045. DOI: 10.1016/S1470-2045(12)70372-8.
- [184] Li Wang et al. "A robust blood gene expression-based prognostic model for castration-resistant prostate cancer". In: *BMC Medicine* 13.1 (Aug. 2015). ISSN: 17417015. DOI: 10.1186/s12916-015-0442-0.
- [185] Laurent Gautier et al. "Affy - Analysis of Affymetrix GeneChip data at the probe level". In: *Bioinformatics* 20.3 (Feb. 2004), pp. 307–315. ISSN: 13674811. DOI: 10.1093/bioinformatics/btg405.
- [186] Jeffrey T Leek et al. *sva: Surrogate Variable Analysis*. 2024. DOI: 10.18129/B9.bioc.sva.
- [187] James W MacDonald. *pd.hta.2.0: Platform Design Info for Affymetrix HTA-2_0*. 2017.
- [188] Matthew E. Ritchie et al. "Limma powers differential expression analyses for RNA-sequencing and microarray studies". In: *Nucleic Acids Research* 43.7 (Jan. 2015), e47. ISSN: 13624962. DOI: 10.1093/nar/gkv007.
- [189] Shuangbin Xu et al. "Using clusterProfiler to characterize multiomics data". In: *Nature Protocols* 19.11 (July 2024), pp. 3292–3320. ISSN: 17502799. DOI: 10.1038/s41596-024-01020-z.
- [190] Suzi A Aleksander et al. "The Gene Ontology knowledgebase in 2023". In: *Genetics* 224.1 (May 2023). ISSN: 19432631. DOI: 10.1093/genetics/iyad031.
- [191] Minoru Kanehisa et al. *KEGG: Kyoto Encyclopedia of Genes and Genomes*. Jan. 2000. DOI: 10.1093/nar/28.1.27.

- [192] Binbin Chen et al. "Profiling tumor infiltrating immune cells with CIBERSORT". In: *Methods in Molecular Biology*. Vol. 1711. NIH Public Access, 2018, pp. 243–259. doi: 10.1007/978-1-4939-7493-1{_}12.
- [193] Chloé B. Steen et al. "Profiling cell type abundance and expression in bulk tissues with CIBERSORTx". In: *Methods in Molecular Biology*. Vol. 2117. NIH Public Access, 2020, pp. 135–157. doi: 10.1007/978-1-0716-0301-7{_}7.
- [194] R Core Team. *R: A Language and Environment for Statistical Computing*. Vienna, Austria, 2024.
- [195] Posit team. *RStudio: Integrated Development Environment for R*. Boston, MA, 2024.
- [196] Terry M Therneau. *A Package for Survival Analysis in R*. 2024.
- [197] Alboukadel Kassambara et al. *survminer: Drawing Survival Curves using 'ggplot2'*. 2024.
- [198] Paul Blanche et al. "Estimating and comparing time-dependent areas under receiver operating characteristic curves for censored event times with competing risks." In: *Statistics in medicine* 32.30 (Dec. 2013), pp. 5381–97. ISSN: 1097-0258. doi: 10.1002/sim.5958.
- [199] Hadley Wickham. *ggplot2: Elegant Graphics for Data Analysis*. Springer-Verlag New York, 2016. ISBN: 978-3-319-24277-4.
- [200] M. Kirby et al. *Characterising the castration-resistant prostate cancer population: A systematic review*. Nov. 2011. doi: 10.1111/j.1742-1241.2011.02799.x.
- [201] Takashi Kawahara et al. "A high neutrophil-to-lymphocyte ratio is a poor prognostic factor for castration-resistant prostate cancer patients who undergo abiraterone acetate or enzalutamide treatment". In: *BMC Cancer* 20.1 (Sept. 2020). ISSN: 14712407. doi: 10.1186/s12885-020-07410-2.
- [202] Manuel Neuberger et al. "Changes in neutrophile-to-lymphocyte ratio as predictive and prognostic biomarker in metastatic prostate cancer treated with taxane-based chemotherapy". In: *Discover Oncology* 13.1 (Dec. 2022). ISSN: 27306011. doi: 10.1007/s12672-022-00603-0.
- [203] Tanja Langsenlehner et al. "Validation of the neutrophil-to-lymphocyte ratio as a prognostic factor in a cohort of European prostate cancer patients". In: *World Journal of Urology* 33.11 (Nov. 2015), pp. 1661–1667. ISSN: 14338726. doi: 10.1007/s00345-015-1494-7.
- [204] Robert J. Van Soest et al. "Neutrophil-to-lymphocyte ratio as a prognostic biomarker for men with metastatic castration-resistant prostate cancer receiving first-line chemotherapy: Data from two randomized phase III trials". In: *Annals of Oncology* 26.4 (Apr. 2015), pp. 743–749. ISSN: 15698041. doi: 10.1093/annonc/mdu569.
- [205] Martin Boegemann et al. "The Role of the Neutrophil to Lymphocyte Ratio for Survival Outcomes in Patients with Metastatic Castration-Resistant Prostate Cancer Treated with Abiraterone." In: *International journal of molecular sciences* 18.2 (Feb. 2017), p. 380. ISSN: 1422-0067. doi: 10.3390/ijms18020380.

- [206] D. Lorente et al. "Baseline neutrophil-lymphocyte ratio (NLR) is associated with survival and response to treatment with second-line chemotherapy for advanced prostate cancer independent of baseline steroid use". In: *Annals of Oncology* 26.4 (Apr. 2015), pp. 750–755. ISSN: 15698041. DOI: 10.1093/annonc/mdu587.
- [207] R. Leibowitz-Amit et al. "Clinical variables associated with PSA response to abiraterone acetate in patients with metastatic castration-resistant prostate cancer". In: *Annals of Oncology* 25.3 (2014), pp. 657–662. ISSN: 15698041. DOI: 10.1093/annonc/mdt581.
- [208] D. R. Cox. "Regression Models and Life-Tables". In: *Journal of the Royal Statistical Society: Series B (Methodological)* 34.2 (Jan. 1972), pp. 187–202. ISSN: 2517-6161. DOI: 10.1111/J.2517-6161.1972.TB00899.X.
- [209] N Mantel. "Evaluation of survival data and two new rank order statistics arising in its consideration." In: *Cancer chemotherapy reports* (Mar. 1966). ISSN: 0069-0112.
- [210] E. L. Kaplan et al. "Nonparametric Estimation from Incomplete Observations". In: *Journal of the American Statistical Association* 53.282 (1958), pp. 457–481. ISSN: 1537274X. DOI: 10.1080/01621459.1958.10501452.
- [211] Jerome Friedman et al. "Regularization paths for generalized linear models via coordinate descent". In: *Journal of Statistical Software* 33.1 (Feb. 2010), pp. 1–22. ISSN: 15487660. DOI: 10.18637/jss.v033.i01.
- [212] Hemant Ishwaran et al. "Random survival forests". In: *Annals of Applied Statistics* 2.3 (Nov. 2008), pp. 841–860. ISSN: 19326157. DOI: 10.1214/08-AOAS169.
- [213] Thomas Alexander Gerds et al. *riskRegression: Risk Regression Models and Prediction Scores for Survival Analysis with Competing Risks*. 2023.
- [214] Cameron A. Wade et al. *Profiling prostate cancer therapeutic resistance*. Mar. 2018. DOI: 10.3390/ijms19030904.
- [215] Camila R. Consiglio et al. "Enzalutamide, an androgen receptor antagonist, enhances myeloid cell-mediated immune suppression and tumor progression". In: *Cancer Immunology Research* 8.9 (Sept. 2020), pp. 1215–1227. ISSN: 23266074. DOI: 10.1158/2326-6066.CIR-19-0371.
- [216] Le Wang et al. "Prostate Cancer Incidence and Mortality: Global Status and Temporal Trends in 89 Countries From 2000 to 2019". In: *Frontiers in Public Health* 10 (Feb. 2022), p. 811044. ISSN: 22962565. DOI: 10.3389/FPUBH.2022.811044.
- [217] Neil K. Jairath et al. "Tumor immune microenvironment clusters in localized prostate adenocarcinoma: Prognostic impact of macrophage enriched/plasma cell non-enriched subtypes". In: *Journal of Clinical Medicine* 9.6 (2020), pp. 1–13. ISSN: 20770383. DOI: 10.3390/jcm9061973.
- [218] Shuang G. Zhao et al. "The immune landscape of prostate cancer and nomination of PD-L2 as a potential therapeutic target". In: *Journal of the National Cancer Institute* 111.3 (Mar. 2019), pp. 301–310. ISSN: 14602105. DOI: 10.1093/jnci/djy141.

- [219] Natalia Alonso-Moreda et al. "Comparative Analysis of Cell Mixtures Deconvolution and Gene Signatures Generated for Blood, Immune and Cancer Cells". In: *International Journal of Molecular Sciences* 24.13 (July 2023), p. 10765. ISSN: 14220067. DOI: 10.3390/ijms241310765.
- [220] Aaron M. Newman et al. "Robust enumeration of cell subsets from tissue expression profiles". In: *Nature Methods* 12.5 (Apr. 2015), pp. 453–457. ISSN: 15487105. DOI: 10.1038/nmeth.3337.
- [221] María P. Fernandez-Perez et al. "A correlative biomarker study and integrative prognostic model in chemotherapy-naïve metastatic castration-resistant prostate cancer treated with enzalutamide". In: *Prostate* 83.4 (Mar. 2023), pp. 376–384. ISSN: 10970045. DOI: 10.1002/pros.24469.
- [222] Agnes E. Coutinho et al. *The anti-inflammatory and immunosuppressive effects of glucocorticoids, recent developments and mechanistic insights*. Mar. 2011. DOI: 10.1016/j.mce.2010.04.005.
- [223] Enrique Perez-Navarro et al. "Prognostic Implications of Blood Immune-Cell Composition in Metastatic Castration-Resistant Prostate Cancer". In: *Cancers* 16.14 (July 2024), p. 2535. ISSN: 20726694. DOI: 10.3390/cancers16142535.
- [224] Susan Halabi et al. "Updated prognostic model for predicting overall survival in first-line chemotherapy for patients with metastatic castration-resistant prostate cancer". In: *Journal of Clinical Oncology* 32.7 (Mar. 2014), pp. 671–677. ISSN: 15277755. DOI: 10.1200/JCO.2013.52.3696.
- [225] Howard I. Scher et al. "Circulating tumor cell biomarker panel as an individual-level surrogate for survival in metastatic castration-resistant prostate cancer". In: *Journal of Clinical Oncology* 33.12 (Apr. 2015), pp. 1348–1355. ISSN: 15277755. DOI: 10.1200/JCO.2014.55.3487.
- [226] Anuradha Jayaram et al. "Plasma DNA and metastatic castration-resistant prostate cancer: The odyssey to a clinical biomarker test". In: *Cancer Discovery* 8.4 (Apr. 2018), pp. 392–394. ISSN: 21598290. DOI: 10.1158/2159-8290.CD-18-0124.
- [227] Manuel Ramirez-Garrastacho et al. *Extracellular vesicles as a source of prostate cancer biomarkers in liquid biopsies: a decade of research*. Nov. 2021. DOI: 10.1038/s41416-021-01610-8.
- [228] Daniel C. Danila et al. "TMPRSS2-ERG Status in Circulating Tumor Cells as a Predictive Biomarker of Sensitivity in Castration-Resistant Prostate Cancer Patients Treated With Abiraterone Acetate". In: *European Urology* 60.5 (Nov. 2011), pp. 897–904. ISSN: 03022838. DOI: 10.1016/j.eururo.2011.07.011.
- [229] Adam Sharp et al. "Androgen receptor splice variant-7 expression emerges with castration resistance in prostate cancer". In: *Journal of Clinical Investigation* 129.1 (Nov. 2018), pp. 192–208. ISSN: 0021-9738. DOI: 10.1172/JCI122819.
- [230] Ross L. Prentice. "Surrogate endpoints in clinical trials: Definition and operational criteria". In: *Statistics in Medicine* 8.4 (Apr. 1989), pp. 431–440. ISSN: 0277-6715. DOI: 10.1002/sim.4780080407.

- [231] Howard I. Scher et al. "Assessment of the validity of nuclear-localized androgen receptor splice variant 7 in circulating tumor cells as a predictive biomarker for castration-resistant prostate cancer". In: *JAMA Oncology* 4.9 (Sept. 2018), pp. 1179–1186. ISSN: 23742445. DOI: 10.1001/jamaoncol.2018.1621.
- [232] Mary Ellen Taplin et al. "Androgen Receptor Modulation Optimized for Response—Splice Variant: A Phase 3, Randomized Trial of Galeterone Versus Enzalutamide in Androgen Receptor Splice Variant-7-expressing Metastatic Castration-resistant Prostate Cancer". In: *European Urology* 76.6 (Dec. 2019), pp. 843–851. ISSN: 18737560. DOI: 10.1016/j.eururo.2019.08.034.
- [233] Howard I. Scher et al. "Circulating tumour cells as prognostic markers in progressive, castration-resistant prostate cancer: a reanalysis of IMMC38 trial data". In: *The Lancet Oncology* 10.3 (Mar. 2009), pp. 233–239. ISSN: 14702045. DOI: 10.1016/S1470-2045(08)70340-1.
- [234] A. J. Armstrong et al. "Development and validation of a prognostic model for overall survival in chemotherapy-naïve men with metastatic castration-resistant prostate cancer". In: *Annals of oncology : official journal of the European Society for Medical Oncology* 29.11 (Nov. 2018), pp. 2200–2207. ISSN: 1569-8041. DOI: 10.1093/ANNONC/MDY406.
- [235] Natalie C. Twine et al. "Disease-associated expression profiles in peripheral blood mononuclear cells from patients with advanced renal cell carcinoma". In: *Cancer Research* 63.18 (2003), pp. 6069–6075. ISSN: 00085472.
- [236] Fray F. Marshall. *Transcriptional profiles in peripheral blood mononuclear cells prognostic of clinical outcomes in patients with advanced renal cell carcinoma: Commentary*. 2006. DOI: 10.1016/S0022-5347(05)00564-1.
- [237] Yoshio Sakai et al. "Common transcriptional signature of tumor-infiltrating mononuclear inflammatory cells and peripheral blood mononuclear cells in hepatocellular carcinoma patients". In: *Cancer Research* 68.24 (Dec. 2008), pp. 10267–10279. ISSN: 00085472. DOI: 10.1158/0008-5472.CAN-08-0911.
- [238] Thomas Zander et al. "Blood-based gene expression signatures in non-small cell lung cancer". In: *Clinical Cancer Research* 17.10 (May 2011), pp. 3360–3367. ISSN: 10780432. DOI: 10.1158/1078-0432.CCR-10-0533.
- [239] Jianjun Gao et al. "VISTA is an inhibitory immune checkpoint that is increased after ipilimumab therapy in patients with prostate cancer". In: *Nature Medicine* 23.5 (May 2017), pp. 551–555. ISSN: 1546170X. DOI: 10.1038/nm.4308.
- [240] Stephanie T. Page et al. "Effect of medical castration on CD4+CD25+ T cells, CD8+ T cell IFN- γ expression, and NK cells: A physiological role for testosterone and/or its metabolites". In: *American Journal of Physiology - Endocrinology and Metabolism* 290.5 (May 2006). ISSN: 01931849. DOI: 10.1152/ajpendo.00484.2005.
- [241] Yang Pu et al. "Androgen receptor antagonists compromise T cell response against prostate cancer leading to early tumor relapse". In: *Science Translational*

- Medicine* 8.333 (Apr. 2016). ISSN: 19466242. DOI: 10.1126/scitranslmed.aad5659.
- [242] Ravi A. Madan et al. "Analysis of overall survival in patients with nonmetastatic castration-resistant prostate cancer treated with vaccine, nilutamide, and combination therapy". In: *Clinical Cancer Research* 14.14 (July 2008), pp. 4526–4531. ISSN: 10780432. DOI: 10.1158/1078-0432.CCR-07-5048.
- [243] Arianna Calcinotto et al. "IL-23 secreted by myeloid cells drives castration-resistant prostate cancer". In: *Nature* 559.7714 (June 2018), pp. 363–369. ISSN: 14764687. DOI: 10.1038/s41586-018-0266-0.
- [244] Marco Bezzi et al. "Diverse genetic-driven immune landscapes dictate tumor progression through distinct mechanisms". In: *Nature Medicine* 24.2 (Feb. 2018), pp. 165–175. ISSN: 1546170X. DOI: 10.1038/nm.4463.
- [245] Diletta Di Mitri et al. "Tumour-infiltrating Gr-1 + myeloid cells antagonize senescence in cancer". In: *Nature* 515.7525 (Nov. 2014), pp. 134–137. ISSN: 14764687. DOI: 10.1038/nature13638.
- [246] Thiago Vidotto et al. "PTEN-deficient prostate cancer is associated with an immunosuppressive tumor microenvironment mediated by increased expression of IDO1 and infiltrating FoxP3+ T regulatory cells". In: *Prostate* 79.9 (June 2019), pp. 969–979. ISSN: 10970045. DOI: 10.1002/pros.23808.
- [247] Eric J. Small et al. "A pilot trial of CTLA-4 blockade with human anti-CTLA-4 in patients with hormone-refractory prostate cancer". In: *Clinical Cancer Research* 13.6 (Mar. 2007), pp. 1810–1815. ISSN: 10780432. DOI: 10.1158/1078-0432.CCR-06-2318.
- [248] Tomasz M. Beer et al. "Enzalutamide in Men with Chemotherapy-naïve Metastatic Castration-resistant Prostate Cancer: Extended Analysis of the Phase 3 PREVAIL Study". In: *European urology* 71.2 (Feb. 2017), pp. 151–154. ISSN: 1873-7560. DOI: 10.1016/J.EURURO.2016.07.032.
- [249] Thomas Powles et al. "Atezolizumab with enzalutamide versus enzalutamide alone in metastatic castration-resistant prostate cancer: a randomized phase 3 trial". In: *Nature Medicine* 28.1 (Jan. 2022), pp. 144–153. ISSN: 1546170X. DOI: 10.1038/s41591-021-01600-6.
- [250] Julie N. Graff et al. "KEYNOTE-641: A Phase III study of pembrolizumab plus enzalutamide for metastatic castration-resistant prostate cancer". In: *Future Oncology* 17.23 (Aug. 2021), pp. 3017–3026. ISSN: 17448301. DOI: 10.2217/fon-2020-1008.
- [251] Kevin Litchfield et al. "Meta-analysis of tumor- and T cell-intrinsic mechanisms of sensitization to checkpoint inhibition". In: *Cell* 184.3 (Feb. 2021), pp. 596–614. ISSN: 10974172. DOI: 10.1016/j.cell.2021.01.002.
- [252] Jun Li Luo et al. "Nuclear cytokine-activated IKK α controls prostate cancer metastasis by repressing Maspin". In: *Nature* 446.7136 (Mar. 2007), pp. 690–694. ISSN: 14764687. DOI: 10.1038/nature05656.

- [253] Massimo Ammirante et al. "B-cell-derived lymphotoxin promotes castration-resistant prostate cancer". In: *Nature* 464.7286 (Mar. 2010), pp. 302–305. ISSN: 00280836. DOI: 10.1038/nature08782.
- [254] W. Peter M. Benten et al. "Functional testosterone receptors in plasma membranes of T cells". In: *The FASEB Journal* 13.1 (Jan. 1999), pp. 123–133. ISSN: 0892-6638. DOI: 10.1096/fasebj.13.1.123.
- [255] Stephanie M. Liva et al. "Testosterone Acts Directly on CD4+ T Lymphocytes to Increase IL-10 Production". In: *The Journal of Immunology* 167.4 (Aug. 2001), pp. 2060–2067. ISSN: 0022-1767. DOI: 10.4049/jimmunol.167.4.2060.
- [256] Magdalena Walecki et al. "Androgen receptor modulates Foxp3 expression in CD4+CD25+Foxp3+ regulatory T-cells". In: *Molecular Biology of the Cell* 26.15 (Aug. 2015), pp. 2845–2857. ISSN: 19394586. DOI: 10.1091/mbc.E14-08-1323.
- [257] Jayne S. Sutherland et al. "Activation of Thymic Regeneration in Mice and Humans following Androgen Blockade". In: *The Journal of Immunology* 175.4 (Aug. 2005), pp. 2741–2753. ISSN: 0022-1767. DOI: 10.4049/jimmunol.175.4.2741.
- [258] Philippe O. Gannon et al. "Characterization of the intra-prostatic immune cell infiltration in androgen-deprived prostate cancer patients". In: *Journal of Immunological Methods* 348.1-2 (Aug. 2009), pp. 9–17. ISSN: 00221759. DOI: 10.1016/j.jim.2009.06.004.
- [259] Maria Mercader et al. "T cell infiltration of the prostate induced by androgen withdrawal in patients with prostate cancer". In: *Proceedings of the National Academy of Sciences of the United States of America* 98.25 (Dec. 2001), pp. 14565–14570. ISSN: 00278424. DOI: 10.1073/pnas.251140998.
- [260] Matthew D. Morse et al. "Prostate cancer patients on androgen deprivation therapy develop persistent changes in adaptive immune responses". In: *Human Immunology* 71.5 (May 2010), pp. 496–504. ISSN: 01988859. DOI: 10.1016/j.humimm.2010.02.007.
- [261] Nancy J. Nesslinger et al. "Standard treatments induce antigen-specific immune responses in prostate cancer". In: *Clinical Cancer Research* 13.5 (Mar. 2007), pp. 1493–1502. ISSN: 10780432. DOI: 10.1158/1078-0432.CCR-06-1772.
- [262] Jessica E. Hawley et al. "Anti-PD-1 immunotherapy with androgen deprivation therapy induces robust immune infiltration in metastatic castration-sensitive prostate cancer". In: *Cancer Cell* 41.11 (Nov. 2023), pp. 1972–1988. ISSN: 15356108. DOI: 10.1016/j.ccell.2023.10.006.

THESIS CONTRIBUTIONS

This chapter summarizes the contributions to the scientific community and the related projects that have been related projects that have been worked on throughout the development of the thesis.

Articles

The Prostate Fernandez-Perez M.P, Perez-Navarro E., Alonso-Gordoa T., et al. A correlative biomarker study and integrative prognostic model in chemotherapy-naïve metastatic castration-resistant prostate cancer treated with enzalutamide. *The Prostate*. 2023; 83: 376-384. <https://doi.org/10.1002/pros.24469>

Cancers Perez-Navarro, E.; Conteduca, V.; Funes, J.M.; Dominguez, J.I.; Martin-Serrano, M.; Cremaschi, P.; Fernandez-Perez, M.P.; Gordoa, T.A.; Font, A.; Vazquez-Estevez, S.; et al. Prognostic Implications of Blood Immune-Cell Composition in Metastatic Castration-Resistant Prostate Cancer. *Cancers* 2024, 16, 2535. <https://doi.org/10.3390/cancers16142535>

Patent

A key outcome of this research has been the development of a novel gene signature with prognostic value in mCRPC. This signature has been patented, highlighting its potential for clinical application and commercialization.

- Submission number: 300549454
- Application number: EP25382005.4

- File Number (for priority declarations): EP25382005

This acknowledgement confirms the formal reception and processing of the patent application by the EPO, marking a significant step toward the potential commercial viability and clinical application of the developed gene signature.

International Congress

ESMO Congress 2021 589P Dynamics of peripheral blood immune profiling associated with tumour progression in metastatic castration-resistant prostate cancer (mCRPC) Perez-Navarro, E. et al. *Annals of Oncology*, Volume 32, S637 - S638

National Congress

VI Jornadas IMIB Oral Presentation: "Dynamics of peripheral blood immune profiling associated with tumour progression in metastatic castration-resistant prostate cancer"

Academic Supervision

Throughout the course of this doctoral research, I have had the opportunity to contribute significantly to the academic development of other students. This involvement has included the supervision of both Master's theses and undergraduate degree projects, allowing for the dissemination of research methodologies and findings to the next generation of researchers.

I have co-directed two Master's thesis, focussing on critical aspects of prostate cancer research:

Master's Thesis Supervision:

- Africa Martínez Blanco. "Signature of non-coding genes involved in survival and death in patients with castration-resistant prostate cancer (mCRPC)". 2021
- Domingo Murciano Olivares. "Molecular-clinical study of gene expression in patients with metastatic prostate cancer". 2022

Additionally, I have supervised two undergraduate degree projects, expanding the scope of our research to include aspects of the tumour microenvironment and immune system in prostate cancer:

Degree Project Supervision:

- Katia Molina Barrio. "Characterization of the tumour microenvironment in patients with metastatic prostate cancer and loss of PTEN by Digital Spatial Profiling". 2023
- Jessica Rafaela Gregorio Cardoso. "Estudio del sistema inmune en el cáncer de próstata" (Study of the immune system in prostate cancer). 2024

ANNEXES

A correlative biomarker study and integrative prognostic model in chemotherapy-naïve metastatic castration-resistant prostate cancer treated with enzalutamide

María P. Fernandez-Perez PhD¹ | Enrique Perez-Navarro BSc²  |
Teresa Alonso-Gordoa MD³  | Vicenza Conteduca MD⁴  | Albert Font MD⁵ |
Sergio Vázquez-Estévez MD⁶ | Aránzazu González-del-Alba MD⁷ |
Daniel Wetterskog PhD⁸ | Emmanuel S. Antonarakis MD⁹ |
Begona Mellado MD, PhD¹⁰ | Ovidio Fernandez-Calvo MD¹¹ |
María J. Méndez-Vidal MD¹² | Miguel A. Climent MD¹³ | Ignacio Duran MD, PhD¹⁴ |
Enrique Gallardo MD¹⁵ | Angel Rodriguez Sanchez MD¹⁶ |
Carmen Santander MD¹⁷ | Maria I. Sáez MD¹⁸ | Javier Puente MD, PhD¹⁹ |
Julian Tudela MD²⁰ | Alberto Martínez BSc²¹ | Maria J. López-Andreo PhD²² |
José Padilla BSc¹ | Rebeca Lozano MD, PhD^{23,24} | David Hervas BSc²⁵ |
Jun Luo PhD²⁶ | Ugo de Giorgi MD⁴ | Daniel Castellano MD² |
Gerhardt Attard MD, PhD⁸ | Enrique Grande MD²⁷ |
Enrique Gonzalez-Billalabeitia MD, PhD^{1,2,28} 

¹Department of Haematology and Medical Oncology, Hospital Universitario Morales Meseguer, IMIB, Murcia, Spain

²Department of Medical Oncology, Instituto de Investigación, Hospital Universitario 12 de Octubre, Madrid, Spain

³Department of Medical Oncology, Hospital Ramón y Cajal, Madrid, Spain

⁴Department of Medical Oncology, Istituto Scientifico Romagnolo per lo Studio e la Cura dei Tumori (IRST) "Dino Amadori" IRCCS, Meldola, Italy

⁵Department of Medical Oncology, Catalan Institute of Oncology, Badalona Applied Research Group in Oncology (BARGO), Badalona, Spain

⁶Department of Medical Oncology, H. Universitario Lucus Augusti, Lugo, Spain

⁷Department of Medical Oncology, H.U. Son Espases, Palma de Mallorca, Spain

⁸University College London Cancer Institute, Paul O'Gorman Building, London, UK

⁹Department of Oncology, Johns Hopkins University School of Medicine, Baltimore, Maryland, USA

¹⁰Department of Medical Oncology, IDIBAPS, Hospital Clinic, Universidad de Barcelona, Barcelona, Spain

¹¹Department of Medical Oncology, Complejo Hospitalario Universitario Ourense, Ourense, Spain

¹²Department of Medical Oncology, Hospital Universitario Reina Sofía (HURS), Maimonides Institute for biomedical research of Córdoba (IMIBIC), Córdoba, Spain

¹³Servicio de Oncología Médica, Instituto Valenciano de Oncología, Valencia, Spain

¹⁴Instituto de Biomedicina de Sevilla, IBIH/Hospital Universitario Virgen del Rocío/CSIC/Universidad de Sevilla, Seville, Spain

¹⁵Department of Medical Oncology, Servicio de Oncología Médica, Parc Taulí Hospital Universitari, Institut d'Investigació i Innovació Parc Taulí I3PT, Universitat Autònoma de Barcelona, Sabadell, Spain

¹⁶Department of Medical Oncology, Hospital Universitario de León, León, Spain

¹⁷Department of Medical Oncology, Hospital Universitario Miguel Servet, Zaragoza, Spain

¹⁸Medical Oncology Intercenter Unit, Regional and Virgen de la Victoria University Hospitals, IBIMA, Málaga, Spain

This is an open access article under the terms of the Creative Commons Attribution-NonCommercial-NoDerivs License, which permits use and distribution in any medium, provided the original work is properly cited, the use is non-commercial and no modifications or adaptations are made.

© 2022 The Authors. *The Prostate* published by Wiley Periodicals LLC.

¹⁹Department of Medical Oncology, Hospital Clínico San Carlos, Instituto de Investigación Sanitaria del Hospital Clínico San Carlos (IdISSC), CIBERONC, Madrid, Spain

²⁰Department of Pathology, Hospital Morales Meseguer, Murcia, Spain

²¹Biobanco de la región de Murcia, IMIB, Nodo 3, Murcia, Spain

²²Department of Molecular Biology, SAI-IMIB-Universidad de Murcia, Murcia, Spain

²³Prostate Cancer Clinical Research Unit, Spanish National Cancer Research Centre, Madrid, Spain

²⁴Genitourinary Translational Research Group, Instituto de Investigación Biomédica de Málaga, Málaga, Spain

²⁵Data Science Unit, Instituto de Investigación Sanitaria La Fe, Valencia, Spain

²⁶Department of Urology, Johns Hopkins University School of Medicine, Baltimore, Maryland, USA

²⁷MD Anderson Cancer Center Madrid, Madrid, Spain

²⁸Universidad Católica San Antonio de Murcia-UCAM, Murcia, Spain

Correspondence

Enrique Gonzalez-Billalabeitia, MD, PhD,
Department of Medical Oncology, Hospital
Universitario "12 de Octubre",
Madrid 28041, Spain.
Email: egbillalabeitia@salud.madrid.org

Funding information

Astellas; Instituto de Salud Carlos III,
Grant/Award Number: PI18/00883;
SEOM-CRIS Cancer Foundation

Abstract

Background: There is a considerable need to incorporate biomarkers of resistance to new antiandrogen agents in the management of castration-resistant prostate cancer (CRPC).

Methods: We conducted a phase II trial of enzalutamide in first-line chemo-naïve asymptomatic or minimally symptomatic mCRPC and analyzed the prognostic value of *TMPRSS2-ERG* and other biomarkers, including circulating tumor cells (CTCs), androgen receptor splice variant (AR-V7) in CTCs and plasma Androgen Receptor copy number gain (AR-gain). These biomarkers were correlated with treatment response and survival outcomes and developed a clinical-molecular prognostic model using penalized cox-proportional hazard model. This model was validated in an independent cohort.

Results: Ninety-eight patients were included. *TMPRSS2-ERG* fusion gene was detected in 32 patients with no differences observed in efficacy outcomes. CTC detection was associated with worse outcome and AR-V7 in CTCs was associated with increased rate of progression as best response. Plasma AR gain was strongly associated with an adverse outcome, with worse median prostate specific antigen (PSA)-PFS (4.2 vs. 14.7 m; $p < 0.0001$), rad-PFS (4.5 vs. 27.6 m; $p < 0.0001$), and OS (12.7 vs. 38.1 m; $p < 0.0001$). The clinical prognostic model developed in PREVAIL was validated (C-Index 0.70) and the addition of plasma AR (C-Index 0.79; $p < 0.001$) increased its prognostic ability. We generated a parsimonious model including alkaline phosphatase (ALP); PSA and AR gain (C-index 0.78) that was validated in an independent cohort.

Conclusions: *TMPRSS2-ERG* detection did not correlate with differential activity of enzalutamide in first-line mCRPC. However, we observed that CTCs and plasma AR gain were the most relevant biomarkers.

KEYWORDS

AR gain, AR-V7, CTCs, enzalutamide, prostate cancer, *TMPRSS2-ERG*

1 | INTRODUCTION

Prostate cancer (PCa) is the second cause of death from cancer in males.¹ Its growth is dependent upon androgen receptor (AR) signaling, and androgen deprivation therapy (ADT) is the mainstay

of treatment in advanced patients.² Virtually all patients progress to a castration-resistant state where androgen signaling is potentially driving tumor progression.³ Enzalutamide is a potent AR-targeted agent that competitively binds the AR ligand-binding domain and inhibits AR signaling.⁴ Treatment with enzalutamide has

improved overall survival and quality of life in PCa.⁵ However benefit from this treatment is variable and several clinical and molecular events have been proposed to explain this heterogeneity.^{6–8}

Fusion genes involving E26 transformation-specific (ETS) oncogenes are the most common driver events affecting 30%–70% of PCa.^{9–11} The most frequent fusion gene involves transmembrane protease serine 2 (*TPRSS2*) on 21q22.3 and v-ets erythroblastosis virus E26 oncogene homolog (*ERG*) on 21q22.2, either by intrachromosomal deletion or translocation, and as a result of the oncogene *ERG* becomes AR-regulated. *TPRSS2-ERG* is involved in tumor initiation,¹² invasion,¹³ and progression,¹⁴ and has been associated with increased efficacy in abiraterone-treated patients.^{15,16} Other biomarkers, including plasma AR gain,^{17–19} circulating tumor cells (CTCs),^{20,21} and AR-V7 in CTCs^{22,23} have demonstrated prognostic and/or predictive value in pretreated metastatic castration-resistant prostate cancer (mCRPC). However, the prognostic value of these biomarkers in first-line mCRPC needs to be further explored.

Clinical prognostic models in mCRPC, including a prognostic model in patients treated with enzalutamide in first-line mCRPC²⁴ are intended to deal with this heterogeneity. This latter model needs to be externally validated and can potentially be improved including molecular information.

In this phase 2 multicenter biomarker study with enzalutamide in first-line chemo-naïve mCRPC, we aimed to evaluate the clinical significance of *TPRSS2-ERG* fusion gene, and to explore other relevant biomarkers, including plasma AR, CTCs, and AR-V7 in CTCs, and its contribution to the available clinical prognostic models.

2 | MATERIALS AND METHODS

2.1 | Study design and conduct

The PREMIERE trial is a translational multicenter single-arm open-label phase 2 clinical trial (NCT02288936) of enzalutamide in first-line mCRPC, originally designed to analyze the prognostic value of the gene fusion *TPRSS2-ERG* and other correlative laboratory studies, including plasma DNA and CTC analysis. The study was approved by a central independent review board (IRB).

The validation cohort consisted of a single institution cohort from patients participating in a protocol approved by the Istituto Scientifico Romagnolo per lo Studio e la Cura dei Tumori (IRST), Meldola, Italy (REC 2192/2013) with plasma samples collected prospectively with the primary aim of biomarker evaluation.

2.2 | Participants

The PREMIERE trial consisted of patients with histologically confirmed adenocarcinoma of the prostate with documented metastases and tumor progression and a serum testosterone level of 50 ng per deciliter or less with continued androgen-deprivation therapy. Eligible patients had Eastern Cooperative Oncology Group

(ECOG) 0–1, and were asymptomatic or mildly symptomatic (Brief Pain Inventory Short Form question 3 of less than 4).

The IRST cohort consisted of patients with histologically confirmed prostate adenocarcinoma without neuroendocrine differentiation, progressive disease despite “castration levels” of serum testosterone (<50 ng/dl), ongoing LHRH analog treatment or prior surgical castration, and no prior treatment with enzalutamide or abiraterone.

Treatment in both cohorts consisted of enzalutamide at a dose of 160 mg once daily. Treatment continued until the occurrence of unacceptable side effects or confirmed radiographic progression. Written informed consent was obtained from all patients.

2.3 | Procedures

In the PREMIERE trial, tumor tissue and blood samples were shipped before study entry and a central pathologist reviewed all histological FFPE samples. Blood samples were collected before study entry, at 12 weeks and at progression, and included three 5 ml EDTA tubes: two were locally processed to obtain plasma that was stored at –80°C and centrally shipped at study completion and one was shipped overnight at 4°C to a central laboratory and processed in less than 24 h for CTC analyses. In the IRST cohort, plasma samples were collected before treatment initiation and analyzed at a central laboratory.

TPRSS2-ERG fusion gene was studied in FFPE tumor tissue from the PREMIERE trial. In brief, an 8-μm FFPE slide was macrodissected and DNA/RNA was extracted and quantitative PCR (qPCR) was performed in duplicate with the TaqMan primer probe for *TPRSS2-ERG* fusion transcript (Hs03063375 ft, Applied Biosystems) following manufacturer's instructions. *ERG* immunohistochemistry was performed using *ERG* rabbit monoclonal antibody (EPR3864, Epitomics; dilution 1:100) and correlated with qPCR results. Fluorescence in situ hybridization (FISH) for *TPRSS2-ERG* fusion gene was independently performed as previously described²⁵ at two different institutions (HMM and CNIO).

- *Plasma AR copy number.* Plasma was collected within 30 days before treatment initiation and plasma aliquots were stored at –80°C and centrally analyzed upon study completion. ddPCR assays were carried out as previously described.¹⁸ In brief, for each individual sample, AR CN was estimated using each of the reference genes *NSUN3*, *EIF2C1*, and *AP3B1* and using *ZXDB* at *Xp11.21* as a control gene to determine X chromosome CN. An AR gain cutoff of ≥ 1.92 was considered as AR gain, as previously published.¹⁹
- *CTC and AR-V7 analysis.* The CTC analyses were conducted using the commercially available AdnaTest platform (Qiagen) following the manufacturer's instructions with a minor modification previously described.²² Custom primers, as previously described, were used to detect AR-V7 mRNA. Sanger sequencing confirmed the accuracy of the PCR product. AR-V7 cross-validation was

performed between PREMIERE central laboratory (CL) and Johns Hopkins University (JH).

2.4 | Outcomes

The primary endpoint for the PREMIERE clinical trial was prostate specific antigen (PSA) progression-free survival (PSA-PFS) and secondary endpoints included PSA response, radiographic progression-free survival (rad-PFS), and overall survival (OS). PSA and blood tests were assessed monthly and radiographic disease was evaluated with the use of computed tomography (CT) and bone scan at the time of screening and every 12 weeks thereafter. Response was evaluated according to the Prostate Cancer Clinical Trials Working Group 2 (PCWG2) criteria²⁶ and soft tissue disease was assessed on the basis of Response Evaluation Criteria in Solid Tumors (RECIST), version 1.1.²⁷ CTC conversion was defined considering the analysis at basal and after 12 weeks of treatment.

2.5 | Statistical analyses

Statistical analyses were performed using the R software, version 3.3.0. The statistical plan for biomarkers included descriptive and prognostic analyses of TMPRSS2-ERG, CTC, AR-V7 in CTCs, and AR gain using the primary and secondary outcomes of the trial, as previously described. Post hoc exploratory analyses included correlation with primary progression. Qualitative variables were compared using the Fisher exact test. Time variables were evaluated using Kaplan-Meier analysis and cox-proportional hazards models. All tests were two-sided, and an alpha-error of less than 0.05 was required to be considered statistically significant. Cohen's Kappa test was used to study concordance between the central and the external laboratory. A Cox-proportional hazards model via penalized maximum likelihood, using the package *glmnet* 2.0-18,²⁸ was used to generate a parsimonious clinical-molecular model.

3 | RESULTS

Ninety-eight chemotherapy-naïve mCRPC patients initiated enzalutamide as first-line treatment between February and November 2015 at 16 Spanish institutions in the PREMIERE trial. Patients' characteristics are described in Table 1. Survival outcomes for all patients included in the study are shown in Supporting Information: Figure S1. With a median follow-up of 37 months, median PSA-PFS was 14.1 months (95% confidence interval [CI]: 10.2–20.2), median rad-PFS was 25.2 months (95% CI: 21.7–32.1) and median OS was 37.5 months (95% CI: 33.7 vs. NR). Treatment responses are described in Supporting Information: Table S2. PSA-50 (decrease $\geq 50\%$) was observed in 82%, and PSA-90 (decrease $\geq 90\%$) in 53%, with radiographic response observed in 49% of the patients ($N = 21$).

TABLE 1 Patients' characteristics

Patient characteristics	All ($n = 98$)
Age median (range)	77 (57–95)
Metastases, no. (%)	
Bone	80 (82%)
Visceral	16 (16%)
Liver	4 (4%)
Lymph nodes	47 (48%)
Bone metastasis, no. (%)	
<4	50 (51%)
≥ 4	30 (31%)
ECOG, no. (%)	
0	53 (54%)
1	45 (46%)
Pain, N (%)	
No pain	45 (46%)
Mild (≤ 3 BPI score)	52 (54%)
PSA, ng/dl, median (range)	24.95 (0.59–4319)
Albumin ($\mu\text{g/dl}$)	4.16 (3.29–5.00)
Hemoglobin median (range)	13.20 (7.50–17.30)
ALP ratio median (range)	0.71 (0.24–17.46)
High ($> \text{UNL}$)	28 (29%)
LDH ratio median (range)	0.84 (0.29–3.36)
High ($> \text{UNL}$)	31 (32%)
NLR median (range)	2.14 (0.52–12.33)
CTC positive, no. (%)	35 (36%)
Plasma DNA, ng/ml, median (range)	18.64 (0.05–1585)
AR gain, no. (%)	11 (11%)

Abbreviations: ALP, alkaline phosphatase; AR, androgen receptor; BPI, Brief Pain Inventory; CTC, circulating tumor cell; ECOG, Eastern Cooperative Oncology Group; LDH, lactate dehydrogenase; NLR, neutrophil to lymphocyte ratio.

Enzalutamide was well tolerated with no unexpected toxicities, as shown in Supporting Information: Table S4.

3.1 | TMPRSS2-ERG status

TMPPSS2-ERG fusion gene was detected in 32 patients (33%). All positive samples expressed high ERG in the nucleus by IHC ($r = 0.93$; $p < 0.0001$). Baseline patients' characteristics were similar between both groups and no differences were observed in any efficacy outcome based on the detection of *TMPPSS2-ERG*. Further details are described in Supporting Information: Tables S1–S3 and Figures S2 and S3.

3.2 | Plasma AR gain

Baseline plasma AR gain was detected in 11 patients (11%). Plasma AR-based survival analyses are shown in Figure 1A–C. AR gain was associated with worse survival outcomes than AR normal: median PSA-PFS 4.2 versus 14.7 months (hazard ratio [HR] 4.03, 95% confidence interval [CI] 1.87–8.72; $p < 0.001$), median rad-PFS was 4.5 versus 27.6 months (HR 9.83, 95% CI 4.50–21.44; $p < 0.0001$) and median OS of 12.7 versus 38.1 months (HR 6.65, 95% CI 3.18–13.91; $p < 0.0001$), respectively. AR gain was also associated with worse PSA response, as shown in Figure 1D.

AR gain was detected in 19.4% (6/31) versus 7.6% (5/66) in *TMPRSS2-ERG* positive and negative, respectively ($p = 0.166$), as shown in Supporting Information: Table S5.

3.3 | CTCs by Adna-Test®

Baseline CTCs were present in 35 patients (36%). Survival outcomes by baseline CTC status are described in Figure 2A–C. The presence of CTC at baseline was associated with worse evolution in all survival outcomes. Median PSA-PFS for positive patients was 7.4 versus 20.2 months (HR 3.37, 95% CI 2.01–5.66; $p < 0.0001$), median rad-PFS was 11.5 versus 33.1 months (HR 5.21, 95% CI 2.82–9.64; $p < 0.0001$) and median OS was 25.4 months versus not reached

(HR 4.68, 95% CI 2.64–8.28; $p < 0.0001$). CTC conversion analysis using landmark survival analysis is shown in Figure 2D. Conversion of CTC detection from positive to negative was associated with improved evolution in all survival outcomes, including PSA-PFS ($p < 0.001$), rad-PFS ($p < 0.001$), and OS ($p < 0.001$). No association was observed between *TMPRSS2-ERG* expression and CTC detection ($p = 0.825$), as described in Supporting Information: Table S5.

3.4 | AR-V7 expression in CTCs

AR-V7 was detected in 16% of CTC-positive evaluable patients (5/32). Progression as best response at 12 weeks was observed in 60% (3/5) in AR-V7 positive patients, compared with 30% (8/27) in AR-V7 negative and 8% (5/63) in CTC negative patients ($p = 0.0014$). However, two externally validated AR-V7 patients had tumor responses lasting for 14 and 25 months, as shown in Supporting Information: Figure S4A. AR-V7-based survival analyses are shown in Figure 2B–D. No differences were observed for survival outcomes. Intriguingly, at baseline all AR-V7 positive patients were *TMPRSS2-ERG* negative (5/21 vs. 0/11, $p = 0.134$), as shown in Supporting Information: Table S5. A numerical increase, not statistically significant, was observed for AR gain in AR-V7 positive when compared with AR-V7 negative and CTC negative patients: 40% (2/5), 16% (4/24), and 8% (5/66), respectively.

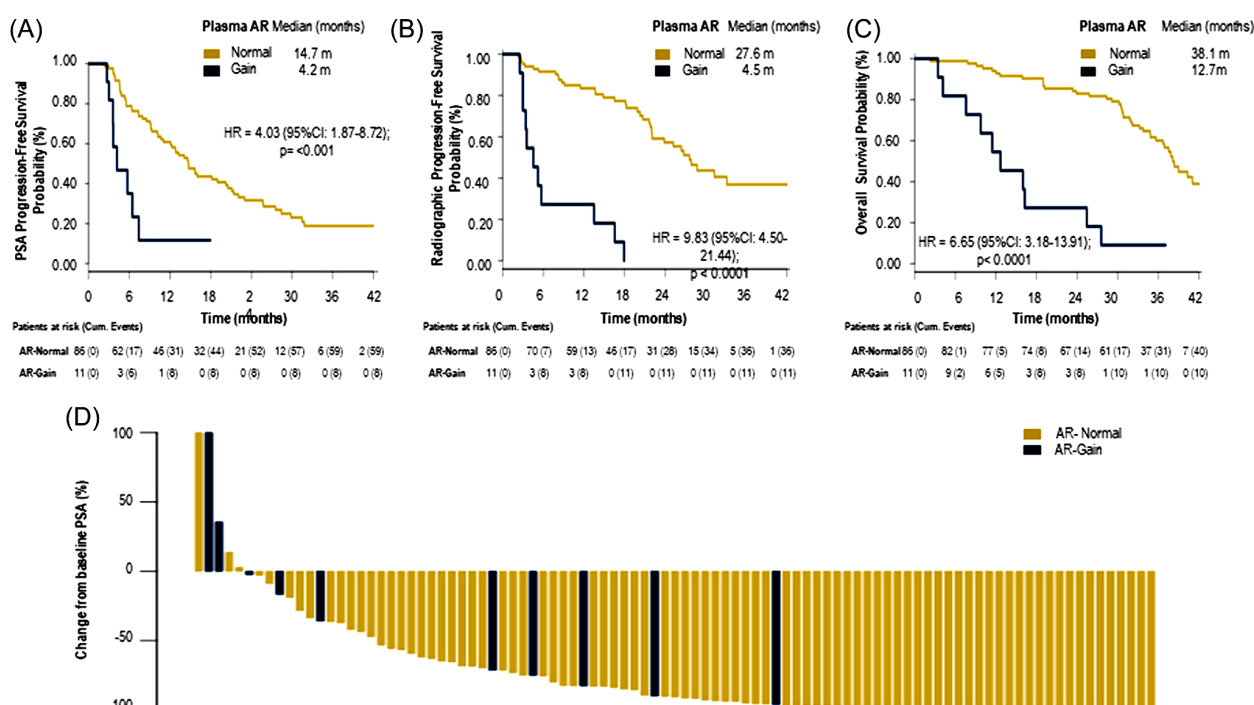


FIGURE 1 Survival outcomes and response by AR gain in plasma DNA. Kaplan-Meier and Cox-regression models were used for survival analyses: (A) PSA progression-free survival; (B) radiographic progression-free survival; (C) overall survival; and (D) waterfall plot representing maximum PSA decrease by plasma AR status. AR, androgen receptor. [Color figure can be viewed at wileyonlinelibrary.com]

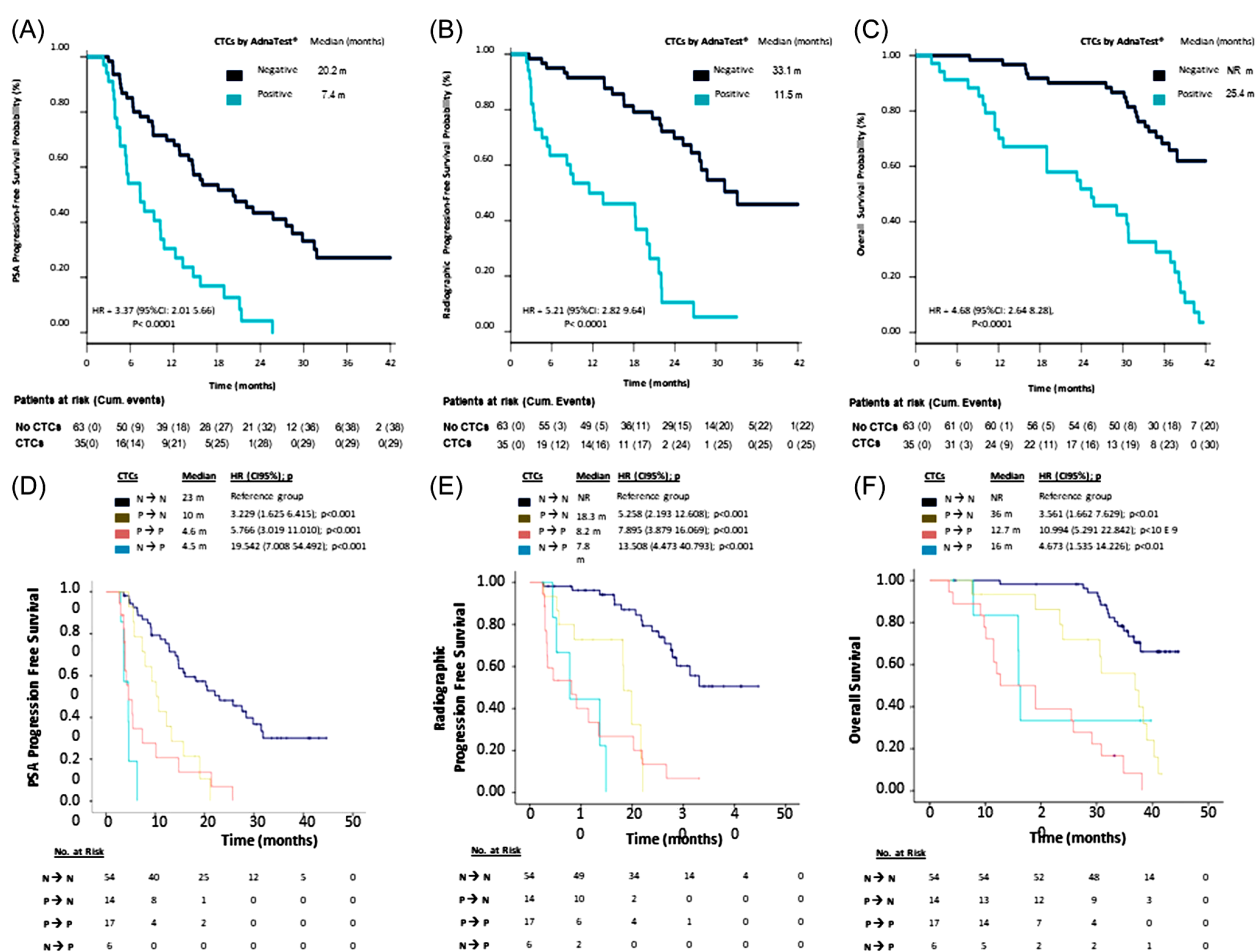


FIGURE 2 Survival outcomes by CTC and CTC conversion. Kaplan-Meier and Cox-regression models were used for survival analyses: (A, D) PSA progression-free survival in CTCs and by CTC conversion; (B, E) radiographic progression-free survival in CTCs and by CTC conversion; and (C, F) overall survival in CTCs and by CTC conversion. CTC, circulating tumor cell. [Color figure can be viewed at wileyonlinelibrary.com]

3.5 | Development of an integrated clinical-molecular model

We evaluated in our series the clinical prognostic model previously developed based on the PREVAIL trial externally validating it in our series, with a Concordance Index (C-Index) of 0.70. Interestingly, most patients in our study were included in the low (61%) and intermediate (37%) risk groups, as shown in Supporting Information: Figure S5.

A multivariate analysis of all clinical variables included in the clinical model, CTC, and AR is shown in Table 2. We then integrated AR gain with the clinical variables included in the clinical model into a new comprehensive clinical and molecular model that obtained a bootstrap-validated C-Index of 0.79. The addition of AR to the clinical model increased the prognostic ability of the clinical model ($p < 0.001$). Using a penalized regression model, we obtained a clinical-molecular parsimonious model that included three variables: ALP ratio, PSA, and AR gain Table 3, and a bootstrap-validated C-Index of 0.78. This model was validated in an independent cohort

of patients treated at IRST with enzalutamide obtaining a C-Index of 0.71. We then designed a nomogram capable to predict the survival probability at 12, 24, and 36 months, as shown in Figure 3.

4 | DISCUSSION

We here show the final results of a biomarker phase 2 multicentre clinical trial of enzalutamide in first-line chemo-naïve mCRPC. The primary aim of the study was to evaluate the association between TMPRSS2-ERG and the efficacy of enzalutamide and we did not find any difference. However, we observed that CTCs by AdnaTest® and AR gain are strong and independent prognostic variables. In addition, we externally validated a clinical prognostic model developed in the PREVAIL trial and observed that both CTCs and AR gain are able to improve the prognostic ability of the model. We then developed a parsimonious model including clinical variables and AR gain, that validated an independent data set of mCRPC patients treated with enzalutamide in the same clinical scenario.

TABLE 2 Multivariable analysis for the clinical and molecular variables

Premiere		
Prognostic	HR (95% CI)	p*
Albumin	0.57 (0.21–1.57)	0.276
ALP	0.44 (0.23–0.87)	0.018
Number of bone metastases	0.94 (0.82–1.08)	0.355
Hemoglobin	1.00 (0.79–1.27)	0.985
LDH	0.66 (0.35–1.26)	0.207
NLR	0.77 (0.36–1.64)	0.499
Pain score	2.13 (1.12–4.05)	0.021
Pattern of spread	0.63 (0.14–2.83)	0.543
Log _e PSA	1.39 (1.10–1.74)	0.005
Time from diagnosis to randomization	1.00 (0.99–1.01)	0.863
AR gain	8.25 (3.17–21.45)	<0.001
CTC	2.74 (1.34–5.61)	0.006

Abbreviations: ALP, alkaline phosphatase; AR, androgen receptor; BPI, Brief Pain Inventory; CI, confidence interval; CTC, circulating tumor cell; ECOG, Eastern Cooperative Oncology Group; HR, hazard ratio; LDH, lactate dehydrogenase; NLR, neutrophil to lymphocyte ratio.

*p Value was calculated using Cox regression.

TABLE 3 Clinical-molecular parsimonious model

	Coefficient	p*
ALP ratio (log)	0.73	<0.001
PSA ng/dl (log)	0.36	<0.001
AR gain (yes vs. no)	2.15	<0.001

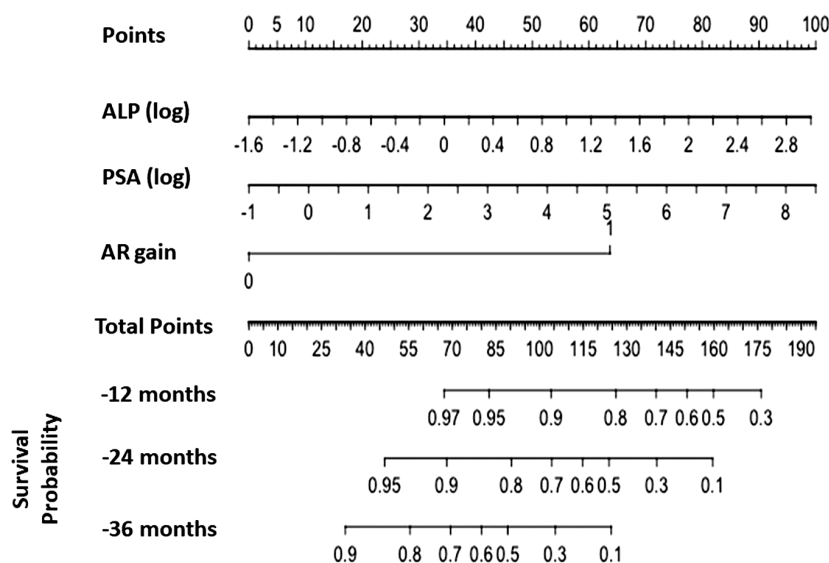
*p Value was calculated using Cox regression.

Previous results regarding the predictive value of *TMPRSS2-ERG* to new antiandrogens were controversial with abiraterone, with an early phase I/II trial of abiraterone that reported increased PSA responses in *TMPRSS2-ERG* associated tumors.^{15,29} Our results with enzalutamide-treated patients, together with previous studies with abiraterone, support that *TMPRSS2-ERG* fusion gene has limited value as predictive biomarker in mCRPC treated with anti-androgen therapies.

We also evaluated plasma AR-gain and other promising biomarkers including CTCs measured by AdnaTest® and AR-V7 expression in CTCs. We previously published the association of plasma AR-gain with an adverse outcome to enzalutamide with a median follow-up of 11 months. Here we present the final updated survival, with a median follow-up of 37 months that confirms its strong independent prognostic value in first-line mCRPC. AR-gain prognostic value was independent of other clinical and molecular prognostic variables. We observed a numerical increase in AR gain in AR-V7 positive patients compared with AR-V7 negative and CTC negative (40% vs. 17% vs. 8%). This result, although limited by the low numbers, is in agreement with previous publications in PCa metastatic tissue, that observe an association between AR gain and AR-V7 expression in PCa metastases.³⁰

We show that CTCs can be detected using AdnaTest® in almost one third (35%) of low-intermediate risk mCRPC patients, and that it is a strong and independent prognostic biomarker. We also observe, using landmark survival analysis, that CTC conversion at 12 weeks of treatment is associated with treatment outcome, including a favorable outcome when it turns negative and an adverse outcome when it becomes positive. However, prospective randomized clinical trials are needed to fulfill the Prentice criteria³¹ and fully qualify as a meaningful biomarker for regulatory matters.

AR-V7 in CTCs has previously demonstrated clinical value in mCRPC patients treated with a new anti-androgen therapy.^{22,23} In this first-line study, we observed a low detection rate for AR-V7 (5% of all

**FIGURE 3** Nomogram for the clinical-molecular parsimonious model. Nomogram developed using the integrated parsimonious three variables prognostic model. ALP ratio and PSA were included in logarithmic scale. This nomogram predicts survival probability at 12, 24, and 36 months. ALP, alkaline phosphatase.

patients; $N = 5/98$) and low PSA50 response rate (40% vs. 82%). These results are consistent with a recently published phase 3 trial³² in this same scenario, with a detection rate of 7%–10% ($N = 38/953$) and a response rate of 42% in 19 patients treated with enzalutamide.

Investigators from the pivotal trial of enzalutamide in first-line mCRPC published a clinical prognostic model able to stratify patients based on pretreatment clinical variables. This model was limited by the lack of external validation and the absence of molecular variables. We here validated this clinical prognostic model, obtaining a C-index of 0.70 and observed that both CTCs and AR-gain were independent variables that were able to improve the prognostic ability of the model. We then built a parsimonious clinical-molecular model, composed of three variables: AR gain, ALP, and PSA that was independently validated. LDH has been previously selected in multiple prognostic models in mCRPC, including models that include CTCs.^{33,34} Intriguingly, LDH was not significant in our penalized regression model. The association of LDH with high-risk features, that were not represented in our model, might explain the lack of statistical significance in our study.

5 | CONCLUSIONS

In this phase 2 biomarker trial, we report additional evidence with long follow-up on the prognostic impact of AR gain together with other biomarkers, including CTCs and AR-V7 chemo-naïve mCRPC patients. We demonstrate its ability to improve clinical prognostic models and propose a new parsimonious model including plasma AR gain. Further studies, including comprehensive biomarker panels and well-annotated clinical data sets, are required to redefine prognostic models in PCa.

ACKNOWLEDGMENTS

The authors would like to acknowledge all the staff at SOGUG for their support to run the PREMIERE trial, Astellas for supporting this research, ISCIII from the Spanish Ministry of Health, and Cris Cancer Foundation for their support. This trial was promoted by SOGUG and received a grant from Astellas. EGB received a travel grant (BA16/00038) and funding support from the "Instituto de Salud Carlos III" (PI18/00883) and support from SEOM-CRIS Cancer Foundation.

CONFLICTS OF INTEREST

TG has received travel grants from Sanofi and participated in advisory boards for Sanofi, Janssen, Astellas, and Bayer. AF has received travel grants from Astellas, Astra-Zeneca, Sanofi and participated in advisory boards for Janssen, Sanofi, Eisai, and Bayer. SVE has received travel grants from Astellas, Janssen, and Bayer, and has participated in advisory boards for Janssen, Astellas, Sanofi, and Bayer. AGdA has received research funding from Astellas, travel grants from Astellas, Jansen, Sanofi, BMS, Roche, Pfizer, and Ipsen, and honoraria for speaker engagements, advisory boards, and continuous medical education from Janssen, Astellas, Sanofi, Bayer, Roche, Ipsen, BMS, MSD, Pfizer, Eusa Pharma, Eisai, and Astra Zeneca. ESA is the codeveloper of a patented AR-V7 biomarker technology that has been licensed to Qiagen. ID has received travel grants and research funding from Astellas and has

participated in advisory boards for Astellas, Janssen, Sanofi, and Bayer. EG has received travel grants from Astellas, Janssen, Sanofi, Bayer, Roche, BMS, and Eisai, honoraria for speaking engagements for Astellas, Janssen, Sanofi, Bayer, Pfizer, Roche, BMS, Novartis, Rovi, Daiichi Sankyo, Leo Pharma, Menarini, Eisai, MSD, Boehringer Ingelheim, Merck, and EUSA Pharma and participated in advisory boards for Astellas, Janssen, Sanofi, Bayer, Pfizer, Roche, Novartis, Eisai, EUSA Pharma, BMS, AstraZeneca, Merck, Rovi, Daiichi Sankyo, and Techdow. JP has received research funding from Astellas and Roche and received honoraria for speaker engagements, advisory roles, or continuous medical education from Astellas, Astra Zeneca, Janssen, MSD, Bayer, Pfizer, Eisai, Ipsen, Sanofi, Roche, BMS, and Merck. BM has served advisory role from Roche, Sanofi, Janssen, Astellas, Pfizer, Novartis, Bristol-Myers Squibb, and Ipsen, research funding from Roche, Bayer, and Janssen, and accommodation expenses from Pfizer and Janssen. MA Climent has received travel grants from Astellas, Jansen, Sanofi, Pfizer, Roche, and Ipsen. And honoraria for speaker engagements, advisory boards, and continuous medical education from Janssen, Astellas, Sanofi, Bayer, Roche, Ipsen, BMS, MSD, Pfizer, and Astra Zeneca MJMV has received travel grants from Astellas and Janssen and has participated in advisory boards for Janssen, Astellas, Sanofi, and Bayer. María Isabel Sáez Medina has received travel grants from Sanofi and Roche and participated in advisory boards from Sanofi, Ipsen, and Astellas. DC has received research funding from Astellas, educational grants from Pfizer and Janssen, travel grants from Pfizer and BMS, and has participated in advisory boards for Pfizer, Astellas, Janssen, Sanofi, Bayer, and Roche. JL is an inventor of AR-V7-related technologies that have been licensed to A&G Pharmaceuticals and Qiagen. GA reported receiving grants, personal fees, nonfinancial support, and speaker fees from Janssen, Astellas, and Sanofi; personal fees, nonfinancial support, and speaker fees from AstraZeneca; and personal fees from Novartis and Bayer outside the submitted work; in addition, GA reported having a patent (GB1915469.9; blood signatures for prostate cancer detection) pending and is on the Institute of Cancer Research list of rewards to inventors for abiraterone acetate. EG Research funding from Astellas, Astra Zeneca, IPSEN, Pfizer, and Roche and has participated in advisory boards for Adacap, AMGEN, Angelini, Astellas, Astra Zeneca, Bayer, Blueprint, Bristol Myers Squibb, Caris Life Sciences, Celgene, Clovis-Oncology, Eisai, Eusa Pharma, Genetracer, Guardant Health, HRA-Pharma, IPSEN, ITM-Radiopharma, Janssen, Lexicon, Lilly, Merck KGaA, MSD, Nanostring Technologies, Natera, Novartis, ONCODNA (Biosequence), Palex, Pharmamar, Pierre Fabre, Pfizer, Roche, Sanofi-Genzyme, Servier, Taiho, Thermo Fisher Scientific. EGB has received travel grants from Astellas, Janssen, and Sanofi and has participated in advisory boards for Astellas, Janssen, Sanofi, Astra-Zeneca, and Bayer.

DATA AVAILABILITY STATEMENT

The authors confirm that the data supporting the findings of this study are available within the article and its Supporting Information.

ORCID

Enrique Perez-Navarro  <http://orcid.org/0000-0003-1091-8926>

Teresa Alonso-Gordoa  <http://orcid.org/0000-0002-8966-7236>

Vicenza Conteduca  <http://orcid.org/0000-0002-6921-714X>

Enrique Gonzalez-Billalabeitia  <http://orcid.org/0000-0003-3143-3143>

REFERENCES

- Siegel RL, Miller KD, Fuchs HE, Jemal A. Cancer statistics, 2021. *CA Cancer J Clin*. 2021;71(1):7-33. doi:10.3322/caac.21654
- Attard G, Parker C, Eeles RA, et al. Prostate cancer. *Lancet*. 2016;387(10013):70-82.
- Beer TM, Armstrong AJ, Rathkopf DE, et al. Enzalutamide in metastatic prostate cancer before chemotherapy. *N Engl J Med*. 2014;371(5):424-433.
- Tran C, Ouk S, Clegg NJ, et al. Development of a second-generation antiandrogen for treatment of advanced prostate cancer. *Science*. 2009;324(5928):787-790.
- Beer TM, Armstrong AJ, Rathkopf D, et al. Enzalutamide in men with chemotherapy-naïve metastatic castration-resistant prostate cancer: extended analysis of the phase 3 PREVAIL study. *Eur Urol*. 2017;71(2):151-154.
- Armenia J, Wankowicz SAM, Liu D, et al. The long tail of oncogenic drivers in prostate cancer. *Nature Genet*. 2018;50(5):645-651.
- Quigley DA, Dang HX, Zhao SG, et al. Genomic hallmarks and structural variation in metastatic prostate cancer. *Cell*. 2018;174(3):758-769.
- Abida W, Cyrta J, Heller G, et al. Genomic correlates of clinical outcome in advanced prostate cancer. *Proc Natl Acad Sci USA*. 2019;116(23):11428-11436.
- Tomlins SA, Rhodes DR, Perner S, et al. Recurrent fusion of TMPRSS2 and ETS transcription factor genes in prostate cancer. *Science*. 2005;310(5748):644-648. doi:10.1126/science.1117679
- Cancer Genome Atlas Research Network. The molecular taxonomy of primary prostate cancer. *Cell*. 2015;163(4):1011-1025.
- Robinson D, Van Allen EM, Wu YM, et al. Integrative clinical genomics of advanced prostate cancer. *Cell*. 2015;161(5):1215-1228.
- Carver BS, Tran J, Chen Z, et al. ETS rearrangements and prostate cancer initiation. *Nature*. 2009;457(7231):E1. doi:10.1038/nature07738
- Wang J, Cai Y, Yu W, Ren C, Spencer DM, Ittmann M. Pleiotropic biological activities of alternatively spliced TMPRSS2/ERG fusion gene transcripts. *Cancer Res*. 2008;68(20):8516-8524.
- Yu J, Yu J, Mani RS, et al. An integrated network of androgen receptor, polycomb, and TMPRSS2-ERG gene fusions in prostate cancer progression. *Cancer Cell*. 2010;17(5):443-454. doi:10.1016/j.ccr.2010.03.018
- Attard G, Swennenhuis JF, Olmos D, et al. Characterization of ERG, AR and PTEN gene status in circulating tumor cells from patients with castration-resistant prostate cancer. *Cancer Res*. 2009;69(7):2912-2918. doi:10.1158/0008-5472.CAN-08-3667
- Attard G, de Bono JS, Logothetis CJ, et al. Improvements in radiographic progression-free survival stratified by ERG gene status in metastatic castration-resistant prostate cancer patients treated with abiraterone acetate. *Clin Cancer Res*. 2015;21(7):1621-1627.
- Carreira S, Romanel A, Goodall J, et al. Tumor clone dynamics in lethal prostate cancer. *Sci Transl Med*. 2014;6(254):254ra125.
- Conteduca V, Wetterskog D, Sharabiani MTA, et al. Androgen receptor gene status in plasma DNA associates with worse outcome on enzalutamide or abiraterone for castration-resistant prostate cancer: a multi-institution correlative biomarker study. *Ann Oncol*. 2017;28(7):1508-1516.
- Jayaram A, Wingate A, Wetterskog D. Plasma androgen receptor copy number status at emergence of metastatic castration-resistant prostate cancer: a pooled multicohort analysis. *JCO Precis Oncol*. 2019;3:1-13.
- Danila DC, Heller G, Gignac GA, et al. Circulating tumor cell number and prognosis in progressive castration-resistant prostate cancer. *Clin Cancer Res*. 2007;13(23):7053-7058.
- Scher HI, Heller G, Molina A, et al. Circulating tumor cell biomarker panel as an individual-level surrogate for survival in metastatic castration-resistant prostate cancer. *J Clin Oncol*. 2015;33(12):1348-1355.
- Antonarakis ES, Lu C, Wang H, et al. AR-V7 and resistance to enzalutamide and abiraterone in prostate cancer. *N Engl J Med*. 2014;371(11):1028-1038.
- Scher HI, Graf RP, Schreiber NA, et al. Assessment of the validity of nuclear-localized androgen receptor splice variant 7 in circulating tumor cells as a predictive biomarker for castration-resistant prostate cancer. *JAMA Oncol*. 2018;4(9):1179-1186.
- Armstrong AJ, Lin P, Higano CS, et al. Development and validation of a prognostic model for overall survival in chemotherapy-naïve men with metastatic castration-resistant prostate cancer. *Ann Oncol*. 2018;29(11):2200-2207. doi:10.1093/annonc/mdy406
- Mehra R, Tomlins SA, Shen R, et al. Comprehensive assessment of TMPRSS2 and ETS family gene aberrations in clinically localized prostate cancer. *Mod Pathol*. 2007;20(5):538-544. doi:10.1038/MODPATHOL.3800769
- Scher HI, Halabi S, Tannock I, et al. Design and end points of clinical trials for patients with progressive prostate cancer and castrate levels of testosterone: recommendations of the Prostate Cancer Clinical Trials Working Group. *J Clin Oncol*. 2008;26(7):1148-1159.
- Eisenhauer EA, Therasse P, Bogaerts J, et al. New response evaluation criteria in solid tumours: revised RECIST guideline (version 1.1). *Eur J Cancer*. 2009;45(2):228-247.
- Friedman J, Hastie T, Tibshirani R. Regularization paths for generalized linear models via coordinate descent. *J Stat Softw*. 2010;33(1):1-22. doi:10.18637/jss.v033.i01
- Danila DC, Anand A, Sung CC, et al. TMPRSS2-ERG status in circulating tumor cells as a predictive biomarker of sensitivity in castration-resistant prostate cancer patients treated with abiraterone acetate. *Eur Urol*. 2011;60(5):897-904. doi:10.1016/j.eururo.2011.07.011
- Sharp A, Coleman I, Yuan W, et al. Androgen receptor splice variant-7 expression emerges with castration resistance in prostate cancer. *J Clin Invest*. 2019;129(1):192-208.
- Prentice RL. Surrogate endpoints in clinical trials: definition and operational criteria. *Stat Med*. 1989;8(4):431-440.
- Taplin ME, Antonarakis ES, Ferrante KJ, et al. Androgen receptor modulation optimized for response-splice variant: a phase 3, randomized trial of galeterone versus enzalutamide in androgen receptor splice variant-7-expressing metastatic castration-resistant prostate cancer. *Eur Urol*. 2019;76:843-851.
- Scher HI, Jia X, de Bono JS, et al. Circulating tumour cells as prognostic markers in progressive, castration-resistant prostate cancer: a reanalysis of IMMC38 trial data. *Lancet Oncol*. 2009;10(3):233-239.
- Scher HI, Heller G, Molina A, et al. Circulating tumor cell biomarker panel as an individual-level surrogate for survival in metastatic castration-resistant prostate cancer. *J Clin Oncol*. 2015;33(12):1348-1355. doi:10.1200/JCO.2014.55.3487








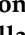


SUPPORTING INFORMATION

Additional supporting information can be found online in the Supporting Information section at the end of this article.

How to cite this article: Fernandez-Perez MP, Perez-Navarro E, Alonso-Gordoa T, et al. A correlative biomarker study and integrative prognostic model in chemotherapy-naïve metastatic castration-resistant prostate cancer treated with enzalutamide. *The Prostate*. 2023;83:376-384. doi:10.1002/pros.24469

Article

Prognostic Implications of Blood Immune-Cell Composition in Metastatic Castration-Resistant Prostate Cancer

Enrique Perez-Navarro ^{1,2} , Vincenza Conteduca ³, Juan M. Funes ¹ , Jose I. Dominguez ¹, Miguel Martin-Serrano ¹ , Paolo Cremaschi ⁴, Maria Piedad Fernandez-Perez ⁵, Teresa Alonso Gordoa ⁶, Albert Font ⁷, Sergio Vázquez-Estévez ⁸, Aránzazu González-del-Alba ⁹ , Daniel Wetterskog ⁴, Begona Mellado ¹⁰, Ovidio Fernandez-Calvo ¹¹ , María José Méndez-Vidal ¹², Miguel Angel Climent ¹³, Ignacio Duran ¹⁴, Enrique Gallardo ¹⁵ , Angel Rodriguez Sanchez ¹⁶, Carmen Santander ¹⁷, Maria Isabel Sáez ¹⁸, Javier Puente ¹⁹, Julian Tudela ²⁰, Cecilia Marinas ¹, Maria Jose López-Andreo ²¹ , Daniel Castellano ¹, Gerhardt Attard ⁴, Enrique Grande ²² , Antonio Rosino ²³ , Juan A. Botia ², Jose Palma-Mendez ², Ugo De Giorgi ²⁴ , and Enrique Gonzalez-Billalabeitia ^{1,25,*}

- ¹ Department of Medical Oncology, Instituto de Investigación Imas12, Hospital Universitario 12 de Octubre, 28041 Madrid, Spain; enrique.perez2@um.es (E.P.-N.); jmfunes.imas12@h12o.es (J.M.F.); mmartin.imas12@h12o.es (M.M.-S.)
- ² Departamento de Ingeniería de la Información y las Comunicaciones, Universidad de Murcia, 30100 Murcia, Spain; jtpalma@um.es (J.P.-M.)
- ³ Unit of Medical Oncology and Biomolecular Therapy, Department of Medical and Surgical Sciences, University of Foggia, 71122 Foggia, Italy
- ⁴ University College London Cancer Institute, London WC1E 6DD, UK
- ⁵ Department of Haematology and Medical Oncology, Hospital Universitario Morales Meseguer, Instituto Murciano de Investigaciones Biosanitarias (IMIB), 30005 Murcia, Spain
- ⁶ Medical Oncology Department, Hospital Universitario Ramón y Cajal, 28034 Madrid, Spain; talonso@salud.madrid.org
- ⁷ Institut Català d'Oncologia, Hospital Universitari Germans Trias i Pujol, 08029 Badalona, Spain
- ⁸ Hospital Universitario Lucus Augusti, 27003 Lugo, Spain; svazquezestevez@gmail.com
- ⁹ Medical Oncology Department, Hospital Universitario Puerta de Hierro-Majadahonda, 28222 Madrid, Spain
- ¹⁰ Medical Oncology Department, Hospital Clínic, 08036 Barcelona, Spain
- ¹¹ Department of Medical Oncology, Complejo Hospitalario Universitario Ourense, 32005 Ourense, Spain
- ¹² Medical Oncology Department, Maimonides Institute for Biomedical Research of Cordoba (IMIBIC), Hospital Universitario Reina Sofía, 14004 Córdoba, Spain
- ¹³ Instituto Valenciano de Oncología, 46009 Valencia, Spain
- ¹⁴ Hospital Universitario Marqués de Valdecilla, Instituto de Investigación Valdecilla (IDIVAL), 39011 Santander, Spain
- ¹⁵ Medical Oncology Service, Parc Taulí Hospital Universitari, Institut d'Investigació i Innovació Parc Taulí I3PT, Universitat Autònoma de Barcelona, 08208 Sabadell, Spain; enrqgllrd@gmail.com
- ¹⁶ Department of Medical Oncology, University Hospital of León, 24071 León, Spain
- ¹⁷ Department of Medical Oncology, Hospital Universitario Miguel Servet, 50009 Zaragoza, Spain
- ¹⁸ UGCI Oncología Médica, Hospital Universitario Virgen de la Victoria, 29010 Málaga, Spain
- ¹⁹ Medical Oncology Department, Hospital Clínico San Carlos, Instituto de Investigación Sanitaria del Hospital Clínico San Carlos (IdISSC), CIBERONC, 28040 Madrid, Spain
- ²⁰ Department of Pathology, Hospital Morales Meseguer, 30008 Murcia, Spain; jtpallares@gmail.com
- ²¹ Department of Molecular Biology, Servicio de Apoyo a la Investigación-Instituto Murciano de Investigación Biosanitaria (SAI-IMIB), Universidad de Murcia, 30100 Murcia, Spain
- ²² Medical Oncology Department, MD Anderson Cancer Center Madrid, Universidad Francisco de Vitoria, 28223 Madrid, Spain
- ²³ Urology Department, Hospital Universitario Morales Meseguer, 30005 Murcia, Spain
- ²⁴ IRCCS Istituto Romagnolo per lo Studio dei Tumori (IRST) "Dino Amadori", 47014 Meldola, Italy
- ²⁵ Facultad de Medicina, Universidad Católica San Antonio de Murcia (UCAM), 30107 Murcia, Spain
- * Correspondence: egbillalabeitia@salud.madrid.org



Citation: Perez-Navarro, E.; Conteduca, V.; Funes, J.M.; Dominguez, J.I.; Martin-Serrano, M.; Cremaschi, P.; Fernandez-Perez, M.P.; Gordoa, T.A.; Font, A.; Vázquez-Estévez, S.; et al. Prognostic Implications of Blood Immune-Cell Composition in Metastatic Castration-Resistant Prostate Cancer. *Cancers* **2024**, *16*, 2535. <https://doi.org/10.3390/cancers16142535>

Academic Editor: Anait S. Levenson

Received: 17 June 2024

Revised: 7 July 2024

Accepted: 12 July 2024

Published: 14 July 2024



Copyright: © 2024 by the authors. Licensee MDPI, Basel, Switzerland. This article is an open access article distributed under the terms and conditions of the Creative Commons Attribution (CC BY) license (<https://creativecommons.org/licenses/by/4.0/>).

Simple Summary: Metastatic castration-resistant prostate cancer (mCRPC) represents a lethal stage of prostate cancer, characterized for its resistance to androgen deprivation therapy and variable survival outcomes. This study investigates how the composition of specific immune cells in the blood affects the prognosis of mCRPC patients who have not yet received chemotherapy. In looking at blood samples taken before treatment with the drug enzalutamide, we discovered significant correlations

between lower levels of CD8 T cells and higher levels of monocytes, which were consistently linked to poorer survival rates. The prognostic value of blood CD8 T cells was independently validated in multivariate prognostic models and in an independent cohort of mCRPC patients. This study highlights the feasibility of blood immune-cell profiling in patients included in clinical trials and the association of blood CD8 T cells with the prognosis for mCRPC patients.

Abstract: The prognosis for patients with metastatic castration-resistant prostate cancer (mCRPC) varies, being influenced by blood-related factors such as transcriptional profiling and immune cell ratios. We aimed to address the contribution of distinct whole blood immune cell components to the prognosis of these patients. This study analyzed pre-treatment blood samples from 152 chemotherapy-naïve mCRPC patients participating in a phase 2 clinical trial (NCT02288936) and a validation cohort. We used CIBERSORT-X to quantify 22 immune cell types and assessed their prognostic significance using Kaplan–Meier and Cox regression analyses. Reduced CD8 T-cell proportions and elevated monocyte levels were substantially connected with a worse survival. High monocyte counts correlated with a median survival of 32.2 months versus 40.3 months for lower counts (HR: 1.96, 95% CI 1.11–3.45). Low CD8 T-cell levels were associated with a median survival of 31.8 months compared to 40.3 months for higher levels (HR: 1.97, 95% CI 1.11–3.5). These findings were consistent in both the trial and validation cohorts. Multivariate analysis further confirmed the independent prognostic value of CD8 T-cell counts. This study highlights the prognostic implications of specific blood immune cells, suggesting they could serve as biomarkers in mCRPC patient management and should be further explored in clinical trials.

Keywords: prostate cancer; castration-resistant prostate cancer (CRPC); enzalutamide; whole blood; prognostic factors

1. Introduction

Prostate cancer (PCa) is the most common and the second-most deadly cancer among men [1]. Most patients with metastatic prostate cancer eventually develop castration resistance and succumb to the disease [2,3]. Enzalutamide is an androgen receptor (AR) inhibitor that works by directly binding to AR on its ligand-binding domain and blocking AR activation and signaling, which is critical for the growth and survival of prostate cancer cells. By inhibiting AR signaling, enzalutamide can reduce tumor proliferation and progression. Treatment with enzalutamide has demonstrated to improve survival in advanced prostate cancer patients [4–6].

The prognosis of metastatic prostate cancer is highly variable, ranging from a few months to several years [7]. Several prognostic factors are available, and distinct prognostic models have been proposed, depending on the clinical scenario and treatment received.

The peripheral blood of patients with mCRPC can be informative of the prognosis of the disease, besides the identification of tumor components. This is due to a complex interplay between the tumor, the bone marrow, and the immune system of the host. Previous reports support the prognostic value of whole-blood RNA signatures [8,9], including genes involved in hematopoiesis and the immune system. In addition, the composition of blood according to the cell types available in the hemogram can also have a prognostic value, as is a high neutrophil-to-lymphocyte ratio [10–16]. Further understanding of the dynamic interplay between the cancer and the immune cells might provide crucial prognostic information concerning mCRPC.

Blood immune-cell composition includes more than 22 distinct cell populations that can be identified either by flow cytometry or recently by blood cell deconvolution using gene expression arrays. CIBERSORT-X is a machine learning deconvolution algorithm validated for blood immune cell analyses [17,18]. It offers technical advantages for sample analysis at central referral laboratories and provides a method that can be implemented in multicenter clinical trials.

In this study, we aimed to understand the contribution of distinct immune cell types to the prognosis of mCRPC patients. We analyzed prospectively collected pre-treatment blood samples from patients included in a phase 2 multicenter biomarker study investigating the use of enzalutamide as a first-line treatment in mCRPC. Results were further validated in an independent cohort of mCRPC patients.

2. Materials and Methods

2.1. Study Design and Conduct

The PREMIERE trial represented a multicenter, open-label, single-arm, phase 2 clinical trial (NCT02288936). Its purpose was to explore the use of enzalutamide as a first-line treatment option for metastatic castration-resistant prostate cancer (mCRPC). This study was approved by the Germans Trias i Pujol independent review board (IRB) in Spain (AC-14-112-R). A separate validation cohort was established at the Istituto Scientifico Romagnolo per lo Studio e la Cura dei Tumori (IRST) in Meldola, Italy, with approval from their IRB (REC 2192/2013). The PREMIERE trial constituted a cohort of 98 mCRPC patients, all of whom had not received prior chemotherapy treatments. These participants were recruited across 17 established hospitals within Spain. The selection criteria for patient inclusion incorporated individuals with histologically verified prostate adenocarcinoma, documented metastases, and tumor progression, alongside a serum testosterone level equal to or below 50 ng per deciliter, despite the continuation of androgen-deprivation therapy. In addition, the participants were required to have an Eastern Cooperative Oncology Group (ECOG) rating between 0 and 1 and display either for asymptomatic or for mildly symptomatic conditions (a Brief Pain Inventory Short Form question 3 score less than 4). Detailed outcomes, including primary and secondary findings, have been documented in earlier publications [19–22].

Additionally, a distinct validation cohort was obtained at the Istituto Scientifico Romagnolo per lo Studio e la Cura dei Tumori (IRST) in Meldola, Italy. This was conducted under the approved protocol REC 2192/2013 and comprised 54 mCRPC patients.

2.2. Sample Collection

Serial whole-blood samples from all participants were obtained using PAXgene®RNA Blood RNA tube (PreAnalytiX, Qiagen BD, Valencia, Spain). Samples were stored at -80°C until processing. Time points for whole blood sample collection included the following: before treatment, on-treatment at 12 weeks, and at tumor progression or end of treatment. For this study, we will focus on analyzing samples taken prior to the initiation of treatment.

2.3. RNA Extraction and Microarray Analysis

Whole-blood samples collected in PAXgene RNA tubes were subjected to isolation and purification following the manufacturer's prescribed protocol. Spectrophotometry and electrophoresis on a microfluidic solution with the NanoDrop 2000 (Thermo Scientific, Newark, DE, USA) and the Bioanalyzer 2100 (Agilent Technologies, Palo Alto, CA, USA), respectively, were utilized for RNA quantification and quality assessment. Only purified RNA samples with an RNA integration number (RIN) of seven or above were chosen for subsequent analyses. Complementary DNA (cDNA) was synthesized from 100 ng of each RNA sample using the WT PLUS Reagent Kit (Thermo Scientific, Newark, DE, USA), following the standard protocol. This cDNA was then amplified, fragmented, and labelled with biotin for hybridization.

For hybridization, the GeneChip™ Human Transcriptome Array HTA 2.0 (902162, Affymetrix, ThermoFisher, Newark, DE, USA) was incubated with 5.2 μg of single-strand DNA (ssDNA) over a period of 16 h. Any non-specific probes were then washed away, and the hybridized array was scanned using the GeneChip Scanner 3000 (Affymetrix, Thermo Scientific, Newark, DE, USA).

2.4. Gene Expression Analysis

Gene microarray analyses were derived after quality control, background correction, normalization, logarithmic conversion, and removal of batch effects processing using Transcriptome Analysis Console (TAC) software (version 4.0.1, Thermo, Newark, DE, USA). All samples that had not passed quality control were filtered out, and the resulting data were annotated and analyzed by R packages “affy”, “limma” and “pd.hta.2.0” [23–25]. Gene identification relied on the presence of a unique Symbol identifier, with duplicates removed to retain distinct isoforms. The complete dataset includes a comprehensive list of all recognized genes, which is available upon request.

The entire microarray datasets can be accessed through the Gene Expression Omnibus (GSE248619).

2.5. CTC and AR-V7 Analysis

The Circulating Tumor Cell (CTC) analyses were performed using the AdnaTest platform (Qiagen, Hilden, Germany), following the manufacturer’s instructions. Custom primers were used for the detection of AR-V7 mRNA. The accuracy of the PCR product was confirmed through Sanger sequencing.

2.6. Statistical Analysis

R software (version 4.4.0) was used for statistical analyses [26–28]. Survival analyses included Cox proportional hazards regression, log-rank, and the Kaplan–Meier method. Hazard ratios (HRs) were reported as relative risks with corresponding 95% confidence intervals (CIs). A two-sided $p < 0.05$ was considered statistically significant.

Survival curves were constructed to visualize the impact of various immune cell populations on patient outcomes. Patients were stratified into ‘high’ and ‘low’ groups, defined by whether their immune cell counts were above or below the median values, respectively. This method of stratification facilitates an unbiased comparison of survival outcomes across the groups.

Multivariable, Cox proportional hazards models were employed to evaluate the association between immune cell proportions and patient survival, adjusting for potential confounders such as the Eastern Cooperative Oncology Group (ECOG) performance status, pattern of spread, prostate-specific antigen (PSA) levels, alkaline phosphatase, lactate dehydrogenase (LDH), pain score, as measured by the Brief Pain Inventory, neutrophil-to-lymphocyte ratio, and corticosteroid usage. Adjustments were made to account for these variables, providing a comprehensive evaluation of their independent contributions to survival outcomes.

3. Results

3.1. Study Population

This study involved 152 chemotherapy-naïve participants diagnosed with mCRPC, with blood samples obtained before treatment with enzalutamide. The training cohort consisted of 98 patients participating in a phase 2 biomarker clinical trial. All patients had pre-treatment whole-blood samples available for analyses. Gene expression arrays were available from 95 patients. Three patients were excluded due to technical challenges stemming from poor-quality RNA (Figure 1). The patients’ characteristics for the training cohort are described in Table S1.

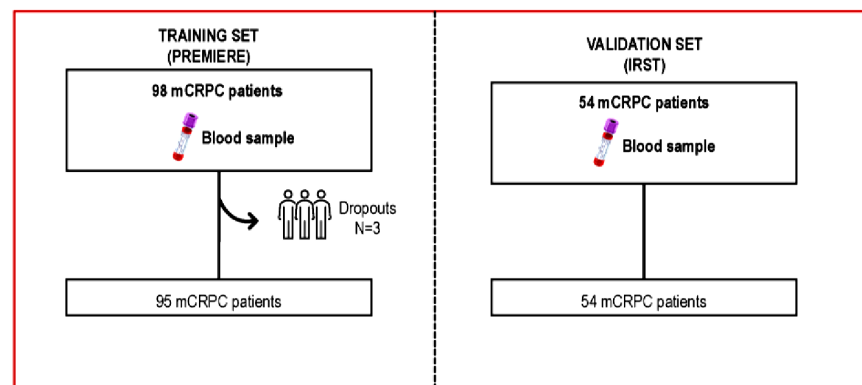


Figure 1. Consort diagram. This study analyzes pre-treatment whole blood samples from mCRPC patients prospectively treated with enzalutamide, including a training cohort comprised of 98 patients from a phase 2 biomarkers clinical trial, and an independent validation cohort including 54 patients.

3.2. Blood Immune-Cell Composition

The distribution of the blood immune cells within the training cohort is depicted in Figure 2 and further detailed in Table S2.

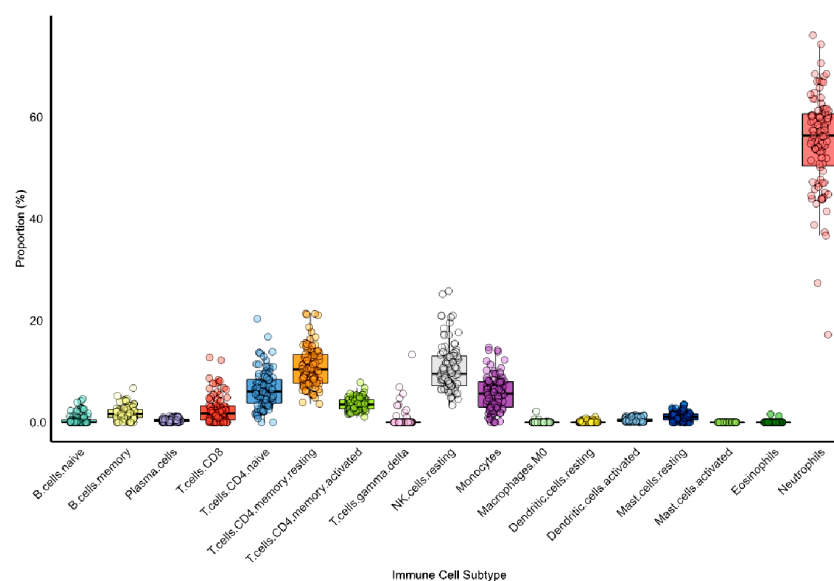


Figure 2. Blood immune-cell composition. The figure shows the relative proportion of immune cell components in the blood in the training set.

As expected, neutrophils represented the largest segment of immune cells. They were followed, in decreasing order, by resting NK cells, resting and both naïve and activated memory CD4 T-cells, monocytes, CD8 T-cells, memory B-cells, and resting mast cells. Other immune cells were present in a markedly smaller proportion.

3.3. Prognostic Significance of Individual Immune Cell Types

We used Cox-regression analyses to address the contribution of individual immune cell types to overall survival in the training cohort. The results are shown in Table 1. We observed that both an increase in monocytes ($p < 0.05$) and a decrease in CD8 T-Cell lymphocytes ($p < 0.01$) were associated with worse prognosis, after correcting for multiple testing. This prognostic significance remained consistent after stratification based on median values, as depicted in Figure S1. Specifically, patients with high-monocytes (median 32.2 months vs. 40.3 months; HR 1.96, 95%, CI 1.11–3.45) and those with low-CD8

T cells (median 31.8 months vs. 40.3 months; HR 0.51, 95% CI 0.29–0.9) were associated with worse survival (Figure 3A,B), respectively.

Table 1. Survival analyses by blood immune cell type. Cox-regression survival analyses was conducted for each individual immune cell population.

Blood Immune Cell Type	HR (95% CI)	<i>p</i> Value
Memory B cells	1.21 (0.69–2.12)	0.506
Plasma cells	1.32 (0.76–2.31)	0.323
T cells CD8	0.51 (0.29–0.9)	0.018
T cells CD4-naïve	1.11 (0.64–1.94)	0.71
T cells CD4 memory, resting	0.72 (0.41–1.26)	0.252
T cells CD4 memory, activated	0.87 (0.50–1.51)	0.617
NK cells, resting	0.92 (0.53–1.61)	0.78
Monocytes	1.96 (1.11–3.45)	0.019
Dendritic cells, activated	1.65 (0.94–2.89)	0.081
Mast cells, resting	0.92 (0.53–1.61)	0.775
Neutrophils	0.98 (0.56–1.71)	0.935

Abbreviations: HR = hazard ratio. CI = confidence interval. HR compares high versus low values, according to the median. *p* values < 0.05 are considered statistically significant. The following cell types were below the quantifiable limit of detection, and survival analyses are not shown: follicular helper T cells, regulatory T cells (Tregs), gamma delta T cells, activated NK cells, naïve B cells, macrophages M0, macrophages M1, macrophages M2, resting dendritic cells, activated mast cells, and eosinophils.

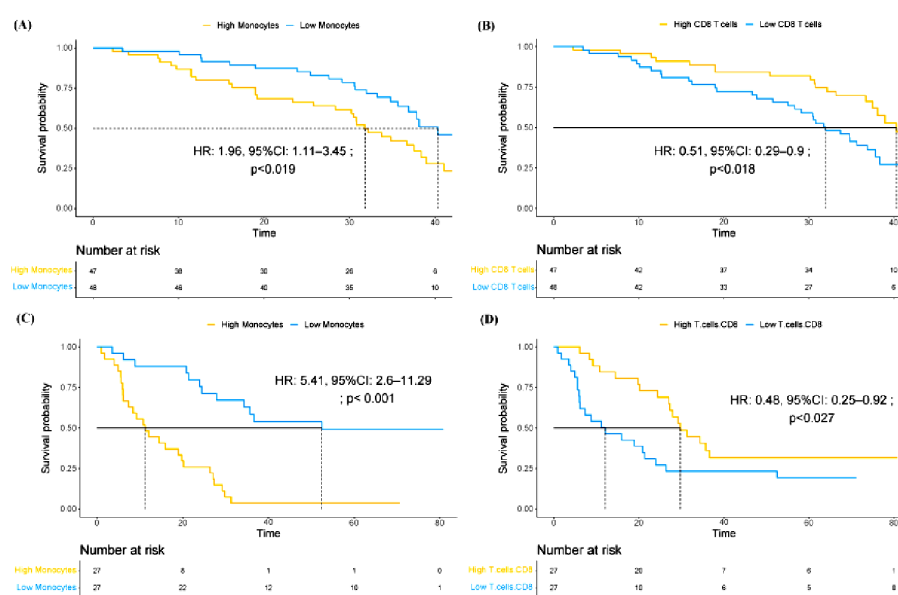


Figure 3. Overall survival analysis in PREMIERE and IRST validation cohorts. Kaplan–Meier survival curves and Cox proportional hazards regression analyses showing the impact of immune cell levels on patient survival in the PREMIERE (A,B) and IRST validation (C,D) cohorts. (A) Survival based on monocyte counts in PREMIERE cohort. (B) Survival based on CD8 T-cell levels in PREMIERE cohort. (C) Survival based on monocyte counts in IRST validation cohort. (D) Survival based on CD8 T-cell levels in IRST validation cohort. Time is expressed in months. Curves show survival probabilities for groups with varying immune cell levels. Numbers below each graph indicate patients at risk at specific time points. Hazard ratios (HR), 95% confidence intervals (CI), and *p*-values from Cox regression analyses are provided for each comparison.

These results were validated in an independent cohort (Table S3), reproducing the adverse prognosis associated with the presence of high monocyte levels (HR 5.41, 95% CI 2.60–11.3) and a low CD8 T-cell proportion (HR 0.48, 95% CI 0.25–0.92) (Figure 3C,D), respectively.

We then analyzed the contribution of monocytes and CD8 T-lymphocytes to other well-established prognostic variables, including ECOG, pattern of spread, PSA, alkaline phosphatase, LDH, pain score, neutrophil-to-lymphocyte ratio, and use of corticoids. This multivariable analysis is shown in Table 2.

Table 2. Multivariable analysis including clinical and molecular variables.

Prognostic	HR (95% CI)	<i>p</i> Value
ALP_Mod	1.84 (0.99–3.342)	0.055
LDH_Mod	1.91 (1.02–3.60)	0.045
Pattern Of Spread	1.08 (0.24–4.82)	0.922
NLR	0.70 (0.36–1.34)	0.279
BPI	0.59 (0.30–1.14)	0.117
LogPSA	1.44 (1.18–1.76)	0.001
Monocytes	1.05 (0.74–1.49)	0.770
CD8 T cells	0.63 (0.41–0.98)	0.04
ECOG	1.33 (0.71–2.50)	0.371

Abbreviations: ALP = alkaline phosphatase; LDH = lactate dehydrogenase; NLR = neutrophil-to-lymphocyte ratio; ECOG = Eastern Cooperative Oncology Group; BPI: Brief Pain Inventory; CI = confidence interval; HR = hazard ratio. *p* value was calculated using Cox regression.

The CD8 T-cell prognostic value was also independent of known molecular variables such as AR gain or the presence of CTCs. The data are shown in Table 3. The CD8 T cells retained their independent prognostic association with survival, reinforcing their pivotal role as a prognostic factor.

Table 3. Multivariable analysis including ARgain and CTCs.

	HR (95% CI)	<i>p</i> Value
T cells CD8	0.54 (0.35–0.83)	0.006
ARgain	6.17 (2.83–13.46)	<0.001
CTCs	4.63 (2.58–8.31)	<0.001

Abbreviations: AR = androgen receptor; CTC = circulating tumor cells.

4. Discussion

This is the first study to demonstrate that the proportion of blood monocytes and CD8 T cells are prognostic in mCRPC patients. We studied twenty-two blood immune cell types in pre-treatment samples from mCRPC patients included in a multicenter phase 2 biomarker clinical trial using enzalutamide. Our observations revealed that the presence of high monocytes and low CD8 T cells was associated with worse survival. These results were validated in an independent cohort of mCRPC patients. Low CD8 T cells retained independent prognostic significance when included in a validated clinical prognostic model. These results confirm the feasibility of analyzing the immune cell components in a central laboratory in samples obtained from patients participating in a multicenter clinical trial. These results could be valuable for patient stratification in future studies, in particular for clinical trials involving immune cell-activating agents.

The blood of patients with mCRPC has been previously demonstrated to be informative of the prognosis of the disease, besides the presence of tumor components. These studies include gene expression analyses [8,9] and the relative proportion of cells obtained from the hemogram, in particular the neutrophil-to-lymphocyte ratio (NLR) [10–16]. Gene expression analyses in whole blood have demonstrated prognostic significance in advanced prostate cancer. Interestingly, Olmos et al. [9] developed a nine-gene signature associated

with T-cell immune response, and Ross et al. [8] developed a six-gene expression signature, including genes related to the regulation of the cellular immunity and monocyte differentiation. However, this is the first study to evaluate the contribution of twenty-two distinct blood immune cell components that are not routinely provided in the hemogram.

We assessed the blood immune-cell composition using CIBERSORT, a machine learning computational method for characterizing the cell composition of complex tissues obtained from gene expression arrays. It has been demonstrated to accurately quantify the immune-cell constituents of blood samples [17,18,29], and it accurately correlates with flow cytometry techniques to enumerate the phenotypic repertoire of the twenty-two immune-cell subsets included for the analyses [29]. It constitutes a validated method that can substitute flow cytometry for the assessment of immune blood cell components, a technique difficult to implement for central evaluation in multicenter clinical trials.

Several prognostic models are currently available in mCRPC, based on the clinical scenario and treatment of choice. A model was developed for chemotherapy-naïve mCRPC patients treated with enzalutamide based on the clinical data obtained from the PREVAIL clinical trial, a pivotal phase 3 trial for this indication, and the scenario and treatments used in our study. We have recently updated this prognostic model to include molecular variables such as the presence of circulating tumor cells (CTCs) and the amplification of the androgen receptor (AR) in circulating plasma DNA [22]. We addressed the independent prognostic value of these cell components relative to the validated clinical models using a multivariable analysis and demonstrated that the CD8 T-cell lymphocyte proportion remained independently prognostic. Intriguingly, the NLR was not prognostic in our series, probably because most patients had a low NLR, associated with the predominance in our study of patients with low tumor burden.

Testosterone is known to act as an immune-suppressor, affecting T-cell function and blocking IFN γ production [30]. Tumors with greater response to anti-androgen therapy are associated with increased proportion of tumor-associated CD8 T cells in the tumor microenvironment [31]. Enzalutamide is an antiandrogen therapy that has demonstrated to increase PD-L1 [32] and tumor immune-cell infiltration. On the contrary, castration-resistant tumors' progression on enzalutamide is associated with an immunosuppressive microenvironment [33]. In our study, we observed that in patients progressing on androgen-deprivation therapy, the presence of higher levels of CD8 T cells in blood is associated with improved prognosis in a series of patients treated with enzalutamide. This improved prognosis might be related to an increased immune activation that could contribute to the increased prognosis observed.

Several factors, including steroid treatments, could influence the blood immune cell components and could act as confounding factors on the prognosis. In particular, steroid treatment is associated with increased neutrophil counts and decreased lymphocyte counts [34]. We noted that a small subgroup of our patients were receiving low-dose steroids at baseline, including six patients receiving low-dose prednisone (≤ 10 mg). In order to exclude a confounding effect of steroids on the prognostic value of these immune-cell components, we included the use of steroids in a comprehensive multivariable analysis comprising the accepted clinical and laboratory variables, in addition to the prognostic immune cell components. The use of steroids did not modify the prognostic value for CD8 T cells nor for monocytes, and steroids lacked prognostic significance. Therefore, we can conclude that the minority of patients receiving low-dose steroids did not affect the results reported on the prognostic value of these immune cell components (Table S4).

Immune-cell composition assessment using CIBERSORT, similar to all gene expression-based methods, can be limited by the fidelity of the reference profiles, which can be deviated under particular conditions. In addition, some cell types can be systematically over- or under-estimated, an effect that can be limited by inter-group relative comparisons. However, it is a validated method for the assessment and monitoring of the immune-cell population in complex tissues such as the blood. Another limitation of this study is related to the inclusion of patients with asymptomatic or mildly symptomatic chemo-naïve

mCRPC. Despite the fact that this is the most frequent scenario in the clinic, it would also be interesting to address the immune components in the blood of patients with other clinical characteristics, including patients with pain and with aggressive or neuroendocrine features of the disease, and on treatment with other approved agents in this scenario, including other androgen receptor pathway inhibitors (ARPIs), docetaxel, Radium-223, or ¹⁷⁷Lu-PSMA.

Our study is unable to address the predictive value of CD8 T cells and monocytes in mCRPC. This question could be assessed in patients participating in a randomized trial preferentially including immunotherapy. A fine dynamic assessment of the blood immune components during treatment could be key to understanding the systemic effects of the prostate cancer treatments, including hormonal agents and the immune-checkpoint inhibitors, among others. This understating is going to be essential to move forward immunotherapy in prostate cancer.

5. Conclusions

In conclusion, this study highlights the contribution of blood CD8 T cells and monocytes to the prognosis of patients with mCRPC treated with new hormonal agents. Further understanding of the complex interplay between the immune system, prostate cancer, and the treatments is necessary to design more effective immunotherapies.

Supplementary Materials: The following supporting information can be downloaded at: <https://www.mdpi.com/article/10.3390/cancers16142535/s1>, Figure S1: Kaplan–Meier Estimator for different types of immune cells; Table S1: Patients' characteristics. Characteristics of patients included in the PREMIERE clinical trial; Table S2: Blood immune-cell composition from CIBERSORTx; Table S3: Survival analyses by blood immune cell type in validation dataset. Cox regression survival analyses were conducted for each individual immune cell population; Table S4: Multivariable analysis including steroids treatment and molecular variables.

Author Contributions: Conceptualization, E.P.-N., V.C., D.C., G.A., E.G. (Enrique Gallardo), U.D.G. and E.G.-B.; methodology, E.P.-N., V.C., P.C., D.C., G.A., E.G. (Enrique Grande), U.D.G. and E.G.-B.; software, E.P.-N., E.G.-B., J.A.B. and J.P.-M.; validation, E.P.-N., V.C., U.D.G., E.G.-B. and J.M.F.; formal analysis, E.P.-N. and E.G.-B.; investigation, E.P.-N., V.C., U.D.G. and E.G.-B.; resources, E.P.-N., V.C., M.P.F.-P., D.C., U.D.G., E.G.-B., T.A.G., A.F., S.V.-E., A.G.-d.-A., D.W., B.M., O.F.-C., M.J.M.-V., M.A.C., I.D., E.G. (Enrique Grande), A.R.S., C.S., M.I.S., J.P., J.T., M.J.L.-A. and A.R.; data curation, E.P.-N. and E.G.-B.; writing—original draft preparation, E.P.-N., E.G.-B., J.M.F., J.I.D., C.M. and M.M.-S.; writing—review and editing, E.P.-N., E.G.-B., J.M.F., J.I.D., C.M. and M.M.-S.; visualization, E.P.-N., E.G.-B., J.M.F., J.I.D. and M.M.-S.; supervision, E.G.-B.; project administration, E.G.-B.; funding acquisition, E.G. (Enrique Grande) and E.G.-B. All authors have read and agreed to the published version of the manuscript.

Funding: This trial was promoted by SOGUG and received a grant from Astellas. EGB received a travel grant (BA16/00038) and funding support from the “Instituto de Salud Carlos III” (FI19/00079), as well as support from the SEOM-CRIS cancer foundation. The laboratory led by Dr. Enrique González Billalabeitia has the support of the FERRO Foundation (<https://ferro.org/en/>, accessed on 13 June 2022).

Institutional Review Board Statement: This study was conducted in accordance with the ethical principles outlined in the Declaration of Helsinki. The PREMIERE trial received approval from the IRB of Germans Trias i Pujol (AC-14-112-R) in Spain. The validation cohort study at the Istituto Scientifico Romagnolo per lo Studio e la Cura dei Tumori (IRST) in Meldola, Italy, was approved by their IRB (REC 2192/2013). Patient information and biological samples for both cohorts were managed in alignment with data protection laws and regulations.

Informed Consent Statement: Written informed consent was obtained from all patients.

Data Availability Statement: The datasets generated and/or analyzed during the current study include gene expression data that have been deposited in the Gene Expression Omnibus (GEO) under the accession number GSE248619. For additional data not publicly available, access can be provided by the corresponding author, EGB, on reasonable request.

Acknowledgments: We would like to acknowledge all the staff at SOGUG for their support to run the PREMIERE trial, Astellas for supporting this research, and ISCIII from the Spanish Ministry of Health and Cris Cancer Foundation for their support. We want to particularly acknowledge the patients, as well as the Biobank IMIB (PT23/00026) integrated in the Platform ISCIII Biomodels and Biobanks, for their collaboration.

Conflicts of Interest: V.C. has served as a consultant/advisory board member for Janssen, Astellas, Merck, AstraZeneca, Amgen, Bayer, Novartis, Ipsen, Eisai, and Recordati and has received speaker honoraria or travel support from Astellas, Janssen, Ipsen, Bayer, Gilead, and BristolMyers Squibb. T.G. has received travel grants from Sanofi and participated in advisory boards for Sanofi, Janssen, Astellas, and Bayer. A.F. has received travel grants from Astellas, Astra-Zeneca, Sanofi and participated in advisory boards for Janssen, Sanofi, Eisai, and Bayer. S.V.-E. has received travel grants from Astellas, Janssen, and Bayer and has participated in advisory boards for Janssen, Astellas, Sanofi, and Bayer. A.G.-d.A. has received research funding from Astellas, A; travel grants from Astellas, Jansen, Sanofi, BMS, Roche, Pfizer, MSD, AZ, and Ipsen; and honoraria for speaker engagements, advisory boards, and continuous medical education from Janssen, Astellas, Sanofi, Bayer, Roche, Ipsen, BMS, MSD, Pfizer, Eusa Pharma, Eisai, Casen Recordati, AAA, Novartis, and AstraZeneca. I.D. has received travel grants and research funding from Astellas and has participated in advisory boards for Astellas, Janssen, Sanofi, and Bayer. E.G. has received travel grants from Astellas, Janssen, Sanofi, Bayer, Roche, BMS, and Eisai; honoraria for speaking engagements for Astellas, Janssen, Sanofi, Bayer, Pfizer, Roche, BMS, Novartis, Rovi, Daiichi Sankyo, Leo Pharma, Menarini, Eisai, MSD, Boehringer Ingelheim, Merck, and EUSA Pharma; and participated in advisory boards for Astellas, Janssen, Sanofi, Bayer, Pfizer, Roche, Novartis, Eisai, EUSA Pharma, BMS, AstraZeneca, Merck, Rovi, Daiichi Sankyo, and Techdow. E.G. has received travel grants from Astellas, Janssen, Sanofi, Bayer, Roche, BMS, and Eisai; honoraria for speaking engagements for Astellas, Janssen, Sanofi, Bayer, Pfizer, Roche, BMS, Novartis, Rovi, Daiichi Sankyo, Leo Pharma, Menarini, Eisai, MSD, Boehringer Ingelheim, Merck, and EUSA Pharma; and participated in advisory boards for Astellas, Janssen, Sanofi, Bayer, Pfizer, Roche, Novartis, Eisai, EUSA Pharma, BMS, AstraZeneca, Merck, Rovi, Daiichi Sankyo, and Techdow. J.P. has received research funding from Astellas and Roche and honoraria for speaker engagements, advisory roles, or continuous medical education from Astellas, AstraZeneca, Janssen, MSD, Bayer, Pfizer, Eisai, Ipsen, Sanofi, Roche, BMS, and Merck. BM has served in an advisory role for Roche, Sanofi, Janssen, Astellas, Pfizer, Novartis, Bristol-Myers Squibb, and Ipsen; received research funding from Roche, Bayer, and Janssen; and accommodation expenses from Pfizer and Janssen. M.A.C. has received travel grants from Astellas, Jansen, Sanofi, Pfizer, Roche, and Ipsen; and honoraria for speaker engagements, advisory boards, and continuous medical education from Janssen, Astellas, Sanofi, Bayer, Roche, Ipsen, BMS, MSD, Pfizer, and AstraZeneca. M.J.M.-V. has received travel grants from Astellas and Janssen and has participated in advisory boards for Janssen, Astellas, Sanofi, and Bayer. M.I.S. has received travel grants from Sanofi and Roche and participated in advisory boards for Sanofi, Ipsen, and Astellas. D.C. has received research funding from Astellas, educational grants from Pfizer and Janssen, travel grants from Pfizer and BMS, and has participated in advisory boards for Pfizer, Astellas, Janssen, Sanofi, Bayer, and Roche. Gerard Attard reported receiving grants, personal fees, nonfinancial support, and speaker fees from Janssen, Astellas, and Sanofi; personal fees, nonfinancial support, and speaker fees from AstraZeneca; and personal fees from Novartis and Bayer outside the submitted work; in addition, GA reported having a patent (GB1915469.9; blood signatures for prostate cancer detection) pending and is on the Institute of Cancer Research list of rewards to inventors for abiraterone acetate. E.G. has received research funding from Astellas, AstraZeneca, IPSEN, Pfizer, and Roche and has participated in advisory boards for Adacap, AMGEN, Angelini, Astellas, AstraZeneca, Bayer, Blueprint, Bristol Myers Squibb, Caris Life Sciences, Celgene, Clovis-Oncology, Eisai, Eusa Pharma, Genetracer, Guardant Health, HRA-Pharma, IPSEN, ITM-Radiopharma, Janssen, Lexicon, Lilly, Merck KGaA, MSD, Nanostring Technologies, Natera, Novartis, ONCODNA (Biosequence), Palex, Pharmamar, Pierre Fabre, Pfizer, Roche, Sanofi-Genzyme, Servier, Taiho, Thermo Fisher Scientific. UDeG reports serving as a consultant for Janssen, Astellas Pharma Inc., Sanofi, Bayer, Pfizer Inc., Bristol Myers Squibb, Novartis, Ipsen, and Merck Sharp & Dohme. E.G.-B. has received research grants from MSD and AstraZeneca; travel grants from Astellas, Janssen, and Sanofi; and has participated in advisory boards for Astellas, Janssen, Sanofi, Astra-Zeneca, and Bayer.

References

1. Siegel, R.L.; Giaquinto, A.N.; Jemal, A. Cancer Statistics, 2024. *CA Cancer J. Clin.* **2024**, *74*, 12–49. [\[CrossRef\]](#) [\[PubMed\]](#)
2. Shelley, M.; Harrison, C.; Coles, B.; Staffurth, J.; Wilt, T.J.; Mason, M.D. Chemotherapy for Hormone-Refractory Prostate Cancer. *Cochrane Database Syst. Rev.* **2006**, CD005247. [\[CrossRef\]](#) [\[PubMed\]](#)
3. Sartor, A.O. Progression of Metastatic Castrate-Resistant Prostate Cancer: Impact of Therapeutic Intervention in the Post-Docetaxel Space. *J. Hematol. Oncol.* **2011**, *4*, 18. [\[CrossRef\]](#) [\[PubMed\]](#)
4. Scher, H.I.; Fizazi, K.; Saad, F.; Taplin, M.-E.; Sternberg, C.N.; Miller, K.; de Wit, R.; Mulders, P.; Chi, K.N.; Shore, N.D.; et al. Increased Survival with Enzalutamide in Prostate Cancer after Chemotherapy. *N. Engl. J. Med.* **2012**, *367*, 1187–1197. [\[CrossRef\]](#) [\[PubMed\]](#)
5. Davis, I.D.; Martin, A.J.; Stockler, M.R.; Begbie, S.; Chi, K.N.; Chowdhury, S.; Coskinas, X.; Frydenberg, M.; Hague, W.E.; Horvath, L.G.; et al. Enzalutamide with Standard First-Line Therapy in Metastatic Prostate Cancer. *N. Engl. J. Med.* **2019**, *381*, 121–131. [\[CrossRef\]](#) [\[PubMed\]](#)
6. Beer, T.M.; Armstrong, A.J.; Rathkopf, D.E.; Loriot, Y.; Sternberg, C.N.; Higano, C.S.; Iversen, P.; Bhattacharya, S.; Carles, J.; Chowdhury, S.; et al. Enzalutamide in Metastatic Prostate Cancer before Chemotherapy. *N. Engl. J. Med.* **2014**, *371*, 424–433. [\[CrossRef\]](#) [\[PubMed\]](#)
7. Kirby, M.; Hirst, C.; Crawford, E.D. Characterising the Castration-Resistant Prostate Cancer Population: A Systematic Review. *Int. J. Clin. Pract.* **2011**, *65*, 1180–1192. [\[CrossRef\]](#) [\[PubMed\]](#)
8. Ross, R.W.; Galsky, M.D.; Scher, H.I.; Magidson, J.; Magidson, K.; Lee, G.S.M.; Katz, L.; Subudhi, S.K.; Anand, A.; Fleisher, M.; et al. A Whole-Blood RNA Transcript-Based Prognostic Model in Men with Castration-Resistant Prostate Cancer: A Prospective Study. *Lancet Oncol.* **2012**, *13*, 1105–1113. [\[CrossRef\]](#) [\[PubMed\]](#)
9. Olmos, D.; Brewer, D.; Clark, J.; Danila, D.C.; Parker, C.; Attard, G.; Fleisher, M.; Reid, A.H.M.; Castro, E.; Sandhu, S.K.; et al. Prognostic Value of Blood mRNA Expression Signatures in Castration-Resistant Prostate Cancer: A Prospective, Two-Stage Study. *Lancet Oncol.* **2012**, *13*, 1114–1124. [\[CrossRef\]](#)
10. Kawahara, T.; Kato, M.; Tabata, K.; Kojima, I.; Yamada, H.; Kamihira, O.; Tsumura, H.; Iwamura, M.; Uemura, H.; Miyoshi, Y. A High Neutrophil-to-Lymphocyte Ratio Is a Poor Prognostic Factor for Castration-Resistant Prostate Cancer Patients Who Undergo Abiraterone Acetate or Enzalutamide Treatment. *BMC Cancer* **2020**, *20*, 919. [\[CrossRef\]](#)
11. Neuburger, M.; Weiß, C.; Goly, N.; Skladny, J.; Nitschke, K.; Wessels, F.; Kowalewski, K.F.; Waldbillig, F.; Hartung, F.; Nientiedt, M.; et al. Changes in Neutrophil-to-Lymphocyte Ratio as Predictive and Prognostic Biomarker in Metastatic Prostate Cancer Treated with Taxane-Based Chemotherapy. *Discover. Oncol.* **2022**, *13*, 140. [\[CrossRef\]](#) [\[PubMed\]](#)
12. Langsenlehner, T.; Thurner, E.M.; Krenn-Pilko, S.; Langsenlehner, U.; Stojakovic, T.; Gerger, A.; Pichler, M. Validation of the Neutrophil-to-Lymphocyte Ratio as a Prognostic Factor in a Cohort of European Prostate Cancer Patients. *World J. Urol.* **2015**, *33*, 1661–1667. [\[CrossRef\]](#) [\[PubMed\]](#)
13. Boegemann, M.; Schlack, K.; Thomes, S.; Steinestel, J.; Rahbar, K.; Semjonow, A.; Schrader, A.J.; Aringer, M.; Krabbe, L.M. The Role of the Neutrophil to Lymphocyte Ratio for Survival Outcomes in Patients with Metastatic Castration-Resistant Prostate Cancer Treated with Abiraterone. *Int. J. Mol. Sci.* **2017**, *18*, 380. [\[CrossRef\]](#)
14. Van Soest, R.J.; Templeton, A.J.; Vera-Badillo, F.E.; Mercier, F.; Sonpavde, G.; Amir, E.; Tombal, B.; Rosenthal, M.; Eisenberger, M.A.; Tannock, I.F.; et al. Neutrophil-to-Lymphocyte Ratio as a Prognostic Biomarker for Men with Metastatic Castration-Resistant Prostate Cancer Receiving First-Line Chemotherapy: Data from Two Randomized Phase III Trials. *Ann. Oncol.* **2015**, *26*, 743–749. [\[CrossRef\]](#) [\[PubMed\]](#)
15. Lorente, D.; Mateo, J.; Templeton, A.J.; Zafeiriou, Z.; Bianchini, D.; Ferraldeschi, R.; Bahl, A.; Shen, L.; Su, Z.; Sartor, O.; et al. Baseline Neutrophil-Lymphocyte Ratio (NLR) Is Associated with Survival and Response to Treatment with Second-Line Chemotherapy for Advanced Prostate Cancer Independent of Baseline Steroid Use. *Ann. Oncol.* **2015**, *26*, 750–755. [\[CrossRef\]](#)
16. Leibowitz-Amit, R.; Templeton, A.J.; Omlin, A.; Pezaro, C.; Atenafu, E.G.; Keizman, D.; Vera-Badillo, F.; Seah, J.A.; Attard, G.; Knox, J.J.; et al. Clinical Variables Associated with PSA Response to Abiraterone Acetate in Patients with Metastatic Castration-Resistant Prostate Cancer. *Ann. Oncol.* **2014**, *25*, 657–662. [\[CrossRef\]](#)
17. Chen, B.; Khodadoust, M.S.; Liu, C.L.; Newman, A.M.; Alizadeh, A.A. Profiling Tumor Infiltrating Immune Cells with CIBERSORT. In *Methods in Molecular Biology*; Humana Press Inc.: Totowa, NJ, USA, 2018; Volume 1711, pp. 243–259.
18. Steen, C.B.; Liu, C.L.; Alizadeh, A.A.; Newman, A.M. Profiling Cell Type Abundance and Expression in Bulk Tissues with CIBERSORTx. In *Methods in Molecular Biology*; NIH Public Access: Milwaukee, WI, USA, 2020; Volume 2117, pp. 135–157.
19. Conteduca, V.; Wetterskog, D.; Sharabiani, M.T.A.A.; Grande, E.; Fernandez-Perez, M.P.; Jayaram, A.; Salvi, S.; Castellano, D.; Romanel, A.; Lolli, C.; et al. Androgen Receptor Gene Status in Plasma DNA Associates with Worse Outcome on Enzalutamide or Abiraterone for Castration-Resistant Prostate Cancer: A Multi-Institution Correlative Biomarker Study. *Ann. Oncol.* **2017**, *28*, 1508–1516. [\[CrossRef\]](#)
20. Jayaram, A.; Wingate, A.; Wetterskog, D.; Conteduca, V.; Khalaf, D.; Sharabiani, M.T.A.A.; Calabrò, F.; Barwell, L.; Feyerabend, S.; Grande, E.; et al. Plasma Androgen Receptor Copy Number Status at Emergence of Metastatic Castration-Resistant Prostate Cancer: A Pooled Multicohort Analysis. *JCO Precis. Oncol.* **2019**, *3*, 1–13. [\[CrossRef\]](#)
21. Wu, A.; Cremaschi, P.; Wetterskog, D.; Conteduca, V.; Franceschini, G.M.; Klefogiannis, D.; Jayaram, A.; Sandhu, S.; Wong, S.Q.; Benelli, M.; et al. Genome-Wide Plasma DNA Methylation Features of Metastatic Prostate Cancer. *J. Clin. Investig.* **2020**, *130*, 1991–2000. [\[CrossRef\]](#)

22. Fernandez-Perez, M.P.; Perez-Navarro, E.; Alonso-Gordoa, T.; Conteduca, V.; Font, A.; Vázquez-Estévez, S.; González-del-Alba, A.; Wetterskog, D.; Antonarakis, E.S.; Mellado, B.; et al. A Correlative Biomarker Study and Integrative Prognostic Model in Chemotherapy-Naïve Metastatic Castration-Resistant Prostate Cancer Treated with Enzalutamide. *Prostate* **2023**, *83*, 376–384. [CrossRef]
23. James, W. *MacDonald Pd.Hta.2.0: Platform Design Info for Affymetrix HTA-2_0*, R Package Version 3.12.2; 2017. Available online: <https://www.bioconductor.org/packages/release/data/annotation/html/pd.hta.2.0.html> (accessed on 16 June 2024).
24. Ritchie, M.E.; Phipson, B.; Wu, D.; Hu, Y.; Law, C.W.; Shi, W.; Smyth, G.K. Limma Powers Differential Expression Analyses for RNA-Sequencing and Microarray Studies. *Nucleic Acids Res.* **2015**, *43*, e47. [CrossRef] [PubMed]
25. Gautier, L.; Cope, L.; Bolstad, B.M.; Irizarry, R.A. Affy—Analysis of Affymetrix GeneChip Data at the Probe Level. *Bioinformatics* **2004**, *20*, 307–315. [CrossRef]
26. Therneau, T.M. *A Package for Survival Analysis in R version 4.4.0*; 2021. Available online: <https://mirrors.sustech.edu.cn/CRAN/web/packages/survival/vignettes/survival.pdf> (accessed on 16 June 2024).
27. Therneau, T.M.; Grambsch, P.M. *Modeling Survival Data: Extending the Cox Model*; Springer: New York, NY, USA, 2000; ISBN 0-387-98784-3.
28. Dexter, T.A. R: A Language and Environment for Statistical Computing. *Quat. Res.* **2014**, *81*, 114–124. [CrossRef]
29. Newman, A.M.; Liu, C.L.; Green, M.R.; Gentles, A.J.; Feng, W.; Xu, Y.; Hoang, C.D.; Diehn, M.; Alizadeh, A.A. Robust Enumeration of Cell Subsets from Tissue Expression Profiles. *Nat. Methods* **2015**, *12*, 453–457. [CrossRef] [PubMed]
30. Kissick, H.T.; Sanda, M.G.; Dunn, L.K.; Pellegrini, K.L.; On, S.T.; Noel, J.K.; Arredouani, M.S. Androgens Alter T-Cell Immunity by Inhibiting T-Helper 1 Differentiation. *Proc. Natl. Acad. Sci. USA* **2014**, *111*, 9887–9892. [CrossRef] [PubMed]
31. Guan, X.; Polesso, F.; Wang, C.; Sehrawat, A.; Hawkins, R.M.; Murray, S.E.; Thomas, G.V.; Caruso, B.; Thompson, R.F.; Wood, M.A.; et al. Androgen Receptor Activity in T Cells Limits Checkpoint Blockade Efficacy. *Nature* **2022**, *606*, 791–796. [CrossRef] [PubMed]
32. Bishop, J.L.; Sio, A.; Angeles, A.; Roberts, M.E.; Azad, A.A.; Chi, K.N.; Zoubeidi, A. PD-L1 Is Highly Expressed in Enzalutamide Resistant Prostate Cancer. *Oncotarget* **2015**, *6*, 234–242. [CrossRef] [PubMed]
33. Xu, P.; Yang, J.C.; Chen, B.; Nip, C.; Van Dyke, J.E.; Zhang, X.; Chen, H.W.; Evans, C.P.; Murphy, W.J.; Liu, C. Androgen Receptor Blockade Resistance with Enzalutamide in Prostate Cancer Results in Immunosuppressive Alterations in the Tumor Immune Microenvironment. *J. Immunother. Cancer* **2023**, *11*, e006581. [CrossRef]
34. Coutinho, A.E.; Chapman, K.E. The Anti-Inflammatory and Immunosuppressive Effects of Glucocorticoids, Recent Developments and Mechanistic Insights. *Mol. Cell. Endocrinol.* **2011**, *335*, 2–13. [CrossRef]

Disclaimer/Publisher’s Note: The statements, opinions and data contained in all publications are solely those of the individual author(s) and contributor(s) and not of MDPI and/or the editor(s). MDPI and/or the editor(s) disclaim responsibility for any injury to people or property resulting from any ideas, methods, instructions or products referred to in the content.

Acknowledgement of receipt

We hereby acknowledge receipt of your request for grant of a European patent as follows:

Submission number	300549454	
Application number	EP25382005.4	
File No. to be used for priority declarations	EP25382005	
Date of receipt	07 January 2025	
Your reference	909 356	
Applicant	FUNDACIÓN PARA LA INVESTIGACIÓN BIOMÉDICA DEL HOSPITAL UNIVERSITARIO 12 DE OCTUBRE	
Country	ES	
Title	Method for Predicting Progression of Prostate Cancer	
Documents submitted	package-data.xml application-body.xml OLF-ARCHIVE.zip\909 356 Text.zip SPECEPO-2.pdf\908 356 - Claims.pdf (4 p.) SPECEPO-4.pdf\908 356 - Figures.pdf (1 p.)	ep-request.xml ep-request.pdf (5 p.) SPECEPO-1.pdf\908 356 - Abstract.pdf (1 p.) SPECEPO-3.pdf\908 356 - Description.pdf (26 p.) f1002-1.pdf (2 p.)
Submitted by	CN=FUSTER OLAGUIBEL GUSTAVO NICOLAS - 33530042K,SN=FUSTER OLAGUIBEL,givenName=GUSTAVO NICOLAS,serialNumber=IDCES-33530042K,C=ES	
Method of submission	Online	
Date and time receipt generated	07 January 2025, 12:02:41 (CET)	

Official Digest of
Submission

D8:7D:37:F0:88:48:5D:79:7F:70:29:93:1D:A5:EE:6F:20:B7:4B:4A

/Madrid, Oficina Receptora/



Request for grant of a European patent

For official use only		
1 Application number:	<input type="text" value="MKEY"/>	
2 Date of receipt (Rule 35(2) EPC):	<input type="text" value="DREC"/>	
3 Date of receipt at EPO (Rule 35(4) EPC):	<input type="text" value="RENA"/>	
4 Date of filing:		

- 5 Grant of European patent, and examination of the application under Article 94, are hereby requested. ☒

Request for examination in an admissible non-EPO language:

Se solicita el examen de la solicitud según el artículo 94.

- 5.1 The applicant waives his right to be asked whether he wishes to proceed further with the application (Rule 70(2)) ☐

Procedural language:

en

Filing Language:

en

- 6 Applicant's or representative's reference

909 356

Filing Office:

ES

Applicant 1

- 7-1 Name:

FUNDACIÓN PARA LA INVESTIGACIÓN
BIOMÉDICA DEL HOSPITAL UNIVERSITARIO
12 DE OCTUBRE

- 8-1 Address:

Avda de Córdoba s/n, Hospital Universitario 12
de Octubre centro de Actividades Ambulatorias 6ª
planta, Bloque D
28041 Madrid
Spain

- 10-1 State of residence or of principal place of business:

Spain

Applicant 2

- 7-2 Name:

Universidad de Murcia

- 8-2 Address:

Avda. Teniente Flomesta 5
30003 Murcia
Spain

10-1 State of residence or of principal place of business: Spain

Applicant 3

7-3 Name: Fundación MD Anderson International España
8-3 Address: C/ Gómez Hemans, 2
28033 Madrid
Spain

10-1 State of residence or of principal place of business: Spain

14.1 The/Each applicant requests a reduction of fees under Rule 7a(1) EPC and is a natural person or entity under Rule 7a(2) EPC. ☒

14.2 The/Each applicant requests a reduction of fees under Rule 7a(3) EPC and is a micro-entity under Rule 7a(3) EPC. ☐

Representative 1

15-1 Name: HOFFMANN EITLE S.L.U.
Association No.: 151
16-1 Address of place of business: Paseo de la Castellana 140
3ª Planta, Edificio Lima
28046 Madrid
Spain

17-1 Telephone: +34917822780

17-1 E-mail: gfuster@hoffmanneitle.com

Inventor(s)

23 Designation of inventor attached ☒

24 Title of invention

Title of invention: Method for Predicting Progression of Prostate Cancer

25 Declaration of priority (Rule 52) and search results under Rule 141(1)

A declaration of priority is hereby made for the following applications

25.2 Re-establishment of rights

Re-establishment of rights under Article 122 EPC in respect of the priority period is herewith requested for the following priority/priorities

25.3 The EPO is requested to retrieve a certified copy of the following previous application(s) (priority document(s)) via the WIPO Digital Access Service (DAS) using the indicated access code(s):

Request	Application number:	Access Code
---------	---------------------	-------------

25.4 This application is a complete translation of the previous application ☐

25.5 It is not intended to file a (further) declaration of priority ☒

26 Reference to a previously filed application

27 Divisional application ☐

28 Article 61(1)(b) application ☐

29 Claims

Number of claims:

29.1 ☒ as attached

29.2 ☐ as in the previously filed application (see Section 26.2)

29.3 ☐ The claims will be filed later

30 Figures

It is proposed that the abstract be published together with figure No.

31 Designation of contracting states

All the contracting states party to the EPC at the time of filing of the European patent application are deemed to be designated (see Article 79(1)).

32 Different applicants for different contracting states

33 Extension/Validation

This application is deemed to be a request to extend the effects of the European patent application and the European patent granted in respect of it to all non-contracting states to the EPC with which extension or validation agreements are in force on the date on which the application is filed. However, the request is deemed withdrawn if the extension fee or the validation fee, whichever is applicable, is not paid within the prescribed time limit.

33.1 It is intended to pay the extension fee(s) for the following state(s):

33.2 It is intended to pay the validation fee(s) for the following state(s):

34 Biological material

38 Nucleotide and amino acid sequences

38.1 The description contains a sequence listing. ☐

38.2 The sequence listing is attached in XML format, in compliance with WIPO Standard ST.26 (Rule 30(1) EPC). ☐

Further indications

- 39** Additional copies of the documents cited in the European search report are requested

Number of additional sets of copies:

- 40** Refund of the search fee under Article 9(2) of the Rules relating to Fees is requested

☐

Application number or publication number of earlier search report:

42 Payment

Method of payment

Debit from deposit account

The European Patent Office is hereby authorised, to debit from the deposit account with the EPO any fees and costs indicated on the fees section below.

Currency:

EUR

Deposit account number:

28120316

Account holder:

Hoffmann Eitle S.L.U.

43 Refunds

Any refunds should be made to EPO deposit account:

28120316

Account holder:

Hoffmann Eitle S.L.U.

Fees

	Factor applied	Fee schedule	Amount to be paid
001 Filing fee - EP direct - online	1	135.00	135.00
002 Fee for a European search - Applications filed on/after 01.07.2005	1	1 520.00	1 520.00
015 Claims fee - For the 16th to the 50th claim	0	275.00	0.00
015e Claims fee - For the 51st and each subsequent claim	0	685.00	0.00
501 Additional filing fee for the 36th and each subsequent page	0	17.00	0.00
Total:	EUR 1 655.00		

44-A Forms

Details:

System file name:

A-1

Request

as ep-request.pdf

A-2

1. Designation of inventor

1. Inventor

as f1002-1.pdf

44-B Technical documents

Original file name:

System file name:

B-1	Specification	908 356 - Abstract.pdf abstract	SPECEPO-1.pdf
B-2	Specification	908 356 - Claims.pdf 15 claims	SPECEPO-2.pdf
B-3	Specification	908 356 - Description.pdf Description	SPECEPO-3.pdf
B-4	Specification	908 356 - Figures.pdf 1 figure(s)	SPECEPO-4.pdf
B-9	Pre-conversion archive	909 356 Text.zip	OLF-ARCHIVE.zip

44-C Other documents

Original file name:

System file name:

45

General authorisation:

46 Signature(s)

Place:

MADRID

Date:

07 January 2025

Signed by:

FUSTER OLAGUIBEL GUSTAVO NICOLAS - 33530042K

Association:

HOFFMANN EITLE S.L.U.

Representative name:

Gustavo Fuster

Capacity:

(Representative)

Form 1002 - 1: Public inventor(s)

Designation of inventor

User reference: 909 356
Application No:

Public

	Inventor Name: GONZÁLEZ BILLALABEITIA, Mr. Enrique Address: 28041 Madrid Spain The applicant has acquired the right to the European patent: As employer
	Inventor Name: PÉREZ NAVARRO, Mr. Enrique Address: 28041 Madrid Spain The applicant has acquired the right to the European patent: As employer
	Inventor Name: BOTÍA BLAYA, Mr. Juan Antonio Address: 30003 Murcia Spain The applicant has acquired the right to the European patent: As employer
	Inventor Name: PALMA MÉNDEZ, Mr. José Tomás Address: 30003 Murcia Spain The applicant has acquired the right to the European patent: As employer
	Inventor Name: GRANDE PULIDO, Mr. Enrique Address: 28033 Madrid Spain The applicant has acquired the right to the European patent: As employer

Signature(s)

Place: MADRID
Date: 07 January 2025
Signed by: FUSTER OLAGUIBEL GUSTAVO NICOLAS - 33530042K
Association: HOFFMANN EITLE S.L.U.
Representative name: Gustavo Fuster
Capacity: (Representative)

User reference: 909 356
Application No:

Method for Predicting Progression of Prostate Cancer

Field of the Invention

5 The present invention relates to methods for predicting the progression of prostate cancer, specifically metastatic castration-resistant prostate cancer (mCRPC), in an individual. The invention employs gene expression profiling combined with predictive modeling to assess the likelihood of overall survival and biochemical recurrence following treatment.

Background of the Invention

- 10 Prostate cancer is a leading cause of cancer-related mortality among men. Metastatic castration-resistant prostate cancer (mCRPC) represents an advanced stage of the disease characterized by poor prognosis and limited treatment options. Accurate prediction of disease progression is critical for guiding therapeutic strategies and improving patient outcomes.
- 15 Currently, clinical assessments such as PSA levels and imaging studies are commonly used to monitor prostate cancer progression; however, they lack precision in predicting overall survival and recurrence. Despite the availability of various genomic panels and clinical metrics, there remains a significant unmet need for a robust and reproducible molecular signature that can accurately predict progression and overall survival after
- 20 mCRPC therapies such as enzalutamide. Classic tests often fail due to low predictive power, irreproducibility across cohorts, and unsatisfactory inclusion of changes in gene expression over time. Advances in gene expression profiling have revealed molecular signatures that are associated with prostate cancer behavior, offering a novel approach to prognostic assessment.
- 25 The present invention addresses these challenges by providing a method to predict prostate cancer progression using a predictive model based on expression levels of a collection of signature genes derived from a biological sample of the individual.

Summary of the invention

An initial aspect of the invention refers to a method for predicting progression of prostate cancer in an individual, the method comprising:

- 5 (a) receiving expression levels of a collection of signature genes from a biological sample taken from said individual, wherein said collection of signature genes comprises at least 2, 3, 4, 5, 6, 7, 8, 9 ... 22 genes selected from the group consisting of: SNORD88C, SYT14L, MS4A2, AC092755.4, MAP2K4, CXADRP2, MS4A6A, SLC31A1, IL5RA, RNU6.286P, MIR142, SRGAP2B, ADAM17, IFI27, CLC, RELL1, TSPAN2, NUDT4, MIR4503, PTBP3, NFKBIA and MMP8;
- 10 (b) applying the expression levels to a predictive model relating expression levels of said collection of signature genes with prostate cancer progression; and
- (c) evaluating an output of said predictive model to predict progression of prostate cancer in said individual.

In an embodiment, the method comprises:

- 15 (a) receiving expression levels of a collection of signature genes from a biological sample taken from said individual, wherein said collection of signature genes comprises at least all genes selected from the group consisting of: SNORD88C, SYT14L, MS4A2, AC092755.4, MAP2K4, CXADRP2, MS4A6A, SLC31A1, IL5RA, RNU6.286P, MIR142, SRGAP2B, ADAM17, IFI27, CLC, RELL1, TSPAN2, NUDT4,
- 20 MIR4503, PTBP3, NFKBIA and MMP8, and
- (b) applying the expression levels to a predictive model relating expression levels of said collection of signature genes with prostate cancer progression; and
- (c) evaluating an output of said predictive model to predict progression of prostate cancer in said individual.
- 25 In another embodiment, the prostate cancer is metastatic castration-resistant prostate cancer (mCRPC).

In another embodiment, said output of the predictive model predicts a likelihood of clinical recurrence of prostate cancer in the individual after said individual has undergone treatment for prostate cancer, wherein said treatment is enzalutamide.

In another embodiment, said output of the predictive model predicts a likelihood of
5 biochemical recurrence of prostate cancer in the individual after said individual has undergone treatment for prostate cancer.

In another embodiment, said output of the predictive model predicts a likelihood of overall survival of the individual after said individual has undergone treatment for prostate cancer.

10 In another embodiment, the method further comprises combining the gene expression levels of said signature genes with one or more other biomarkers to predict progression of prostate cancer in said individual such as one or more other biomarkers selected from the group consisting of germline mutations, somatic mutations, DNA methylation markers, protein markers, and any combinations thereof.

15 In another embodiment, the expression levels of a collection of signature genes comprise gene expression levels measured at multiple times.

In another embodiment, the biological sample is a biological fluid selected from the group consisting of blood, preferably whole blood.

A further aspect of the invention refers to a system for predicting progression of prostate
20 cancer in an individual, the system comprising:

an apparatus configured to determine expression levels of nucleic acids from a biological sample taken from the individual; and

hardware logic designed or configured to perform operations comprising:

25 (a) receiving expression levels of a collection of signature genes from a biological sample taken from said individual, wherein said collection of signature genes comprises at least two genes selected from the group consisting of: SNORD88C, SYT14L, MS4A2, AC092755.4, MAP2K4, CXADRP2, MS4A6A, SLC31A1, IL5RA, RNU6.286P, MIR142, SRGAP2B,

ADAM17, IFI27, CLC, RELL1, TSPAN2, NUDT4, MIR4503, PTBP3, NFKBIA and MMP8;

5 (b) applying the expression levels to a predictive model relating expression levels of said collection of signature genes with prostate cancer progression; and

(c) evaluating an output of said predictive model to predict progression of prostate cancer in said individual.

In an embodiment, said collection of signature genes comprises at least all genes selected from the group consisting of: SNORD88C, SYT14L, MS4A2, AC092755.4, 10 MAP2K4, CXADRP2, MS4A6A, SLC31A1, IL5RA, RNU6.286P, MIR142, SRGAP2B, ADAM17, IFI27, CLC, RELL1, TSPAN2, NUDT4, MIR4503, PTBP3, NFKBIA and MMP8; wherein the prostate cancer is metastatic castration-resistant prostate cancer (mCRPC), and wherein said output of the predictive model predicts a likelihood of clinical recurrence of prostate cancer in the individual after said individual has undergone treatment for prostate 15 cancer, wherein said treatment is enzalutamide.

In another embodiment, the biological sample is a body fluid selected from the group consisting of blood, preferably whole blood.

A still further aspect of the invention refers to a method comprising:

- determining a gene expression level for the signature genes: SNORD88C, SYT14L, 20 MS4A2, AC092755.4, MAP2K4, CXADRP2, MS4A6A, SLC31A1, IL5RA, RNU6.286P, MIR142, SRGAP2B, ADAM17, IFI27, CLC, RELL1, TSPAN2, NUDT4, MIR4503, PTBP3, NFKBIA and MMP8, to obtain a subject expression profile for a subject,

and further comprising:

- classifying the subject as having a good prognosis or a poor prognosis of prostate cancer 25 based on the subject expression profile, wherein the good prognosis predicts an increased likelihood of survival within a predetermined period after initial diagnosis and/or no progression of disease after primary treatment, and the poor prognosis predicts an aggressive disease, a decreased likelihood of survival, and an increased

likelihood of biochemical recurrence, clinical recurrence, and/or the presence of local or distant metastases, within a predetermined period after initial diagnosis; and/or

- classifying the subject as having or not having a predisposition of prostate cancer that is susceptible to disease progression based on the subject expression profile, wherein
5 the predisposition predicts an aggressive disease, decreased likelihood of survival, and an increased likelihood of biochemical recurrence, clinical recurrence, and/or the presence of local or distant metastases, within a predetermined period after initial diagnosis.

In an embodiment, the prostate cancer is metastatic castration-resistant prostate cancer
10 (mCRPC), and said individual has undergone treatment for prostate cancer, wherein preferably said treatment is enzalutamide.

A final aspect refers to a composition comprising enzalutamide for use in the treatment of metastatic castration-resistant prostate cancer (mCRPC) in an individual having said disease and classified as having good prognosis in accordance with the previous aspect
15 of the invention.

Description of embodiments of the invention

Definitions

Unless otherwise indicated, the practice of the method and system disclosed herein
20 involves conventional techniques and apparatus commonly used in molecular biology, microbiology, protein purification, protein engineering, protein and DNA sequencing, and recombinant DNA fields, which are within the skill of the art. Such techniques and apparatus are known to those of skill in the art and are described in numerous texts and reference works (See e.g., Sambrook et al, "Molecular Cloning: A Laboratory Manual,"
25 Third Edition (Cold Spring Harbor), [2001]); and Ausubel et al, "Current Protocols in Molecular Biology" [1987]).

Numeric ranges are inclusive of the numbers defining the range. It is intended that every maximum numerical limitation given throughout this specification includes every lower numerical limitation, as if such lower numerical limitations were expressly written

herein. Every minimum numerical limitation given throughout this specification will include every higher numerical limitation, as if such higher numerical limitations were expressly written herein. Every numerical range given throughout this specification will include every narrower numerical range that falls within such broader numerical range,
5 as if such narrower numerical ranges were all expressly written herein.

Unless defined otherwise herein, all technical and scientific terms used herein have the same meaning as commonly understood by one of ordinary skill in the art. Various scientific dictionaries that include the terms included herein are well known and available to those in the art. Although any methods and materials similar or equivalent
10 to those described herein find use in the practice or testing of the embodiments disclosed herein, some methods and materials are described.

The terms defined immediately below are more fully described by reference to the Specification as a whole. It is to be understood that this disclosure is not limited to the particular methodology, protocols, and reagents described, as these may vary,
15 depending upon the context they are used by those of skill in the art.

The headings provided herein are not intended to limit the disclosure.

As used herein, the singular terms "a," "an," and "the" include the plural reference unless the context clearly indicates otherwise.

"Nucleic acid sequence," "expressed nucleic acid," or grammatical equivalents thereof
20 used in the context of a corresponding signature gene means a nucleic acid sequence whose amount is measured as an indication of the gene's expression level. The nucleic acid sequence can be a portion of a gene, a regulatory sequence, genomic DNA, cDNA, RNA including mRNA and rRNA, or others. A preferred embodiment utilizes mRNA as the primary target sequence. As is outlined herein, the nucleic acid sequence can be a
25 sequence from a sample, or a secondary target such as, for example, a product of a reaction such as a detection sequence from an invasive cleavage reaction, a ligated probe from an OLA or DASL (cDNA- mediated Annealing, Selection, and Ligation) reaction, an extended probe from a PCR reaction, or PCR amplification product (e.g., "amplicon"). A nucleic acid sequence corresponding to a signature gene can be any length, with the
30 understanding that longer sequences are more specific. Probes are made to hybridize to

nucleic acid sequences to determine the presence or absence of expression of a signature gene in a sample.

"Prostate cancer" as used herein includes carcinomas, including, carcinoma in situ, invasive carcinoma, metastatic carcinoma and pre-malignant conditions.

- 5 As used herein the term "comprising" means that the named elements are included, but other element (e.g., unnamed signature genes) may be added and still represent a composition or method within the scope of the claim. The transitional phrase "consisting essentially of" means that the associated composition or method encompasses additional elements, including, for example, additional signature genes, that do not affect the basic
10 and novel characteristics of the disclosure.

- As used herein, the term "signature gene" refers to a gene whose expression is correlated, either positively or negatively, with disease extent or outcome or with another predictor of disease extent or outcome. In some embodiments, a gene expression score (GEX) can be statistically derived from the expression levels of a set of
15 signature genes and used to diagnose a condition or to predict clinical course. In some embodiments, the expression levels of the signature gene may be used to predict progression of PCa without relying on a GEX. A "signature nucleic acid" is a nucleic acid comprising or corresponding to, in case of cDNA, the complete or partial sequence of a RNA transcript encoded by a signature gene, or the complement of such complete or
20 partial sequence. A signature protein is encoded by or corresponding to a signature gene of the disclosure.

- The term "relapse prediction" is used herein to refer to the prediction of the likelihood of cancer recurrence in patients with no apparent residual tumor tissue after treatment. The predictive methods of the present disclosure can be used clinically to make
25 treatment decisions by choosing the most appropriate treatment modalities for any particular patient. The predictive methods of the present disclosure also can provide valuable tools in predicting if a patient is likely to respond favorably to a treatment regimen, such as surgical intervention, chemotherapy with a given drug or drug combination, and/or radiation therapy.

The Gleason grading system is based on the glandular pattern of the tumor. Gleason grade takes into account the ability of the tumor to form glands. A pathologist, using relatively low magnification, performs the histologic review necessary for assigning the Gleason grade. The range of grades is 1-5: 1, 2 and 3 are considered to be low to moderate in grade; 4 and 5 are considered to be high grade. The prognosis for a given patient generally falls somewhere between that predicted by the primary grade and a secondary grade given to the second most prominent glandular pattern. When the two grades are added the resulting number is referred to as the "Gleason score". The Gleason Score is a more accurate predictor of outcome than either of the individual grades. Thus, the traditionally reported Gleason score will be the sum of two numbers between 1-5 with a total score from 2-10. It is unusual for the primary and secondary Gleason grade to differ by more than one, such that the only way that there can be a Gleason score 7 tumor is if the primary or secondary Gleason grade is 4. Because of the presence of grade 4 glandular patterns in tissue having Gleason score 7, these tumors can behave in a much more aggressive fashion than those having Gleason score 6. In a recent study of over 300 patients, the disease specific survival for Gleason score 7 patients was 10 years. In contrast, Gleason score 6 patients survived 16 years and Gleason 4-5 for 20 years. It is therefore clear that the prognosis for men with Gleason score 7 tumors is worse than for men with Gleason score 5 and 6 tumors. Under certain circumstances it is suggested that men with Gleason 7 tumors can be considered for clinical trials.

The terms "polynucleotide," "nucleic acid" and "nucleic acid molecules" are used interchangeably and refer to a covalently linked sequence of nucleotides (i.e., ribonucleotides for RNA and deoxyribonucleotides for DNA) in which the 3' position of the pentose of one nucleotide is joined by a phosphodiester group to the 5' position of the pentose of the next. The nucleotides include sequences of any form of nucleic acid, including, but not limited to RNA and DNA molecules. The term "polynucleotide" includes, without limitation, single- and double-stranded polynucleotide.

The term "Next Generation Sequencing (NGS)" herein refers to sequencing methods that allow for massively parallel sequencing of clonally amplified molecules and of single nucleic acid molecules. Non-limiting examples of NGS include sequencing-by-synthesis using reversible dye terminators, and sequencing-by-ligation.

The term "read" refers to a sequence read from a portion of a nucleic acid sample. Typically, though not necessarily, a read represents a short sequence of contiguous base pairs in the sample. The read may be represented symbolically by the base pair sequence (in ATCG) of the sample portion. It may be stored in a memory device and processed as appropriate to determine whether it matches a reference sequence or meets other criteria. A read may be obtained directly from a sequencing apparatus or indirectly from stored sequence information concerning the sample. In some cases, a read is a DNA sequence of sufficient length (e.g., at least about 25 bp) that can be used to identify a larger sequence or region, e.g., that can be aligned and specifically assigned to a chromosome or genomic region or gene.

As used herein, the terms "aligned," "alignment," or "aligning" refer to the process of comparing a read or tag to a reference sequence and thereby determining whether the reference sequence contains the read sequence. If the reference sequence contains the read, the read may be mapped to the reference sequence or, in certain embodiments, to a particular location in the reference sequence. In some cases, alignment simply tells whether or not a read is a member of a particular reference sequence (i.e., whether the read is present or absent in the reference sequence). For example, the alignment of a read to the reference sequence for human chromosome 13 will tell whether the read is present in the reference sequence for chromosome 13. A tool that provides this information may be called a set membership tester. In some cases, an alignment additionally indicates a location in the reference sequence where the read or tag maps to. For example, if the reference sequence is the whole human genome sequence, an alignment may indicate that a read is present on chromosome 13, and may further indicate that the read is on a particular strand and/or site of chromosome 13.

Aligned reads or tags are one or more sequences that are identified as a match in terms of the order of their nucleic acid molecules to a known sequence from a reference genome. Alignment can be done manually, although it is typically implemented by a computer algorithm, as it would be impossible to align reads in a reasonable time period for implementing the methods disclosed herein. One example of an algorithm from aligning sequences is the Efficient Local Alignment of Nucleotide Data (ELAND) computer program distributed as part of the Illumina Genomics Analysis pipeline. Alternatively, a

Bloom filter or similar set membership tester may be employed to align reads to reference genomes. See US Patent Application No. 61/552,374 filed October 27, 2011 which is incorporated herein by reference in its entirety. The matching of a sequence read in aligning can be a 100% sequence match or less than 100% (non-perfect match).

- 5 The term "mapping" used herein refers to specifically assigning a sequence read to a larger sequence, e.g., a reference genome, by alignment.

The term "subject" herein refers to a human subject as well as a non-human subject such as a mammal, an invertebrate, a vertebrate, a fungus, a yeast, a bacterium, and a virus. Although the examples herein concern humans and the language is primarily
10 directed to human concerns, the concepts disclosed herein are applicable to genomes from any plant or animal, and are useful in the fields of veterinary medicine, animal sciences, research laboratories and such.

The term "condition" herein refers to "medical condition" as a broad term that includes all diseases and disorders, but can include [injuries] and normal health situations, such
15 as pregnancy, that might affect a person's health, benefit from medical assistance, or have implications for medical treatments.

The term "sensitivity" as used herein is equal to the number of true positives divided by the sum of true positives and false negatives.

The term "specificity" as used herein is equal to the number of true negatives divided by
20 the sum of true negatives and false positives.

This disclosure provides improved predictive models that incorporate tumor biomarkers and that better distinguish between indolent cases and metastatic disease. Some embodiments provide a method for predicting progression of prostate cancer, preferably metastatic castration-resistant prostate cancer (mCRPC), in an individual, the method
25 comprising: (a) receiving expression levels of a collection of signature genes from a biological sample taken from said individual, wherein said collection of signature genes comprises at least two or more genes selected from the group consisting of: SNORD88C, SYT14L, MS4A2, AC092755.4, MAP2K4, CXADRP2, MS4A6A, SLC31A1, IL5RA, RNU6.286P, MIR142, SRGAP2B, ADAM17, IFI27, CLC, RELL1, TSPAN2, NUDT4, MIR4503, PTBP3,
30 NFKBIA and MMP8; (b) applying the expression levels to a predictive model relating

expression levels of said collection of signature genes with prostate cancer progression; and (c) evaluating an output of said predictive model to predict progression of prostate cancer in said individual.

5 In some embodiments, the output of the predictive model predicts a likelihood of overall survival or clinical recurrence of prostate cancer in the individual after said individual has undergone treatment for prostate cancer, wherein the prostate cancer is preferably metastatic castration-resistant prostate cancer (mCRPC), and said treatment is enzalutamide.

10 In some embodiments, the 22 markers of the panel are differentially expressed/regulated between PCa cases with and without recurrence, and are predictive of aggressive disease. In some embodiments, the predictive models include these 22 markers along with pre-operative PSA levels, Gleason score, and age at diagnosis, which models show greater prediction than models having clinical variables alone. One skilled in the art understands that further validation of the models using additional datasets will
15 allow improvement of the predictive power of the models, which may include different coefficients of the models. In some embodiments, one or more genes can be selected from the panel to form predictive models for evaluation of PCa progression.

Identifying Gene Expression Panel and Developing Predictive Model

Some embodiments the disclosure provides methods for developing predictive models
20 for determining PCa progression. In some embodiments, the models are developed using data collected from patients known to have prostate cancer. In some embodiments, the predictive models describe the correlation between expression levels of signature genes measured in whole blood and clinical recurrence of PCa or overall survival in patients providing the biological samples. In various embodiments, the
25 disclosure provides a panel of 22 signature genes that correlate with overall survival or PCa recurrence in the prostate cancer patients. In some embodiments, the disclosure further provides methods to predict PCa development, recurrence, and/or overall survival for an individual using the individual's expression levels of one or more of the signature genes. In some embodiments, the predictive model includes the expression
30 levels of at least one gene that is selected from the group including: SNORD88C, SYT14L,

MS4A2, AC092755.4, MAP2K4, CXADRP2, MS4A6A, SLC31A1, IL5RA, RNU6.286P, MIR142, SRGAP2B, ADAM17, IFI27, CLC, RELL1, TSPAN2, NUDT4, MIR4503, PTBP3, NFKBIA and MMP8.

In some embodiments, the gene expression data may be preprocessed by normalization,
 5 background correction, and/or batch effect correction. The pre- processed data may then be analyzed for differential expression of genes for no evidence of disease (NED) group versus clinical recurrence (CR) group.

In some embodiments, one or more of the following genes: SNORD88C, SYT14L, MS4A2, AC092755.4, MAP2K4, CXADRP2, MS4A6A, SLC31A1, IL5RA, RNU6.286P, MIR142,
 10 SRGAP2B, ADAM17, IFI27, CLC, RELL1, TSPAN2, NUDT4, MIR4503, PTBP3, NFKBIA and MMP8, may be used in a predictive model. In some embodiments, the one or more genes may be selected by their correlation with recurrence or overall survival in the training data set to develop the predictive models. In some embodiments, the one or more genes may be selected by their reliability ranks. In some embodiments, the panel
 15 of signature genes include at least 1, 2, 3, 4, 5, 6, 7, 8, 9, or 10 of SNORD88C, SYT14L, MS4A2, AC092755.4, MAP2K4, CXADRP2, MS4A6A, SLC31A1, IL5RA, RNU6.286P, MIR142, SRGAP2B, ADAM17, IFI27, CLC, RELL1, TSPAN2, NUDT4, MIR4503, PTBP3, NFKBIA and MMP8. In some embodiments, the one or more genes may be selected by their predictive power rankings.

20 In some embodiments, various clinical variables (e.g., PSA level, Gleason score, operation year and age) will be included in the same logistic model along with the signature genes. Coefficients will be defined for each variable (gene expression and clinical values). This logistic regression model will provide a probability of having a clinical recurrence given the provided gene expression scores and clinical variables. This
 25 probability will be a number between 0-1, and it will indicate for each given patient the probability of having a clinical recurrence.

In some embodiments, in addition to identifying the coefficients of the predictive model, the disclosure identifies the most useful specificity and sensitivity a user wishes to have for a specific risk probability. Based on the desired specificity and sensitivity levels, the
 30 method will report the risk status of each patient. For example, we may find that given

the specificity and sensitivity of our model, a patient with 45% chance of clinical recurrence might be better off being classified as high-risk of recurrence rather than low-risk or vice versa. In other words, more user-friendly criteria can be chosen based on more detailed analyses in further datasets to determine the most practical interpretation of the risk probability depending on how much clinicians want to risk having a false positive or a false negative.

One skilled in the art can readily determine other combinations of signature genes sufficient to practice the disclosures claimed herein. For example, based on the stability selection ranking of SNORD88C, SYT14L, MS4A2, AC092755.4, MAP2K4, CXADRP2, MS4A6A, SLC31A1, IL5RA, RNU6.286P, MIR142, SRGAP2B, ADAM17, IFI27, CLC, RELL1, TSPAN2, NUDT4, MIR4503, PTBP3, NFKBIA and MMP8 or the p-values of the univariate comparison between the NED and the CR groups, one skilled in the art can readily determine a sub-combination of prostate cancer signature genes suitable for methods of the disclosure. Those exemplary genes having lowest stability selection ranks can be excluded, with the remaining genes providing a sufficient collection of isolated prostate cancer signature genes suitable for relapse prediction of prostate cancer. Similarly, genes having the largest p-value may be excluded.

Thus, the disclosure provides a method of predicting prostate cancer relapse or overall survival based on the expression patterns for any subset of the 22 genes SNORD88C, SYT14L, MS4A2, AC092755.4, MAP2K4, CXADRP2, MS4A6A, SLC31A1, IL5RA, RNU6.286P, MIR142, SRGAP2B, ADAM17, IFI27, CLC, RELL1, TSPAN2, NUDT4, MIR4503, PTBP3, NFKBIA and MMP8 including, for example, at least 1, 2, 3, 4, 5, 6, 7, 8, 9, 10, 11, 12, 13, 14, 15, 16, 17, 18, 19, 20, 21, or 22 genes. In some embodiments, the disclosure also provides a method of predicting prostate cancer progression based on the expression patterns for any subset of the set of genes consisting of SNORD88C, SYT14L, MS4A2, AC092755.4, MAP2K4, CXADRP2, MS4A6A, SLC31A1, IL5RA, RNU6.286P, MIR142, SRGAP2B, ADAM17, IFI27, CLC, RELL1, TSPAN2, NUDT4, MIR4503, PTBP3, NFKBIA and MMP8.

In general, it is preferable to use signature genes for which the difference between the level of expression of the signature gene in prostate cancer cells or prostate-associated body fluids and the level of expression of the same signature gene in normal prostate

cells or prostate-associated body fluids is as great as possible. Although the difference can be as small as the limit of detection of the method for assessing expression of the signature gene, it is preferred that the difference be at least greater than the standard error of the assessment method, and preferably a difference of at least 1.1-, 1.2-, 1.3-, 1.4-, 1.5-, 1.6-, 1.7-, 1.8-, 1.9-, 2-, 3-, 4-, 5-, 6-, 7-, 8-, 9-, 10-, 15-, 20-, 25-, 100-, 500-, 1000-fold or greater.

The disclosure also provides a collection of isolated probes specific for prostate cancer signature genes comprising at least two genes selected from the group consisting of SNORD88C, SYT14L, MS4A2, AC092755.4, MAP2K4, CXADRP2, MS4A6A, SLC31A1, IL5RA, RNU6.286P, MIR142, SRGAP2B, ADAM17, IFI27, CLC, RELL1, TSPAN2, NUDT4, MIR4503, PTBP3, NFKBIA and MMP8. The disclosure includes compositions, kits, and methods for assessing the probability of relapse or overall survival of cancer for an individual from which a sample is obtained.

The practice of the present disclosure employs, unless otherwise indicated, conventional techniques of molecular biology (including recombinant techniques), microbiology, cell biology, and biochemistry, which are within the skill of the art. Such techniques are explained in the literature, such as, "Molecular Cloning: A Laboratory Manual", Second edition (Sambrook et al, 1989); "Oligonucleotide Synthesis" (M. J. Gait, ed., 1984); "Animal Cell Culture" (R. I. Freshney, ed., 1987); "Methods in Enzymology" (Academic Press, Inc.); "Handbook of Experimental Immunology", Fourth edition (D. M. Weir & C. C. Blackwell, eds., Blackwell Science Inc., 1987); "Gene Transfer Vectors for Mammalian Cells" (J. M. Miller & M. P. Calos, eds., 1987); "Current Protocols in Molecular Biology" (F. M. Ausubel et al, eds., 1987); and "PCR: The Polymerase Chain Reaction", (Mullis et al, eds., 1994). [0092] Although the use of the 28 genes, and subsets thereof, has been exemplified with respect to prognosis and diagnosis methods utilizing expression levels of mRNA species produced by these genes, it will be understood that similar diagnostic and prognostic methods can utilize other measures such as methylation levels for the genes which can be correlated with expression levels or a measure of the level or activities of the protein products of the genes. Methylation can be determined using methods known in the art such as those set forth in US 6,200,756 or US 2003/0170684, each of which is incorporated herein by reference. The level and activity of proteins can

be determined using methods known in the art such as antibody detection techniques or enzymatic assays particular to the activity being evaluated. Furthermore, prognosis or diagnosis can be based on the presence of mutations or polymorphisms identified in the genes that affect expression of the gene or activity of the protein product.

- 5 Information relevant to the patient's diagnosis include, but are not limited to, age, ethnicity, serum PSA at the time of surgery, tumor localization, pertinent past medical history related to co-morbidity, other oncological history, family history for cancer, physical exam findings, radiological findings, biopsy date, biopsy result, types of operation performed (radical retropubic or radical perineal prostatectomy), TNM
10 staging, neoadjuvant therapy (i.e. chemotherapy, hormones), adjuvant or salvage radiotherapy, hormonal therapy for a rising PSA (biochemical disease relapse), local vs. distant disease recurrence and survival outcome. These clinical variables may be included in the predictive model in various embodiments.

- In some embodiments, suitable biological samples include, but are not limited to,
15 circulating tumor cells (CTCs) isolated from the blood, urine of the patients or other body fluids, exosomes, and circulating tumor nucleic acids, in particular suitable biological samples are blood samples, in particular whole blood samples.

- In some embodiments, the gene expression levels of the signature genes may be integrated with other biomarkers to predict the progression of PCa. Suitable biomarkers
20 for this purpose include, but are not limited to, germline and somatic mutations, DNA methylation markers, and protein markers. In some embodiments, the combination of the signature genes and other biomarkers can be implemented by including both the signature genes and the biomarkers in the same predictive model. In some
25 embodiments, the effect of the other biomarkers may be accounted for in a computational mechanism in addition to the predictive model, such as a second model that combines the output of the first predictive model with the effects of the other biomarkers. One skilled in the art understands various approaches may be used to combine the effects of the signature genes and biomarkers to predict the progression of PCa.

In some embodiments, the gene expression levels of the signature genes may be measured multiple times. In some embodiments, the dynamics of the expression levels may be used in combination of the signature genes' expression levels to better predict the clinical outcome. One skilled in the art understands various approaches may be used
 5 to combine the effects of the levels and the dynamics of the signature genes' expression to predict the progression of PCa.

Determining Gene Expression Level

The methods of the disclosure depend on the detection of differentially expressed genes for expression profiling across heterogeneous tissues. Thus, the methods depend on
 10 profiling genes whose expression in certain tissues is activated to a higher or lower level in an individual afflicted with a condition, for example, cancer, such as prostate cancer, relative to its expression in a non-cancerous biological sample or in a control subject. Gene expression can be activated to a higher or lower level at different stages of the same conditions and a differentially expressed gene can be either activated or inhibited
 15 at the nucleic acid level or protein level, or may be subject to alternative splicing to result in a different polypeptide product. Such differences can be evidenced by a change in mRNA levels, surface expression, secretion or other partitioning of a polypeptide, for example. For the purpose of this disclosure, differential gene expression is considered to be present when there is at least about 1.1-fold, 1.2-fold, 1.3-fold, 1.4-fold, 1.5-fold, 1.6-
 20 fold, 1.7-fold, 1.8-fold, 1.9-fold, to two-fold.

Differential signature gene expression can be identified or confirmed using methods known in the art such as qRT-PCR (quantitative reverse-transcription polymerase chain reaction) and microarray analysis. In particular embodiments, differential signature gene expression can be identified, or confirmed using microarray techniques.

25 **Practical Implementation in a Clinical Setting**

In some embodiments, the above-described methods are integrated into a routine clinical laboratory workflow. For example, a blood sample from the patient may be collected into an RNA-stabilizing tube (e.g., PAXgene®) and processed according to the manufacturer's instructions. After RNA extraction and quality assessment (with an RNA
 30 Integrity Number (RIN) of ≥ 7), cDNA is synthesized following standard protocols.

Gene expression levels of the 22 signature genes can then be measured using a standardized qPCR assay or a next-generation sequencing (NGS) platform. Appropriate normalization strategies, such as using one or more reference genes or global normalization methods, are employed to ensure accurate quantification. The normalized expression data are then input into the predictive model described herein, applying the previously determined model coefficients to generate a risk score.

Thresholds for clinical interpretation (e.g., distinguishing low-risk from high-risk patients) may be established using Receiver Operating Characteristic (ROC) curve analyses. A higher risk score correlates with an increased likelihood of disease progression, enabling clinicians to tailor treatment strategies—such as deciding whether to initiate, continue, or intensify therapies like enzalutamide—and to consider enrolling the patient in appropriate clinical trials. This systematic approach ensures consistent, reproducible integration of the gene signature into standard oncological care."

Apparatus and Systems for Predicting Progression of PCa

[Analysis of the sequencing data and the diagnosis derived therefrom are typically performed using various computer executed algorithms and programs. Therefore, certain embodiments employ processes involving data stored in or transferred through one or more computer systems or other processing systems. Embodiments disclosed herein also relate to apparatus for performing these operations. This apparatus may be specially constructed for the required purposes, or it may be a general-purpose computer (or a group of computers) selectively activated or reconfigured by a computer program and/or data structure stored in the computer. In some embodiments, a group of processors performs some or all of the recited analytical operations collaboratively (e.g., via a network or cloud computing) and/or in parallel. A processor or group of processors for performing the methods described herein may be of various types including microcontrollers and microprocessors such as programmable devices (e.g., CPLDs and FPGAs) and non-programmable devices such as gate array ASICs or general purpose microprocessors.

In addition, certain embodiments relate to tangible and/or non-transitory computer readable media or computer program products that include program instructions and/or

data (including data structures) for performing various computer-implemented operations. Examples of computer-readable media include, but are not limited to, semiconductor memory devices, magnetic media such as disk drives, magnetic tape, optical media such as CDs, magneto-optical media, and hardware devices that are specially configured to store and perform program instructions, such as read-only memory devices (ROM) and random access memory (RAM). The computer readable media may be directly controlled by an end user or the media may be indirectly controlled by the end user. Examples of directly controlled media include the media located at a user facility and/or media that are not shared with other entities. Examples of indirectly controlled media include media that is indirectly accessible to the user via an external network and/or via a service providing shared resources such as the "cloud." Examples of program instructions include both machine code, such as produced by a compiler, and files containing higher level code that may be executed by the computer using an interpreter.

In various embodiments, the data or information employed in the disclosed methods and apparatus is provided in an electronic format. Such data or information may include reads and tags derived from a nucleic acid sample, counts or densities of such tags that align with particular regions of a reference sequence (e.g., that align to a chromosome or chromosome segment), reference sequences (including reference sequences providing solely or primarily polymorphisms), counseling recommendations, diagnoses, and the like. As used herein, data or other information provided in electronic format is available for storage on a machine and transmission between machines. Conventionally, data in electronic format is provided digitally and may be stored as bits and/or bytes in various data structures, lists, databases, etc. The data may be embodied electronically, optically, etc.

In some embodiments, the disclosure provides a system for predicting progression of prostate cancer in an individual, the system comprising: an apparatus configured to determine expression levels of nucleic acids from a biological sample taken from the individual; and hardware logic designed or configured to perform operations comprising: (a) receiving expression levels of a collection of signature genes from a biological sample taken from said individual, wherein said collection of signature genes comprises at least

two genes selected from the group consisting of: SNORD88C, SYT14L, MS4A2, AC092755.4, MAP2K4, CXADRP2, MS4A6A, SLC31A1, IL5RA, RNU6.286P, MIR142, SRGAP2B, ADAM17, IFI27, CLC, RELL1, TSPAN2, NUDT4, MIR4503, PTBP3, NFKBIA and MMP8; (b) applying the expression levels to a predictive model relating expression levels of said collection of signature genes with prostate cancer progression; and (c) evaluating an output of said predictive model to predict progression of prostate cancer in said individual. In some embodiments, said collection of signature genes comprises at least one gene selected from the group consisting of: SNORD88C, SYT14L, MS4A2, AC092755.4, MAP2K4, CXADRP2, MS4A6A, SLC31A1, IL5RA, RNU6.286P, MIR142, SRGAP2B, ADAM17, IFI27, CLC, RELL1, TSPAN2, NUDT4, MIR4503, PTBP3, NFKBIA and MMP8. In some embodiments, said collection of signature genes comprises at least two genes selected from the group consisting essentially of: SNORD88C, SYT14L, MS4A2, AC092755.4, MAP2K4, CXADRP2, MS4A6A, SLC31A1, IL5RA, RNU6.286P, MIR142, SRGAP2B, ADAM17, IFI27, CLC, RELL1, TSPAN2, NUDT4, MIR4503, PTBP3, NFKBIA and MMP8.

In some embodiments, the apparatus of the system includes a microarray. In some embodiments, the apparatus includes a next generation sequencer. In some embodiments, the apparatus includes a qPCR device.

Sequencing Methods

In various embodiments, determination of gene expression levels may involve sequencing nucleic acids corresponding to genes of interests. Any of a number of sequencing technologies can be utilized.

Some sequencing technologies are available commercially, such as the sequencing-by-hybridization platform from Affymetrix Inc. (Sunnyvale, CA) and the sequencing-by-synthesis platforms from 454 Life Sciences (Bradford, CT), Illumina/Solexa (Hayward, CA) and Helicos Biosciences (Cambridge, MA), and the sequencing-by-ligation platform from Applied Biosystems (Foster City, CA), as described below. In addition to the single molecule sequencing performed using sequencing-by-synthesis of Helicos Biosciences, other single molecule sequencing technologies include, but are not limited to, the

SMRT™ technology of Pacific Biosciences, the ION TORRENT™ technology, and nanopore sequencing developed for example, by Oxford Nanopore Technologies.

It is understood that modifications which do not substantially affect the activity of the various embodiments of this disclosure are also included within the definition of the disclosure provided herein. Accordingly, the following examples are intended to illustrate but not limit the present disclosure.

Examples

MATERIAL AND METHODS

Study design and conduct

10 The PREMIERE trial, a translational multicenter single-arm open-label phase 2 clinical trial (NCT02288936), investigated the use of enzalutamide as first-line treatment for metastatic castration-resistant prostate cancer (mCRPC). The study was approved by a central independent review board (IRB).

15 The chosen patients for the trial had histologically confirmed adenocarcinoma of the prostate with documented metastases and tumor progression, with a serum testosterone level of 50 ng per deciliter or less while continuing androgen-deprivation therapy. They had an Eastern Cooperative Oncology Group (ECOG) 0-1 and were asymptomatic or mildly symptomatic (Brief Pain Inventory Short Form question 3 of less than 4).

20 The validation cohort consisted of a single institution cohort from patients participating in a protocol approved by the Istituto Scientifico Romagnolo per lo Studio e la Cura dei Tumori (IRST), Meldola, Italy (REC 2192/2013) with plasma samples collected prospectively with the primary aim of biomarker evaluation.

Patients

25 The PREMIERE trial included 98 chemo-naïve mCRPC patients from 17 hospitals in Spain treated at a dose of 160 mg as first-line treatment with enzalutamide. Whole-blood samples were serially obtained at pre-treatment, at 12 weeks during the treatment, and at tumour progression.

A total of 237 whole-blood samples were prospectively collected. After quality controls, 3 blood samples were excluded due to poor RNA integrity **Figure 1**.

In the IRST trial, whole-blood samples were obtained at pre-treatment and at tumour progression. A total of 69 whole blood samples were collected from 54 patients.

5 RNA extraction and microarray analysis

Whole-blood samples were collected in whole-blood PAXgene RNA, isolated and purified as established by the manufacturer's instructions. RNA quantification and quality assessment were performed employing spectrophotometry and electrophoresis on microfluidic solution with NanoDrop 2000 (Thermo Scientific, Newark, DE, USA) and
10 Bioanalyzer 2100 (Agilent Technologies, Palo Alto, CA, USA), respectively. Only purified RNA samples with an RNA integration number (RIN) of seven or more were selected for further analyses. 100 ng of RNA of each sample was used to synthesize complementary DNA (cDNA) with the WT PLUS Reagent Kit (Thermo Scientific, Newark, DE, USA) following the standard protocol. The cDNA was amplified, fragmented, and labelled with
15 biotine for the hidridization process.

Microarrays GeneChip™ Human Trascriptome Array HTA 2.0 (902162, Affymetrix, ThermoFisher, Newark, DE, USA) were hybridized using 5.2 ug of single strand DNA (ssDNA) during 16 hours, washed to eliminate the unspecific probes and then scanned with GeneChip Scanner 3000 (Affymetrix, Thermo Scientific, Newark, DE, USA).

20 Differential expression analysis and identification of DEGs

Gene microarray analyses were derived after a quality control, background correction, normalization, logarithmic conversion and remove batch effects processing using Transcriptome Analysis Console (TAC) Software (version 4.0.1, Thermo). All samples that had not passed quality control were filtered out and the resulting data were annotated
25 and analysed by R packages "affy", "limma" and "pd.hta.2.0"^{24–26}. The P-value <0,01, a Q-value <0,05 and $|\log_2FC| > 0.3$ were set as the threshold for screening DEGs.

Clinical Data Processing

Clinical data was initially loaded into a data frame. Preprocessing steps included converting survival time from months to days and reformatting variable names for

consistency. Differential expression analysis was conducted to filter pre-treatment gene expression values, focusing on genes significantly associated with the patients' conditions.

Survival Analysis Methods

5 Univariable Analysis

Univariable Cox regression analyses were performed for each gene using a parallel computing approach (RegParallel) to efficiently handle the high-dimensional data. Genes significantly influencing survival outcomes were identified, with p-values adjusted for multiple testing using the false discovery rate method. This step was crucial
10 in reducing the number of genes to be considered for further analysis.

Model Training

Following the univariable analysis, several advanced survival models were developed to analyze the data, using the selected genes:

1. Cox Proportional Hazards model with Ridge regularization:

- 15 ○ A Ridge regression version of the Cox model was implemented, where regularization parameters were optimized through grid search. This method was employed to control for overfitting and enhance the model's generalizability.

2. LASSO-penalized Cox model:

- 20 ○ The LASSO technique was applied to perform variable selection, effectively shrinking the coefficients of less critical variables to zero. This step helped in reducing model complexity and focusing on the most predictive features.

3. Elastic Net-penalized Cox model:

- 25 ○ Combined both Ridge and LASSO penalties to optimize model complexity and variable selection. This model aimed to balance feature selection with model stability, taking advantage of the benefits of both regularization methods.

4. Random Survival Forest:

- A Random Survival Forest model was trained to manage non-linear relationships between variables and survival times. Feature importance was evaluated through permutation importance tests to identify significant predictors, providing insights into the variables most impacting survival outcomes.

Grid Search and Cross-Validation

For each model, hyperparameters were fine-tuned using GridSearchCV with a K-Fold cross-validation strategy. This method ensured that each model was not only generalizable across different subsets of the data but also robust against variations within the training data.

Feature Selection and Model Coefficients

For each regression-based model, coefficients were examined to determine the influence of each variable on survival predictions. This analysis was essential for identifying key features that significantly impact the survival outcomes, informing further feature selection to refine the prognostic signature.

Validation and Prediction

The optimized models were then applied to a separate validation dataset to assess their predictive performance. This step was crucial for confirming the models' effectiveness in an independent cohort, thereby reinforcing the reliability and applicability of the prognostic signature in clinical settings.

Model Evaluation and Results Visualization

Model performances were visualized using plots of the concordance index (c-index) across different hyperparameter values. Additionally, the coefficients of significant predictors were plotted to highlight their relative importance and impact on the survival outcomes. The final evaluation included a comprehensive comparison of the models'

performance on the validation dataset, summarized in a results table displaying the c-index for each model. Finally, LASSO model was selected.

Combinatorial Testing of Top Features

- 5 The top features identified by the LASSO model were further tested in combinations to evaluate their collective impact on model performance. This step was crucial for refining the prognostic signature and determining the most predictive subset of features.

Validation and Prediction

Independent Validation

- 10 The optimized LASSO model was applied to a separate validation dataset to confirm its effectiveness in an independent cohort. This step assessed the model's predictive performance and robustness.

Prediction and Final Evaluation

- 15 The final evaluation of the model included predictions on the validation dataset and a comprehensive comparison of model performance, summarized in a results table displaying the c-index for both training and validation datasets, obtaining a model of 22 genes:

coefficient

SNORD88C 0.517364

SYT14L 0.469121

MS4A2 -0.310436

AC092755.4 0.290974

coefficient**MAP2K4** 0.290191**CXADRP2** 0.287535**MS4A6A** 0.235089**SLC31A1** 0.231427**IL5RA** -0.224362**RNU6.286P** 0.178509**MIR142** -0.168221**SRGAP2B** 0.131916**ADAM17** 0.129305**IFI27** 0.128270**CLC** -0.120376**RELL1** 0.119308**TSPAN2** 0.100680**NUDT4** 0.058931**MIR4503** -0.039713

coefficient**PTBP3** 0.021022**NFKBIA** 0.011279**MMP8** 0.007688

With the following C-index:

	Modelo	train c-index	val c-index
5	Lasso	0.868 (+- 0.02)	0.735 (+- 0.11)

This structured approach to developing and validating the LASSO model ensures a rigorous assessment of its predictive capabilities and emphasizes its potential for clinical application in predicting patient outcomes based on survival data.

CLAIMS

1. A method for predicting progression of prostate cancer in an individual, the method comprising:

- 5 (a) receiving expression levels of a collection of signature genes from a biological sample taken from said individual, wherein said collection of signature genes comprises at least 2, 3, 4, 5, 6, 7, 8, 9 ... 22 genes selected from the group consisting of: SNORD88C, SYT14L, MS4A2, AC092755.4, MAP2K4, CXADRP2, MS4A6A, SLC31A1, IL5RA, RNU6.286P, MIR142, SRGAP2B, ADAM17, IFI27, CLC, RELL1, TSPAN2, NUDT4, MIR4503, PTBP3, NFKBIA and MMP8;
- 10 (b) applying the expression levels to a predictive model relating expression levels of said collection of signature genes with prostate cancer progression; and
- (c) evaluating an output of said predictive model to predict progression of prostate cancer in said individual.

2. The method for predicting progression of prostate cancer in an individual according to claim 1, the method comprising:

- 15 (a) receiving expression levels of a collection of signature genes from a biological sample taken from said individual, wherein said collection of signature genes comprises at least all genes selected from the group consisting of: SNORD88C, SYT14L, MS4A2, AC092755.4, MAP2K4, CXADRP2, MS4A6A, SLC31A1, IL5RA, RNU6.286P, MIR142, SRGAP2B, ADAM17, IFI27, CLC, RELL1, TSPAN2, NUDT4, MIR4503, PTBP3, NFKBIA and MMP8, and
- 20 (b) applying the expression levels to a predictive model relating expression levels of said collection of signature genes with prostate cancer progression; and
- (c) evaluating an output of said predictive model to predict progression of prostate cancer in said individual.
- 25

3. The method according to any one of claims 1 to 2, wherein the prostate cancer is metastatic castration-resistant prostate cancer (mCRPC).

4. The method of any of the preceding claims, wherein said output of the predictive model predicts a likelihood of clinical recurrence of prostate cancer in the individual after said individual has undergone treatment for prostate cancer, wherein said treatment is enzalutamide.
- 5 5. The method according to claim 4, wherein said output of the predictive model predicts a likelihood of biochemical recurrence of prostate cancer in the individual after said individual has undergone treatment for prostate cancer.
6. The method according to claim 4, wherein said output of the predictive model predicts a likelihood of overall survival of the individual after said individual has undergone
10 treatment for prostate cancer.
7. The method of any of the preceding claims, further comprising combining the gene expression levels of said signature genes with one or more other biomarkers to predict progression of prostate cancer in said individual such as one or more other biomarkers selected from the group consisting of germline mutations, somatic mutations, DNA
15 methylation markers, protein markers, and any combinations thereof.
8. The method of any of the preceding claims, wherein the expression levels of a collection of signature genes comprise gene expression levels measured at multiple times.
9. The method of any of the present claims, wherein the biological sample is a biological
20 fluid selected from the group consisting of blood, preferably whole blood.
10. A system for predicting progression of prostate cancer in an individual, the system comprising:

an apparatus configured to determine expression levels of nucleic acids from a biological sample taken from the individual; and

25 hardware logic designed or configured to perform operations comprising:

(a) receiving expression levels of a collection of signature genes from a biological sample taken from said individual, wherein said collection of signature genes comprises at least two genes selected from the group consisting of: SNORD88C,

SYT14L, MS4A2, AC092755.4, MAP2K4, CXADRP2, MS4A6A, SLC31A1, IL5RA, RNU6.286P, MIR142, SRGAP2B, ADAM17, IFI27, CLC, RELL1, TSPAN2, NUDT4, MIR4503, PTBP3, NFKBIA and MMP8;

5 (b) applying the expression levels to a predictive model relating expression levels of said collection of signature genes with prostate cancer progression; and

(c) evaluating an output of said predictive model to predict progression of prostate cancer in said individual.

11. The system for predicting progression of prostate cancer in an individual according to claim 10, wherein said collection of signature genes comprises at least all genes
10 selected from the group consisting of: SNORD88C, SYT14L, MS4A2, AC092755.4, MAP2K4, CXADRP2, MS4A6A, SLC31A1, IL5RA, RNU6.286P, MIR142, SRGAP2B, ADAM17, IFI27, CLC, RELL1, TSPAN2, NUDT4, MIR4503, PTBP3, NFKBIA and MMP8; wherein the prostate cancer is metastatic castration-resistant prostate cancer (mCRPC), and wherein
15 said output of the predictive model predicts a likelihood of clinical recurrence of prostate cancer in the individual after said individual has undergone treatment for prostate cancer, wherein said treatment is enzalutamide.

12. The system according to any one of claims 10 or 11, wherein the biological sample is a body fluid selected from the group consisting of blood, preferably whole blood.

13. A method comprising:

20 - determining a gene expression level for the signature genes: SNORD88C, SYT14L, MS4A2, AC092755.4, MAP2K4, CXADRP2, MS4A6A, SLC31A1, IL5RA, RNU6.286P, MIR142, SRGAP2B, ADAM17, IFI27, CLC, RELL1, TSPAN2, NUDT4, MIR4503, PTBP3, NFKBIA and MMP8, to obtain a subject expression profile for a subject,
and further comprising:

25 - classifying the subject as having a good prognosis or a poor prognosis of prostate cancer based on the subject expression profile, wherein the good prognosis predicts an increased likelihood of survival within a predetermined period after initial diagnosis and/or no progression of disease after primary treatment, and the poor prognosis predicts an aggressive disease, a decreased likelihood of survival, and an increased

likelihood of biochemical recurrence, clinical recurrence, and/or the presence of local or distant metastases, within a predetermined period after initial diagnosis; and/or

- classifying the subject as having or not having a predisposition of prostate cancer that is susceptible to disease progression based on the subject expression profile, wherein
- 5 the predisposition predicts an aggressive disease, decreased likelihood of survival, and an increased likelihood of biochemical recurrence, clinical recurrence, and/or the presence of local or distant metastases, within a predetermined period after initial diagnosis.

- 14. The method according to claim 13, wherein the prostate cancer is metastatic
- 10 castration-resistant prostate cancer (mCRPC), and wherein said individual has undergone treatment for prostate cancer, and wherein said treatment is enzalutamide.

- 15. A composition comprising enzalutamide for use in the treatment of metastatic castration-resistant prostate cancer (mCRPC) in an individual having said disease and classified as having good prognosis in accordance with any one of claims 13 or 14.

Abstract**Method for Predicting Progression of Prostate Cancer**

The present invention relates to methods for predicting the progression of prostate cancer, specifically metastatic castration-resistant prostate cancer (mCRPC), in an individual. The invention employs gene expression profiling combined with predictive modeling to assess the likelihood of overall survival and biochemical recurrence following treatment.

Figures

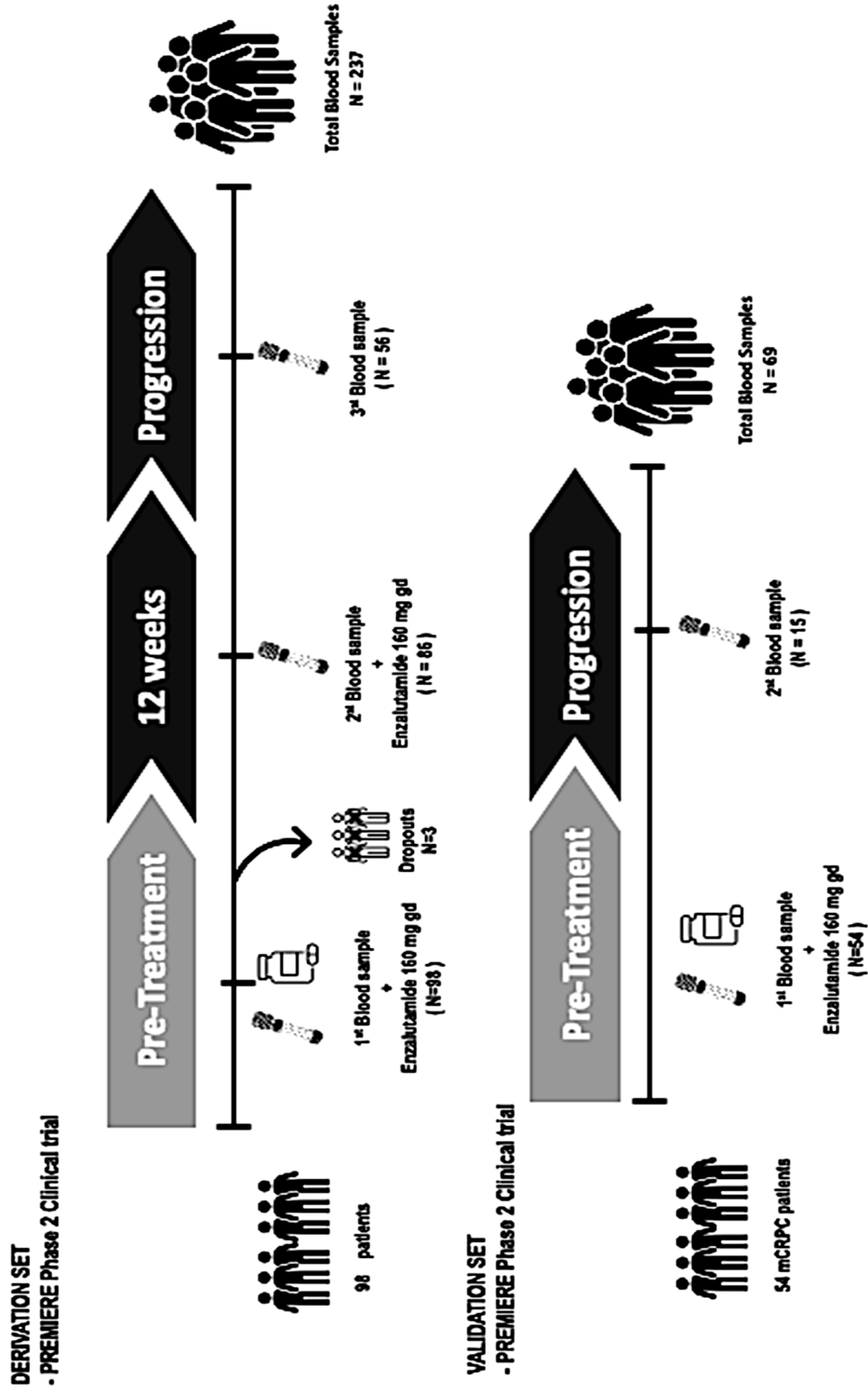


Fig. 1